HEINRICH-HERTZ-INSTITUT

REPORT 1998

HEINRICH-HERTZ-INSTITUT

REPORT 1998

TABLE OF CONTENTS · INHALTSVERZEICHNIS

Mission, Activities, Personnel and Financing

Information technology is of overriding importance for the development and strength of the economy. It is the key technology on the road from an industrial society to an information society, and is itself a leading branch of the economy, with high growth rates world-wide. It is of crucial importance as the basis of global commercial and private communications and for the development of innovative multimedia products for the information society.

The aim of research and development activities at the Heinrich-Hertz-Institut (HHI) is to further develop the principles of information technology and to demonstrate, in partnership with industry, new applications for new products.

The research areas pursued at the Institute derive from the following considerations. Telecommunication applications and infrastructure stimulate each other. The present situation is characterized by an explosive increase in the use of the Internet and mobile communication systems, both by commercial users and increasingly by private users. As a result we can assume that by the year 2010 the traffic in data and image services will be ten times greater than the telephone traffic, which will remain approximately steady.

For this to happen, the capacity of the present telecommunication infrastructure must be enlarged significantly. As this occurs, existing networks will also be modernized using more efficient technologies. Optical communication technology must be considered for the installed network because of the enormous transmission capacities of glass fibres. The resulting challenge is to exploit the possibilities of applied optical communication technology, and to turn research results and pilot projects into industrial products. The HHI meets this challenge through its projects centred on the area of **Photonic Networks**.

Mobile communication is at present still limited to narrowband applications, in contrast to communication on the wired network. But here too a need for broadband transmission systems is developing. The challenge for research is to develop suitable system concepts, to establish the technological principles, and to work

Ziel, Aufgaben, Personal und Finanzierung

Die Informationstechnik spielt eine herausragende Rolle für die Entwicklung und Leistungsfähigkeit der Volkswirtschaft. Sie bildet die Schlüsseltechnologie auf dem Wege von der Industriegesellschaft zur Informationsgesellschaft und ist selbst einer der führenden Wirtschaftszweige mit weltweit hohen Wachstumsraten. Herausragend sind ihre Funktion als Basis für die weltumspannende geschäftliche und private Kommunikation und ihre Bedeutung für die Entwicklung innovativer Multimedia-Produkte für die Informationsgesellschaft.

Das übergeordnete Ziel der F&E-Arbeiten des Heinrich-Hertz-Instituts ist es, die Informationstechnik in ihren Grundlagen weiterzuentwickeln und, in Abstimmung mit der Industrie, neue Anwendungen für neue Produkte zu erschließen.

Die Forschungsthemen des Instituts ergeben sich aus den folgenden Überlegungen. Informationstechnische Anwendungen und Infrastruktur befruchten sich wechselseitig. Derzeit ist die Situation durch eine explosionsartige Zunahme der Nutzung des Internet und mobiler Kommunikationssysteme durch geschäftliche und in steigendem Maß auch durch private Anwender gekennzeichet. Auf der Basis dieser Entwicklung ist davon auszugehen, daß das Verkehrsaufkommen von Daten- und Bilddiensten im Jahr 2010 um das zehnfache über dem etwa konstant bleibenden Telefon-Verkehrsaufkommen liegen wird.

Um diese Entwicklung zu ermöglichen, ist eine erhebliche Kapazitätserweiterung der bestehenden Telekommunikationsinfrastruktur erforderlich. Damit verbunden ist die Modernisierung bestehender Netze durch den Einsatz leistungssteigernder Technologien. Für die Festnetze kommt hierfür wegen der enormen Übertragungskapazität der Glasfaser im wesentlichen die optische Nachrichtentechnik in Betracht. Daraus ergibt sich die Herausforderung, die Anwendungsmöglichkeiten der optischen Nachrichtentechnik auszuloten und die in der Forschung und in Pilotanwendungen erzielten Ergebnisse in Industrieprodukte zu überführen. Diese Herausforderung greift das HHI mit den Projektarbeiten im Schwerpunkt **Photonik-Netze** auf.

Im Gegensatz zur Kommunikation über Festnetze ist die Mobilkommunikation z.Z.

towards standardization. The HHI handles these topics in projects focussed on **Mobile Broadband Systems.**

Data compression is needed if the network capacity is to be used economically, especially for high rate image services. It is necessary to continue research in this area and to develop compression methods with not only better performance than the present methods, but also with new functionalities, especially for interactive applications.

Broadband networks make new applications possible in the area of multimedia communications. The user friendly design of these applications, which penetrate into wide areas of everyday life, and further developments of the multimedia terminals, determine how well these services are received. The HHI handles these tasks through project work focussed on **Electronic Imaging Technology for Multimedia.**

At the end of the reporting year (21.12.1998) a total of 249 positions were occupied, 145 of which were scientific staff and 104 technical and administrative staff. Of these, 123 positions were in the research area of Photonic Networks, 67 in the research area of Electronic Imaging Technology for Multimedia, 11 in the research area of Mobile Broadband Systems and 48 in central areas such as management, planning, administration and workshops. At the end of the year there were also three postgraduate doctoral students, one postdoctoral fellow, eight persons in training, 69 student assistants and one guest scientist working at the HHI.

The Institute's research is financed by both institutional funding, from the Federal Government and the State of Berlin, and by external funding. External funding comes mainly from the development concept for information technology of the Federal Government, especially under the BMBF key development programs Photonik II, and, since May 1998, KomNet, Nano-Optoelectronic (NanOp), MINT (Multimedia Communication on Integrated Networks and Terminals) and ATM*mobil* (Mobile Communication). Further external funding comes from the fourth supporting program of the European Union (ACTS, ESPRIT, etc.), from the Deutsche Forschungsgemeinschaft, and from the program for information and communication technology of the Senate

noch auf schmalbandige Anwendungen begrenzt. Aber auch hier entwickelt sich ein Bedarf an breitbandigen Übertragungswegen. Die Forschung ist herausgefordert, entsprechende Systemkonzepte zu entwerfen, die technologische Basis zu schaffen und die Normung voranzutreiben. Dieses Thema wird im HHI im Schwerpunkt **Mobile Breitbandsysteme** bearbeitet.

Eine wirtschaftliche Nutzung der Übertragungskapazität der Kommunikationsnetze – insbesondere bei hochratigen Bilddiensten – ist nur mit Hilfe der Datenkompression zu erreichen. Es gilt, die Forschung auf diesem Gebiet weiterzuführen und Kompressionsverfahren zu entwickeln, die den Kompressionsgewinn bisheriger Verfahren übertreffen und neue Funktionalität, vor allen Dingen für interaktive Anwendungen, bieten.

Breitbandige Netze schaffen die Voraussetzung für neuartige Anwendungen im Bereich Multimedia-Kommunikation. Die benutzerfreundliche Gestaltung dieser weite Bereiche des täglichen Lebens durchdringenden Anwendungen und die Weiterentwicklung der Endgeräte bestimmt dabei die Akzeptanz der neuen Dienste. Das HHI widmet sich diesen Aufgaben mit den Projektarbeiten im Schwerpunkt **Elektronische Bildtechnik für Multimedia.**

Zum Ende des Berichtsjahres (21.12.1998) waren insgesamt 249 Stellen besetzt, davon 145 Stellen mit Wissenschaftlichen Mitarbeitern und 104 Stellen mit Technischen und Verwaltungsmitarbeitern. 123 Stellen gehörten zum Forschungsgebiet Photonik-Netze, 67 Stellen zum Forschungsgebiet Elektronische Bildtechnik für Multimedia und elf Stellen zum Forschungsgebiet Mobile Breitbandsysteme. In zentralen Einrichtungen (Geschäftsführung, Planung, Verwaltung, Werkstätten) sind 48 Stellen besetzt. Außerdem arbeiteten zum Stichtag drei Doktoranden, ein Postdoktorand, acht Auszubildende, 69 studentische Hilfskräfte und ein Gastwissenschaftler am HHI.

Die Finanzierung der Forschungsarbeit des Instituts erfolgt durch institutionelle Förderung durch Bund und Land und durch Drittmittelförderung. Der überwiegende Teil der Drittmittel wird im Rahmen des Förderkonzepts Informationstechnik der Bundesregierung bereitgestellt, insbesondere innerhalb der BMBF-Förderschwerpunkte Photonik II und, seit Mai 1998, KomNet, Nano-Optoelektronik (NanOp), MINT (Multimediakommunikation auf integrierten

Administration for Commerce and Industry, Berlin.

External funding through direct R&D contracts with companies has been of growing importance to HHI, especially as this leads to a stronger orientation of the research topics and methods towards the long and medium term needs of the telecommunication industries. This policy is also in agreement with the recommendations in the reviews of HHI by the German Association of Electrotechnical Industries and the German Science Council.

To improve our industrial collaboration in all research areas, a number of new R&D contracts with industry have been entered into, aided by the Planning and Marketing Department. In addition, many product-oriented smaller orders have been obtained from industry, mainly in the areas of photonic components and subsystems, system measurements, electronic imaging technology, and feasibility studies. The Institute's participation in technical exhibitions at the major scientific conferences (OFC, ECOC, ECMAST) and our increased public relations activities in the media have been particularly helpful for the marketing of our research products.

In order to better manage the large number of projects and contracts, professional project management and quality management methods are now being introduced.

Netzen und Terminals) und ATM*mobil* (Mobilkommunikation). Weitere Drittmittel erhält das HHI aus dem 4. Rahmenprogramm der Europäischen Union (ACTS, ESPRIT, etc.), von der Deutschen Forschungsgemeinschaft und aus dem Programm Informations- und Kommunikationstechnologie der Senatsverwaltung für Wirtschaft und Betriebe, Berlin.

Von besonderer Bedeutung für das HHI ist die zunehmende Drittmitteleinwerbung aus F&E-Aufträgen aus der Wirtschaft; denn sie führt zu einer stärkeren Orientierung der Forschungsthemen und der Arbeitsmethoden auf den lang- und mittelfristigen Bedarf der Informationstechnischen Industrie und steht damit im Einklang mit den Forderungen der Evaluationen durch den Zentralverband der Elektrotechnischen Industrie (ZVEI) und des Wissenschaftsrates.

Zur Intensivierung der Industriekooperationen wurden mit Unterstützung der Abteilung Planung/Marketing in allen Forschungsschwerpunkten zahlreiche neue Forschungs- und Entwicklungsaufträge abgeschlossen. Dazu kommt die Bearbeitung produktbezogener Kleinaufträge in den Bereichen photonische Komponenten, Systemmeßtechnik und Elektronische Bildtechnik sowie die Durchführung von Studien. Als besonders erfolgreiches Forum für die Vermarktung von Forschungsergebnissen des Instituts haben sich die technischen Ausstellungen auf den einschlägigen internationalen Fachtagungen (OFC, ECOC, ECMAST) erwiesen; mit dem gleichen Ziel wurde die Öffentlichkeitsarbeit in Presse, Funk und Fernsehen intensiviert.

Um die zunehmende Zahl von Projekten und Aufträgen effizient zu bearbeiten, werden derzeit moderne Instrumente für das Projektmanagement und die Gesamtprojektsteuerung sowie für das Qualitätsmanagement eingeführt.

Corporate Bodies

The corporate bodies of the HHI are the General Meeting, the Supervisory Board, the Managing Directors and the Scientific Technical Committee.

Members of the **Supervisory Board** for this report period are:

Organe und Gremien

Die Organe der HHI GmbH sind die Gesellschafterversammlung, der Aufsichtsrat, die Geschäftsführer und der Wissenschaftlich-Technische Rat.

Dem **Aufsichtsrat** gehörten im Berichtsjahr folgende Mitglieder an:

Prof. Dr. J. Hesse, (chairman), Carl Zeiss, Oberkochen
MinDirig Dr. K. Rupf, (1st vice-chairman), BMBF, Bonn
SenR P. Schuhe, (2nd vice-chairman), SenWissForsch und Kultur, Berlin
MinR J. Claus, Deutsche Telekom AG, Bonn
Prof. Dr. H. Berger, Technische Universität Berlin
ORR H.-D. Götze, SenFin, Berlin
Dr. H. Roehle, HHI, Berlin
Dr. H. Venghaus, HHI, Berlin

The **Scientific-Technical Committee** is comprised of heads of departments and an equal number of elected members from the Institute, and advises the Supervisory Board and the Managing Directors on all important scientific and technical matters.

Further, the HHI has appointed a **Scientific Advisory Committee** of experts from industry, the Deutsche Telekom AG and the academic sector. Members of the Scientific Advisory Committee for this report period are:

Der **Wissenschaftlich-Technische Rat** ist paritätisch mit Abteilungsleitern und gewählten Mitarbeitern des Instituts besetzt und berät den Aufsichtsrat und die Geschäftsführung in allen wichtigen wissenschaftlichen und technischen Fragen.

Die Gesellschaft beruft außerdem einen **Wissenschaftlichen Beirat** aus Experten der Industrie, der Deutschen Telekom AG und des Hochschulbereichs. Dem Wissenschaftlichen Beirat gehörten im Berichtsjahr folgende Mitglieder an:

Prof. Dr. G. Kohn, (chairman), Universität Stuttgart
Prof. Dr. J. Eberspächer, Technische Universität München
Dr. H. Eisele, Alcatel-SEL AG, Stuttgart
Dr. R. Gossink, Philips GmbH, Aachen
Dr. H.-G. Junginger, Sony Europe GmbH, Fellbach
Prof. Dr. E. Lüder, Universität Stuttgart
Prof. Dr. H. Melchior, ETH Zürich
Prof. Dr. U. Reimers, Technische Universität Braunschweig
Dr. B. Schwaderer, Bosch Telecom GmbH, Backnang
Prof. Dr. G. Siegle, Robert-Bosch GmbH, Bonn
Werner Späth, Siemens AG, Regensburg
Dr. K. U. Stein, Siemens AG, München
MinR W.-P. Ottenbreit (guest), Deutsche Telekom AG, Bonn

Organisation and Contact Persons · Organisation und Kontaktpersonen

Directors · Geschäftsführer

	Prof. Dr. Clemens Baack	+49-30-31 002-200	baack@hhi.de
	Dr. Wolfgang Grunow	+49-30-31 002-300	grunow@hhi.de

Departments · Abteilungen

Optical Networks Optische Netze	Dipl.-Ing. Godehard Walf	+49-30-31 002-455	walf@hhi.de
Optical Signal Processing Optische Signalverarbeitung	Dr. Hans-Peter Nolting	+49-30-31 002-427	nolting@hhi.de
Broadband Mobile Communication Networks Breitband-Mobilfunknetze	Dr. Dr. Holger Boche	+49-30-31 002-540	boche@hhi.de
Materials Technology Materialtechnologie Photonics Coordination Koordination Photonik	Dr. Norbert Grote	+49-30-31 002-431	grote@hhi.de
Micro Fabrication Technology Strukturtechnologie	Dr. Udo Niggebrügge	+49-30-31 002-550	niggebruegge @hhi.de
Integration Technology Integrationstechnologie	Dr. Herbert Venghaus	+49-30-31 002-555	venghaus@hhi.de
Image Processing Bildsignalverarbeitung	Dr. Ralf Schäfer	+49-30-31 002-560	schaefer@hhi.de
Human Factors Anthropotechnik	Dr. Thomas Sikora	+49-30-31 002-210	sikora@hhi.de

Central Services · Zentrale Einrichtungen

Administration Verwaltung	Dipl.-Ing. Hartmut Mrowka	+49-30-31 002-310	mrowka@hhi.de
Planning + Marketing Planung + Marketing	Dr. Walter Döldissen	+49-30-31 002-253	doeldissen@hhi.de

R&D FIELDS

Photonic Networks

Topics and Results

Worldwide telecommunication is currently experiencing an explosive increase in the demand for transmission capacity. In the USA, where the increase is strongest, growth rates are around 60% every year. The main driving force for this development is the Internet, which will evolve into a broadband Internet with an even higher demand for bandwidth over the next years. A ten-fold increase in transmission capacity is forecast by the year 2010. Telephone traffic, which is expected to remain at a roughly constant level, will then play only a minor part.

Apart from microelectronics, the foundation for this development is optical fibre communication, or photonic networks. The enormous capacity of an optical fibre enables the design and construction of high-capacity communication networks. Multiplexing techniques, such as optical frequency-division multiplexing (OFDM) and optical time-division multiplexing (OTDM), will be further developed in order to exploit the high bandwidth offered by optical fibres. Moreover, in a photonic network the data are not only transmitted over the optical pathway, but they are also routed optically. Thus, the photonic network will be service-independent, offering high capacity pathways for all current and future services.

These predicted developments will also increasingly affect the customer networks, i.e. the communication networks located in either private or commercial premises. As the information has to be transmitted to the user's terminal, the customer network must link these multimedia terminals with the broadband Internet. The prognoses for the year 2010 are data rates of 100 Mbit/s for private and 1 Gbit/s for professional end terminal users.

The objective of research in the area of photonics at the HHI is to make substantial contributions to the development of photonic networks.

The following main areas are being addressed:

- Development of network concepts for the various layers of photonic networks – the core, access and customer networks.
- Investigation of the potential of optical multiplexing techniques such as OFDM and OTDM. The optimum combination of both is of paramount importance.
- Determination of the limits of optical transparency; i.e. the assessment of the transparency path lengths in photonic networks.
- Identification of the requirements for the networks and for their photonic components, including transmission lines and routing subsystems.
- Investigations into the supervision (operation, administration and maintenance – OAM), and control (telecommunication management network – TMN) of photonic networks.
- Development of methods and devices for all-optical 3R signal regeneration.
- Development and fabrication of photonic components and subsystems.

PhotoniK II and KomNet: Most of these activities have been carried out under the national research program Photonik II, which was supported by the Federal Ministry for Education, Science, Research and Technology from 1994 to 1998. The focus of this program was essentially on optical communication systems and techniques, key components and key technologies. The various topics were investigated by the communications industry in cooperation with research institutions and universities. The scientific leadership of the research program was shared between the Fraunhofer Institute for Applied Solid-State Physics (FhG-IAF) in Freiburg and the HHI.

In the new BMBF-sponsored program KomNet the results achieved by Photonik II are to be transferred to product-oriented developments and are to be used to develop a pilot broadband Internet system, which will be built by industry with Deutsche Telekom as network provider. It will be located in Berlin, but with a long distance link to Stuttgart. The HHI participates in the KomNet program through R&D subcontracts from industry and the Deutsche Telekom, and will perform research and development on both system technology and device technology. The HHI is responsible for coordinating the assembly of the KomNet pilot system.

The research area of photonic networks is divided into the specialist areas

Access and *Customer Network* and *Core Network*.

Access and Customer Network

Research and development activities in this area were concentrated on the use of WDM techniques in the access network. The goal was to develop and investigate system concepts and components for WDM applications in the access network.

WDM upgrade of a PON: Research and development activities for a WDM upgrade of an existing passive optical network (PON) are being carried out. Work in this area is based on a system concept that increases capacity without changing the glass fibre network structure between the central office and the optical network units (ONUs) near the subscribers. A WDM overlay of permanent wavelength paths in the region of 1.5 µm is added to the passive optical access network. The key elements used are arrayed waveguide gratings (AWGs) for various multiplexing, demultiplexing and routing functions of the different wavelength signals. Various demonstrators with channel spacings from 9 GHz up to 400 GHz were realized to characterize network elements and components and to investigate possibilities for supervising these elements by a TMN. Arrayed waveguide gratings with channel spacings between 100 GHz and 400 GHz are used in the testbeds. Components such as these were realized by HHI and other partners in Photonik II.

Transponder: For the upgrade of optical transmission systems using WDM techniques, it is necessary to use transponders to interface to an existing system environment. A transponder consists of an optical receiver and an optical transmitter at a given wavelength. Depending on input sensitivity and optical output power, signal gain as well as wavelength conversion can be achieved. In cooperation with industry, a modular bitrate-transparent transponder without temporal regeneration that works over the range 100 Mbit/s to 2.5 Gbit/s was developed. For operation at fixed bitrates (e.g. SDH, STM-16), electronic signal regeneration and clock recovery circuitry can be added. The transponder is provided with appropriate control and supervisory functions for inclusion in a TMN system. A modular bitrate-independent WDM transponder for multi-channel optical systems up to 2.5 Gbit/s was developed and successfully used in a system environment.

WDM filter components: WDM filter devices with various specifications have been developed and fabricated in several technologies, but mainly based on silica (SiO_2/Si) technology because of its superior insertion loss and optimal robustness. Arrayed waveguide grating filters (AWG) have been fabricated as standard devices with 100 and 200 GHz channel spacings and 16 and 8 channels, respectively. These filters usually exhibit Gaussian transmission characteristics. In a more specialized version a filter with a rectangular characteristic has been designed, which eases cascading. This filter uses matched adiabatic horn structures at the inputs and outputs of the AWG waveguides, and also features greatly reduced polarization effects. This achievement, an outcome of a collaborative project with an industrial partner and other research institutions, relies on a special silica deposition process that results in reduced waveguide stress and thereby nearly polarization-free components. Further optimization of this development is under way.

For system applications in a PON/WDM network a special component has been developed that makes it possible to overlay an existing PON with a WDM network. The key component is a specially designed 2-band MUX-AWG with an integrated power divider for the broadcast wavelength at the input. The additional loss of such an 8-channel MUX is 3.5 dB for the WDM Band at 1.55 µm and about 4 dB at 1.50 µm. The crosstalk is less than -25 dB.

AWG devices implemented on polymers as well as silica have been under development. An important part of this activity, which is being carried out in collaboration with an industrial partner, relates to the characterization and application of novel optical polymer materials featuring higher thermal stability than the previously used PMMA. The materials used have been synthesized at the Fraunhofer Institute IZM. For a special application, AWGs were also made on InP.

Drop filters, which separate signals at different carrier frequencies, are further key elements in WDM systems. Such a component, in the form of an active monolithically integrated optoelectronic InP device, is being developed under the framework of

an ACTS project. The device consists of a tunable, polarization-independent optical filter, an optoelectronic detector and an electronic preamplifier. A polarization-independent transfer characteristic with a bandwidth of 400 GHz (3.2 nm), a tuning range of 25 nm and with 20 dB crosstalk was obtained. The first integration of the filter and detector functions has been achieved.

Lasers for WDM: The MQW-DFB lasers with RW structure have been further optimized, the main aim being to achieve high output power and the integration of multi-laser arrays. Single lasers with prescribed wavelengths, 40 mW output powers (at 200 mA driver current) and good aging characteristics can now be reproducibly manufactured. Based on these single lasers, integrated 4-wavelength transmitter chips have been processed. These chips also include a combiner waveguide network, monitor diodes and an integrated temperature sensor. The radiation emitted from all four lasers exits the chip through a single waveguide. A module can therefore be built at very low cost with these transmitter devices. Based on this development, joint R&D projects with small and medium sized companies have been started for the development of laser arrays with special additional characteristics.

Monolithically integrated transceiver: Bidirectional optoelectronic transceivers are being developed for access network applications. The crucial importance of WDM transceiver PICs for optical access networks has been emphasised by the Full Service Access Network (FSAN) Group and also in the Japanese OITDA Report. This project is being carried out in close collaboration with industrial partners. Ultimately, a cost reduction for the fabrication of high volume optical modules is expected by the implementation of Photonic ICs (PICs). The main issues for this project are:

- The ongoing development and availability of a technological toolbox for flexible and economic integration of basic optical and optoelectronic building blocks (e.g. lasers, waveguide networks, photodetectors), without essential loss of performance compared to the fabrication of the separate elements.
- Application of this technology for the realization of complex PICs.
- Demonstration of the functionality of a monolithically integrated solution for a polarization-insensitive heterodyne receiver.
- Extension of the versatile integration technology to the fabrication of WDM transceiver PICs – the first candidates for high volumes.
- Processing of first 1.5/1.3 µm transceiver PICs meeting the system requirements.

A main breakthrough towards the possible economic fabrication of WDM transceiver PICs was achieved with the development of PICs with compact, wavelength-selective photodetector building blocks. First 1.5/1.3 µm transceiver PICs have been fabricated and packaged for implementation in a system demonstrator of the ACTS project Broadband Lightwave Circuits and Systems (BLISS/AC065). The characteristics of these first transceiver PIC demonstrators prove the viability of the developed concepts, even for the challenging FSAN specifications. These results are the basis for work in the follow-up project KomNet.

Power line communication systems (PLC) could contribute to the solution of the 'last-mile' problem. Use of the 230 V power line network for information transmission is seen as a possible low-cost alternative to new installations of communication systems in the access and customer premises area. Under a contract with some power supply companies, a PLC transmission system was developed in cooperation with two engineering enterprises. As an example, video conferencing using 64 kbit/s duplex channels was demonstrated. This was achieved with a spread spectrum technique in a frequency range above the CENELEC band (148.5 kHz). The operational range in a real power line network is about 100 m without a regenerator.

Core Network

Work in this research area is concentrated on high bitrate time division multiplexing (TDM) techniques, optical crossconnects and optically transparent networks. With the high bitrate TDM technique, multiplexing and demultiplexing may be performed either electrically (ETDM) or optically (OTDM). Important issues are the generation, modulation, detection and synchronization of the optical signals. Other topics under investigation are the effects of photonic components and fibre

nonlinearities on the quality of the optical signals and methods of dispersion compensation.

Optical time division multiplexing (OTDM) work includes investigation and realization of optical subsystems such as multiplexers (MUXs), which multiplex 10 Gbit/s optical data signals to generate 40 to 80 Gbit/s signals, and demultiplexers (DEMUXs), which demultiplex these signals back to 10 Gbit/s data signals. Another important subsystem is the RZ data source, which was realized by a modelocked laser. This data source has been demonstrated in 40 Gbit/s transmission experiments using standard fibre and unrepeatered (no optical amplifiers in the transmission line) transmission spans up to 150 km. To compensate for fibre dispersion, we applied passive dispersion compensation using dispersion-compensating fibre.

Experiments in combining the WDM and TDM techniques were performed. A transmission system with a total capacity of 640 Gbit/s was realized. Eight WDM channels, each carrying an 80 Gbit/s OTDM data signal, were generated and simultaneously demultiplexed with a new highly linear demultiplexer switch. This new 'gain transparent' demultiplexer is superior in its performance to the alternatives, and is very promising for future add/drop multiplexer application. It has been realized in a hybrid version so far, but monolithic integration is planned for the future.

Transmission experiments at 40 Gbit/s over 217 km and 433 km lengths of standard fibre (D=16 ps/km nm) were performed using the mid-span spectral inversion technique. These experiments were intended to demonstrate a polarization-insensitive optical phase conjugator (OPC) using the polarization diversity technique. An optical data signal with an arbitrary state of polarization and a CW pump wave with a well defined state of polarization were coupled together into the input of the OPC. At the input of the OPC is a polarization beam splitter, which splits the optical input signal into two orthogonal polarization states, corresponding to the two branches of the OPC. The polarization of the pump wave was chosen in such a way that 50% of its power was in each branch of the OPC. Hence in each OPC branch the well defined polarization components of the data signal and the CW pump were used to generate phase-conjugate data signals by four-wave mixing in a semiconductor optical amplifier. The phase-conjugate signals generated in both OPC branches were combined in a polarization combiner, resulting in a phase-conjugate data signal, which was transmitted as a data signal over the second span of the transmission line in the mid-span spectral inversion arrangement. Polarization independence and error-free operation (with a 3 dB penalty) were demonstrated.

Monolithically integrated OTDM devices: The world's smallest monolithically integrated Mach-Zehnder interferometers have been successfully fabricated at HHI. These are used for all-optical demultiplexing and add-drop functions in OTDM systems at 40 Gbit/s. Optical semiconductor amplifiers (SOAs) are used as nonlinear elements in the interferometer arms. Two different versions have been designed. The asymmetric version comprises a fixed switching window that is set by the geometrical offset of the amplifiers. The advantages of this structure are its small area of only 4×0.75 mm^2 and its simple control (the data and control signals share one input and one output port). The more flexible symmetric version, with two additional branches for the control signal, can also be used for all-optical wavelength conversion, but it needs extra control effort (up to 4 optical inputs and 2 optical outputs) and has a slightly larger device area of 5×1 mm^2.

Transparency lengths and optical crossconnects: The properties of regenerator-free optical communication networks are being investigated theoretically as well as experimentally under a contract with a network provider. The essential elements in the transport layer of such networks are the transmission lines, fibre amplifiers, and optical crossconnects. Non-ideal properties of these components limit the transmission lengths in the optical networks because of signal degradation.

Suitable transparency length diagrams can be used to plan the transport layer of optically transparent networks. The experimental tests are in an eight channel WDM loop test bed in which data packets at transmission rates of up to 10 Gbit/s per wavelength channel circulate around a fibre loop. Cascades of several transmission sections, together with optically transparent crossconnects, can be modelled with

this test bed, and the signal quality can be measured as a function of the number of crossconnects and the fibre link lengths. The measurements show that crosstalk better than -40dB can be demanded with a cascade of 10 sections. Also, the 2R regeneration properties of an electro-optic transponder were measured, and it was shown that its timing jitter limits the number of transponder cascades.

The application of WDM technology in the core network with optical crossconnects at data rates up to 10Gbit/s per WDM channel is being investigated in the ACTS project PHOTON, which is led by Siemens. The HHI is responsible for the development and construction of a wavelength reference for the demonstrator as well as for system studies in this project.

Signal regeneration: Signal degradation in optical networks limits the transmission lengths of the optical paths. Complete 3R (reamplification, reshaping and retiming) regeneration of digital signals can remove this limit. For these functions we are developing optical signal processing methods and components that allow for either full regeneration (3R) or partial regeneration (2R – reamplification and reshaping). The key components for 3R regeneration are the clock recovery and decision stages. Three-section RWG lasers have bistable characteristics if appropriately designed. A module for clock recovery was built which operates from below 5 to more than 20 Gbit/s. The clock rate is continuously adjustable, using an electric current. The clock recovery modules have been demonstrated successfully in several system experiments (at HHI, Denmark Technical University and Alcatel Marcoussis). We are also investigating how specially developed three-section RWG lasers may be used as decision units. Because of the common fabrication technology of the amplifier, clock recovery unit and decision unit, it will be possible in the future to monolithically integrate a 3R regenerator.

Network Modelling: Methods for simulating optical components and signal propagation in an optical path are being developed and tested against the experimental measurements. As well as our own program developments, we use the program package BroadNeD, which is commercially available (from Virtual Photonics Incorporated - VPI). The work towards high bitrate TDM and the combination of TDM with WDM transmission technology is also supported by analytical and numerical investigations. The main topic of investigation is the question of how the transmission line has to be set up to achieve optimum transmission capacity.

Models of national WDM core networks the size of Germany were developed and have been analyzed with respect to their technological limits, traffic capacity and hardware requirements. An evolution of the network based on multiple ring topologies, with various strategies for alternative topologies, is suggested. This could lead to a flexible crossconnected network with both fixed and switchable add-drop nodes.

40 Gbit/s transmitter and receiver: For high bitrate optical transmission systems at 40Gbit/s, transmitters with integrated lasers and modulators (low chirp), together with receivers based on integrated waveguide diodes and high electron mobility transistors (HEMT) for optimal impedance matching, are being developed for the NRZ modulation format, due to the design of our industrial partners. A laser/modulator module with a 3dB frequency of 18GHz that can be tuned over several nanometres had already been built.

For demultiplexing of high bitrate data signals, the ultra-high speed switch reported earlier has been improved for use as an electro-optical demultiplexer. It has a 3dB frequency limit of more than 5 GHz. Polarization-independent switching has been demonstrated using a strained quantum well structure with tunnel barriers for the light holes. Capacitively loaded travelling wave structures, which are suitable for demultiplexing up to 80Gbit/s, were used. The fast switch was successfully used, as part of the ACTS project HIGHWAY, in a system experiment at the Denmark Technical University to demultiplex 40 Gbit/s signals to 10 Gbit/s.

Optoelectronic integrated circuits (OEICs) based on InP have been developed for the reception of high bitrate data streams in TDM transmission systems. They incorporate fast waveguide-integrated PIN photodiodes and MMIC-type electrical amplifiers, which consist of high electron mobility transistors. Bandwidths of up to 37GHz have been achieved. The receiver OEICs, packaged as modules, were successfully applied in system experiments by industrial

partners for the detection of 40 Gbit/s signals modulated in RZ and NRZ formats. As part of the joint project KomNet, the optical receivers have now been optimized for the specific system requirements of our industrial partners, and will be used in field experiments for 40 Gbit/s TDM transmission.

Photodetectors are being developed for operation at high optical power levels for receiver concepts that include optical preamplification. They must be capable of directly driving digital demultiplexing circuits. For this purpose, waveguide-integrated photodiodes that can detect 40 Gbit/s RZ signals at a mean optical power of +16 dBm and that generate peak voltages of 0.7V at 50 Ω have been developed. The -3dB electrical bandwidth is 70 GHz and the sensitivity is 0.35 A/W.

Competencies

Investigation and development of architectures for photonic networks, development of planning guidelines and studies of specific problems of photonic networks.

Characterization and testing of optical networks and network components, including experiments on fibre loops, transmission experiments over large distances and field trials.

Development of high rate optical WDM systems (10x Gbit/s per channel) and the corresponding measurement methods.

Investigation, design and development of optical WDM LANs and MANs, optical access networks, and passive optical networks.

Development of methods for the control and supervision of networks.

Development, application and verification of simulation software for optical transport networks.

Design and development of optical systems using heterodyning.

Development of wavelength conversion methods for WDM systems.

Investigation and development of high rate OTDM subsystems (10 to 40 Gbit/s and above), including multiplex/demultiplex and add/drop techniques.

Development of methods for purely optical clock recovery and signal regeneration (2R and 3R).

Development of methods for the generation of ultra-short optical pulses.

Optimization of methods of dispersion management.

Design and development of optical frequency reference equipment.

Design and fabrication of transponders and optical SDH front ends.

Development, fabrication and characterization of fibre optic components.

Development, fabrication and characterization of methods and devices for PMD compensation.

Development, fabrication and characterization of optoelectrical components and photonic integrated circuits based on InP:
- Tunable lasers (DFB, dBR).
- Multi-wavelength laser arrays.
- Optical amplifiers.
- Fast laser/modulator transmitters.
- Wavelength converters.
- Wavelength drop filters.
- Demultiplexers and add/drop multiplex for OTDM applications.
- Components for optical clock recovery and signal regeneration (self pulsating lasers).
- Integrated transceivers.
- Ultra-fast photodetectors (70 GHz).
- High bitrate optical receivers with integrated MMIC preamplifiers.
- Optical microwave generators.

Development and fabrication of thermo-optical switches and switch matrices with minimal crosstalk using polymers.

Development and fabrication of planar waveguide components in SiO_2/Si (e.g. waveguide grating filters).

Development and fabrication of passive

and of electrically controllable diffractive optical components in SiO_2.

Modelling of photonic components and integrated circuits.

Development, optimization and application of component technologies:
- Clean room laboratories (class 10/1000).
- Epitaxy (MOVPE, MBE, MOMBE) and the characterization of InP-based semiconductor materials.
- Secondary ion mass spectroscopy (SIMS).
- CAD/CAM of photolithography masks.
- Electron beam lithography and optical lithography.
- Dry etch processes (reactive ion etching, ion beam etching) with endpoint detection.
- Rapid thermal short time processing.
- Deposition of metal and dielectric layers (evaporation, sputtering, plasma deposition).
- Optical coatings.
- Characterization and technology of optical polymer materials.
- High resolution scanning electron microscopy.

Development and application of electrical and optical mounting and connection methods for components (flip chip bonding, high frequency packaging, laser welding, fibre-chip coupling).

Mobile Broadband Systems

Topics and Results

In recent years personal and mobile communications systems have experienced an overwhelming increase in the number of users. This, together with additional services such as data transmission, has lead to a growing need for capacity. Capacity can be increased by higher spectral efficiency. Several techniques are being developed to do this. In a cellular system the capacity is limited by the cell density, the frequency spacing and the number of users who can be served simultaneously by each base station.

Smart antenna technology is one of the most significant new techniques for increasing the capacity of mobile networks. It has a great impact on the radio performance – e.g. it decreases the bit error rate in the uplink channel (the link from the mobile unit to the base station) in CDMA cellular radio systems.

Future mobile communications systems are also facing an increasing demand for heterogeneous broadband services and applications. Smart antennas will not only increase the capacity of the system, but also reduce interference and delay spread by means of spatial filtering, thus enhancing the properties of the mobile radio channel, as required for high data rate communications. Although it is generally expected that smart antennas will be used in emerging communication systems such as UMTS/IMT-2000, the design of the Integrated Broadband Mobile System (IBMS) is based completely on smart adaptive antenna technology, which allows the use of more bandwidth-efficient advanced modulation techniques. The IBMS project is sponsored by BMBF, the German Federal Ministry of Education, Science, Research, and Technology.

The performance enhancements that can be achieved by employing constrained beamformers in code division multiple access (CDMA) cellular radio systems were investigated in connection with IMBS. Our investigations focussed on improving the reverse (uplink) channel, the main problem with such systems. The analytical results and simulations demonstrate that constrained beamformers at the base station can dramatically improve the reverse channel bit error performance. To achieve optimal system performance, a new constrained beamforming algorithm was proposed. Whereas existing beamformers allow only the directions of either the zeros or the main beam to be controlled, the new beamforming algorithm allows both to be controlled. The number of zeros in the beam pattern that can be constrained depends on the number of sensors. This new constrained beamforming algorithm can produce an optimized beam pattern that exploits both space division multiple access (SDMA) and spatial filtering for interference reduction (SFIR).

The propagation conditions in indoor environments, where many echoes arrive from different directions, are more difficult than in outdoor environments. Due to the large number of echoes and their angular spread, it is not practical to eliminate the interfering signals by aligning the zeros of the beam pattern with the directions of these signals. A new constrained beamforming algorithm for indoor applications was introduced to generate an optimal beam pattern for indoor environments with many echoes, allowing for their angular distribution.

The newly emerging mobile communication systems of the fourth generation will support higher data rates than current systems. Because of higher data rates the carrier frequencies will also increase, leading to a decrease of cell size. With small cell sizes, the mobility behaviour of the subscribers is a factor that cannot be ignored. The performance of future mobile communication systems will depend strongly on the mobility and calling behaviour of the subscribers. New mobility models were proposed to describe the movements of the subscriber at different scales. These new mobility models can be used to estimate the cell and location area crossing rates, the hence the amount of mobility-related signalling, such as handover and location update signalling. The new models are extensions of the ETSI (European Telecommunication Standards Institute) mobility models, and have been proposed for the standardization of UMTS.

Another research area in the indoor domain focuses on infrared and microwave communications.

For wireless infrared (IR) communication,

two approaches are presently under investigation that exploit directed beam line-of-sight and spot diffusing links. The aim is to realize inexpensive and power-efficient transceivers for data rates up to 155 Mbit/s. Both base station oriented systems and ad hoc LAN systems with spot diffusion are under consideration. The system performance and the power budget are considerably improved by using a tracking architecture. Array technologies for the receiver and transmitter will supersede the use of mechanically moved optics and will allow a single interface for narrowband and broadband services.

Laboratory experiments on an IR ad hoc LAN were carried out at a wavelength of 1.55 µm. The distribution of the transmitter power across the cell was realized by diffuse reflection from the ceiling (spot diffusion with diffusion angle about 100 degrees). The receiver optics (field of view less than one degree) was directed towards the diffusing spot. Error-free digital video transmission (at 140 Mbit/s with CMI coding) could be obtained in a 20 m^2 cell with 5 mW transmitter power in a collimated beam, which is safe for the human eye for wavelengths greater than 1.4 µm.

Well known principles in the area of optical frequency division multiplexing are being applied to broadband mobile communication and satellite systems operating in the 60 GHz band. These investigations have been carried out under the framework of the BMBF program Photonik II. The aim was to combine fibre-based low-loss distribution of broadband signals between the control and base stations with remote microwave generation in low cost base stations. Low phase noise microwave signals were generated at very precise frequencies in the 60 GHz band by using optical heterodyning and the sideband injection locking technique. Components of a commercial mobile broadband system, which was developed in cooperation with our industrial partner Bosch Hildesheim, were used for the transmission of 155 Mbit/s data signals.

Multichannel transmission experiments with different multiplexing techniques have been carried out, and the results agreed with simulations that were done in cooperation with the Fachhochschule Lübeck.

The optic/microwave converter in the base station is a key component for optical microwave systems. In cooperation with the Institute for Solid State Physics at the Technical University of Berlin, monolithically integrated devices for the 60 GHz range were developed.

The optical transmission technique is already used in the area of phased array antennas because of the broadband and low loss properties of the optical fibres. Further advantages of optical methods, especially for space-borne antennas, are the low weight and compactness of the fibres. For the control of phased array antennas, the distribution network connecting the central electronics with the antenna elements should have low loss and high phase stability. The properties of optical delay lines were investigated in cooperation with Dornier Satellitentechnik GmbH. These delay lines can be used for beam forming by controlling the phase relations between the antenna elements.

Electronic Imaging Technology for Multimedia

Topics and Results

The R&D contributions of the HHI to this research area are in the areas of Image Processing and Terminal Systems and Applications.

Image Processing

The HHI activities in the field of image processing are concentrated on signal processing and coding for video services in various applications, on the design of VLSI components, and on system integration. A wide range of image formats, from very low resolution for narrowband video communication up to high resolution for multimedia services, are supported. Typical applications include VLBV (Very Low Bitrate Video) for multimedia communication at low bit rates over the Internet or mobile networks, interactive multimedia services, broadcast and communication services, and studio applications.

As far as hardware projects are concerned, the development of architectures for future multimedia terminals is the central activity, with the focus on key components for 3D graphics, compositing, MPEG encoding and decoding, and format conversion. One emphasis is on Multimedia Communication on Integrated Networks and Terminals (MINT), which is a collaborative project sponsored by BMBF. The main topics of this project were the development of service-integrating fixed and mobile terminals, the development of interfaces for digital fixed and mobile networks, wired and wireless in-house communication, and user interfaces for mobile and stationary terminals. The development of the MPEG-4 standard for image a sound sound compression was a major activity in MINT.

The main issue for HHI under the MINT project was the development of key components for the common demonstrator of the collaborative project. Architectural studies have been carried out for the realization of components for MPEG-4 decoding (including system demultiplexing), for format conversion, and for the decoding and display of stereo images, and these components were implemented in hardware. They were then used in the complete demonstrator, which was presented to the public during the Symposium 'Multimedia Communication on Networks and Terminals', which was organized jointly by the MINT project and by the German TV Platform on 26 November in the International Congress Centre in Berlin.

- A DSP module was developed to implement a real-time MPEG-4 decoder. This module consists of a signal processor, together with a coprocessor for bit-stream decoding, plus memory. Up to four modules can be mounted on a PCI card, which was also developed at HHI and which can be integrated into a PC. This device is currently the most powerful MPEG-4 decoder available, and corresponds to the Simple and the Main Profile of the MPEG-4 standard (Version1).
- An MPEG-4 based client-server application was implemented using this decoder. This application enables the retrieval of video objects from a remote server. An MPEG-4 compositor is used to manipulate (move or resize) the video objects on the screen. The signalling protocol DMIF (Delivery Multimedia Integration Framework), which is still in the process of standardization by MPEG, was implemented for this purpose. This functional implementation is one of the first worldwide.
- An autostereoscopic videophone terminal was developed. It consists of a 3D display with head tracking, which was developed by Zeiss but based on HHI patents, and a specially designed processing unit for parallax compensation. This unit uses a real-time disparity estimator and viewpoint interpolator. Images from virtual camera positions, depending on the position of the viewer's head, are computed. This is the world's first real-time implementation of such a system.
- In order to display stereo images on commercial 100 Hz TV sets or on the above autostereoscopic display, a special decoder (HiBOX) was developed. This unit allows the simultaneous and synchronized decoding of two MPEG-2 encoded bitstreams, representing the left and the right channels of a stereo pair. These signals can be retrieved from a DVD drive connected via a SCSI interface or from a DVB transmission channel connected via a parallel DVB interface. The world's first DVB-T

transmission of stereo TV was demonstrated during the MINT Symposium.

Based on the current status of image coding (MPEG-4, BIFS, SNHC) and of description languages for interactive services (HTML, VRML, JAVA), concepts for the coding, transmission and presentation of interactive video and VR applications are being developed in close cooperation with service providers. The main goal is to define new object, graphics and video oriented user functions, taking into account these standards as well as constraints due to production technology and transmission characteristics. These user functions will be presented to producers and service providers in order to demonstrate their attractiveness and feasibility. Services such as home shopping, business TV and virtual communication platforms are used as examples to show the potential of these new technologies. Tools will also be made available for new interactive services. Image segmentation techniques, which can be used either on-line or off-line, are important tools for such applications and are therefore being developed at HHI.

- A prototype of the world's first distributed virtual video conference system was developed and presented to the public during the above mentioned MINT Symposium. This system consisted of four subscribers, who were connected via ISDN or LANs for a video conference. The images of the three other participants, who are MPEG-4 encoded in their natural shapes, are shown in an artificial 3D conference environment, through which the viewer can navigate. An important feature of this system is a real-time segmentation tool that can separate the participant from an arbitrary background.

The development and verification of technologies that are required for new functionalities in mobile multimedia systems is of crucial importance. Such functionalities have been identified in ISO-MPEG, and the forthcoming MPEG-4 standard will become a basis for image and sound compression in future multimedia systems. These new functionalities, including content manipulation, content-based scalability and content-based access, are obtained with coding algorithms that are both very efficient and robust against transmission errors. New methods of data communication between terminals based on generic languages are also being developed as part of this framework.

- HHI has realized a number of software implementations of MPEG-4 encoders and decoders. These serve as reference models for hardware developments and are also used in MPEG-4 based real-time applications. HHI is also responsible for the integration of the MOMUSYS reference model, which is one of the two official test models of MPEG-4, alongside the Microsoft version.

Image analysis and feature extraction are basic technologies for intelligent network assistance systems. They facilitate access to multimedia information over networks. Methods of processing for image analysis and classification are being developed for this purpose as part of the MPEG-7 standardization process. In addition, object based and model based methods are being investigated and further developed for the extraction of useful visual parameters for such systems.

These techniques will enable the user to search for information among the increasingly overwhelming choice of programs that is available over hundreds of DVB channels and the Internet. To achieve this, the audio and video streams must be provided with standardized index information to enable MPEG-7 based search engines to browse for special features. The selection of a program with given contents can then be either user controlled or event driven (e.g. it could be programmed so that a sports channel could be automatic switched on if a goal is scored in a football match).

- The first prototype of a search engine that allows searching for images of similar content in an image data base was developed. Description parameters based on contour, texture and colour information may be used. This system was presented to the public during Online '98.

HDTV is currently gaining increased attention. HDTV broadcast services based on MPEG-2 coding are to be introduced in the US and Japan in the near future, whereas in Europe mainly niche applications, such as electronic cinemas, advertisements or medical applications, are the main applications under consideration. The MPEG-2 standard, which allows the transmission of HDTV material at about 20 Mbit/s, will be used world wide for this purpose.

- One of the world's first functional single

chip decoders for HDTV that implements the Main Profile@High Level of MPEG-2 was developed at HHI. This chip, called HiPEG, has been used in a complete decoder unit HiBOX, also developed at HHI. This device contains several analogue and digital interfaces for various ITU and DVB standards. HiPEG and HiBOX haven been successfully demonstrated at various events in Asia, the US and Europe. The most important demonstrations were at ECMAST '98 in Berlin, at IBC '98 in Amsterdam and at joint demonstrations with the European DVB project in Hong Kong and Argentina.

Terminal Systems and Applications

The HHI carries out R&D in the area of interactive multimedia services and new media, concentrating on user friendly multimedia applications, interaction technologies and multimedia terminals.

The focus of the work is on autostereoscopic display technologies, concepts for user friendly image communication systems with telepresence techniques, novel and trend-setting technologies for 3D desktop computers, the development of innovative 2D and 3D interaction techniques for man-machine communication, methods for data search and data visualization, and intelligent agent-based information management and user guidance. These main themes are extended by both fundamental and applied work in the area of usability engineering, with special emphasis on human factors constraints.

The autostereoscopic display developments concentrate on approaches that spare the user the need to wear special glasses when viewing natural or computer generated 3D images or videos. Applications of this technology are in the areas of 3D telephony and video conferencing, 3D TV, 3D multimedia desktop computing, 3D virtual worlds, telepresence and telework, telesupervision, vehicular technology, CAD/CAM, 3D computer games, as well as medicine and biology. The work in this area includes the development of flat panel autostereoscopic displays for one or more viewers, as well as large format front or back projection displays based on the use of either lenticular array screens or field lens technology. Prototypes of these developments were introduced to the public last year at many trade fairs and exhibitions.

- An autostereoscopic 14" flat display panel using lenticular array screen tracking was developed jointly with the firm Zeiss, Oberkochen, who also licenced the technology of lenticular screen tracking.
- A high resolution single-person flat panel display ((2×512)×768 pixels) for use in the CAD/CAM area was developed. This does not require mechanical tracking of the lenticular screen – instead, the monitor was mounted on a swinging arm so that the image plane can track the user's head movements.
- A high resolution autostereoscopic single-person display using field lens technology was developed for applications in video communication. In order to show figures in natural size for telepresence applications, the display integrates a collimation lens system to create a virtual image several metres behind the display surface. The display has outstanding resolution and brightness and minimal crosstalk.
- A large format 40" autostereoscopic back projection display with extremely high resolution ((2×1000)×750 pixels) was developed for applications in multimedia desktop computing. This monitor features mechanical tracking of the lenticular screen.
- A video-based head tracker was developed so that the HHI displays can be used without special glasses.

In recognition of the development of new concepts and technologies that point the way to the 3D desktop computer of the future, the work at the HHI concentrates on the vision of a computer with intelligent man-machine interfaces. In order to make operation easier for the user, prototypes of desktop computers were developed that present information in a clearly arranged and adequate form using a 3D display and suitable 3D visualization methods. The wishes of the user are anticipated by innovative multimodal interaction and agent technologies, thus enabling simple and intuitive operation in interactive applications.

A first prototype of an intelligent and 'seeing' 3D desktop computer that overcomes the disadvantages of the common windows desktops and allows novel forms of user interaction was implemented and shown publicly at various trade fairs and exhibitions.

• The development of a novel 3D visual operating system and suitable editors gives the desktop computer a simple and clearly arranged representation of multimedia information, and simple means for the user to interact with it. In contrast to conventional windows based desktops, the new operating system is object oriented and can arrange information in the depth dimension.
• A 50" high resolution autostereoscopic display that was developed in the HHI was used for the prototype of a 3D computer that allows the visualization of multimedia objects arranged in the depth dimension. These objects are generated and managed by the 3D operating system. Because of the autostereoscopic representation, the user can see the objects and information stacked in depth layers, and can view them from different sides by moving his or her head (movement parallax).
• A video-based measurement of the user's head movement and gaze direction that was developed at the HHI spares the user the need to wear either head markings or special glasses.
• An interface agent can recognize what the user is viewing and can then autonomously initiate appropriate actions (visually controlled graphics). In this way the representations of the displayed objects can be changed in a manner that is adapted to the user (e.g. the depth representation of the objects can be changed in a way that models the depth of focus behaviour of the human visual system). Also, the user can initiate actions by means of gaze control.

Research in the area of algorithms for 2D and 3D image processing was carried out in order to equip future generations of multimedia terminals and desktop computers with a large degree of intelligence and new forms of man-machine interaction. Applications are in the areas of 3D desktop computing, teleworking and telepresence. The work in this research area concentrates on user recognition, object recognition and tracking, 3D depth estimation, 3D intermediate view generation, and head and gaze tracking.
• A video-based head tracker was developed with the aim of presenting users of an autostereoscopic display with views of 3D images from various directions. The algorithm that was developed responds reliably to even the smallest changes of head position, even in difficult lighting conditions, and passes the measurements to a head tracking display. This algorithm works in real time and was implemented under IRIX on O2 and under Windows NT.
• The video-based head tracker was extended, using infrared techniques, so that it can also measure gaze direction. Gaze direction measurements are also being investigated for possible use as input variables for interactive purposes in future desktop computers (visually controlled graphics).
• An algorithm for object segmentation of trinocular images was developed for applications in 3D desktop computers. This algorithm can decompose image objects into depth layers and makes possible the recognition of people and spatial structures in images. This information can be used for a depth oriented representation of images and videos, with the depth of focus matched to the human visual system if the viewer's gaze direction is measured at the same time. It can also be used by an intelligent and 'seeing' computer that is equipped with a trinocular camera system to distinguish and recognize spatial structures (e.g. people, hands, physical objects) in its neighbourhood – in appropriate cases it could then act autonomously.
• New representations of objects in space were investigated and optimized in a series of psycho-optical experiments, in order to extend the ways in which 3D images can be represented in autostereoscopic multimedia displays, while still maintaining compatibility with the human eye. By measuring the fixation point of the viewer, using gaze direction measurements, the depth of focus of the stereo pair is changed by digital filtering so that it matches the natural depth of focus behaviour of the human eye (synthetic depth of focus).

The development of operating concepts that are adequate for the users of future multimedia TV is being carried out as part of the BMBF joint project MINT (Multimedia on Integrated Networks and Terminals). The aim is the development of prototype TV receivers that integrate many multimedia applications. A central challenge, apart from the service integration, is their operation and guidance for the user; these must be simple and user friendly because of the complexity of the services.

• A prototype of a multimedia TV set was implemented. This gives the user typical Internet services (e.g. email, www, home shopping) and new communication services (e.g. video telephony, digital audio broadcasts – DAB, MPEG-4 virtual conferencing) as well as conventional television.
• A user desktop, which was developed by rapid prototyping after user tests, gives the user simple and easily understandable control of all the services integrated into the TV receiver.

A further major research area was the investigation of communication systems with a high degree of telepresence. Concepts were developed and demonstrated in the laboratory, and also empirically checked by means of user tests. 3D imaging techniques were shown to be useful for increasing telepresence and effectiveness in communication experiments with studio video conferences at the HHI. Similar advantages are expected for workplace conferences, and generally for workplace systems.

Since this style of communication will increase in importance, the use of 3D technology in workplace systems was also investigated. In this case the main considerations were the undistorted reproduction of movement parallax, the perceptually conflict-free mixing of 2D and 3D images, and user friendly remote pointing in stereoscopic images.
• Following investigations, guidelines for applications that include modelling of movement parallax were developed to include a mechanism for the viewer to adjust the relation between changes of the perspective centre of the image and changes of head position.
• Based on user investigations, rules for mixing 3D images were developed to avoid disturbing artifacts in the picture plane.
• An autostereoscopic workplace display using field lenses was developed that separates the stereo images using directed light. It features bright stereo images with good contrast that are easily viewed, even with the lighting conditions in office workplaces.

Informal communication is an important aspect of human communication. This includes spontaneous and mostly confidential conversations, e.g. on the fringes of conferences, in coffee breaks or at other chance meetings. Since this form of communication has a positive significance for the individual worker as well as for the organization, means of providing technical support for informal communication among distributed work groups (for either telework or telecooperation) are being sought. A questionnaire to potential users of telecooperation systems showed that informal communication in many areas connected with work is viewed as absolutely essential.
• In order to find the essential features needed for telecooperation systems to support informal communication, various field studies were carried out using a chat system, a chat system extended by still images, and a virtual environment. The results showed that informal communication is possible with text-based communication systems, but that they should be augmented by indicators of the degree of communication readiness of potential communication partners.
• For telework applications, the telepresence of a work group was simulated using a virtual office environment generated by computer graphics. Each participant of the telework group, including his or her position and actions in space, was given a computer graphic representation (avatar). This concept appeared to be promising, especially for informal communication among teleworkers. It delivered a high degree of telepresence with a sufficient degree of privacy protection.

Competencies

Development of algorithms and hardware architectures for image and sound compression (MPEG2, MPEG4).

Development of algorithms and hardware architectures for 2D and 3D image analysis and synthesis using motion and stereo information.

Image segmentation and feature extraction.

Development of applications based on MPEG2/4/7 and JAVA for interactive services over the Internet, over DVB/DAB/DMD, over ISDN, over DSL, and over mobile networks (DECT, GPRS, HSCSD, UMTS).

Coding methods for videophones and video conferencing (H.26x, MPEG-4).

MPEG and ITU-based signalling and transport protocols (H.32x, MPEG-TS, DMIF).

Development and design of integrated circuits for image processing.

Design, integration and implementation of prototypes and experimental systems for video-based applications in communication and for tests and demonstrations of new communication technologies and hardware architectures.

Development of 3D display technologies.

Conception and evaluation of user interfaces for multimedia applications using VRML, JAVA, MSDL and dVS.

Analysis and optimization of communication terminals and services on the basis of human factors and usability criteria.

Development of video-based pattern recognition and photogrammetry methods.

Modelling and development of integrated circuits for image processing.

Design and construction of experimental systems for the development of video-based communications applications and for testing and demonstrating new communication technologies and hardware architectures.

Analysis of human sensory and sensorimotor functions in relation to communication applications.

Expertise in desktop computer graphics design.

Research in the area of high voltage electroluminescence (SrS:Ce, ZnS:Mn).

Development of multilayer electroluminescent structures, blue-emitting phosphors, full colour flat displays and transparent displays.

Development of diffractive optical components for read/write heads for optical disks.

F&E-SCHWERPUNKTE

Photonik-Netze

Themen und Ergebnisse

In der Telekommunikation ist weltweit eine explosionsartige Zunahme des Bedarfs an Übertragungskapazität zu verzeichnen. In den USA, wo die Zuwachsraten am stärksten sind, liegen die jährlichen Zuwachsraten bei 60%. Besonders getrieben wird diese Entwicklung durch das Internet, das sich in den nächsten Jahren zu einem Breitband-Internet mit einem noch höheren Kapazitätsbedarf entwickeln wird. Es wird prognostiziert, daß im Jahr 2010 das gesamte Verkehrsaufkommen um das Zehnfache über dem heutigen liegen und der nahezu konstant bleibende Telefonverkehr eine untergeordnete Rolle spielen wird.

Basis dieser Entwicklung ist neben der Mikroelektronik die optische Nachrichtentechnik bzw. das photonische Netz. Durch die enorme Übertragungskapazität der Glasfaser ist die Voraussetzung für den Aufbau hochkapazitiver Kommunikationsnetze gegeben. Im photonischen Netz werden die Nachrichten nicht nur optisch übertragen, sondern auch optisch vermittelt. Die außerordentlich hohe Bandbreite der Lichtwellenleiter wird durch optische Frequenzmultiplextechniken und durch optische Zeitmultiplextechniken genutzt. Das Photonik-Netz ist ein diensteunabhängiges Netz, das sehr breitbandige Transportwege zur Verfügung stellt, über die alle heutigen und alle zukünftigen Dienste abgewickelt werden können.

Die dargestellte Entwicklung hat auch zunehmende Auswirkungen auf die Customer Networks, d.h. auf die Kommunikationsnetze beim Teilnehmer, sowohl beim geschäftlichen als auch beim privaten Teilnehmer. Die Informationsmengen müssen bis zum Endgerät transportiert werden. Das Customer Network stellt das Bindeglied zwischen dem Breitband-Internet und dem multimedialem Endgerät dar. Es werden bis zum Jahr 2010 Übertragungsraten von 100 Mbit/s zum privaten und von 1 Gbit/s zum professionellen Endgerät prognostiziert.

Ziel des HHI ist es, mit seinen Forschungsarbeiten maßgeblich zur Weiterentwicklung des Photonik-Netzes beizutragen. Hierbei sind alle drei Ebenen des Telekommunikationsnetzes – Core Network, Access- und Customer Network – zu betrachten. Folgende Themen werden schwerpunktmäßig behandelt:

- Entwicklung von Netzkonzepten für die verschiedenen Ebenen des Photonik-Netzes.
- Ausloten des Potentials der optischen Frequenzmultiplextechnik und der optischen Zeitmultiplextechnik zur besseren Nutzung der Lichtwellenleiterkapazität sowie zur Gestaltung flexibler Netze. Von besonderer Bedeutung ist hierbei die optimale Kombination beider Multiplexverfahren.
- Ausloten der Grenzen der optischen Transparenz, d.h. die Ermittlung der Transparenzfeldlänge von photonischen Netzen.
- Ermittlung der Anforderung an die Netzkonzepte, die Netzkomponenten, d.h. an die Übertragungsstrecken und Vermittlungseinrichtungen sowie an die photonischen Komponenten.
- Untersuchungen zum Betrieb, zur Überwachung (OAM, Operation, Administration and Maintenance) sowie zur Steuerung (TMN, Telecommunication Management Network) von photonischen Netzen.
- Entwicklung von Verfahren und Bauelementen zur rein optischen 3R-Signalregeneration.
- Entwicklung und Herstellung photonischer Komponenten.

Photonik II und KomNet: Ein Großteil der unten beschriebenen Aktivitäten wurde im Rahmen des nun abgeschlossenen nationalen Forschungsprogramms Photonik II, gefördert vom Bundesministerium für Bildung, Wissenschaft, Forschung und Techologie, durchgeführt. Während der Laufzeit von 1994-1998 zählten optische Kommunikationsysteme, die optische Verbindungstechnik sowie Schlüsselkomponenten und -technologien zu den wesentlichen thematischen Schwerpunkten. Die Themen wurden von der nachrichtentechnischen Industrie zusammen mit Forschungseinrichtungen und Universitäten bearbeitet. Die wissenschaftliche Federführung des Forschungsprogramms teilten sich das Fraunhofer Institut für Angewandte Festkörperphysik (FhG-IAF), Freiburg, und das HHI.

In Rahmen des neuen BMBF-Förderprogramms KomNet sollen die im Photonik II Programm gewonnenen Ergebnisse in pro-

duktorientierte Entwicklungen umgesetzt und zum Aufbau eines Breitband-Internet-Pilotsystems genutzt werden, das von der Industrie und der Deutschen Telekom als Netzbetreiber in Berlin mit einer Weitverkehrsverbindung nach Stuttgart errichtet werden soll. Das HHI ist in Form von F&E-Unteraufträgen der Industrie und der Deutschen Telekom sowohl mit systemtechnischen als auch technologischen Forschungs- und Entwicklungsarbeiten an dem KomNet-Programm beteiligt. Die Koordination des Aufbaus des KomNet-Pilotsystems liegt in der Hand des HHI.

Der Forschungsschwerpunkt Photonik-Netze gliedert sich in die Fachgebiete Access und Customer Network sowie Core Network.

Access und Customer Network

Die Forschungs- und Entwicklungsarbeiten konzentrierten sich auf den Einsatz der WDM-Technik im Access Network. Ziel war es, Systemkonzepte und Komponenten für WDM-Anwendungen im Access-Network zu entwickeln und zu untersuchen.

WDM-Upgrade eines PON: Es wurden Forschungs- und Entwicklungsarbeiten zum WDM-Upgrade eines bestehenden passiven optischen Netzes (PON) durchgeführt, deren Anwendung sowohl in zukünftigen breitbandigen Teilnehmerzugangsnetzen als auch im professionellen LAN/MAN-Bereich liegt. Hierbei wurde auf einem Systemkonzept aufgebaut, das eine Kapazitätserweiterung ohne Änderung der Glasfasernetzstruktur zwischen der Zentrale und den teilnehmernahen Optical Network Units (ONU) erlaubt. Das passive optische Zugangsnetz wird mit einem WDM-Overlay von permanenten Wellen längenpfaden im Bereich 1,5 µm versehen. Zentrales Bauelement ist ein Arrayed Waveguide Grating (AWG), das zum Multiplexen, Demultiplexen und zum Routen der Signale unterschiedlicher Wellenlänge eingesetzt wird. Zur Untersuchung der Eigenschaften von Netzelementen und Komponenten, sowie deren Überwachbarkeit durch ein TMN wurden Demonstratoren mit Kanalabständen von 9 GHz bis 400 GHz realisiert. Arrayed Waveguide Gratings mit Kanalabständen zwischen 100 GHz und 400 GHz gemäß dem dem von der International Telecommunication Union (ITU) vorgeschlagenen 100-GHz-Kanalraster wurden untersucht, die von den Photonik II Kooperationspartnern und dem HHI bereitgestellt wurden.

Transponder: Bei dem Upgrade von optischen Übertragungssystemen mit Hilfe der WDM-Technik ist es notwendig, diese mit Hilfe von Transpondern an eine bereits existierende Systemumgebung zu adaptieren. Ein Transponder besteht aus einem optischen Empfänger und einem optischen Sender, der auf einer vorgegebenen Wellenlänge sendet. Je nach Eingangsempfindlichkeit und optischer Ausgangsleistung kann mit einem solchen elektro-optischen Wellenlängenkonverter neben der Wellenlängenumsetzung auch eine Signalverstärkung erreicht werden. In Kooperation mit der Industrie erfolgte die Entwicklung eines modularen Transponders, der ohne zeitliche Regeneration bitratentransparent von 100 Mbit/s bis 2,5 Gbit/s arbeitet. Für den Betrieb bei festen Bitraten (z.B. SDH, STM-16) kann eine elektronische Signal- und Taktrückgewinnung eingefügt werden. Für die Einbindung in ein TMN-System ist der Transponder mit entsprechenden Steuer- und Überwachungsfunktionen versehen.

Filterkomponenten: Das HHI entwickelt und fertigt WDM-Filter mit unterschiedlichen Spezifikationen und Technologien. Hauptsächlich werden diese Komponenten in Silica-Technik (SiO_2/Si) hergestellt. Standardkomponenten sind sog. "Arrayed Waveguide Grating"-Filter (AWG), die für 8 und 16 Wellenlängenkanäle mit 100 GHz und 200 GHz Kanalabstand hergestellt wurden. Es wurden sowohl Filter mit einer Gauß-förmigen Transmissions-Charakteristik als auch Filter mit einem Rechteckverlauf entwickelt. Letztere eignen sich besser für eine Kaskadierung. Diese Filter benutzen angepaßte adiabatische Horn-Strukturen an ihren Ein- und Ausgängen zur Modenaufweitung. Weiterhin wurde die Polarisationsabhängigkeit weitgehend reduziert. Diese Entwicklungen, die das Abscheiden streßfreier und damit polarisationsunabhängiger Silica-Schichten zum Ziel hatten, wurden zusammen mit einem deutschen Industriepartner und weiteren Instituten durchgeführt.

Für Systemanwendungen in einem PON/WDM-Netz wurde eine spezielle Komponente entwickelt und zum Patent

angemeldet. Diese erlaubt als Erweiterung eines bestehenden PON-Netzes die Überlagerung mit einem WDM-Netz. Schlüsselelement hierin ist ein speziell entworfenes 2-Band-MUX-AWG mit integriertem Leistungsteiler im Eingang für die Broadcast-Wellenlänge. Die Zusatzverluste einer 8-Kanal-MUX-Komponente betragen 3,5 dB für das WDM-Band bei einer Wellenlänge von 1,55 µm und ca. 4 dB einschließlich des Leistungsteilers für die Broadcastwellenlänge bei 1,50 µm. Das Nebensprechen ist <-25 dB.

In Zusammenarbeit mit einem Industriepartner werden AWG's auch auf der Basis von Polymermaterialien entwickelt, was auch die Charakterisierung und Anwendung neuer, temperaturstabiler Polymermaterialien einschließt. Letztere werden am Fraunhofer-Institut IZM entwickelt. Für Spezialanwendungen wurden AWG darüber hinaus auch für das Materialsystem InP realisiert.

Eine weitere zentrale Komponente in WDM-Netzen sind 'Drop'-Filter, die einzelne Wellenlängenkanäle aus dem Kanalensemble herausfiltern können. Eine solche Komponente in Form eines aktiven, monolithisch integrierten optoelektronischen Bauelements auf InP-Basis wird im Rahmen eines ACTS-Vorhabens entwickelt. Sie besteht aus einem abstimmbaren, polarisationsunabhängigen optischen Filter, einem optoelektronischen Detektor und einem elektronischen Vorverstärker. Für eine polarisationsunabhängige Durchlaßcharakteristik wurde eine Filterbreite von 400 GHz (3,2nm) bei einem Nebensprechen von 20 dB und ein Durchstimmbereich von 25 nm erreicht. Erste Integrationen von Filter und Photodiode wurden erfolgreich durchgeführt.

Laser für WDM: Die Optimierung von MQW-DFB-Lasern mit RW-Struktur wurde weitergeführt mit den vorrangigen Zielen hoher Ausgangsleistung und der Integrierbarkeit zu Multi-Laser-Arrays. Einzellaser mit vorgegebener Wellenlänge, 40 mW Ausgangsleistung (bei 200 mA Treiberstrom) und gutem Alterungsverhalten können reproduzierbar hergestellt werden. Auf der Basis dieser Einzellaser wurden integrierte 4-Wellenlängen-Sendechips prozessiert, die außer den Lasern ein Combiner-Wellenleiter-Netzwerk, Monitordioden und einen integrierten Temperatursensor auf dem Chip enthalten, so daß die emittierte Strahlung aller vier Laser den Chip über einen einzigen Wellenleiter verläßt. Damit wird der Modulaufbau dieser Sendebausteine besonders kostengünstig. Auf der Basis dieser technologischen Entwicklung wurden gemeinsame F&E-Vorhaben mit KMUs zur Entwicklung von Laser-Arrays mit ganz speziellen Zusatzeigenschaften begonnen.

Monolithisch integrierter Transceiver: Für den Einsatz im Access-Bereich werden bidirektionale optoelektronische Wandler (Transceiver) entwickelt. Die entscheidende Bedeutung der Verfügbarkeit von WDM-Transceiver-PICs für optische Teilnehmeranschlußnetze wurde sowohl von der internationalen Arbeitsgruppe "Full Services Access Network" (FSAN) als auch im japanischen OITDA-Report unterstrichen. Eine größtmögliche Kostensenkung bei der Massenproduktion optischer Module wird mit der Einbringung von Photonischen ICs (PICs) erwartet. Davon abgeleitet sind die Hauptziele dieses Projektes:

- die Weiterentwicklung und Verfügbarkeit einer flexiblen technologischen "Toolbox" für eine wirtschaftliche Integration von optischen und optoelektronischen Grundzellen (z.B. Laser, Wellenleiternetzwerk, Photodetektor) ohne wesentliche Qualitätseinbußen gegenüber der Herstellung der entsprechenden diskreten Bauelemente,
- die Anwendung dieser Technologie zur Realiserung komplexer PICs,
- die Demonstration der Funktionalität einer monolithisch integrierten Lösung eines polarisationsunempfindlichen Heterodynempfängers,
- die Erweiterung der Integrationstechnologie für die Herstellung von WDM-Transceiver-PICs,
- die Prozessierung erster 1,5 µm/1,3 µm Transceiver-PICs, die den Systemanforderungen genügen.

Der entscheidende Durchbruch in Richtung einer ökonomischen Herstellung von WDM-Transceiver-PICs konnte mit der erstmaligen Entwicklung von kompakten Wellenlängen-selektiven Photodetektorzellen erbracht werden. Erste 1,5 µm/1,3 µm Transceiver-PICs wurden hergestellt und für den Einsatz in einem System-Demonstrator des ACTS-Projektes "Broadband Lightwave Circuits and Systems" (BLISS/AC065) zu Modulen aufgebaut. Die Eigenschaften dieser ersten Transceiver-PIC-Muster stellen die Tragfähigkeit des entwickelten Konzepts unter Beweis und lassen die Herstellung von Komponenten mit FSAN-

Spezifikationen realistisch erscheinen. Die Ergebnisse bilden die Basis für Weiterentwicklungen im Rahmen von KomNet.

Power Line Communication Systeme (PLC) könnten zur Lösung des Problems der sogenannten letzten Meile beitragen. Die Nutzung des 230 Volt-Niederspannungsnetzes zur Informationsübertragung wird als mögliche kostengünstige Alternative zur Neuinstallation von Kommunikationssystemen im Access- und Customer-Bereich angesehen. Im Auftrag einiger Energieversorgungsunternehmen wurde in Zusammenarbeit mit zwei Ingenieurbüros ein PLC-Übertragungssystem entwickelt. Mit einem Demonstratorsystem konnte zum Beispiel eine Videokonferenz über 64-kbit/s-Duplexkanäle im Frequenzbereich oberhalb des CENELEC-Bandes (148,5 kHz) mit Hilfe eines Bandspreizverfahrens demonstriert werden. Die Reichweite im realen Niederspannungsnetz beträgt etwa 100 m ohne Regenerator.

Core Network

Die Arbeiten in diesem Fachgebiet sind auf die Themen höchstbitratige Übertragung im Zeit- (TDM) und Wellenlängenmultiplex (WDM), optischer Crossconnect, optisch transparentes Netz und 3R-Regeneration ausgerichtet. Für die höchstbitratige Übertragung (TDM) kann das Multiplexen und Demultiplexen sowohl elektrisch (ETDM) als auch optisch (OTDM) erfolgen. Wichtige Aufgaben sind dabei die Generierung, Modulation, Detektion und Synchronisation der optischen Signale. Weitere Untersuchungspunkte sind der Einfluß von photonischen Netzkomponenten und Faser-Nichtlinearitäten auf die Qualität der optischen Signale sowie die Techniken der Dispersionskompensation.

Die Arbeiten zur optischen Zeitmultiplextechnik (OTDM) beinhalteten die Untersuchung und Realisierung optischer Subsysteme, die in der Lage sind, optische Signale von 10 Gbit/s zu einem 40- bis 80-Gbit/s-Signal zusammenzufassen (MUX) und anschließend wieder rein optisch zu demultiplexen (DEMUX). Zur Übertragung wurden hier – mit modengekoppelten Lasern generierte – RZ-Signale verwendet. Es wurde in Systemexperimenten gezeigt, daß als Übertragungsmedium die Standardfasern mit Dispersionskompensation auch für 40 Gbit/s geeignet ist.

Experimentelle Untersuchungen zur Kombination von WDM- und TDM-Techniken in einem Übertragungssystem mit der Gesamtkapazität von 640 Gbit/s zeigten folgendes Ergebnis. Es wurden acht WDM-Kanäle, jeder bestehend aus einem 80-Gbit/s-OTDM-Signal, generiert und mittels eines neuen, hoch linearen Demultiplexers wieder in jeweils acht einzelne 10 Gbit Kanäle zerlegt. Dieser "Gain-Transparent-Semiconductor Optical Amplifier"- Schalter ist z.Z. der Schalter mit den besten Eigenschaften für die Anwendungen als Optischer Demultiplexer und speziell auch als Add/Drop-Multiplexer geeignet. Dieser Schalter wurde bisher in einer hybriden Realisierung betrieben. Eine monolithische Integration ist beabsichtigt.

Mit der Methode der optischen Phasenkonjugation (Mid-Span Spectral Inversion) wurden 40 Gbit/s-Übertragungsexperimente über 217 km und über 433 km Standardfaser durchgeführt. Das Ziel dieses Experimentes war die Demonstration eines polarisationsunabhängigen Phasenkonjugators (OPC-optical phase conjugator) nach dem Prinzip der Polarisationsdiversität. In einen Polarisationsteiler am Eingang des OPC (Mach-Zehnder Interferometer) werden das Datensignal mit einem beliebigen Polarisationszustand und eine kontinuierliche optische Welle (CW-Pump) mit einem festen Polarisationszustand zu gleichen Teilen eingekoppelt. In jedem Zweig des OPC befinden sich ein SOA, in dem mittels Vierwellenmischung (FWM-four wave mixing) eine FWM-Komponente (phasenkonjugiertes Datensignal) generiert wird. Mit Hilfe eines zweiten Polarisationsteilers am Ausgang des OPC werden die beiden orthogonalen FWM-Komponenten zu einer resultierenden FWM-Komponente zusammengesetzt, die dann nach Filterung das zum Eingangsdatensignal phasenkonjugierte Datensignal bildet. Die Polarisationsunabhängigkeit des OPC und eine fehlerfreie Übertragung (Penalty 3 dB) konnten nachgewiesen werden.

Monolithisch integrierte OTDM-"Add-Drop"-Multiplexer: Für rein optische Demultiplex- und "Add-Drop"-Funktionen in OTDM-Systemen wurden die weltweit kleinsten monolithisch integrierten Mach-Zehnder Interferometer hergestellt. Als optisch nichtlineare Elemente werden

optische Halbleiterverstärker in den Armen der Interferometer verwendet. Die Interferometer wurden in zwei Varianten designed. Bei der asymmetrischen Version wird durch den örtlichen Versatz zwischen den Verstärkern in den beiden Armen des Interferometers die zeitliche Größe des Schaltfensters festgelegt. Der Vorteil dieser Struktur liegt in den kleinen Dimensionen von (4x0,75) mm^2 und einer einfachen Ansteuerung (Daten und Kontrolleingang nutzen jeweils ein Eingangs- und Ausgangsport gemeinsam). Bei der zweiten Version werden zwei zusätzliche Abzweige zur optischen Signalkontrolle eingesetzt. Dadurch ist das Bauelement auch als rein optischer Wellenlängenumsetzer einsetzbar, hat aber bei höheren Anforderungen an die optische Steuerung (je zwei Dateneingänge und Ausgänge, zwei Kontrolleingänge) einen etwas größeren Flächenbedarf von (5 x 1) mm^2.

Transparenzlänge und optische Crossconnects: Im Auftrag eines Netzbetreibers wurden die Eigenschaften von regeneratorfreien optischen Kommunikationsnetzen sowohl theoretisch als auch experimentell untersucht. Die wesentlichen Elemente in der Transportebene solcher Netze sind die Übertragungsstrecken, Faserverstärker und optischen Crossconnects. Nichtideale Eigenschaften dieser Komponenten führen, bedingt durch Signaldegradation, zu einer Begrenzung der Übertragungslänge im optischen Netz. Entsprechende Transparenzlängendiagramme können als Grundlage für die Planung der Transportebene optisch transparenter Netze dienen. Die experimentelle Überprüfung erfolgt in einem achtkanaligen WDM-Doppelringtestbed, in dem Datenpakete mit einer Übertragungsrate von bis zu 10 Gbit/s pro Wellenlängenkanal in einem Faserring umlaufen. Mit dem Ringtestbed kann die Kaskadierung mehrerer Übertragungsabschnitte in der Zusammenschaltung mit optisch transparenten Crossconnects nachgebildet und die Signalqualität als Funktion der Anzahl der durchlaufenen Crossconnects und der Faserstreckenlänge bestimmt werden. Die Messungen zeigen, daß bei 10 Kaskadierungen ein Nebensprechen von <-40 dB zu fordern ist. Zum anderen wurde ein elektrooptischer Transponder auf seine Eigenschaften als 2R-Regenerator unter Kaskadierungsaspekten untersucht. Dabei zeigte sich, daß hauptsächlich die Akkumulation des zeitlichen Jitters die Zahl der Kaskadierungen begrenzt.

Die Anwendung der WDM-Technik im Core Network mit optischen Crossconnects bei Datenraten bis zu 10 Gbit/s pro WDM-Kanal wurde in dem von der Firma Siemens geführten ACTS-Vorhaben PHOTON untersucht. Das HHI hat eine Wellenlängenreferenz für den Demonstrator hergestellt und das Vorhaben durch Systemstudien unterstützt.

Signalregeneration: Die Signaldegradation in optischen Netzen begrenzt die Länge der optischen Pfade. Durch vollständige Regeneration der digitalen Signale (3R: reamplification, reshaping, retiming) kann diese Begrenzung überwunden werden. Für diese speziellen Funktionen der optischen Signalverarbeitung werden Verfahren und Komponenten entwickelt, die es erlauben, digitale optische Signale teilweise (2R, reamplification, reshaping) oder völlig (3R) zu regenerieren. Schlüsselkomponenten der 3R-Regeneration sind die Taktrückgewinnung und Entscheiderstufen. 3-Sektions-RWG-Laser zeigen bei geeignetem Design eine bistabile Charakteristik. Es wurde ein Modul zur Taktrückgewinnung aufgebaut, das im Bereich von unter 5 bis über 20 Gbit/s arbeitet. Die Taktrate ist über einen Strom kontinuierlich einstellbar. In mehreren Systemexperimenten (HHI, Technische Universität Dänemark, Alcatel Marcoussis) wurde ihr Einsatz erfolgreich demonstriert. Darüber hinaus wird untersucht, inwieweit speziell entwickelte 3-Sektions-RWG-Laser auch als Entscheider verwendet werden können. Die technologischen Gemeinsamkeiten dieser Verstärker, Taktextraktions- und Entscheiderstufen ermöglichen in der Zukunft die monolithische Integration eines optischen 3R-Regenerators.

Modellierung von Netzen: Begleitend zu diesen Arbeiten werden Methoden zur Simulation der Signalausbreitung und zur Modellierung der Komponenten im optischen Pfad entwickelt und mit den experimentellen Messungen überprüft. Dafür kommt neben eigenen Programmentwicklungen auch das Programmpaket BroadNeD zum Einsatz, das kommerziell erhältlich ist (Virtual Photonics Incorporated – VPI). Die Arbeiten zur höchstbitratigen TDM-Übertragungstechnik und zur Kombination von TDM mit der WDM-Technik werden ebenfalls unterstützt durch ana-

lytische und numerische Untersuchungen. Schwerpunkt ist dabei die Fragestellung, wie die Übertragungsstrecke aufgebaut werden muß, um eine maximale Übertragungskapazität zu erreichen.

Netzmodelle für ein WDM Core Netz der Größe Deutschlands wurden entworfen und bezüglich der technologischen Grenzen, der Netzkapazität und des Hardware-Aufwandes analysiert. Mehrfach-Ring-Topologien mit verschiedenen Ersatzschaltungsstrategien bieten eine günstige Basis für eine Netzevolution, die über starre und schaltbare Add-Drop Knoten zu einem flexiblen Crossconnect Netz führen kann.

40Gbit/s Sender und Empfänger: Für hochratige Systeme bei 40 Gbit/s wurden Transmitter mit integriertem Laser/Modulator (geringer Chirp) und Empfänger mit integrierten Wellenleiterdioden und High-Electron-Mobility-Transistoren (HEMT) für die optimale Impedanzanpassung entwickelt. Diese Komponenten werden gemäß den Vorgaben der industriellen Partner designed und für NRZ-Signale ausgelegt. Ein Laser/Modulator-Modul, das im Bereich einiger nm abstimmbar ist und eine 3-dB-Grenzfrequenz von 18 GHz aufweist, wurde bereits früher aufgebaut.

Der Modulator wurde als elektrisch-optischer DEMUX weiterentwickelt und erreicht eine 3 dB-Grenzfrequenz von über 50 GHz. Verwendet werden zum polarisationsunabhängigen Schalten elektro-optische (verspannte MQW-Strukturen) Mach-Zehnder Interferometer. Es werden kapazitätsbelastete Lauffeldleitungen eingesetzt, die für das Demultiplexen bis 80 Gbit/s geeignet sind. Der schnelle Schalter wurde im Rahmen des ACTS-Projektes HIGHWAY in einem Systemexperiment in Zusammenarbeit mit der Technischen Universität Dänemark zum Demultiplexen von 40 Gbit/s Signalen auf 20 Gbit/s erfolgreich eingesetzt.

Für den Empfang von Datenströmen hoher Bitrate in TDM-Übertragungssystemen wurden optoelektronische integrierte Schaltungen (OEICs) auf der Basis von InP entwickelt. Sie vereinigen in sich schnelle wellenleiter-integrierte PIN-Photodioden und MMIC-artige elektrische Verstärker, die aus High-Electron-Mobility Transistoren aufgebaut sind. Es wurden Bandbreiten bis 37 GHz erreicht. Die Empfänger-OEICs, verpackt als Module, wurden in Systemexperimenten bei Industriepartnern erfolgreich zur Detektion von 40 Gbit/s Signalen, moduliert sowohl im RZ- als auch im NRZ-Format, angewendet. Im Verbundprojekt KomNet werden die optischen Empfänger nunmehr im Hinblick auf die spezifischen Systemanforderungen der verschiedenen Industriepartner optimiert. Sie sollen in Feldversuchen bei 40 Gbit/s eingesetzt werden.

Im Hinblick auf Empfängerkonzepte mit optischer Vorverstärkung werden Photodetektoren für den Einsatz bei hohen optischen Leistungen entwickelt. Sie sollen in der Lage sein, digitale elektrische Demultiplexer direkt anzusteuern. Dazu wurden bereits wellenleiter-integrierte Photodioden realisiert, die 40 Gbit/s RZ-Signale mit einer durchschnittlichen Leistung von +16 dBm detektieren können und dabei 0,7 V Spitzenspannung an 50 Ω erzeugen. Ihre Bandbreite (-3 dB elektrisch) beträgt ca. 70 GHz bei einem Konversionsgrad von 0.35 A/W.

Kompetenzen

Untersuchung und Entwicklung der Architekturen photonischer Netzwerke, Erstellung von Planungsrichtlinien und Studien zu spezifischen Problemen photonischer Netzwerke

Charakterisierung und Test von optischen Netzwerken und Netzwerkelementen einschließlich Experimenten an ringförmigen Fasertrassen, Übertragungsexperimente über große Längen und Feldversuche

Entwicklung von hochratigen optischen WDM-Systemen (10 Gbit/s pro Kanal) und entsprechenden WDM-Meßtechniken

Untersuchung, Entwurf und Entwicklung von optischen WDM-LANs/MANs, optischen Netzen im Teilnehmerbereich und passiven optischen Netzwerken

Entwicklung von Verfahren zur Steuerung und Überwachung von Netzwerken

Entwicklung, Anwendung und Verifikation von Simulations-Software für optische Transportnetzwerke

Entwurf und Entwicklung von auf Heterodyn-Techniken beruhenden optischen Systemen

Entwicklung von Verfahren der Wellenlängenkonversion für WDM-Systeme

Untersuchung und Entwicklung von hochratigen OTDM-Subsystemen (10 bis 40 Gbit/s und höher) einschließlich Multiplex/Demultiplex- und "Add/Drop"-Techniken

Entwicklung von Verfahren zur rein optischen Taktrückgewinnung und Signalregeneration (2R und 3R)

Entwicklung von Methoden zur Erzeugung ultrakurzer optischer Pulse

Optimierung von Verfahren zum Dispersionsmanagement

Entwurf und Entwicklung von optischen Frequenzreferenz-Geräten

Entwurf und Herstellung von Transpondern und optischen SDH-Frontends

Entwicklung, Herstellung und Charakterisierung von faseroptischen Komponenten

Entwicklung, Herstellung und Charakterisierung von Verfahren und Geräten zur PMD-Kompensation

Entwurf, Herstellung und Charakterisierung von optoelektronischen Bauelementen und photonisch integrierten Schaltungen auf der Basis von InP:
- abstimmbare Laser (DFB, DBR)
- Multi-Wellenlängen-Emitter (Laser-Arrays)
- optische Verstärker
- schnelle Laser/Modulator-Transmitter
- Wellenlängen-Konverter
- Wellenlängen-"Drop"-Filter
- Demultiplexer und "Add/Drop" Multiplexer für OTDM-Anwendungen
- Bauelemente zur optischen Taktrückgewinnung und Signalregeneration (selbstpulsierende Laser)
- integrierte Transceiver
- ultra-schnelle Photodetektoren (70 Ghz)
- hochbitratige optische Empfänger mit integriertem MMIC-Vorverstärker
- optische Mikrowellengeneratoren

Entwicklung und Herstellung von thermooptischen Schaltern und Schaltmatrizen mit geringem Nebensprechen auf der Basis von Polymeren

Entwurf und Herstellung von planaren Wellenleiterkomponenten in SiO_2/Si (z.B. Wellenleitergitter-Filter)

Entwurf und Herstellung von passiven und von elektrisch steuerbaren diffraktiven optischen Elementen in SiO_2

Modellierung von photonischen Bauelementen und photonischen Schaltkreisen sowie integrierten Schaltungen

Entwicklung, Optimierung und Anwendung von Bauelement-Technologien:
- Reinraumlabore (Klasse 10/1000)
- Epitaxie (MOVPE, MBE, MOMBE) und Charakterisierung von InP-basierenden Halbleitermaterialien
- Sekundärionen-Massenspektrometrie (SIMS)
- CAD und Herstellung von Photolithographie-Masken
- Elektronenstrahl-Lithographie und optische Lithographie
- Trockenätzprozesse (reaktive Ionenätzung, Ionenstrahlätzung) mit Endpunkterkennung
- thermische Kurzzeitprozessierung
- Deposition von Metall- und Dielektrika-Schichten (Aufdampfung, Sputtern Plasma-Deposition)
- optische Beschichtungen
- Charakterisierung und Technologie von optischen Polymermaterialien
- hochauflösende Rasterelektronenmikroskopie

Entwicklung und Anwendung von elektrischen und optischen Aufbau- und Verbindungstechniken für Bauelemente (Chip- und Draht-Bonden, Hochfrequenz-Gehäusung, Laserschweißen, Faser-Chip-Kopplung)

Mobile Breitbandsysteme

Themen und Ergebnisse

In den letzten Jahren ist die Teilnehmeranzahl von Mobilfunksystemen stark angestiegen. Aufgrund dieses Zuwachses von Teilnehmern und zusätzlichen Diensten, z.B. der Datenübertragung, werden weitere Systemkapazitäten benötigt. Diese können durch eine Verbesserung der Spektrumseffizienz der Systeme erhöht werden. Eine ganze Reihe unterschiedlicher Techniken wurde für die Verbesserung der Spektrumseffizienz vorgeschlagen. Die Systemkapazität von Mobilfunksystemen wird durch eine ganze Reihe von Parametern beeinflußt. Dies sind unter anderem die Zellstrukturierung, der Frequenzwiederholungs-Abstand und die Anzahl der möglichen Mobilstationen, die gleichzeitig durch eine Basisstation bedient werden können. Die Smart Antennas stellen hierbei die wichtigste neue Technik zur Steigerung der Kapazität von Mobilfunksystemen und zur Verbesserung der Systemperformance, wie z.B. der Verringerung der Bitfehlerrate des Uplink-Kanals (Verbindung von der Mobilstation zur Basisstation) von CDMA-basierten Mobilfunksystemen dar.

Mit Hilfe der räumlichen Filterung mit Smart Antennas ist es möglich, die Interferenz im System und das Delay Spread zu verringern. Somit können Parameter des Mobilfunkkanals beeinflußt werden. Dieses Potential der Smart Antennas ist insbesondere für die Übertragung von hohen Datenraten interessant.

In dem zukünftigen Mobilfunksystem der 3. Generation UMTS/IMT 2000 ist der Einsatz von Smart Antennas als zusätzliche Funktionalität vorgesehen. Dagegen werden die Mobilfunksysteme der 4. Generation, wie z.B. das Integrated Broadband Mobile System (IBMS, Teilprojekt des Verbundprojekts ATM*mobil*), vollständig auf den Einsatz von Smart Antennas ausgerichtet sein. In diesem Zusammenhang wurde die Möglichkeit der Verbesserung der Systemperformance von CDMA-basierten Mobilfunksystemen mit Hilfe von Constrained Beamformern untersucht. Hierbei stellt die Beherrschung des Uplink-Kanals eine Hauptschwierigkeit in CDMA Systemen dar. Es wurde in den Forschungsarbeiten gezeigt, daß die Bitfehlerrate von Mobilfunkteilnehmern für den Uplink-Kanal mit Hilfe von Constrained Beamformern wesentlich verbessert werden kann. Zur Erzielung der optimalen Systemperformance wurde ein neuer Beamforming Algorithmus vorgeschlagen. Für diesen neuen Beamforming Algorithmus kann eine bestimmte Anzahl von Nullstellen, entsprechend der Anzahl der Sensoren, vorgegeben werden. Er erlaubt eine Kontrolle sowohl der Lage der Nullstellen des Beampatterns als auch der Lage des Hauptbeams. Das durch diesen Beamformer erzeugte optimale Beampattern ermöglicht die Ausnutzung des räumlichen Vielfachzugriffs (Space Division Multiple Access-SDMA) und der räumlichen Filterung zur Interferenzreduktion (spatial filtering for interference reduction – SFIR).

Weiterhin wurde der Einsatz von Smart Antennas für Indoor-Anwendungen untersucht. Im Indoor-Bereich sind die Ausbreitungsbedingungen aufgrund der großen Anzahl von Echos aus unterschiedlichsten Richtungen meist komplizierter als im Outdoor-Bereich. Aufgrund der großen Anzahl der Echos und des Angular-Spread ist es durch die begrenzte Anzahl der Antennen eines Arrays nicht möglich, Nullstellen des Beampatterns in Richtung der Störsignale zu erzeugen. Deshalb wurde speziell für Indoor-Anwendungen ein neuer Beamforming Algorithmus entworfen. Dieser neue Algorithmus nutzt den Angular-Spread zur Erzeugung eines optimalen Beampatterns.

Eine weitere Forschungsaktivität stellen die Analyse und der Entwurf von Mobilitätsmodellen von Mobilfunkteilnehmern zur Simulation und Evaluierung vonzukünftigen Mobilfunksystemen dar. Die zukünftigen Mobilfunksysteme der 4. Generation zeichnen sich im Vergleich zu den gegenwärtigen Mobilfunksystemen unter anderem dadurch aus, daß sie höherratige Dienste unterstützen. Dies führt zu einer Erhöhung der Trägerfrequenzen der Systeme und somit zu einer Verkleinerung der Zellgrößen der Funkzellen. Auch bei dem zukünftigen Mobilfunksystemder 3. Generation UMTS/IMT 2000 kann von einer Verkleinerung der Funkzellen, hier verursacht durch den Wunsch einer hohen Teilnehmerkapazität, ausgegangen werden. Aufgrund dieser Verkleinerung der Funkzellen ist die Systemperformance der zukünftigen Mobilunksysteme sehr stark

von dem Mobilitätsverhalten und der Statistik der Dienstenutzung der Mobilfunkteilnehmer abhängig. Zur Erzeugung realistischer Szenarien für die Systemevaluierung wurden neue Mobilitätsmodelle entwickelt. Diese Mobilitätsmodelle stellen Erweiterungen der von ETSI (European Telecommunication Standard Institute) vorgeschlagenen Modelle zur Evaluierung von UMTS dar. Mit Hilfe der neuen Mobilitätsmodelle können realistische Daten über Handover-Raten und über den durch die Mobilität bedingten Signalisierungsaufwand ermittelt werden.

Einen weiteren Forschungsschwerpunkt im Indoor-Bereich stellen die Infrarot- und die Mikrowellenkommunikation dar.

Bezüglich drahtloser Infrarotkommunikation werden derzeit zwei Ansätze untersucht, die auf Konzepten mit direkter Strahlausbreitung und diffuser Strahlausbreitung mit direkter Sichtverbindung basieren. Es ist das Ziel, kostengünstige und leistungseffiziente Transceiver zu realisieren, wobei Datenraten von 155 Mbit/s angestrebt werden. Es werden sowohl Systeme mit Basisstation als auch ad-hoc LANs betrachtet, die ohne Basisstation auskommen und auf der diffusen Reflektion eines Lichtflecks beruhen. Die Systemeigenschaften und die Leistungsbilanz werden beträchtlich durch Anwendungen eines Nachführsystems verbessert. Array-Technologien der Sende- und Empfangselemente können später mechanisch bewegte Teile ersetzen und würden ein einziges Interface für Schmal- und Breitbanddienste ermöglichen.

Für ein ad-hoc IR LAN bei 1,55 µm Wellenlänge wurde in einem Laborversuch die Verteilung des Sendesignals durch diffuse Reflexion an der Decke realisiert (Spot Diffusing mit einem Streuwinkel = 100 Grad). Die Empfängeroptik (Gesichtsfeld < 1 Grad) wurde auf den Reflexionspunkt ausgerichtet. Mit 5 mW Leistung in dem kollimierten Sendestrahl konnte ein Videosignal (140 Mbit/s, CMI codiert) in einer 20 m^2 Zelle fehlerfrei übertragen werden. Für Wellenlängen > 1,4 µm ist diese Sendeleistung augensicher.

Für die kostengünstige Erzeugung und Verteilung von Mikrowellensignalen in zellularen Breitband-Funknetzen wurden im Rahmen des BMBF-Förderschwerpunktes Photonik II Methoden der optischen Mikrowellentechnik untersucht. Das Ziel war, neben der verlustarmen glasfasergebundenen Übertragung zwischen den Kontroll- und Basisstationen auch die für die Funkübertragung erforderliche Mikrowellensignale in aufwandsarmen Basisstationen mit optischen Mitteln zu erzeugen. Hierfür wurde das optische Heterodynprinzip angewandt. Mit Hilfe der "Seitenband Injection Locking"-Technik wurden quarzstabile, phasenrauscharme Mikrowellensingnale im 60 GHz-Band generiert. Für die elektrische Signalverarbeitung der 155 Mbit/s Datensignale im OQPSK-Format wurden Komponenten des kommerziellen Digitalrichtfunksystems unseres Industriepartners Bosch-Hildesheim eingesetzt. Ein wichtiges Ziel des Projekts waren Untersuchungen zum Mehrkanalbetrieb in optischen Mikrowellensystemen. Es wurden Übertragungsversuche mit zwei unterschiedlichen Multiplexverfahren durchgeführt. Die Ergebnisse wurden mit Simulationsrechnungen in Zusammenarbeit mit der FH-Lübeck bestätigt. Eine Schlüsselkomponente für die optische Mikrowellentechnik ist der Optik/Mikrowellen-Konverter in der Basisstation. In Kooperation mit dem Institut für Festkörperphysik der Technischen Universität Berlin werden monolithisch integrierte Komponenten für den 60 GHz Bereich entwickelt.

Bei Phased Array Antennen hat die optische Mikrowellenübertragung wegen der vorteilhaften Eigenschaften wie z.B. hohe Übertragungsgeschwindigkeit, große Bandbreite und problemlose Leitungsführung Eingang gefunden. Für den Einsatz in einer Satellitenantenne sind auch das geringe Gewicht und das geringe Volumen der Glasfaser wichtig. Phased Array Antennen benötigen ein Verteilnetzwerk, das eine möglichst verlustarme und phasenstabile Verbindung zwischen der Zentralelektronik und den Antennenelementen herstellt. Im Rahmen eines Auftrags der Firma Dornier Satellitentechnik GmbH wurden Basisexperimente mit einer schaltbaren optischen Übertragungungsstrecke durchgeführt, mit der die Phasenbelegung der Antennenelemente und damit die Schwenkrichtung der Antennencharakteristik gesteuert wird.

Elektronische Bildtechnik für Multimedia

Themen und Ergebnisse

Die F&E-Beiträge des HHI zu diesem Schwerpunkt sind den Fachgebieten Bildsignalverarbeitung und Endsysteme und Anwendungen zuzuordnen.

Bildsignalverarbeitung

Die Aufgaben im Themenbereich Bildsignalverarbeitung sind auf Signalaufbereitung, -verarbeitung und Codierung für Bilddienste unterschiedlichster Auflösungen und Anwendungen sowie auf die Realisierung von VLSI-Komponenten und die Systemintegration ausgerichtet. Dabei wird ein breites Feld von kleinsten Bildformaten für schmalbandige Videokommunikationsdienste bis hin zu hochauflösenden Multimediadiensten abgedeckt. Typische Anwendungen sind VLBV (Very Low Bitrate Video) für die niedrigratige Multimediakommunikation über das Internet und Mobilfunkkanäle, interaktive Multimediadienste, Verteil- und Kommunikationsdienste sowie Studioapplikationen. Im Hardwarebereich spielen die Entwicklung von Architekturen für zukünftige Multimediaterminals eine zentrale Rolle, wobei die Realisierung von Schlüsselkomponenten für 3D-Grafik, Compositing, MPEG-Codierung und Decodierung sowie Formatkonversion im Vordergrund steht. Ein Schwerpunkt der Arbeiten lag bei der Multimediakommunikation auf Integrierten Netzen und Terminals (MINT), einem vom BMBF geförderten Verbundprojekt. Die Hauptziele dieses Projekts lagen bei der Entwicklung von diensteintegrierenden, stationären und portablen Terminals, bei der Entwicklung von Interfaces zu digitalen Fest- und Mobilnetzen, bei der drahtlosen und drahtgebundenen Inhouse-Kommunikation, sowie bei den Benutzerplattformen für mobile und stationäre Endgeräte. Dabei stand der sich z.Z. entwickelnde Bild- und Tonkompressionsstandard MPEG-4 im Mittelpunkt.

Im Rahmen des MINT-Projekts stand die Entwicklung von Kernkomponenten zum Gesamtdemonstrator des Verbundprojekts im Vordergrund. Es wurden Architekturstudien zur Realisierung von Komponenten zur MPEG-4-Decodierung inklusive Systemdemultiplex, zur Formatkonversion sowie zur Decodierung und Darstellung von 3D-Bildern durchgeführt, und diese Komponenten wurden realisiert. Sie wurden dann als Teil des Gesamtdemonstrators auf dem Symposium "Multimediakommunikation auf Netzen und Terminals", das am 26.11.1998 gemeinsam vom MINT-Projekt und von der Deutschen TV-Plattform organisiert wurde und im ICC in Berlin stattfand, der Öffentlichkeit präsentiert.

- Für einen MPEG-4 Echtzeitdecoder wurde ein DSP-Modul entwickelt, das aus einem Digitalen Signal-Prozessor, einem Co-Prozessor zu Bitstromdecodierung und Speicherbausteinen besteht. Bis zu vier solcher Module können auf einer eigens entwickelten PCI-Trägerkarte untergebracht werden, die in einen PC gesteckt werden kann. Damit wurde der z.Z. wohl weltweit leistungsfähigste MPEG-4 Decoder entwikkelt, der dem Simple und Main Profile des endgültigen MPEG-4 Standards (Version 1) entspricht.
- Auf Basis des o.g. MPEG-4 Decoders wurde eine Client-Server-Applikation entwickelt, die einen Abruf von MPEG-4 Videoobjekten von einem Server gestattet. Mit Hilfe eines MPEG-4 Compositors können diese Videoobjekte dann auf dem Bildschirm manipuliert (verkleinert, vergrössert, verschoben) werden. Dazu wurde das Signalisierungsprotokoll DMIF (Delivery Multimedia Integration Framework), das sich noch in der Standardisierungsphase befindet, implementiert. Diese funktionsfähige Implementierung gilt als weltweit eine der ersten.
- Es wurde ein autostereoskopisches Bildtelephonie-Terminal entwickelt, das aus einem 3D-Display mit Headtracking der Fa. Zeiss, welches auf HHI-Patenten basiert, sowie einer speziell entwickelten Signalverarbeitungseinrichtung zur Kompensation der Bewegungsparallaxe besteht. Diese Einrichtung setzt sich aus einem Echtzeit-Disparitätsschätzer und einem Viewpoint-Interpolator zusammen. Mit diesem System werden in Abhängigkeit vom Blickwinkel des Betrachters Bilder von virtuellen Kamerapositionen berechnet. Hierbei handelt es sich um die weltweit erste Hardware-Implementierung eines solchen Systems.
- Zur Darstellung von Stereo-TV-Bildern auf handelsüblichen 100 Hz Fernsehgeräten

oder dem o.g. autostereoskopischen Display wurde eine Decoder-Box (HiBOX) entwickelt. Diese gestattet die simultane und synchronisierte Decodierung von zwei MPEG-2 codierten Bitströmen, die den linken und rechten Komponenten eines Stereopaares entsprechen. Diese Signale können entweder von einem DVD-Laufwerk, das über ein SCSI-Interface angeschlossen werden kann oder von einer DVB-Übertragungstrecke, die über ein paralleles DVB-Interface angeschlossen werden kann, stammen. Entsprechende Übertragungen über eine digitale terrestrische (DVB-T) Strecke wurden im Rahmen des o.g. Symposiums durchgeführt.

Ausgehend vom aktuellen Stand bei der Videocodierung (MPEG-4, BIFS, SNHC) und bei den Beschreibungssprachen für interaktive Dienste (HTML, VRML,JAVA) werden in enger Kooperation mit Diensteanbietern Konzepte für die Codierung, Übertragung und Präsentation interaktiver Video- und VR-Anwendungen entwickelt. Die zentrale Zielsetzung besteht darin, unter Berücksichtigung der oben genannten Standards sowie produktions-, netz- und dienstespezifischer Randbedingungen neue objekt-, grafik- und videoorientierte Nutzerfunktionen zu definieren und deren Attraktivität im Rahmen einer Machbarkeitsstudie zu demonstrieren. Anhand konkreter Anwendungsbeispiele wie "Home-Shopping", "Business-TV" oder "Virtuelle Kommunikationsplattformen" soll Programm- und Diensteanbietern das Potential der zu entwickelnden Techniken aufgezeigt werden und diesen gleichzeitig Werkzeuge und Konzepte für die Entwicklung zukünftiger interaktiver Dienste zur Verfügung gestellt werden. Ein hierfür wichtiges Arbeitsgebiet ist die Bildsegmentierung, die sowohl für On-line als auch für Off-line Anwendungen weiterentwickelt wird.

- Im Rahmen dieser Arbeiten wurde der Prototyp des weltweit ersten, verteilten virtuellen Videokonferenzsystems entwikkelt und auf dem o.g. MINT-Symposium der Öffentlichkeit präsentiert. Dieses System besteht aus vier Teilnehmern, die verteilt über ISDN oder LANs miteinander eine Bildkonferenz abhalten können. Dabei werden jeweils die drei Gesprächspartner, die MPEG-4 codiert in ihren Konturen als Videoobjekte übertragen werden, in einem synthetischen Konferenzraum gezeigt, durch den man navigieren kann. Ein wichtiger Baustein dieses Systems ist die Echtzeitsegmentierung, die den Teilnehmer von einem beliebigen Hintergrund separieren kann.

Die Entwicklung und Verifizierung von Techniken, die für neuartige audio-visuelle Funktionalitäten in mobilen Multimedia-Systemen benötigt werden, steht im Mittelpunkt der Arbeiten des HHI. Solche Funktionalitäten wurden im Rahmen von ISO-MPEG identifiziert, und der zukünftige MPEG-4-Standard wird die Grundlage zur Bild- und Tonkompression in zukünftigen Multimediasystemen werden. Die neuen audio-visuellen Funktionalitäten, die Inhaltsmanipulationen, eine inhaltsabhängige Skalierbarkeit und einen inhaltsbasierten Datenzugriff beinhalten, werden mit Algorithmen erreicht, die einerseits sehr kompressionseffizient und andererseits sehr robust gegen Übertragungsfehler sind. Deshalb werden neue Verfahren zur Datenkommunikation zwischen Terminals entwickelt, die nicht auf einer speziellen, sondern auf einer generellen generischen Sprache basieren.

- Das HHI hat eine Reihe von Softwareimplementierungen für MPEG-4-Coder und -Decoder durchgeführt. Diese Implementierungen dienen einerseits als Referenzmodelle für Hardware Entwicklungen und kommen andererseits in MPEG-4 basierten Echtzeit- und Off-line-Anwendungen zum Einsatz. In diesem Zusammenhang ist das HHI für die Integration des MOMUSYS-Referenz modells verantwortlich, das neben jenem von Microsoft als offizielles Referenzmodell von MPEG-4 gilt.

Die Bildanalyse/Merkmalextraktion ist eine zentrale Technologie für intelligente Netzassistenz-Systeme, die den Zugang zu visuellen Informationsressourcen erleichtern. Hierzu werden Verarbeitungsverfahren zur Bildanalyse und -klassifizierung für den intelligenten Zugriff auf Multimediainformationen entwickelt. Diese Arbeiten fließen in die MPEG-7 Standardisierung ein. Darüber hinaus werden auch objekt- bzw. modellbasierte Verfahren hinsichtlich einer sinnvollen Extraktion von visuellen Parametern für solche Systeme untersucht und weiterentwickelt. Diese Technologien werden es dem Nutzer ermöglichen, gezielt nach Informationen in dem immer unübersichtlicher werdenden Programmangebot zu suchen, das über Hunderte von DVB-Kanälen und über das Internet

zugänglich ist. Hierzu müssen die Audio- und Videoströme mit standardisierter Indexinformation versehen werden, so daß MPEG-7 basierte Suchmaschinen nach bestimmten Merkmalen suchen können. Die Auswahl eines Programms mit den gesuchten Inhalten kann dann entweder nutzergesteuert oder aber ereignisgesteuert (z.B. Einblenden eines Fußballspiels, wenn ein Tor gefallen ist) ablaufen.

• Es wurde der erste Prototyp einer Search-Engine entwickelt, die eine gezielte Suche nach Bildern ähnlichen Inhalts in einer Datenbank ermöglicht. Dazu wurden Beschreibungsparameter verwendet, die auf Kontur-, Textur- und Farbinformationen beruhen. Dieses System wurde auf der Online '98 zum ersten Mal der Öffentlichkeit präsentiert.

Die HDTV-Codierung hat in der letzten Zeit wieder an Aktualität gewonnen. Während in Europa hauptsächlich Nischenanwendungen wie "Elektronische Kinos" oder Werbungs- und Medizinapplikationen im Vordergrund stehen, steht auf MPEG-2 basierendes digitales HDTV in den USA kurz vor der Einführung bzw. ist dessen Einführung in Japan für das Jahr 2000 geplant. Weltweit hat man sich für die Verwendung des MPEG-2 Standards für die Kompression der HDTV-Signale entschieden, die eine Übertragung der HDTV-Programme mit ca. 20 Mbit/s gestattet.

• Im HHI wurde einer der weltweit ersten funktionsfähigen Ein-Chip-HDTV-Decoder "HiPEG" entsprechend dem Main Profile @ High Level von MPEG-2 entwickelt. Weiterhin wurde um diesen Chip herum eine komplette Decoder-Box (HiBOX), die mit standardisierten digitalen und analogen Interfaces gemäß den entsprechenden ITU- und DVB-Standards ausgerüstet ist, aufgebaut. HiPEG und HiBOX wurden mit großem Erfolg in Asien, den USA und Europa einzelnen Firmen bzw. der Öffentlichkeit präsentiert. Zu den wichtigsten Demonstrationen gehörten die ECMAST '98 in Berlin, die IBC '98 in Amsterdam sowie gemeinsame Präsentationen mit dem europäischen DVB-Projekt in Hongkong und Argentinien.

Anthropotechnik – Multimedia Endsysteme und Anwendungen

Im Rahmen von interaktiven Multimediadiensten und neuen Medien beschäftigt sich das HHI mit der Forschung und Entwicklung von nutzerfreundlichen Multimediaanwendungen, Interaktions-Technologien und Endgeräten.

Im Mittelpunkt der Arbeiten stehen autostereoskopische Displaytechnologien, Konzepte für nutzerfreundliche Bild-Kommunikationssysteme mit Telepräsenz-Techniken, neue und richtungweisende Systeme und Technologien für 3D Desktop Computer, die Entwicklung innovativer 2D und 3D Interaktionstechnologien für die Mensch-Maschine-Kommunikation, die Erforschung von Technologien zur Datensuche und Datenvisualisierung sowie für die intelligente, agentenbasierte Informationsverwaltung und Nutzerführung. Ergänzt werden diese Schwerpunkte durch grundlagen- und anwendungsorientierte Arbeiten auf dem Gebiet des Usability Engineering unter besonderer Berücksichtigung anthropotechnischer Randbedingungen.

Die Entwicklung von autostereoskopischen Displays konzentriert sich auf Konzepte, die dem Nutzer das Betrachten natürlicher oder computergraphisch generierter 3D Bilder und Videos ohne "Zusatzbrillen" ermöglichen. Anwendungen ergeben sich aus den Bereichen 3D Fernsprechen und 3D Videokonferenzen, 3D TV, 3D Multimedia-Desktop-Computing, 3D virtuelle Welten, Telepräsenz und Telearbeit, Teleüberwachung, Fahrzeugtechnik, CAD/CAM, 3D Computerspiele, sowie aus der Medizin und der Biologie. Die Arbeiten auf diesem Gebiet umfassen die Entwicklung von autostereoskopischen Einpersonen-Displays und Mehrpersonen-Displays mit Flachbildschirmen sowie großformatigen Front- bzw. Rückprojektions-Displays basierend auf der Linsenraster- und Feldlinsentechnik. Prototypen dieser Entwicklungen wurden in den vergangenen Jahren auf einer Vielzahl von Messen und Ausstellungen der Öffentlichkeit vorgestellt:

• in Zusammenarbeit mit der Fa. Zeiss, Oberkochen, wurde ein autostereoskopischer 14 Zoll Flachbildschirm mit Linsenrastertracking entwickelt. Die Technologie für das Linsenrastertracking wurde an die Fa. Zeiss lizensiert.

• Für Anwendungen im Bereich CAD/CAM wurde ein hochauflösender autostereoskopischer Einpersonen-Flachbildschirm ((2x512)x768 pixel) entwickelt, der kein mechanisches Tracking des Linsenrasters benötigt. Zur Nachführung der Bildebene bei Änderung der Kopfposition des Betrachters wurde der Monitor auf einen Schwenkarm projektiert.
• Auf Basis der Feldlinsentechnologie wurde ein hochauflösendes autostereoskopisches Einpersonen-Display für Anwendungen bei der Videokommunikation entwickelt. Um für Telepräsenz-Anwendungen Personen mit "natürlicher Größe" zeigen zu können, erlaubt das Display durch die Integration einer Kollimationsoptik das Abbilden eines virtuellen Bildes einige Meter hinter der Displayoberfläche. Das Display zeichnet sich durch ausgezeichnete Auflösung, Helligkeit und geringes Übersprechen aus.
• Ein großformatiges und extrem hochauflösendes 40 Zoll autostereoskopisches Rückprojektions-Display ((2x1000)x750 pixel) wurde für Anwendungen im Bereich Multimedia Desktop Computing entwikkelt. Dieser Monitor führt ein mechanisches Tracking des Linsenrasters durch.
• Ein videobasierter Head-Tracker wurde entwickelt um die am HHI entwickelten autostereoskopischen Displays ohne Zusatzbrille zu nutzen.

In Hinblick auf die Entwicklung neuer und richtungweisender Konzepte und Technologien für 3D Desktop Computer der Zukunft konzentrieren sich die Arbeiten des HHI auf die Vision eines Computers mit "intelligenten" Mensch-Maschine-Schnittstellen. Um den Nutzer bei der Bedienung zu entlasten, werden Prototypen von Desktop Computern entwickelt, die dem Nutzer Informationen übersichtlich und nutzeradäquat mit Hilfe eines 3D Displays und geeigneter 3D Visualisierung präsentieren. Durch innovative, multimodale Interaktionstechnologien und Agententechnologien werden Wünsche des Nutzers antizipiert und eine einfache und intuitive Nutzung von interaktiven Anwendungen ermöglicht.

Ein erster Prototyp eines "intelligenten" und "sehenden" 3D Desktop-Computers, der die Nachteile herkömmlicher Windows-Oberflächen überwindet und neuartige Formen der Nutzerinteraktion erlaubt, wurde implementiert und auf verschiedenen Messen und Ausstellungen vorgestellt.

• Die Entwicklung eines neuartigen visuellen 3D Betriebssystemes und geeigneter Editoren ermöglicht dem Desktop Computer und dem Nutzer eine einfache und übersichtliche Darstellung von – und Interaktion mit – multimedialen Informationen. Im Gegensatz zu herkömmlichen Windows-basierten Nutzeroberflächen ist das entwickelte Betriebssystem objektbasiert und kann Informationen in der Tiefe staffeln.
• Der Prototyp des 3D Computers nutzt ein im HHI entwickeltes hochauflösendes, autostereoskopisches 50 Zoll Display für eine tiefengestaffelte Visualisierung multimedialer Objekte, die durch das 3D Betriebsystem generiert und verwaltet werden. Aufgrund der stereoskopischen Darstellung kann der Nutzer die Objekte und Informationen in der Tiefe gestaffelt sehen und mittels Kopfbewegung von verschiedenen Seiten betrachten (Bewegungsparallaxe).
• Eine am HHI entwickelte videobasierte Messung der Kopfbewegung und Blickrichtung des Nutzers erübrigt das Tragen von Markierungspunkten und Spezialbrillen.
• Ein Interface-Agent kann erkennen, was der Nutzer betrachtet und kann autonom entsprechende Aktionen auslösen (Visually Controlled Graphics). So kann einerseits nutzeradaptiv die Darstellung der Objekte am Display verändert werden (z.B. kann eine an dem menschlichen visuellen System modellierte Schärfentiefe bei der in der Tiefe gestaffelten Darstellung der Objekte nachgebildet werden). Andererseits kann ein Nutzer Interaktionen mittels Blicksteuerung auslösen.

Forschung auf dem Gebiet der Algorithmen für 2D und 3D Bildverarbeitung wird durchgeführt, um zukünftige Generationen von Multimedia-Endgeräten und Desktop-Computern mit einem großen Potential an Intelligenz und neuen Formen der Mensch-Maschine-Interaktion ausstatten zu können. Anwendungen ergeben sich im Bereich des 3D Desktop-Computings und bei der Telearbeit und Telepräsenz. Die Arbeiten in diesem Schwerpunkt konzentrieren sich auf die Nutzererkennung Objekterkennung und -verfolgung, 3D Tiefenschätzung, 3D-Zwischenbildberechnung und das Head- und Gaze-Tracking.
• Ein videobasierter Head-Tracker wurde entwickelt mit dem Ziel, dem Nutzer von

autostereoskopischen Displays das Betrachten von 3D Bildern aus unterschiedlichen Richtungen zu ermöglichen. Der entwikkelte Algorithmus erkennt selbst kleinste Änderungen der Kopfposition eines Betrachters – robust auch bei schwierigen Beleuchtungsbedingungen – und stellt die Messung einem Display zum Head-Tracking zur Verfügung. Der Algorithmus arbeitet in Echtzeit und wurde unter IRIX auf O2 und unter Windows NT implementiert.

• Der videobasierte Head-Tracker wurde um eine Komponente zur Infrarotbasierten Blickrichtungsmessung erweitert. Eine Blickrichtungsmessung wird unter anderem als Eingabevariable und Interaktionsform für zukünftige Desktop Computer untersucht (Visually Controlled Graphics).

• Für die Anwendung bei 3D Desktop Computern wurde ein Algorithmus für die Objektsegmentierung von trinokularen Bildern entwickelt. Der Algorithmus kann Objekte in Bildern tiefengestaffelt zerlegen und ermöglicht das Erkennen von Personen und räumlichen Strukturen in Bildern. Diese Information kann einerseits für eine tiefengestaffelte Darstellung von Bildern und Videos mit einer dem visuellen System angepaßten Schärfentiefe genutzt werden (bei gleichzeitiger Blickrichtungsmessung des Betrachters). Andererseits kann der mit einem trinokularen Kamerasystem ausgestattete "intelligente" und "sehende" Computer so räumliche Strukturen in seinem Umfeld differenzieren und erkennen (z.B. Personen, Hände, physikalische Objekte, etc.) und ggf. autonom interagieren.

• Für die augenverträgliche Erweiterung der 3D-Darstellungsmöglichkeit für (auto-) stereoskopische Multimedia-Displays wurden in psycho-optischen Experimenten neue Formen der Darstellung von Objekten im Raum untersucht und optimiert. Durch Messung des Fixationspunktes des Betrachters mittels Blickrichtungsmessung wird die Schärfentiefe des gerade gezeigten Stereopaares mittels digitaler Filterung so verändert, daß ein dem natürlichen Sehen angepaßter Schärfentiefenverlauf nachgebildet wird (synthetische Schärfentiefe).

Die Entwicklung nutzeradäquater Bedienkonzepte für zukünftiges Multimedia TV wird im Rahmen des deutschen BMBF-Verbundprojektes MINT (Multimedia auf Integrierten Netzen und Terminals) untersucht. Ziel ist die Entwicklung von prototypischen TV-Empfängern, die eine Vielzahl von Multimediaanwendungen integrieren. Eine zentrale Herausforderung stellt neben der Diensteintegration insbesondere die Bedienung und Nutzerführung dar, die aufgrund der Komplexität der Dienste einfach und nutzerfreundlich gestaltet werden muß.

• Es wurde ein Prototyp eines Multimedia TV-Gerätes implementiert, das dem Nutzer neben herkömmlichem TV auch die Nutzung typischer Internetdienste (Email, www, Homeshopping), und neuer Kommunikationsdienste (z.B. Videotelefonie, Digital Audio Broadcast – DAB, MPEG-4 virtuelle Konferenzen) ermöglicht.

• Eine mit Hilfe von Nutzeruntersuchungen im Rapid-Prototyping entwickelte Bedienoberfläche ermöglicht dem Nutzer eine einfache und übersichtliche Bedienung aller im TV-Empfänger integrierten Dienste.

In einem weiteren Forschungsschwerpunkt werden Kommunikationssysteme mit hoher Telepräsenz untersucht. Es werden Konzepte entwickelt, die in Form von Laborsystemen realisiert und demonstriert sowie in Nutzeruntersuchungen empirisch überprüft werden. Im Rahmen von am HHI durchgeführten Kommunikationsexperimenten mit Studio-Videokonferenzen hatten sich 3D-Bildtechniken als nützlich für die Erhöhung der Telepräsenz und Effektivität erwiesen. Entsprechende Vorteile werden auch bei Arbeitsplatzkonferenzen bzw. allgemein bei Arbeitsplatzsystemen erwartet. Da diese Art der Kommunikation in Zukunft weiter an Bedeutung gewinnen wird, wurde der Einsatz von 3D-Techniken auch bei Arbeitsplatzsystemen untersucht. Dabei ging es u.a. um eine unverzerrte Wiedergabe der Bewegungsparallaxe, um eine wahrnehmungsmäßig konfliktfreie Mischung von 2D- und 3D-Bildern sowie um das benutzerfreundliche 3D-Fernzeigen in stereoskopischen Bildern.

• Durch Untersuchungen konnten Hinweise erarbeitet werden, die für Anwendungen mit Abbildung der Bewegungsparallaxe einen Mechanismus vorsehen, der es dem Betrachter ermöglicht, das Übersetzungsverhältnis der Änderung des Perspektivzentrums der Wiedergabe und der Kopfbewegung einzustellen.

• Für die Mischung von 3D-Bildern wurden mit Hilfe von Nutzeruntersuchungen Vorschläge erarbeitet, die beschreiben, wie störende Mischkanten in der Bildschirmebene vermieden werden können.

• Als autostereoskopisches Display für den Arbeitsplatz wurde ein Feldlinsen-Display entwickelte, das eine Trennung der Stereoteilbilder durch gerichtetes Licht erzielt. Es liefert helle und kontrastreiche Stereobilder, die auch bei den Lichtverhältnissen an Büroarbeitsplätzen gut zu betrachten sind.

Ein wichtiger Aspekt zwischenmenschlicher Kommunikation ist die informelle Kommunikation. Gemeint sind damit die spontanen und überwiegend vertraulichen Gespräche z.B. am Rande von Konferenzen, bei Kaffeepausen oder bei anderen zufälligen Begegnungen. Da diese Formen der Kommunikation eine positive Bedeutung für den einzelnen Mitarbeiter ebenso wie für das Unternehmen haben, wird für verteilte Arbeitsgruppen bei Telearbeit und Telekooperation nach einer technischen Unterstützung der informellen Kommunikation gesucht. Eine Befragung potentieller Nutzer von Telekooperationssystemen ergab, daß informelle Kommunikation in vielen Arbeitszusammenhängen als unverzichtbar angesehen wird.

• Um herauszufinden, welche Merkmale Telekooperationssysteme aufweisen müssen, um informelle Kommunikation möglichst gut zu unterstützen, wurden verschiedene Feldversuche durchgeführt: mit einem Chat-System, einem um Standbilder erweiterten Chat-System und einer virtuellen Umgebung. Ergebnisse zeigen, daß textbasierte Kommunikationssysteme informelle Kommunikation ermöglichen; sie sollten aber durch Indikatoren für den Grad der Kommunikationsbereitschaft potentieller Kommunikationspartner ergänzt werden.

• Für die Anwendung bei der Telearbeit wurde die Telepräsenz einer Arbeitsgruppe durch eine "virtuelle Büroumgebung" mit Hilfe von computergraphischen virtuellen Welten nachgebildet. Jeder Teilnehmer einer Telearbeitsgruppe – und dessen Position und Aktion im Raum – wird durch einen computergraphischen Repräsentanten (Avatar) dargestellt. Insbesondere für die informelle Kommunikation bei der Telearbeit erscheint ein solches Konzept erfolgversprechend; es ermöglicht eine hohe Telepräsenz bei ausreichendem Schutz der Privatsphäre.

Kompetenzen

Entwicklung von Algorithmen und Hardwarearchitekturen zur Bild- und Tonkompression (MPEG-2, MPEG-4)

Entwicklung von Algorithmen und Hardwarearchitekturen zur 2D- und 3D-Bildanalyse und Synthese auf der Grundlage von Bewegungs- und Stereoinformation

Bildsegmentierung und Merkmalsextraktion

Entwicklung von Anwendungen auf Basis von MPEG-2/4/7 und JAVA für interaktive Dienste im Internet, über DVB/DAB/DMB, über das ISDN, über xDSL und über Mobilfunknetze (DECT, GPRS, HSCSD, UMTS)

Codierverfahren für Bildtelephonie und Videokonferenz (H.26x, MPEG-4)

MPEG- und ITU-T basierte Signalisierungs- und Transportprotokolle (H.32x, MPEG-TS, DMIF)

Modellierung und Entwurf von integrierten Schaltkreisen für die Bildsignalverarbeitung

Entwurf, Integration und Aufbau von Prototypen und Experimentalsystemen für videobasierte Kommunikationsanwendungen und für Test und Demonstration neuer Kommunikationstechnologien und neuer Hardwarearchitekturen

Entwicklung von 3D-Displaytechnologien

Konzeption und Bewertung von Benutzerschnittstellen für Multimediaanwendungen auf der Basis von VRML, JAVA, MSDL und dVS

Analyse und Optimierung von Kommunikations-Endgeräten und -Diensten nach anthropotechnischen Kriterien

Entwicklung von videobasierten Mustererkennungs-und Photogrammetrieverfahren

Modellierung und Entwurf von integrierten Schaltkreisen für die Bildsignalverarbeitung

Entwurf und Aufbau von Experimentalsystemen für die Entwicklung von videobasierten Kommunikationsanwendungen

und für Test und Demonstration neuer Kommunikationstechnologien und neuer Hardwarearchitekturen

Analyse sensorischer und sensomotorischer Funktionen des Menschen mit Bezug zu Kommunikationsanwendungen

Expertise in Desktop Computer Graphics Design

Forschung auf dem Gebiet der Hochfeld-Elektrolumineszenz (SrS:Ce, ZnS:Mn)

Entwicklung von Vielschicht-Elektrolumineszenzstrukturen, blau emittierenden Phosphoren, vollfarbigen Flach-Displays, transparenten Displays

Entwicklung von Diffraktiven Optischen Elementen für den Schreib-/Lesekopf einer Optischen Disk

R & D PROJECTS · F & E-PROJEKTE

Project	Projekt	Project Manager · Projektleiter phone · Telefon email	Provider of Grant/Contractor · Förderer/ Auftraggeber Period · Laufzeit
Photonic Networks	**Photonik-Netze**		
OFDM-LAN with Optical Filters, PHOTONIK II, 2 Subprojects:	OFDM-LAN mit optischer Filtertechnik, PHOTONIK II, 2 Teilprojekte:	Godehard Walf +49(0)30-31002-455 walf@hhi.de	BMBF 4/94-3/98
1) OFDM-LAN/MAN	1) OFDM-LAN/MAN	Fritz-Joachim Westphal +49(0)30-31002-288 westphal@hhi.de	
2) Optically Transparent Interconnection of OFDM Networks	2) Optisch transparente Zusammenschaltung von OFDM-Inselnetzen	Jürgen Saniter +49(0)30-31002-288 saniter@hhi.de	
Frequency Selective Tunable Receiver OEICs Based on Indiumphosphide for OFDM Systems, PHOTONIK II	Frequenzselektive abstimmbare Empfänger-OEICs auf Indiumphosphid-Basis für OFDM-Systeme, PHOTONIK II	Helmut Heidrich +49(0)30-31002-538 heidrich@hhi.de	BMBF 4/94-3/98
Broadband Lightwave Sources and Systems, ACTS BLISS	Broadband Lightwave Sources and Systems, ACTS BLISS	Niraj Agrawal +49(0)30-31002-510 agrawal@hhi.de Helmut Heidrich +49(0)30-31002-538 heidrich@hhi.de	EU 9/95-8/98
WDM Transmitter PIC for Industrial Applications	WDM-Transmitter-Chip für den industriellen Einsatz	Frank Fidorra +49(0)30-31002-538 fidorra@hhi.de	HHI 5/96-4/97
Selective Area MOMBE for Laser/Waveguide Integration, PHOTONIK II	Flächenselektive MOMBE für die Laser/Wellenleiter Integration, PHOTONIK II	Harald Künzel +49(0)30-31002-546 kuenzel@hhi.de	BMBF 1/95-3/98
Integrated Waveguide Components on SiO_2/Si for OFDM Systems	Integrierte Wellenleiterkomponenten auf SiO_2/Si-Basis für OFDM-Systeme	Berndt Kuhlow +49(0)30-31002-448 kuhlow@hhi.de	HHI 4/94-3/98
Plasma Etching Techniques for Micro-Optical Elements with Highly Precise Profiles for Micro Systems	Plasmastimulierte Ätztechniken für mikrostrukturierte optische Elemente mit hochpräzisen Profilen für die Mikrosystemtechnik	Margit Ferstl +49(0)30-31002-430 ferstl@hhi.de	State of Berlin 10/96-5/98

Components and Subsystems for Optical Time Division Multiplexing, PHOTONIK II, 2 Subprojects:	Komponenten und Subsysteme für die optische Zeitmultiplextechnik, PHOTONIK II, 2 Teilprojekte:	Hans-Georg Weber +49(0)30-31002-443 hgweber@hhi.de	BMBF 4/94-/98
1) Subsystems for Optical Time Division Multiplexing	1) Subsysteme für die optische Zeitmultiplextechnik	Hans-Georg Weber +49(0)30-31002-443 hgweber@hhi.de	
2) Semiconductor Laser Amplifier Components for OTDM Applications	2) Halbleiterverstärkerkomponenten für OTDM-Anwendungen	Niraj Agrawal +49(0)30-31002-510 agrawal@hhi.de	
Photonic Technologies for Ultra High Speed Information Highways, ACTS HIGHWAY	Photonic Technologies for Ultra High Speed Information Highways, ACTS HIGHWAY	Detlef Hoffmann +49(0)30-31002-454 hoffmann@hhi.de	EU 9/95-8/98
High Bit Rate Receiver OEICs Based on InP, PHOTONIK II	Höchstfrequente Empfänger-OEICs auf InP-Basis, PHOTONIK II	Heinz-Gunter Bach +49(0)30-31002-503 bach@hhi.de	BMBF 4/94-3/98
Investigations on a Regenerator Free Optical Network	Untersuchungen zu einem regeneratorfreien optischen Netz	Bernhard Strebel +49(0)30-31002-586 strebel@hhi.de	Industry 5/96-9/98
Paneuropean Photonic Transport Overlay Network, ACTS PHOTON	Paneuropean Photonic Transport Overlay Network, ACTS PHOTON	Clemens v. Helmolt +49(0)30-31002-506 helmolt@hhi.de	EU 9/95-8/98
Metropolitan Optical Network, ACTS METON	Metropolitan Optical Network, ACTS METON	Dirk Trommer +49(0)30-31002-526 trommer@hhi.de	EU 9/95-8/98
Architectures in Optical Networks, PHOTONIK II	Architekturen in optischen Netzen, PHOTONIK II	Josef Giglmayr +49(0)30-31002-366 giglmayr@hhi.de	BMBF 4/94-3/98
Planning Guidelines for Photonic Networks	Planung Photonisches Netz	Ernst-Jürgen Bachus +49(0)30-31002-457 bachus@hhi.de	Industry 7/96-3/98
Data Communication Using Low Voltage Power Lines	Datenübertragung über Niederspannungs Energienetze	Klaus-Dieter Langer +49(0)30-31002-457 langer@hhi.de	Industry 11/97-9/98
Transponders for 2,5 Gbit/s	Transponder für 2,5 Gbit/s	Jürgen Saniter +49(0)30-31002-288 saniter@hhi.de	Industry 12/97-11/98
Arrayed Waveguide Grating Filters	Arrayed Waveguide Grating-Filter	Berndt Kuhlow +49(0)30-31002-448 kuhlow@hhi.de	Industry 7/97-12/98

InP-Based Micro-Mechanical Tunable and Selective Photo-detector for WDM-systems	InP-Based Micro-Mechanical Tunable and Selective Photo-detector for WDM-systems	Harald Künzel +49(0)30-31002-546 kuenzel@hhi.de	EU 1/97-12/99
Development of Basic Technological Processes and Components	Entwicklung technologischer Basisverfahren und Bauelemente	Helmut Heidrich +49(0)30-31002-538 heidrich@hhi.de	Industry 3/97-12/04
Active Resonant Grating-Waveguide Structures for Rapidly Tuning Semiconductor Lasers with no Moving Elements	Gitterwellenleiter-Struktur für den Einsatz in einem modengekoppelten Halbleiterlaser mit Wellenlängendurchstimmbarkeit ohne mechanisch bewegliche Elemente	Hans-Georg Weber +49(0)30-31002-443 hgweber@hhi.de	BMBF 7/97-6/00
Electroabsorption Modulated DFB-Laser Diodes (EML)	Electroabsorption Modulated DFB-Laser Diodes (EML)	Martin Möhrle +49(0)30-31002-503 moehrle@hhi.de	HHI/Industry 9/98-12/99
KomNet System Integration Office	KomNet System-integrationsbüro	Godehard Walf +49(0)30-31002-455 walf@hhi.de	BMBF/Industry (KomNet) 5/98-4/02
System Studies and the Test of Components for City Ring Networks	Systemstudien und Komponententest für Cityringe	Ernst-Jürgen Bachus +49(0)30-31002-457 bachus@hhi.de	BMBF/Industry (KomNet) 9/98-4/01
Planning Guidelines for WDM-Systems in City- and Access-Networks	Planunggrundlagen für WDM-Netz im City- und Access-Bereich	Ernst-Jürgen Bachus +49(0)30-31002-457 bachus@hhi.de	IBMBF/Industry (KomNet) 6/98-4/02
Low-Cost Transceiver-PIC for the Access Network	Low-Cost Transceiver-PIC für den Teilnehmerzugangsbereich	Helmut Heidrich +49(0)30-31002-538 heidrich@hhi.de	BMBF/Industries (KomNet) 6/98-/02
Development of an Integrated Multi Channel Transmitter	Entwicklung eines integrierten Mehrwellensenders	Frank Fidorra +49(0)30-31002-538 fidorra@hhi.de	Industry 8/98-10/98 HHI 11/98-4/99
Polymeric Optical Waveguide Enhanced Router (POWER)	Polymeric Optical Waveguide Enhanced Router (POWER)	Norbert Keil +49(0)30-31002-590 keil@hhi.de	Industry 2/98 -1/00
Planar Optical SiO_2 /Polymer Switch Matrix	Planare optische SiO_2/ Polymer-Schaltmatrix	Norbert Keil +49(0)30-31002-590 keil@hhi.de	Industry 3/98-2/00
40 Gbit/s OTDM for KomNet	40 Gbit/s OTDM für KomNet	Hans-Georg Weber +49(0)30-31002-443 hgweber@hhi.de	BMBF 9/98-8/02

REgeneration of Pulse shapE, Amplitude and Timing, REPEAT	REgeneration of Pulse shapE, Amplitude and Timing, REPEAT	Detlef Hoffmann +49(0)30-31002-454 hoffmann@hhi.de	EU 3/98-12/99
All-optical Signal Processing	All-optical Signal Processing	Bernd Sartorius +49(0)30-31002-508 sartorius@hhi.de	Industry 1/98-12/00
Nonlinear Interferometer Photonic Integrated Circuits for all Optical Demultiplexing in OTDM Systems	Integrierte nichtlineare Interferometer als rein optische Demultiplexer für die OTDM-Technik	Michael Schlak +49(0)30-31002-407 schlak@hhi.de	Industry 1/98-12/00
Gain-Clamped Optical Amplifier in Fibre-optical Transmission Systems	Gain-Clamped Halbleiter-verstärker als optischer Schalter in faseroptischen Übertragungssystemen	Hans-Georg Weber +49(0)30-31002-443 hgweber@hhi.de	DFG 4/98-3/00
Semiconductor Saturable Absorber Structures for Femtosecond Demulti-plexer	Sättigbare Absorber-strukturen für Femtosekunden-Demulti-plexer	Harald Künzel +49(0)30-31002-546 kuenzel@hhi.de	MBI/HHI 11/98-10/01
Development of Twin Photodiode-Photo-receivers for a 40 Gbit/s Field Experiment in KomNet	Entwicklung von Twin-Photodioden-Empfängern für einen 40 Gbit/s TDM Feldversuch in KomNet	Andreas Umbach +49(0)30-31002-526 umbach@hhi.de	BMBF/Industry (KomNet) 5/98-4/02
40 Gbit/s Photoreceiver Module Development for the GIGATRANSPORT Field Experiment in KomNet	40 Gbit/s Photoempfänger -Modul-Entwicklung für das GIGATRANSPORT Feldversuchsystem in KomNet	Heinz-Gunter Bach +49(0)30-31002-503 bach@hhi.de	BMBF/Industry (KomNet) 6/98-5/01
40 Gbit/s Frontend Development for an ETDM Long Haul Transmission in KomNet	40 Gbit/s Frontend-Entwicklung für eine ETDM Weitverkehrs-strecke in KomNet	Heinz-Gunter Bach +49(0)30-31002-503 bach@hhi.de	BMBF/Industry (KomNet) 6/98-5/01
Optical Sampling of High Bitrate Data Signals	Optisches Sampling von hochratigen Daten-signalen	Hans-Georg Weber +49(0)30-31002-443 hgweber@hhi.de	DFG 6/98-5/00
Picosecond Laserdiode System	Pikosekunden-Laser-dioden-System	Agnostis Paraskevopoulos +49(0)30-31002-527 paraskevopoulos@hhi.de	State of Berlin 11/98-1/00

Mobile Broadband Systems	**Mobile Breitbandsysteme**		
Integrated Mobile Broadband System, 2 Subprojects:	Integrierendes breitbandiges Mobilkommunikations-System, 2 Teilprojekte:	Holger Boche +49(0)30-31002-540 boche@hhi.de	BMBF 10/96-6/00
1) Integrated Mobile Broadband System – Inhouse	1) Integrierendes breitbandiges Mobilkommunikations-System Inhouse	Holger Boche +49(0)30-31002-540 boche@hhi.de	
2) Broadband Mobile Communication System Based on IR	2) Breitbandiges Mobilkommunikationssystem auf Infrarotbasis	Clemens v. Helmolt +49(0)30-31002-506 helmolt@hhi.de	
Optical Millimetre-Wave Generation for Mobile Communication, PHOTONIK II	Optische Mikrowellenerzeugung für die Mobilkommunikation, PHOTONIK II	Gerd Großkopf +49(0)30-31002-317 grosskopf@hhi.de	BMBF 4/94-3/98
Optical Time Delay Network	Optische Verzögerungsnetzwerke	Gerd Großkopf +49(0)30-31002-317 grosskopf@hhi.de	Industry 7/97-3/99
Optoelectronic Converter OEIC for 38/60 GHz as Component for Future Integrated Antenna Base Stations for Mobile Communication	Optoelektronischer Wandlerschaltkreis für 38/60 GHz als Bestandteil zukünftiger integrierter Antennenbasisstationen für die Mobilkommunikation	Heinz-Gunter Bach +49(0)30-31002-503 bach@hhi.de	NaFög 4/97-4/99
Electronic Imaging Technology for Multimedia	**Elektronische Bildtechnik für Multimedia**		
Decoding and Signal Processing Systems for Network Independant Multimedia Communication	Decodier- und Signalverarbeitungseinrichtungen für die netzübergreifende Multimediakommunikation	Peter Stammnitz +49(0)30-31002-570 stammnitz@hhi.de	BMBF 1/96-12/98
AV Processors for Network Independant Multimedia Communication	AV-Prozessoren für die netzübergreifende Multimediakommunikation	Maati Talmi +49(0)30-31002-293 talmi@hhi.de	BMBF 1/96-12/98
Mobile Multimedia Systems, ACTS MOMUSYS	Mobile Multimedia Systems, ACTS MOMUSYS	Guido Heising +49(0)30-31002-619 heising@hhi.de	EU 10/95-12/99
Architectures, Software and Hardware for MPEG4 Systems, ACTS EMPHASIS	Architectures, Software and Hardware for MPEG4 Systems, ACTS EMPHASIS	Thorsten Selinger +49(0)30-31002-404 selinger@hhi.de	EU 10/95-9/98

Package for New Operational Autosteroscopic Multiview Systems and Applications, ACTS PANORAMA	Package for New Operational Autosteroscopic Multiview Systems and Applications, ACTS PANORAMA	Jens-Rainer Ohm +49(0)30-31002-617 ohm@hhi.de	EU 9/95-8/98
Videocompression and -Presentation for Interactive Services (VPID)	Videokompression und -präsentation für interaktive Dienste (VPID)	Peter Kauff +49(0)30-31002-615 kauff@hhi.de	BMBF 1/97-12/99
Integration and Optimization of the MPEG-4 Video Verification Model of MOMUSYS	Pflege und Optimierung des MPEG-4- Video verifikationsmodells von MOMUSYS	Minhua Zhou +49(0)30-31002-616 zhou@hhi.de	Industry 4/97-1/98
MPEG-4 Fo(u)r Mobile Communications – M4M	MPEG-4 Fo(u)r Mobile Communications – M4M	Ralf Schäfer +49(0)30-31002-560 schaefer@hhi.de	Industry 7/97-6/98
MPEG-4 for Mobile Multimedia Service	MPEG-4 für Mobile Multimedia-Dienste	Jens-Rainer Ohm +49(0)30-31002-617 ohm@hhi.de	BMBF 7/97-6/00
Virtual Interactive Video Shop - VITO	Virtueller T-Punkt mit Online-Fachberater im Internet – VITO	Peter Kauff +49(0)30-31002-615 kauff@hhi.de	Industry 10/97-5/98
Coding of Contour- and Surface Data Using Wavelets	Codierung von Kontur- und Oberflächendaten unter Verwendung von Wavelets	Jens-Rainer Ohm +49(0)30-31002-617 ohm@hhi.de	DFG 10/97-9/99
Development of an Evaluation Board	Erstellung eines Evaluierungsboards	Maati Talmi +49(0)30-31002-293 talmi@hhi.de	Industry 9/97-11/98
New Multimedia Services Using Analysis and Synthesis 3D, NEMESIS	New Multimedia Services Using Analysis and Synthesis 3D, NEMESIS	Peter Kauff +49(0)30-31002-615 kauff@hhi.de	EU 9/98-8/00
Package for New Operational Autostereoscopic Multiview Systems and Applications, ACTS PANORAMA	Package for New Operational Autostereoscopic Multiview Systems and Applications, ACTS PANORAMA	Siegmund Pastoor +49(0)30-31002-345 pastoor@hhi.de	EU 9/95-8/98
Approaches for Gaze-Controlled Interactions with Autostereoscopic Multimedia-Displays	Verfahren zur blickgesteuerten Interaktion mit autostereoskopischen Multimedia-Displays	Siegmund Pastoor +49(0)30-31002-345 pastoor@hhi.de	BMBF 1/95-12/98
Telepresence in the Workplace	Telepräsenz am Arbeitsplatz	Lothar Mühlbach +49(0)30-31002-237 muehlb@hhi.de	BMBF 8/94-6/98

User Interfaces for Cross-Network and Cross-Service Multimedia Applications, MINT	Benutzerschnittstellen für netz- und diensteüber-greifende Multimedia-anwendungen, MINT	Thomas Meiers +49(0)30-31002-218 meiers@hhi.de	BMBF 1/96-12/98
Usability in ACTS, ACTS USINACTS	Usability in ACTS, ACTS USINACTS	Lothar Mühlbach +49(0)30-31002-237 muehlb@hhi.de	EU 7/96-12/98
Evaluation of The Global Learning Platform of the Deutsche Telekom AG	Evaluation der Global Learning Plattform der Deutschen Telekom AG	Jens Faber +49(0)30-31002-235 faber@hhi.de	Industry 5/97-7/98
Autostereoscopic Single User Monitors with Tracking System	Autostereoskopische Einpersonen-Monitore mit Trackingsystem	Reinhard Börner +49(0)30-31002-259 boerner@hhi.de	BMBF 4/96-3/00
Full Colour Electroluminescence Based on IIa-VIa Compounds	Vollfarb-Elektrolumines-zenz auf der Basis von IIa-VIa-Verbindungen	Karl-Otto Velthaus +49(0)30-20377-326 velthaus@hhi.de	BMBF 7/95-6/98
Next Generation Colour Electroluminescent Displays, ESPRIT ELDISP	Next Generation Colour Electroluminescent Displays, ESPRIT ELDISP	Karl-Otto Velthaus +49(0)30-20377-326 velthaus@hhi.de	EU 11/96-10/99
New S+S:Ce,Mn,Ag Multi-source Deposition Process for Active-Matrix Electro-luminescent-Devices	New S+S:Ce,Mn,Ag multi-source deposition process for Active-Matrix Electro-luminescent-Devices	Karl-Otto Velthaus +49(0)30-20377-326 velthaus@hhi.de	Industry 10/97-9/98
Active Matrix Electroluminescence (AMEL)	Active Matrix Electroluminescence (AMEL)	Karl-Otto Velthaus +49(0)30-20377-326 velthaus@hhi.de	Industry 1/98-12/99
Diffractive Optical Elements for a Write/ Read Optical Pickup of a Disk	Diffraktive Optische Elemente für den Schreib/Lesekopf einer optischen Disk	Berndt Kuhlow +49(0)30-31002-448 kuhlow@hhi.de	TH Darmstadt 10/96-12/99

Selected Achievements

H.-G. BACH, G. GROSSKOPF, H. HEIDRICH, J. SANITER, H.-G. WEBER, F.-J. WESTPHAL AND G. WALF

PHOTONIK II – OVERVIEW OF THE HHI-PROJECTS

Abstract

"Photonics" has been one of the main R&D programs in Information Technology initialized and financed by the German government and carried out by industry and research institutes. Its second four-year phase was completed in April 1998. This covered the development of various advanced technologies for broadband optical fibre systems. Several system and technology oriented projects in the fields of access networks, core networks and optical microwave generation were carried out at HHI under the framework of this R&D program.

1. Introduction

The German Ministry of Education, Science, Research and Technology (BMBF) started the national R&D program "Photonics" in 1990. The second four-year phase of this program was completed in 1998. Photonics was subdivided into the branches "Optical Interconnects" and "Optical Communication Systems". The latter was coordinated by HHI. All major IT companies (Alcatel, Bosch Telecom, Daimler Benz, Lucent Technologies and Siemens), governmental research institutes and universities were involved in this program. The program covered system oriented as well as component-oriented research and development.

An overview of the results of the Photonics projects that were carried out by the HHI under this R&D program is given here.

2. WDM access and the local area network

The activities in the area of customer and access networks are concentrated on the use of wavelength division multiplexing with different channel spacings (WDM or OFDM techniques). Different demonstrators were built to verify concepts experimentally and to characterize key components and network elements in a system environment.

The activities can be divided into two phases. The focus during the first phase was on the use of OFDM networks with small channel spacings (e.g. 9 GHz) and the all-optical interconnection of these networks. For this channel spacing a polarization-insensitive heterodyne receiver was successfully implemented, using an OIEC developed and monolithically integrated at the HHI (see next section for details). The stable and error-free operation of the receiver was demonstrated over a long period of time.

During the second phase the centre of interest was the use of WDM with a wider channel spacing (100 GHz – 400 GHz) for broadband access networks, especially the development of a WDM upgrade of existing passive optical networks (PON). To verify experimentally the concepts and innovative components that had been developed, a PON operating at 1.3 µm with a WDM overlay at 1.55 µm was realized. Due to the WDM overlay, permanent optical wavelength paths are established between the central office and the optical network unit at the subscriber side, dramatically enhancing the transmission capacity of the PON. The existing fibre infrastructure of the PON remains unaltered and the WDM overlay can be installed gradually, depending on the demand. Also, protection against eavesdropping and intentional disturbances is enhanced by this configuration.

Optical multiplexer/demultiplexers are key components of the WDM technique. Arrayed Waveguide Gratings (AWG) with a channel spacing of 100 GHz are used in the experimental testbed. Such AWGs were developed and fabricated by the HHI in SiO2/Si technique and by the University of Dortmund and the company IOT on glass substrates. The integrated components produced by these partners, as well as transmitter and receiver modules developed at the HHI, were characterized and operated in the experimental testbed.

Various proposals for supervision and controlling optical access networks were developed. For example, concepts for the

remote supervision of the AWG in the PON from the central office and for the supervision of the PON fibre infrastructure by means of a frequency selective OTDR were experimentally verified.

It is necessary to use WDM transponders to interface existing terminal equipment with new WDM systems. A WDM transponder consists of an optical receiver and a transmitter which transmits at a given wavelength, matched to the WDM system. A modular bitrate-independent transponder for data rates from 100 Mbit/s up to 2.5 Gbit/s has been developed. For a fixed bit rate, e.g. 2.5 Gbit/s, a clock recovery circuit can be added. The transponder is provided with appropriate control and supervision functions for integration in a TMN system [1].

3. WDM transceiver and frequency selective tunable receiver OEICs on InP

The implementation of Photonic ICs (PICs) should lead ultimately to a cost reduction for the fabrication of high volume optical modules. This cost reduction is one prerequisite for the implementation of fibre systems in access and customer networks. The main issues of this project, which has the title "Integration Technology: Frequency Selective Tunable Receiver OEICs Based on InP for OFDM Systems", were:

1. The ongoing development and availability of a technological toolbox for flexible and economic integration of optical and optoelectronic basic building blocks (e.g. lasers, waveguide networks, photodetectors), without substantial loss of performance compared to the fabrication of the separate elements.
2. The application of this technology for the realization of complex PICs.
3. The demonstration of the functionality of a monolithically integrated, polarization-insensitive heterodyne receiver.
4. The extension of the versatile integration technology to the fabrication of WDM transceiver PICs – the first high volume candidates.
5. The processing of first transceiver PICs meeting the system requirements.

A main breakthrough towards the possible economic fabrication of WDM transceiver PICs was achieved with the development of PICs including compact wavelength-selective photodetector building blocks. The developed integration technology and transceiver designs offer the possibility of also fabricating TRx-PICs with the potential to meet even the demanding FSAN performance specifications. For this purpose further improvements will follow in future (e.g. optimization of the external receiver responsivity [2]).

Besides the WDM transceiver, a polarization diversity heterodyne receiver PIC has also been developed The polarization diversity heterodyne receiver PIC represents the highest degree of integration complexity to date. The parallel processing on the same wafer of the very first optical sweeper PIC for the generation of millimetre wave signals [3] demonstrated the universality and the potential of the developed integration technology. Both components – the WDM transceiver and the polarization diversity heterodyne receiver PIC – have been tested successfully in laboratory systems.

4. Optical transmission of 40 Gbit/s – 80 Gbit/s on standard fibres and a 640 Gbit/s WDM/TDM experiment

An optical time division multiplexing system was realized in the project "Components and Subsystems for Optical Time Division Multiplexing". The 10 Gbit/s optical data signals were all-optically multiplexed by bit interleaving to 40 Gbit/s or 80 Gbit/s optical data signals. The multiplexed data stream was transmitted over a fibre link and subsequently demultiplexed to 10 Gbit/s data signals. 40 Gbit/s transmission over 434 km standard fibre (D = 17 ps/km nm) and 4×40 Gbit/s transmission over 100 km standard fibre were performed. For these experiments an optical pulse source was developed, which is tunable in wavelength (1540 – 1560 nm), in fundamental mode repetition rate (1 – 14 GHz) and in pulse width (0.18 – 17 ps). Monolithically integrated switches based on semiconductor optical amplifiers in interferometers were realized and used as a demultiplexer in the 40 Gbit/s transmission experiments.

In contrast to previous interferometric

switches based on semiconductor optical amplifiers, a novel concept of an all-optical switch was developed. In the new switch the control signal changes only the phase and not the amplitude of the data signal. The switch is of great interest for demultiplexing and add/drop multiplexing applications in high bit rate TDM and combined TDM/WDM systems. Operation of the switch was successfully demonstrated in a 640 Gbit/s demultiplexing experiment, where 8 WDM channels, each with a 80 Gbit/s data stream in the time domain, were simultaneously demultiplexed to 8 WDM channels, each at 10 Gbit/s [4].

The high linearity of the switch with regard to the data input power gives promising potential applications as an optical switch and as an optical sensor (optical sampling) with a time resolution of around 1 ps. The commercial use of this invention is additionally indicated by the fact that the switch, including all its components, can be monolithically integrated.

5. High-speed receiver OEICs on InP

High bit rate photoreceivers, operating in the 1.3 to 1.55 µm wavelength range, are needed in optical networks employing fast TDM techniques. At project start such high-speed receivers were only available as hybrids. This project aimed at incorporating a detection capability in the InP-based receiver OEICs, and this was achieved at 40 Gbit/s. Together with the excellent material properties of the InP material, the travelling wave design that was used allows continual further upgrade of the OEICs towards higher bit rates up to 100 Gbit/s. An optical input waveguide, a pin photodiode, and high-electron mobility transistors (HEMTs) are integrated in the receiver. The HEMTs form a travelling wave amplifier (TWA) using MMIC technology. The work program :

- The development of an MBE process (overgrowth of MOVPE-based semi-insulating waveguide layer stacks).
- The development of basic technologies, such as selective etching of the GaInAsP/AlGaInAs material system and a coplanar waveguide technique, including air bridges.
- The optimization of waveguide-integrated photodiodes with respect to their bandwidth-efficiency product by applying MOVPE growth of a semi-insulating waveguide layer stack.
- The development of HEMTs, including gate lithography, using optical and electron beam exposure.
- The circuit design in cooperation with a university partner (Universität-GH-Duisburg, FG HLT).
- The development of an optoelectronic packaging technology.
- An extension of the detector/receiver optical heterodyne measurement technique up to 75 GHz.

Waveguide-integrated photodiodes (0.35 A/W) have been fabricated with cut-off frequencies as high as 70 GHz. A basic process was developed for a monolithically integrated optical waveguide taper, which enables future photodiode conversion efficiencies above 0.5 A/W. The HEMT process on Fe-doped semi-insulating optical waveguide layers employing electron-beam written gates ($f_T/f_{max} \geq 100/200$ GHz) was adapted to the pin TWA integration process. Photoreceiver OEICs, mounted into modules, were tested in system experiments by Siemens AG and Alcatel SEL. The receiver OEIC had a bandwidth of 28 GHz and was tested by Alcatel SEL in an optical TDM experiment at 40 Gbit/s. Improved OEICs comprising e-beam HEMTs achieved a bandwidth of 37 GHz [5].

6. Optical millimetre wave generation for mobile communication

In this project two different optical techniques for the generation of low phase noise millimetre wave signals, which are used for the remote feeding of antenna stations in broad-band mobile communication systems, have been investigated. In the first case the signals of two lasers at a frequency spacing equal to the desired millimetre wave frequency were heterodyned in an optic/millimetre-wave converter. The phase noise was suppressed by applying modulation sideband injection locking. This technique simultaneously stabilizes the generated frequency. In the second case only a single laser diode was used. The desired millimetre wave signal was obtained by optical upconversion, using nonlinear effects caused by the laser chirp in combination with the fibre

dispersion. An experimental system was built up in cooperation with R. Bosch GmbH, Hildesheim. Error-free full duplex operation was demonstrated with 155 Mbit/s data signals in the frequency ranges 18-20 and 60-70 GHz [6, 7]. Further experimental and theoretical investigations proved the feasibility of the optical millimetre wave technique in multichannel systems. Optic/millimetre-wave converters with a large conversion efficiency were developed in cooperation with our partners Fraunhofer Institut für angewandte Festkörperphysik (IAF) and DASA.

The results obtained in this project demonstrate the advantages of the optical millimetre wave technique in broadband mobile communication systems. Low phase noise millimetre wave signals with high frequency flexibility and stability were generated by the two photonic methods. Hence remotely fed low-cost antenna stations can be built.

Further cost savings are possible by applying this technique in combination with monolithic integration of the components. It was demonstrated experimentally that the control stations of a mobile communication system can also be simplified by using monolithically integrated optical millimetre wave transmitters comprising two tunable laser diodes and a waveguide coupler.

7. Conclusion

The HHI has carried out system and technology oriented projects under the framework of the R&D program "Photonics" of the German government in the fields of access networks, core networks and optical microwave generation. System concepts for WDM access networks and OFDM local area networks were developed and verified in system experiments. The potential of optical time division multiplexing and transmission of signals up to 80 Gbit/s and up to 640 Gbit/s in combination with WDM techniques was investigated in transmission experiments.

Monolithic optoelectronic integrated circuits on InP were developed in technology oriented projects. As well as the WDM transceiver for access networks and 40 Gbit/s photoreceiver OEICs with a bandwidth of 37 GHz for high-speed transmission systems, a polarization diversity heterodyne receiver for OFDM systems, with the highest degree of integration complexity to date, was also fabricated. For application in broadband mobile communication systems the optical generation of millimetre wave signals with frequencies up to 60 GHz with high stability and low phase noise was also investigated.

In continuation of the German Photonics program, a new program KomNet (Innovative Communication) started in May 1998. The target of this program is to convert the results of the Photonics program into products. In collaboration between German IT companies, German Telekom and Institutes, a field system will be built, consisting of a WDM city ring with access networks located in the city of Berlin and, in addition, a 800 km long high-speed trunk line from Berlin to Stuttgart.

Acknowledgments

The work presented in this article was supported by grants from the German Ministry for Education, Science, Research and Technology (BMBF) and from the State of Berlin. The responsibility for the contents rests exclusively with the authors.

References

[1] Saniter J., Hermes Th., Hilbk U. and Westphal F.-J., **"WDM overlay for access networks"**, ECOC'97 Workshop "Multiwavelength Access Networks".

[2] M. Hamacher et al., **"Full-duplex WDM-transceiver PICs"**, Proc. 24th Europ. Conf. on Optical Communication (ECOC '98), 20-24.9.1998, Madrid, ThA07, pp. 639-640.

[3] R.P. Braun, R. Kaiser, D. Rohde, R. Stenzel, D. Trommer, H. Heidrich and G. Großkopf, **"Optical microwave generation and transmission experiments using a monolithically integrated tunable optical signal source"**, Proc. 21st Europ. Conf. on Optical Communication, Brussels, 17-21.9.1995, vol. 3, pp. 1023-1026, post-deadline paper.

[4] S. Diez, R. Ludwig and H.G. Weber,

"All-optical switch for TDM and WDM/TDM systems demonstrated in a 640 Gbit/s demultiplexing experiment", Electronics Letters, vol. 34, no. 8, 1998, pp. 803-805.

[5] H.-G. Bach, W. Schlaak, G.G. Mekonnen, R. Steingrüber, A. Seeger, Th. Engel, W. Passenberg, A. Umbach, C. Schramm and G. Unterbörsch, **"50 Gbit/s InP-based photoreceiver OEIC with gain flattened transfer characteristics"**, Proc. 24th Europ. Conf. on Optical Communication (ECOC'98), ISBN 84-89900-15-9, vol. 1, pp. 55-56, Madrid, 1998.

[6] R.-P. Braun, G. Grosskopf, D. Rohde and F. Schmidt, **"Low phase noise millimetre-wave generation at 64 GHz and data transmission using optical side band injection locking"**, IEEE Photonics Technology Letters, vol. 10, no. 5, pp. 728-730, May 1998.

[7] R.-P. Braun, G. Grosskopf, D. Rohde and F. Schmidt, **"Optical millimetre-wave systems for broadband mobile communications, devices and techniques"**, Invited Paper, 1998 International Zürich Seminar on Broadband Communications – Accessing, Transmission, Networking, ETH-Zürich, Switzerland, February 1998, Conference Proc., pp. 51-58.

C. CASPAR, F. SCHMIDT,
E. SCHULZE AND B. STREBEL

INFLUENCE OF CASCADED CROSSCONNECTS AND DISPERSION COMPENSATION ON TRANSPARENT OPTICAL WDM SYSTEMS

Abstract

The maximum length of a transparent transmission without optoelectronic repeaters is an important parameter for network planning. A single loop test bed and a new double loop test bed were used to investigate the influence of crossconnects and dispersion compensation on the transparency length of WDM links with standard single-mode fibres. The results show that dispersion compensation of 98 % is optimal for post-compensated and pre-compensated fibres with input power levels of + 2 dBm and - 2 dBm in the SMFs and DCFs. The inband crosstalk of each crossconnect should be limited to less than - 40 dB for links of 2000 km length at a 10 Gbit/s transmission rate with 10 cascaded crossconnects and 80 km amplifier spacings.

1. Introduction

Extended high capacity WDM networks are composed of high speed fibre links, complex optical crossconnects (OXCs), amplifiers and add/drop multiplexers. An optical network path concept and an effective network restoration capability can be used in the network [1]. The system components and their properties determine the overall system performance. The influences of cascaded crossconnects, their crosstalk and dispersion compensation of fibres were investigated.

2. Cascaded crossconnects

In WDM networks the routing of optical signals is done by optical crossconnects (OXCs). These crossconnects can be realized as transparent switches, optical space switches, and frequency domain switches. Two critical performance parameters of crossconnects are crosstalk and loss, which influence the maximum length of a transparent transmission. Even a small amount of crosstalk may cause serious problems in network operation in large area multichannel WDM networks, where many crossconnects are cascaded.

Laboratory experiments were done at the HHI using a loop testbed setup to evaluate the influence of crossconnects on network performance. The questions of the number of crossconnects that can be cascaded and the fibre link length that can be bridged without optoelectronic regeneration of the optical signal were investigated to determine the transparency lengths of the links.

The cascadability of crossconnects has been experimentally demonstrated for fibre loops with equally spaced crossconnects [2], whereas so far only simulations have been done for fibre links with non-uniformly located crossconnects [3, 4].

The transmission path can be switched between two different loops with the fibre double loop structure used, one loop containing the OXC and one bridging it (Fig. 1). The signal can therefore be routed to either pass through or bypass the crossconnect. This allows the number of crossconnects in the transmission path to be varied, and also allows the fibre lengths between crossconnects to be independently adjusted. This loop structure has enabled the preparation of transparency length diagrams that show the transparency length as a function of the crosstalk and the number of crossconnects in the signal path.

The experimental loop is realized as an 8-channel WDM system at wavelengths between 1544.53 nm and 1555.75 nm with 10 Gbit/s per channel data rate. In several of the experiments the measurements have been restricted to a single channel only, for reasons of simplicity.

The loop setup is composed of a transmitter, a receiver, and an intermediate double loop fibre link with dispersion compensated fibres (SMFs and DCFs). The link contains fibres, fibre amplifiers (EDFAs), loop switches, a crossconnect, and a filter. The fibre length was chosen to be 162 km without the dispersion compensating fibres. For the experiments the gains and signal round trip lengths of the two loops were made equal to avoid dynamic power peaks of the signal due to the EDFAs.

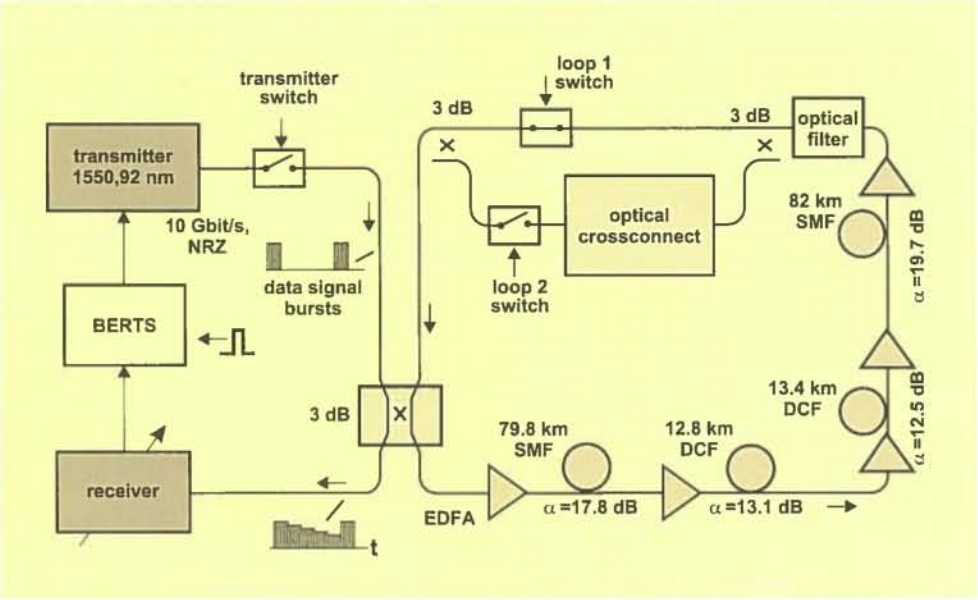

Fig. 1:
Double loop structure (schematic diagram) for the measurement of the transparency length.

The transmitter generated an optical 10 Gbit/s NRZ signal by external modulation with a 215-1 length PRBS at a wavelength of l = 1550.92 nm. It was fed into the loop, which contained standard single mode fibres (SMFs) and dispersion compensating fibres (DCFs). A dispersion compensation scheme with post-compensation and pre-compensation by DCFs was employed. The input power levels of the SMFs and DCFs were adjusted to + 2 dBm and - 2 dBm, respectively. Fibre amplifiers (EDFAs) were used to maintain the power levels in the link. Directional couplers and two computer-controlled acousto-optical switches were inserted to switch between the paths of the double loop. For simplicity, instead of using a typical OXC architecture based on a WDM multiplexer/demultiplexer and switches, the OXC properties were simulated by an attenuator (EDFA) and an adjustable inband crosstalk signal. This allows the influences of loss and crosstalk to be separated from other possible effects. The crosstalk was adjusted to a polarization parallel to that of the signal, which is the worst case.

The transparency length was determined by BER measurements for a BER =10^{-9}. The measurements were done for different receiver input powers, crosstalk levels, number of crossconnects, and fibre link lengths. The achievable fibre link length for a 3 dB penalty was determined by

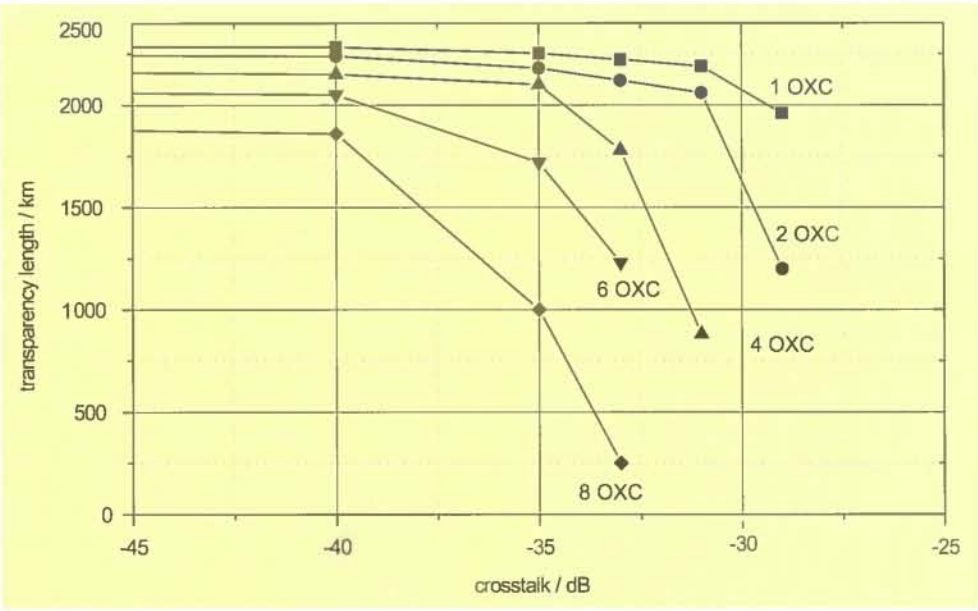

Fig. 2:
Transparency length diagram of a 10 Gbit/s link with crossconnects, measured with decorrelated in band crosstalk and parallel polarization of signal and crosstalk. The parameter is the number of crossconnects.

increasing the fibre link length and number of crossconnects (i.e. the number of signal round trips in the loops). The fibre link length for this 3 dB penalty characterizes the transparency length.

Figure 2 shows the transparency length as a function of the crosstalk level per crossconnect, with the number of cascaded crossconnects as parameter. It can be seen that the transparency length drops slowly with increasing crosstalk if there are only one or two crossconnects and if the crosstalk is less than - 30 dB. The transparency length falls more rapidly if there are more crossconnects. We therefore conclude that crosstalk becomes more critical if many crossconnects are cascaded in the network. To ensure proper WDM network operation, the crosstalk level must not exceed - 40 dB per crossconnect in the case of in-band decorrelated crosstalk with the same polarization as the signal.

3. Dispersion compensation of fibres

In high speed optical networks the transparency length is influenced not only by the crosstalk in the crossconnects, but also by chromatic dispersion, the signal power in the fibre and the polarization mode dispersion. The investigations at HHI concentrated on fibre dispersion compensation and the adjustment of signal power in the SMFs and DCFs to minimize the BER. Several proposals for dispersion compensation of fibres have been made in the literature [5, 6].

The signal power per channel may rise so high in the fibres that self-phase modulation occurs. This effect can partly compensate for the distortion caused by chromatic dispersion.

To investigate experimentally the influence of fibre dispersion and input power on the BER, different dispersion compensation schemes and fibre input power levels were investigated. As testbed, a single loop structure was used in which only the path via the loop 1 switch was implemented (Fig. 1). The loop was composed of two single-mode fibres of about 80 km length each and two dispersion compensation fibres of about 13 km length each. Dispersion compensation was done by post-compensation and pre-compensation using the DCFs. The loop experiments show that 2400 km can be bridged by transparent transmission using proper dispersion compensation and power management in the loop. This corresponds to 15 signal round trips in the loop.

In addition to these experiments, simulations were done at the Deutsche Telekom AG, Berlin, to evaluate possible dispersion compensation schemes and grades (e.g. post-compensation only or both pre-compensation and post-compensation). The simulations took into account chromatic dispersion, self phase modulation, and polarization mode dispersion. From the simulations it became clear that a compensation ratio of 98 % is optimal

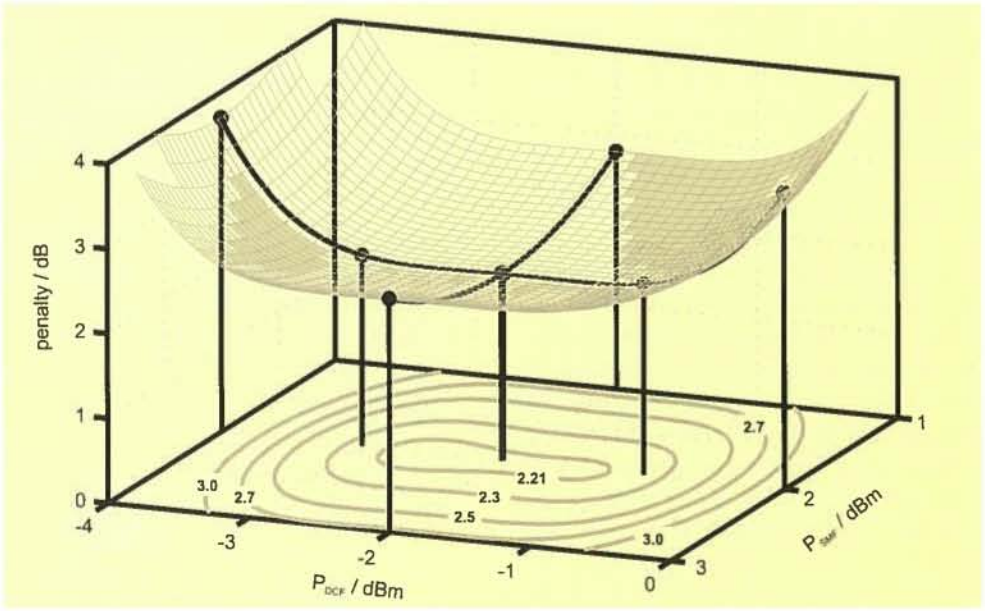

Fig. 3:
Dependence of the BER penalty on the input power levels of the single-mode fibres and dispersion-compensating fibres (dispersion-compensation 98 %).

for cascaded 80 km fibre links if post-compensation and pre-compensation together with suitable power management are used. The same result was obtained in the experiments.

Tests were done using different input power levels for the loop fibres from + 1 to + 3 dBm for the SMF and - 4 to - 1 dBm for the DCF. The bit-error rate was employed as test criterion. From the back-to-back measurements in comparison to the loop measurements the penalty was derived and it is shown in Fig. 3. This figure shows that the optimum transmission, with a minimum penalty of 2.2 dB, is achieved for an input power of + 2 dBm in the SMF and -2 dBm in the DCF. However, the curves are quite flat so that power management in the fibres is not all that critical.

The single-channel measurements as in Fig. 3 were also expanded to multi-channel measurements. These experiments show basically similar results if the power in each channel is regarded.

4. Summary

The influences of crossconnects and dispersion compensation of fibres on the achievable transparent transmission in WDM systems have been investigated. A single loop setup and a new flexible and powerful double loop setup have been constructed to determine the transparency length of WDM links.

Investigations with different numbers of crossconnects, fibre segments of unequal lengths between crossconnects, and variable crosstalk levels have been carried out using the new double loop structure. The experiments show that the transparency length decreases with a growing number of crossconnects and a rising crosstalk level. For 10 Gbit/s links bridging long distances (more than 2000 km), the crosstalk per crossconnect should be limited to less than - 40 dB, assuming in-band decorrelated crosstalk with a polarization parallel to that of the signal. In the setup used, the longest transparency length is obtained at a dispersion compensation grade of 98 % and with power levels of + 2 dBm in the SMF and - 2 dBm in the DCF.

Acknowledgment

The work described here was done by the HHI under a contract with the Deutsche Telekom AG, whose agreement to publish the results is gratefully acknowledged. The responsibility for the contents rests exclusively with the authors.

References

[1] A. Watanabe et al., **"Optical path crossconnect system architecture suitable for large scale expansion"**, J. Lightwave Technol., vol 14, no. 10, Oct. 1996, pp. 2122-2172.

[2] C. Caspar et al., **"4 * 2.5 Gbit/s NRZ transmission experiment over transparent crossconnects with opto-electronic frequency converters and dispersion compensated standard single-mode fiber links"**, Techn. Digest, OECC'98, Makuhari Exhibition Chiba, Japan, July 12-16, pp. 426-427.

[3] B. Strebel et al., **"Optical transparency in future core networks"**, Technical Digest, Photonics in Switching, Stockholm, 1997, pp. 68-71.

[4] B. Strebel et al., **"Loop experiments and simulations for the wavelength division multiplex network signal path"**, **Proc. SPIE**, " Fiber Optic Components and Optical Communication", Beijing, China, 18-19 Sept.1998, vol. 3552, pp. 31-40.

[5] D. M. Rothnie and J. E. Midwinter, **"Improved standard fibre performance by positioning the dispersion compensating fiber"**, Electron. Lett., vol. 32, no. 20, 1996, pp. 1907-1908.

[6] D. Breuer et al., **"Optical schemes for dispersion compensation of standard monomode fibre based on links"**, Optics Comm., 140, 1997, pp. 15-18.

R. LUDWIG, L. KÜLLER,
C. FRÖHLICH, S. DIEZ,
C. SCHMIDT, U. FEISTE AND
H. G. WEBER

AN OPTICAL PULSE SOURCE FOR HIGH BIT RATE OTDM SYSTEMS

Abstract

We describe the properties of an external cavity modelocked semiconductor laser with tunable wavelength, pulse width and repetition rate. This modelocked laser generates optical pulses with pulse widths down to 180 fs and with repetition rates up to 20 GHz in a 120 nm wavelength range near 1.55 µm or 1.3 µm. The generated pulses are close to the transform limit and are therefore suitable for very high speed communication systems. This pulse source is not only highly tunable but is also a compact and mechanically stable device. The pulse source is a subsystem in various functional blocks in a high bit rate optical time division multiplexing (OTDM) system, including transmitters and retiming clock recovery components.

1. Introduction

A pulse source with a pulse width of some picoseconds and a pulse repetition frequency in the GHz range is of interest, particularly for the development of high speed optical communication systems. Monolithically integrated extended cavity lasers are desired for installed systems. However, experimental systems operated in the laboratory require pulse sources with widely tunable wavelength, pulse width and repetition rate.

In this contribution we report on an external cavity modelocked semiconductor laser that was developed for a high speed OTDM system. It is applicable in systems with data rates in excess of 160 Gbit/s. The properties of this tunable modelocked laser (TMLL) are as follows: The pulses are tunable in wavelength over the range 1440 - 1560 nm, in fundamental mode repetition rate over the range 1-20 GHz, and in pulse width over the range 180 fs-17 ps. The fibre-coupled average output power is about -5 dBm. Except for pulse widths less than 500 fs, the pulses have a sech^2 shape with a spectrum close to the transform limit ($\Delta\nu\,\Delta t = 0.316$). These values were measured for a particular TMLL in the 1.5 µm wavelength range. Other TMLLs, including those operating at 1.3 µm, have also been constructed, with similar tunability ranges as above.

Such an optical pulse source is an essential part of an OTDM system such as the one shown in Fig.1. It can be used in various functional blocks in such a system. It was used as a transmitter laser in several all-optical demultiplexing experiments with data rates up to 80 Gbit/s [1]. A TMLL can also be used for retiming in a 3R regenerator. Finally, the TMLL was used for clock recovery in an optical demultiplexer in OTDM transmission experiments.

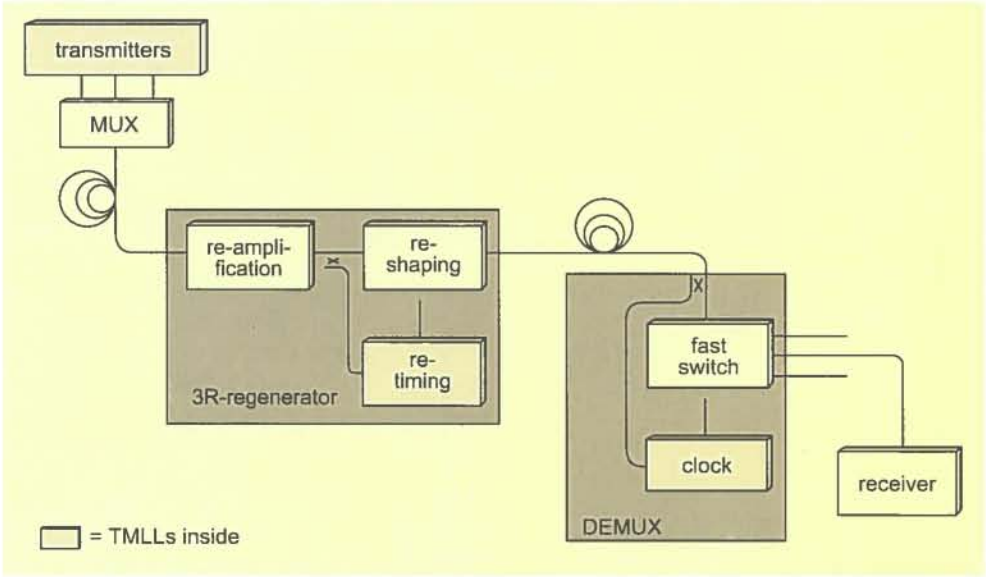

Fig. 1:
Overview of an OTDM system showing the potential for the use of TMLLs.

2. The tunable mode-locked laser (TMLL)

Figure 2 shows a schematic setup of the TMLL. The laser diode is a 1.5 µm InP Fabry Perot laser. One facet of the laser is antireflection (AR) coated. This side is coupled via a GRIN rod lens to a grating. The other facet was bombarded with high energy ions to create a fast saturable absorber (for details see [2]). Compared to a similar external cavity laser (ECL) without an absorber, the threshold current is significantly increased and curves of power versus current show multiple hysteresis. The laser diode is passively modelocked above the threshold. However, for optical communication systems, active mode locking is required.

The complete TMLL is mounted in a standard 19 inch rack unit, together with the DC electronics. A DC bias of 50–100 mA (depending on the wavelength and the repetition rate) and an RF driving power of +30 dBm are applied. The device is turnkey ready and an optical bench is not needed. For practical reasons, the output of the TMLL comprises 30 cm of standard fbre (SMF). The pulses are not compressed by this fibre.

The large tunability ranges of the TMLL are achieved by the following operations. To select the wavelength the grating is rotated. To set the fundamental mode repetition rate the cavity length is changed. The distance between the GRIN rod lens and the laser diode, which directs either a collimated or focussed light beam onto the grating, can also be varied.Finally, different gratings from 150 to 1200 lines/mm were used.

The temporal width, spectral width and peak power of the TMLL pulses were measured for various wavelengths, various gratings, collimated and focussed beams on the grating, and various repetition rates. Selected results are shown in Figs. 3 and 4. If the beam is collimated onto the 150 line/mm grating and transmitted over about 10 m of standard fibre, we obtain nearly transform limited ($\Delta\nu\ \Delta t = 0.316$) sech2 pulses with widths of 570 fs. The 10 m SMF is used to compensate for the small linear chirp that the pulses exhibit directly at the TMLL output. No significant changes in the pulse characteristics are observed by tuning the repetition rate from 1 to 14 GHz and the wavelength from 1440 to 1560 nm.

Inserting the 150, 300, 600, 900 or 1200 line/mm gratings results in pulse widths of 0.57, 1.3, 2.5, 5.1 or 17 ps, respectively. The pulse peak powers vary between 2 and 330 mW. If the beam is focussed on the grating, we obtain corresponding pulse widths of 180, 190, 195, 450 or 910 fs. For example, the minimum pulse width (FWHM) of 180 fs is obtained with a focussed beam on the 150 line/mm grating and with 2 m of standard single mode fibre (D=16 ps/nm/km). In this case the best fit to the autocorrelation trace is the Lorentzian function. The FWHM of the spectrum is 21.41 nm, corresponding to 1.4 times the transform limit.

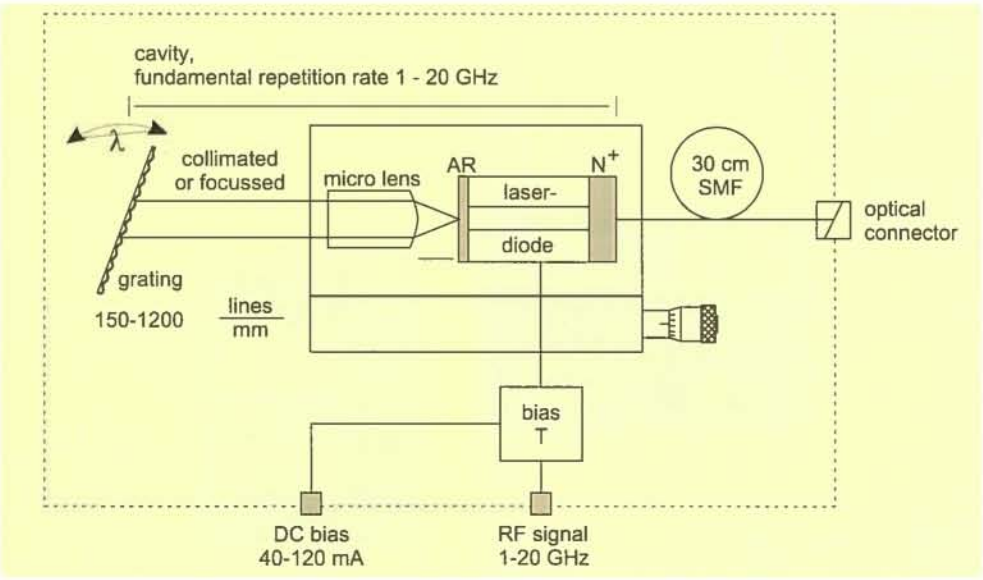

Fig. 2: Schematic setup of the tunable mode locked laser.

The measurement of pulse width was perhaps hampered by the spectral selectivity of the autocorrelator. From our experiments, it can thus not be determined whether the difference in the measured pulse shape results from the pulse shape of the actual pulses or from the measurement technique.

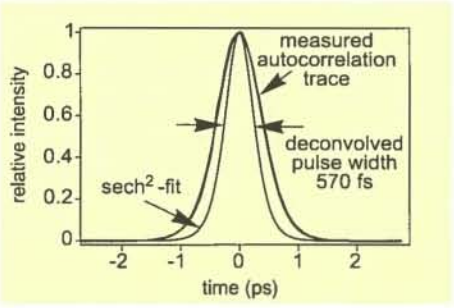

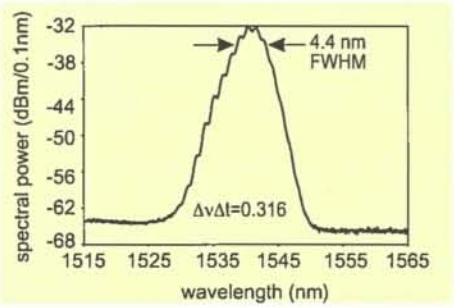

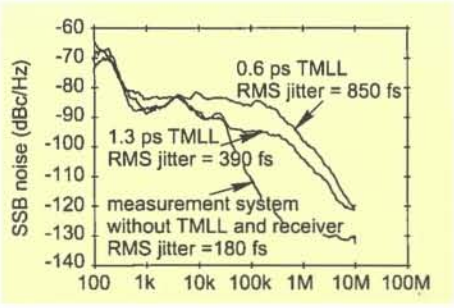

The timing jitter of the TMLL is an important parameter for applications of the TMLL in OTDM systems. Fig. 5 shows measurements of the single sideband (SSB) phase noise versus the frequency offset from the 10 GHz carrier frequency of a 10 GHz pulse train. The measurement system comprised the TMLL driven by a synthesizer, a BER test set and an optical receiver with an RF spectrum analyser. Three sets of measurements are shown in Fig. 5: firstly the SSB noise without the TMLL and optical receiver, which represents the electrical jitter of the measurement system; secondly and thirdly, the SSB noise with 0.6 ps and 1.3 ps optical pulses, respectively. The latter measurements represent a combination of electrically and optically generated phase noise. By using the phase noise measurement utility of the HP 85671A spectrum analyser, we calculated from the data in Fig. 5 RMS timing jitters of 850 fs for the 0.6 ps pulse source and 390 fs for the 1.3 ps pulse source. Measurements with 2.7 ps pulses yielded an RMS jitter below 300 fs. Similar results were obtained by cross-correlation measurements of two TMLLs.

3. TMLL for clock recovery

An important application of the TMLL in an OTDM system is for clock recovery. The clock recovery circuit extracts a timed clock signal from the received data signal at the receiver. To do that, the data signal is coupled into the TMLL at the absorber facet. This causes the TMLL to oscillate at its fundamental mode repetition rate in phase with the data signal. The pulse train generated by the TMLL may for example be used as the clock signal in an all optical demultiplexer.

This technique was demonstrated in a 40 Gbit/s to 10 Gbit/s all-optical demultiplexing experiment [3]. The multiplexed 40 Gbit/s data signal synchronized directly the TMLL at its fundamental mode repetition rate of 10 GHz. This 10 GHz pulse train was fed as a control signal into the monolithically integrated Mach-Zehnder interferometer, which acted as a fast switch in the demultiplexer. Therefore, both the clock recovery circuit and the switch used purely optical signal processing in a very compact arrangement.

We investigated the optical synchronization properties of the TMLL as a clock recovery device. We achieved synchronization of the TMLL within a wavelength range of about $\Delta\lambda = 100$ nm around the data wavelength. The laser remained synchronized when the injected power was changed over a range of up to 20 dB, depending on the wavelength of the injected light. The line width of the synchronized clock pulse was measured to be less than 10 Hz, which is the resolution of the electrical spectrum analyser that was used. We also measured the locking range of the TMLL clock recovery circuit, as follows. We detuned the resonator length of the TMLL

Fig. 3:
Temporal pulse width of the generated pulses.

Fig. 4 :
Spectral pulse width of the generated 570 fs pulses.

Fig. 5:
Single side band (SSB) noise measurements for 0.6 ps and 1.3 ps TMLL pulses.

until the synchronization failed. Then we measured the oscillation frequency of the detuned and free running laser. It turned out that optical locking of the TMLL can be achieved for detunings up to 5 MHz when injecting optical data signal powers up to 3 dBm. Also, the locking range increases with increasing power of the injected data signal, mainly due to a shift of the lower frequency limit.

The pulse width and the optical spectrum of the slave laser were compared in the free running and in the locked state. No significant difference was measured. Synchronization was also possible when the TMLL delivered harmonics ($N(f_0)$ with $N = 1 - 8$ and subharmonics (f_0/N) of the line data rate f_0, with $N = 1 - 112$.

4. Conclusion

We described the properties of an external cavity modelocked semiconductor laser with large tunability ranges for wavelength, pulse width and repetition rate. This modelocked laser generates optical pulses with pulse widths down to 180 fs and with repetition rates up to 20 GHz in a 120 nm wavelength range near 1.55 µm or 1.3 µm. These pulses are among the shortest ever created with an all-semiconductor laser diode system. The generated 0.6 ps $sech^2$ pulses are close to the transform limit. They are therefore suitable for very high speed communication systems and possess the potential to be passively multiplexed up to more than 160 Gbit/s.

This pulse source is not only highly tunable but is also a compact and mechanically stable device. In particular, it is useful for laboratory and high speed system test applications. We reported on the application of this pulse source as a clock recovery device.

Acknowledgments

This work was supported by the German Ministry for Education, Science, Research and Technology (BMBF) and by the State of Berlin under contract 01 BP 436/1 in the national photonics program.

References

[1] S. Diez, R. Ludwig and H.G. Weber, **"All-optical switch for TDM and WDM/TDM systems demonstrated in a 640 Gbit/s demultiplexing experiment"**, Electronics Letters, vol. 34, no. 8, 1998, pp. 803-805.

[2] R. Ludwig, S. Diez, A. Ehrhardt, L. Küller, W. Pieper and H.G. Weber, **"A tunable femtosecond modelocked semiconductor laser for applications in OTDM systems"**, IEICE Trans. Electron., vol. E81-C, no. 2, 1998, pp. 140-145.

[3] R. Ludwig, W. Pieper, A. Ehrhardt, E. Jahn, N. Agrawal, H.-J. Ehrke, L. Küller and H.G. Weber, **"40 Gbit/s demultiplexing experiment with a 10 GHz all-optical clock recovery using a modelocked semiconductor laser"**, Electronics Letters, vol. 32, no. 4, 15 February 1996, pp. 327-328.

B. SARTORIUS,
C. BORNHOLDT, O. BROX,
D. HOFFMANN, M. MÖHRLE
AND H.P. NOLTING

ALL-OPTICAL 3R SIGNAL REGENERATION: INNOVATIVE CLOCK RECOVERY AND DECISION DEVICES

Abstract

Optical signal regeneration is required for the implementation of all-optical telecommunication networks. Critical nonlinear optical processing functions that must be improved for full 3R signal regeneration are optical clock recovery and clocked decisions. A novel device type is presented that can be used for both clock recovery and the decision unit. It is a multi-section DFB laser that is modulated by controlled reflectivity of the laser mirrors. The concept of dispersive mirror modulation and the function of the multi-section laser are described. The required basic functions for signal processing are verified in experiments.

1. Introduction to 3R signal regeneration

In current telecommunication systems light is used only for the transport of signals via point-to-point fibre links. Switching, routing and processing of the signals within the nodes is still performed in the electrical domain. With increasing bit rates and a number of wavelength channels, the repeated opto-electronic conversion combined with electronic signal processing appears as a bottleneck.

Optical solutions for switching, wavelength conversion, demultiplexing, and add-drop functions are under development in order to construct optical crossconnects. In optical networks the signals pass through a variable number of optical amplifiers, cascaded crossconnects and long distance fibre links. All these elements contribute to signal degradation by the accumulation of noise and crosstalk, and to pulse degradation by non-linearities, resulting in a limited transmission distance and a limited number of acceptable nodes in a path in the network. Signal regeneration is required to increase the network size. The regeneration must be performed in the optical domain to maintain the advantages of an all-optical network.

A full 3R signal regeneration scheme consists of Reamplification, Retiming, and Reshaping of the signals [1]. The functional blocks for achieving such regeneration are optical amplifiers, optical clock recovery circuits, and clocked decision circuits. The clock recovery circuit is an optical oscillator that locks in frequency and phase to an injected optical data signal. The output of the clock is a continuous stream of optical pulses, stable in amplitude and time intervals and synchronized to the data stream. Both the clock and the data signal are injected into the decision element. The decision element works as a monostable, generating a pulse if the sum of the two signals exceeds a certain threshold level.

It is evident that optical signal processing requires strong optical nonlinearities. However, for 3R regeneration very special optical transfer functions also have to be designed to realize clocking and decisions. In this paper we report on a new concept that allows the design of all-optical switching functions in novel multi-section laser devices.

2. Q-switched lasers – novel devices for signal processing

A laser can be modulated by controlling the reflectivity of the laser mirrors. Our new functional devices that apply this behaviour are built of at least three sections: a DFB gain section, a phase section and a reflector section (Fig. 1a). The reflector is a DFB section that is operated close to transparency. It has a similar function to a DBR section, but is easier to fabricate [2].

To understand the signal processing operation of the device, we look at the device as a DFB laser with an additional reflector at a very short distance (the length of the phase section). The reflector has a strongly wavelength dependent reflectivity at the lasing wavelength, due to the Bragg grating. Varying the spectral positions of reflector and laser modulates the reflectivity (Q factor of the additional resonator). In a semiconductor the index of refraction depends on the carrier density, and thus

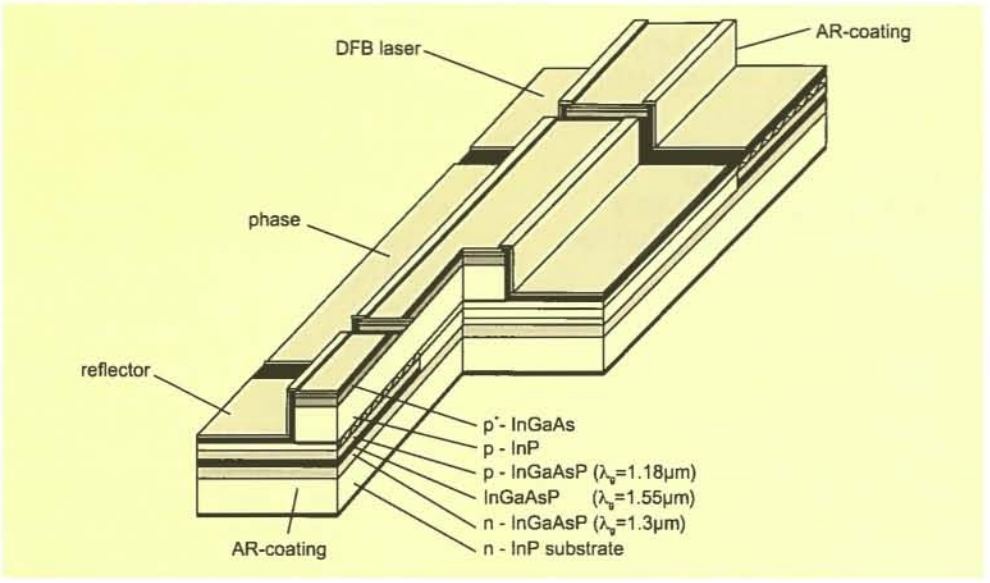

Fig. 1:
(a) Architecture of a Q-switched laser: 3 section DFB laser with DFB laser, phase and reflector sections.

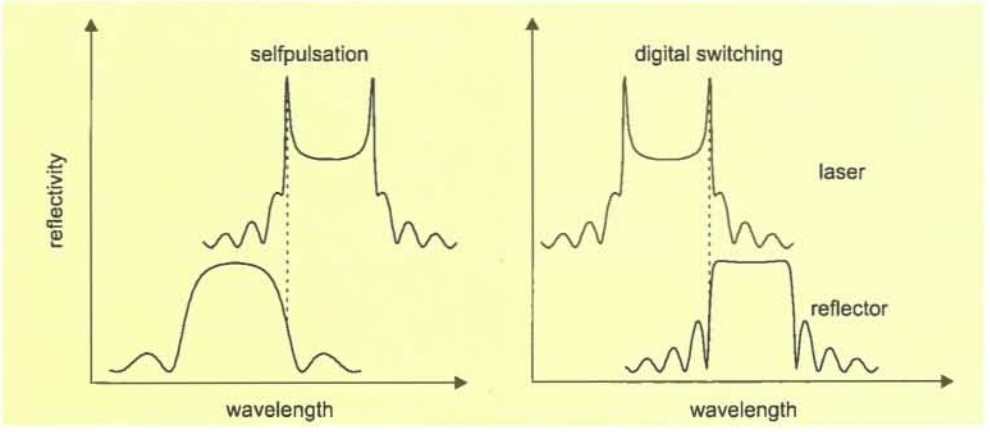

(b) Detuning of laser and reflector section determines the function as either a clock recovery element or a decision element.

modulation of the carrier density modulates the feedback from the reflector (electrical Q switching) [3]. In addition the carrier density in a semiconductor can be optically controlled. Absorption of light generates carriers, and light injected into a highly pumped optical amplifier structure consumes carriers. The required optical control of the dispersive reflector is thus also possible.

The integrated phase tuning section is essential for tuning a selected lasing mode to the correct operating point on one of the reflectivity slopes. Different functionalities can be obtained by operation on the negative or positive slopes of the reflector. We have found both theoretically and experimentally that the negative slope leads to self pulsation, whereas on the positive slope there can be bistable digital switching as in a monostable (Fig. 1b) [4]. Thus an oscillator and a monostable can be constructed from basically the same device; the only difference is the detuning of the Bragg grating relative to the lasing wavelength. For optimized operation the section length, the coupling efficiency of the Bragg grating and the operating currents have to be chosen differently in the two cases. Both devices can be integrated on the same chip with current technology.

3. Decision element

For decision elements the laser section has to be short (about 200 μm). In this case, even at a high pumping level (e.g. 70 mA) lasing is achieved only if there is phase-matched feedback from the reflector section. The dispersive reflector has to be long (300 μm) to obtain a step-like profile of the dispersive reflectivity. A short (150 μm) phase section is chosen to tune the lasing mode to the short wavelength side of the reflector stop band. At a

positive reflectivity slope the chirping of a laser mode that is switched on or off gives a bistable digital switching action, as required for a decision function. Dispersive Q switching means that the laser is switched on and off by varying the phase conditions in the device. To show this, the dispersive reflector was operated close to transparency, and pumping of the laser section was adjusted to a value above the threshold with feedback, but below the threshold without feedback. Switching was performed in three ways:

- The phase current was varied and the output peak power of the single mode emission was measured (Fig. 2a). The laser was switched on and off with a contrast of 30 dB via the phase conditions at fixed pumping.
- Carrier injection into a laser section varies not only the gain but also the index of refraction. Increasing the laser current switches the laser abruptly off. Reducing the pump current switches the laser on again. Bistable switching with a contrast of 30 dB and a hysteresis width of 0.5 mA is obtained (Fig. 2b).
- An optical signal injected into a pumped laser heterostructure causes carrier depletion. This allows us to optically modulate the carrier density and the index of refraction, whereby optical power and pump current have opposite effects. To investigate this optical control the device was set to the operating conditions (74.2 mA) for laser off. Then an optical signal was injected into the device. By increasing the input power we could switch the laser on. Fig. 2c shows the measured all-optical switching characteristic.

Note that the mode of operation of this Q-switched laser is quite different from the well known gain cross-modulation in conventional lasers.

4. Self-pulsating lasers and optical clock recovery

Self pulsations at high and tunable frequencies can be generated by dispersive self Q switching in DFB lasers. One DFB section (300 µm long) is strongly pumped (about 100 mA) and is called the laser section. A second DFB section (150 µm long) is driven with low current (about 10 mA, close to transparency) and acts as a dispersive reflector (the facets are AR coated). The lasing mode has to be adjusted to the negative reflectivity slope (Fig. 1b) to create the self pulsations. Chirping of the lasing mode can then modulate the feedback from the reflector in such a way that the laser switches itself on and off. The integrated phase tuning section (600 µm long) has a spectral control function that can be used for adjusting the required condition. The phase current is therefore the electrical switch for turning on and off the self pulsation. The frequency of the resulting self pulsation is tunable via the laser current and covers the present target value of 10 GHz.

It is important for practical applications that the clock recovery circuitry is not sensitive to wavelength and polarization. Therefore the laser has a bulk heterostructure designed for low polarization dependency. Resonance effects between the injected signal and DFB modes were avoided by setting the DFB grating to 1570 nm, which is spectrally far enough away from the planned data wavelengths close to

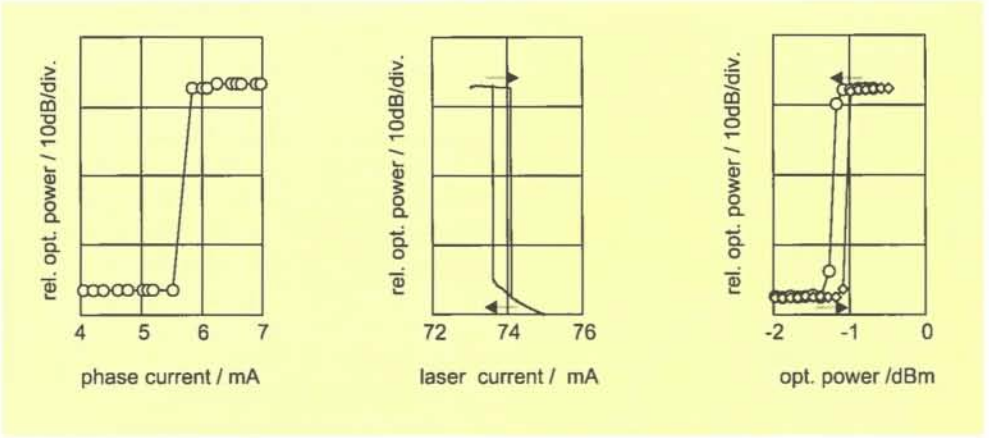

Fig. 2:
(a) Digital Q switching via the phase current at fixed pump current.
(b) Bistable Q switching via the laser current. Note that the laser is switched off with increasing pump current!
(c) Optically controlled bistable switching. The device is electrically operated in the "off" state close to the switching point in (b).

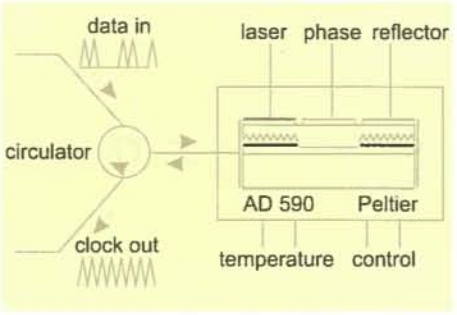

Fig. 3:
Scheme of the clock recovery module.

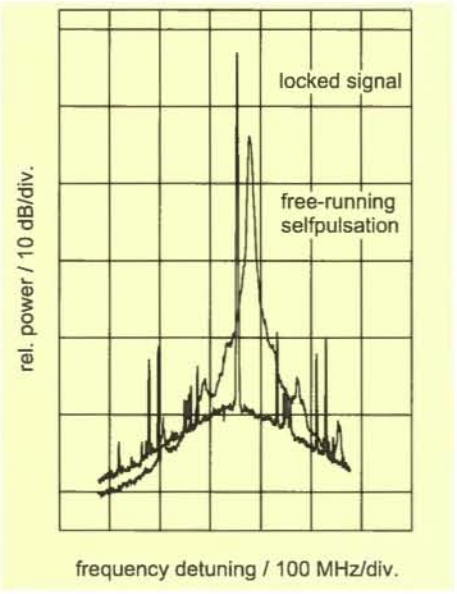

Fig. 4:
Investigation of the all-optical locking function of the assembled module. The two RF spectra shown are those of the 10 GHz free running self pulsation and of the clock signal when synchronized to an optically injected PRBS data pattern.

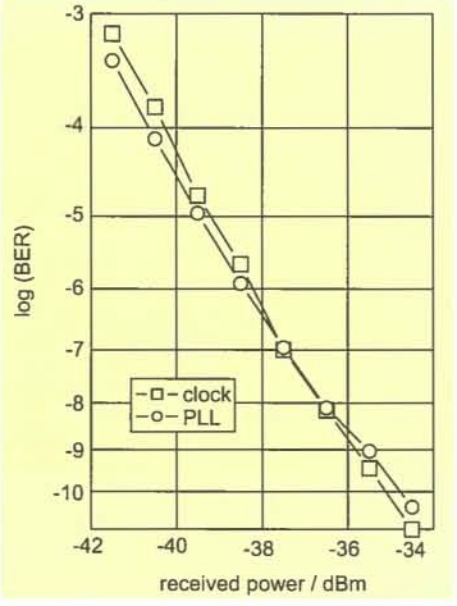

Fig. 5:
BER curve for a 10 Gb/s PRBS 2^{31}-1 signal, measured using both an electronic PLL and the new optical clock for triggering the BER receiver.

1550 nm. All together, wavelength and polarization insensitive synchronization of the self pulsation to optically injected signals is ensured, at least in the spectral range from 1540 to 1560 nm [5].

The device has been packaged into a temperature controlled module with only one fibre attached for both injection of the optical data signals and extraction of the synchronized clock pulses from the device. Input data and output clock signals are separated in a three port circulator (Fig. 3). The function of the optical clock module was investigated at 10 Gb/s. Optical 10 Gb/s PRBS data signals (1550 nm, 3 dBm) were injected into the device, with the self-pulsation frequency was adjusted close to 10 GHz. Synchronization was observed in the RF spectra (Fig. 4). The frequency adjusted itself to the data rate and the RF line became very sharp.

The system quality of the optical clock is characterized by BER measurements in the following way. Firstly, the BER curve of an optical PRBS data signal is measured using an electronic PLL for clock extraction. Then the measurement is repeated using the self-pulsating DFB laser for clock extraction. In Fig. 5 the resulting BER curves are compared. One cannot observe any penalty of the optical clock relative to the electronic PLL for a PRBS word length of 2^{31}-1 in a testbed with a sensitivity of -35 dBm [6]. This shows that the developed all-optical clock has good system performance.

5. System experiments

The penalty-free function of the new optical clock relative to an electronic PLL was demonstrated in a 105 km transmission experiment at 10 Gb/s. The module operates in the range from 1540 to1560 nm, is insensitive to wavelength and polarization, and requires no RF electronics. Bit rate flexible operation is anticipated over the continuous electrical frequency tuning range from 5 to 22 GHz [7].

Error-free demultiplexing from 40 to 10 Gb/s has been demonstrated using the all-optical clock recovery module based on a self-pulsating DFB laser for synchronization [8]. The advantages of self-pulsating lasers for clock recovery are variable speed operation (5-22 GHz for the present device) and simplicity of operation without RF components.

The full benefits of the optical clock will be exploited by using an all-optical DEMUX in a following experiment. Self-pul-

sating DFB lasers and SOA-based demultiplexers can be integrated to create full photonic DEMUX circuits.

6. Summary

Novel all-optical functional elements for 3R signal regeneration are presented. The devices are based on multi-section DFB lasers: a DFB laser, a phase section, and a reflector section. These lasers can be designed as optical oscillators or as monostables. It is shown that these functionalities can be used for both clock extraction and for decisions, which are the most important functions needed for full 3R regeneration.

Static dispersive Q switching has been performed in three ways: changing the phase by (i) current injection into the phase section, (ii) current injection into the laser section, and (iii) photon injection into the laser section.

An optical clock recovery module based on a self-pulsating DFB laser has been developed and tested in system experiments at bitrates of 10 Gbit/s. The optical clock worked as well as an electronic PLL. The device is insensitive to both polarization and wavelength. Bit rate flexible operation is anticipated over the continuous electrical frequency tuning range from 5 to 22 GHz.

References

[1] B. Sartorius, **"All-optical 3R signal regeneration – a challenge for integrated optics"**, SPIE, vol. 2954, pp. 30-41, 1996.

[2] M. Möhrle, B. Sartorius, R. Steingrüber and P. Wolfram, **"Electrically switchable self-pulsations in integratable multi-section DFB lasers"**, IEEE Photon. Technol. Lett., vol. 8, pp. 28-30, 1996.

[3] B. Sartorius and M. Möhrle, **"Mirror modulated lasers, a concept for high speed transmitters"**, Electron. Lett., vol. 32, pp. 1781-1782, 1996.

[4] B. Sartorius, M. Möhrle, S. Reichenbacher, H. Preier, H.J. Wünsche and U. Bandelow, **"Dispersive self Q-switching in self-pulsating DFB-lasers"**, IEEE J. Quantum Electron., vol. 33, pp. 211-218, 1997.

[5] B. Sartorius, M. Möhrle, S. Malchow and S. Reichenbacher, **"Wavelength and polarisation independent all optical synchronisation of high frequency DFB type self-pulsations"**, Electron. Lett., vol. 32, no. 11, pp. 1026-1028, 1996.

[6] B. Sartorius, C. Bornholdt, O. Brox, H.J. Ehrke, D. Hoffmann, R. Ludwig and M. Möhrle, **"All-optical clock recovery module based on a self-pulsating DFB laser"**, Electron. Lett., vol. 34, pp. 1664-1665, 1998.

[7] B. Sartorius, C. Bornholdt, O. Brox, H.J. Ehrke, D. Hoffmann, R. Ludwig and M. Möhrle, **"Bit-rate flexible all-optical clock recovery"**, accepted for OFC '99, San Diego, California, paper FB1.

[8] A. Buxens, A.T. Clausen, H.N. Poulsen, K.S. Jepsen, K.E. Stubkjaer, C. Bornholdt, O. Brox and B. Sartorius, **"40 to 10 Gb/s demultiplexing using a self-pulsating DFB laser for clock recovery"**, Conf. Proc. ECOC '98, Madrid, pp. 507-508, 1998.

H. HEIDRICH, R. KAISER,
M. HAMACHER, P. ALBRECHT,
D. FRANKE, G. JACUMEIT,
S. MALCHOW, W. REHBEIN,
H. SCHROETER-JANßEN AND
R. STENZEL

MONOLITHICALLY INTEGRATED 1.5 µM/1.3 µM TRANSCEIVERS FOR FULL-DUPLEX OPERATION

Abstract

The development of monolithically integrated bidirectional, full duplex WDM GaInAsP/InP transceivers is sketched and first results on 1.5 µm/1.3 µm transceiver PICs are summarized.

1. Introduction

The optical paths to the subscribers in future high capacity optical access networks will require millions of low cost full-duplex WDM transceiver (TRx) components to receive and transmit optical data via a single fibre [1]. A cost reduction for the fabrication of such a huge number of optical modules is ultimately expected with the availability of WDM TRx Photonic ICs (PICs). The crucial importance of such transceiver PICs as the first candidates for high volume PICs has been expressed for example by the 'Full Services Access Network' (FSAN) Group [2] and in the Japanese OITDA Report [3].

HHI developed first 1.5 µm/1.3 µm TRx PICs (transmission at 1.5 µm, detection at 1.3 µm), which were targeted for implementation in a recent system demonstrator in the European ACTS program (project AC065/ BLISS) and for use in datacom point-to-point links. At the same time, an important requirement was that the PIC should operate in a future commercial transceiver module without the need for complex external control circuits (e.g. for temperature stability or signal crosstalk suppression). Moreover, the chosen integration concept is suitable for fabricating WDM TRx PICs to be implemented in FSAN which require much more challenging optical and electrical crosstalk suppression data on chip [3].

2. Design and fabrication

The developed 1.5 µm/1.3 µm TRx PICs are based on inline [6, 7] and y-junction waveguide designs as shown in Fig 1. Those architectures are relatively simple to fabricate and operate with low sensitivity to polarization and wavelength. They also enable smaller chip sizes and higher fabrication yields compared with other transceiver PIC designs that use more complex and space consuming wavelength-selective elements (e.g. arrayed waveguide gratings or grating duplexers [4]).

As active elements we integrated a 1.5 µm strained layer (SL) multi-quantum well (MQW) ridge waveguide (RW) DFB laser for signal transmission as well as wavelength-selective photodiodes for 1.3 µm signal reception and for 1.5 µm optical crosstalk reduction. The optical waves are guided in semi-insulating (si) GaInAsP:Fe/InP:Fe rib waveguides on the chip. All semiconductor layers are grown on a si InP:Fe substrate for maximum electrical crosstalk suppression.

Altogether only three MOVPE growth steps are necessary, including one selective area regrowth of the waveguide and photodiode layers to achieve laser integration by butt coupling. The received optical signals at 1.3 µm are fed from the waveguide into the photodiode by vertical (evanescent field) coupling. The entire fabrication is based on a versatile and extendable integration process with the potential to produce not only different transceiver PICs but also other kinds of PIC architectures (e.g. multi-wavelength sources, optical millimetre wave generators [5]).

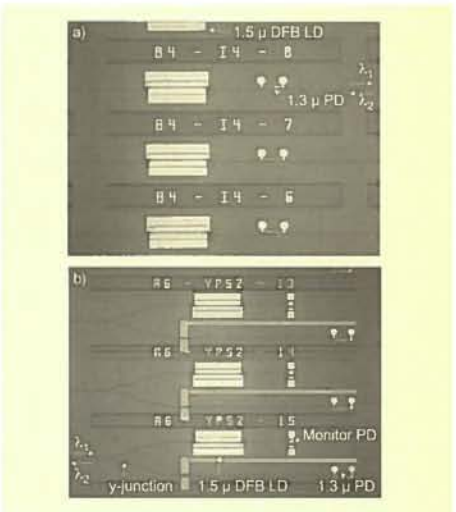

Fig. 1: Photographs of: (a) inline and (b) y-junction 1.5 µm/1.3 µm TR x PICs.

3. Transmitter

The RW laser structure was chosen at first in order to circumvent possible aging effects (due to the selective area regrowth of Fe-doped waveguide layers needed for the laser integration), and to enable the simultaneous formation of both the laser ridge and the passive waveguide rib without lateral alignment. The laser integration is achieved by a special etching procedure to form masked laser mesas and by a selective area regrowth of waveguide and photodiode layers around these areas.

The developed technology has the potential to integrate laser layer stacks of different architectures fabricated in different production lines. A first demonstration of this flexibility was shown by the integration of si optical rib waveguides with 1.5 µm SL-MQW DFB RW lasers on a si InP:Fe substrate at HHI Berlin and 1.3 µm SL-MQW complex coupled (CC) DFB RW lasers (Siemens Munich) on InP:S substrate.

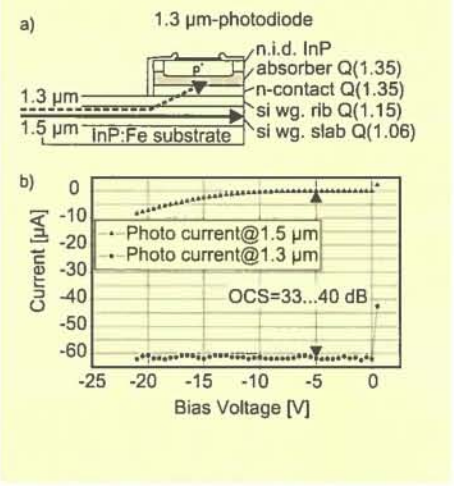

Fig. 2: Wavelength-selective photodiode for 1.5 µm/1.3 µm TRx PICs: (a) Schematic vertical cross section (photodiode length 70 µm, width 18 µm); (b) Photocurrents at 1.3 µm and 1.5 µm vs bias voltage, and optical 1.5/1.3 µm crosstalk suppression [OCS(1.5/1.3)].

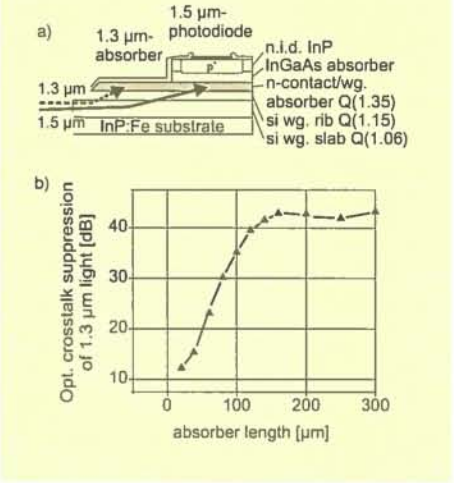

Fig. 3: Wavelength-selective photodiode for 1.3 µm/1.5 µm TRx PICs: (a) Schematic vertical cross section (photodiode length 70 µm, width 18 µm); (b) Optical suppression of 1.3 µm light vs Q-1.35 µm absorber length {OCS(1.3/1.5) = 10*log[Iphoto(1.3) / Iphoto(1.5)]}

4. Wavelength selective photodiodes

An important step towards the future economic fabrication of WDM transceiver PICs was achieved with the development of compact, wavelength-selective photodiodes. Those components suppress unwanted residual laser light in the photodiode and therefore enable maximum optical crosstalk suppression [5].

In the case of 1.5 µm/1.3 µm TRx PICs, the photodiode contains a GaInAsP absorber layer with a bandgap equivalent wavelength of 1.35 µm (Q-1.35).

This material is almost transparent to the residual laser light at 1.5 µm wavelength and absorbs the received signals at 1.3 µm (cf. Fig. 2) [6]. Experimental optical crosstalk suppression data[1] OCS(1.5/1.3) of 33 - 40 dB were obtained for these photodiodes.

In the case of a 1.3 µm/1.5 µm TRx PIC a Q-1.35 waveguide absorber is located in front of a 1.5 µm photodiode with a GaInAs absorption layer (Fig. 2a). From those wavelength selective photodiodes OCS(1.3/1.5) data larger than 40 dB have so far been measured at absorber lengths of 200 µm (Fig. 3).

Theoretical calculations indicate increasing 1.5 µm light suppression by further improvement of the absorber design.

[1]The 1.5/1.3 µm module optical crosstalk suppression OCS (1.5/1.3) is defined as 10*log [photocurrent at 1.5 µm/photocurrent at 1.3 µm] for -10 dBm light power in the optical fibre for transmission and reception.

5. Performance data

The first experimental performance data for TRx PICs and their subelements (Table I) are partly comparable with those of hybrid components and offer the potential for further improvements. An inline and a y-junction PIC have been packaged into a fibre pigtailed butterfly module (Fig. 4).

ing the sensitive fibre fixing operation. Due to this effect the external receiver responsivity decreased from 0.2 A/W to 0.06 A/W. For the inline TRx a simply cleaved fibre was butt-coupled to the PIC input port. The shape of the photodiode allows fibre/chip alignment tolerances greater than 2 µm and acts as an almost 'free space' region for the diverging laser light.

	Inline	y-junction
Ext. response (fibre)	0.35 - 0.45 A/W	0.14 - 0.22 A/W
Dark current photodiodes (PD)	0.25 - 5 nA (T = 20°C, U = -5V) 2 - 110 nA (T = 80°C, U = -5V)	
Opt. crosstalk suppression (OCS)	(37 ± 4) dB	(57 ± 5) dB -no AR coating-
DFB laser (LD) threshold current	15 - 20 mA (L = 400µm, w = 2.7µm)	
Dark current in monitor PD	5 - 50 nA (T = 20°C, U = -5V)	
Photocurrent Monitor PD	7 - 9 mA (T = 20°C, U = -5V) (100 mA injection in 1.5 µm DFB LD)	
PIC output power (100 mA in LD, as cleaved)	0.2 - 1.0 mW, pulsed operation	0.8 - 2 mW, pulsed operation
Chip area	0.5 - 0.7 mm^2	1.0 - 1.3 mm^2

TABLE I: Performance data of 1.5/1.3 µm TRx PICs.

This uncritical behaviour is an important advantage for PIC packaging. Several performance data of an inline and a y-junction transceiver module are summarized in Table II.

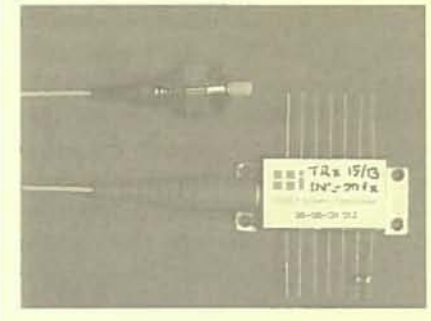

Fig. 4 : 1.5 µm/1.3 µm transceiver module including an inline PIC.

The chips were glued on an alumina subcarrier and bonded. In the case of the y-junction PICs, fibre/chip coupling was performed by using a lensed (tapered) fibre with a lens radius of 10 µm. Unfortunately, the fibre/chip coupling efficiency degraded during hardening of the glue dur-

	Inline	y-junction
Photodiode dark current (25°C, U = -5 V)	10 nA	
Photodiode capacity (U = -5 V)	< 0.7 pF	
Ext. photodiode sensitivity (U = -5 V)	0.45 A/W	0.06 A/W (0.2 A/W before fibre fixation)[2]
DFB threshold currents	15 - 20 mA	
DFB output power in fibre (25°C)	0.1 mW(LD: 31 mA)	0.1 mW(LD:33 mA)
Side mode suppression ratio (LD: 40 mA, 25°C)	35 dBc	> 40 dBc
Opt. crosstalk suppression [1] (photodiode bias: -2 V)	23 dB AR coated [1,3]	26 dB non-AR coated[3]

TABLE II: First performance data of inline and y-junction TRx modules (CW operation).

[1] cf. p. [80]
[2] Due to non-optimized fibre fixation.
[3] Anti-reflection (AR) coated for both wavelengths using a TiO_2/SiO_5 multilayer stack.

The measured optical 1.5/1.3 µm module crosstalk suppression for the inline TRx architecture is relatively small because the high laser power is guided through the photodiode to the PIC input port (Fig. 1). However, for many point-to-point links such a suppression value is sufficient. For the y-junction device the laser light is guided directly to the input port of the PIC without penetrating the photodiode. Only residual non-guided stray light and guided light reflected at the y-junction and AR-coated chip facet can be detected by the photodiode. Therefore, much better module crosstalk suppression is expected. The crosstalk suppression of the y-junction module in Table II is only 3 dB better than that of the inline module, but this result is caused by inefficient fibre fixing (Table II), a non-AR coated chip facet and the fact that optical baffles (e.g. reflectors) for stray light suppression are not integrated. Further improvements will result in much better suppression data.

Bit-error-rate (BER) measurements were made on the y-junction TRx module under simplex and diplex (full duplex) operation at a bitrate of 155 Mb/s using NRZ (2^{23}-1) coded pseudo random bit sequences (PRBS). The receiver sensitivities are -20 dBm under simplex and -16 dBm under diplex operation without external control circuits (BER 10^{-9}). The average optical output power was set to be -10 dBm during the BER experiments in the diplex mode. Taking into account the existing imperfect PIC preparation, packaging and housing, simplex receiver sensitivities of the order of -26 dBm (BER: 10^{-9}) are possible for this TRx module. Better performance data, which can meet the strong FSAN specifications, are expected by further improvements, e.g. improvements of such matters as the optical crosstalk suppression on chip, the external receiver sensitivity, the fibre fixing (integration of an optical spot size transformer!), the facet coating, and the PIC packaging and housing (including electronic preamplifier matching).

The integrated laser and photodiode have also been characterized with respect to their RF response. RIN measurements of a 1.5 µm DFB laser in a fibre pigtailed TRx PIC module indicate a -3 dB laser bandwidth of 6 - 7 GHz. The -3 dB bandwidth of the photodiode is 2 GHz . Both results show that the fabricated transceiver PICs are able to operate at even higher bitrates than 622 Mb/s.

6. Conclusions

First 1.5 µm/1.3 µm TRx PICs have been fabricated with a versatile, extendable integration process. The devices operate without external control circuits and the performance data of the PICs and their subelements were measured at chip level and in first fibre pigtailed modules.

After investigating different TRx PIC architectures, the inline and y-junction designs have been favoured because of their potential for future economic commercial production. The development of a compact wavelength-selective photodiode was an important step towards small size TRx PIC fabrication. The entire fabrication process requires only three epitaxial growth steps, including one selective area MOVPE regrowth for laser integration.

The receiver sensitivities of a first fibre pigtailed TRx module with a y-junction TRx PIC, which is oriented towards a low cost customer product, are -20 dBm under simplex and -16 dBm under diplex operation at 155 Mb/s (BER = 10^{-9}). The causes of the limited crosstalk suppression data were found and adequate improvements will be implemented in the next generation of components.

The developed integration technology and transceiver designs also offer the possibility of fabricating TRx PICs with the potential to meet even the stringent FSAN performance specifications. For this purpose further improvements will be incorporated in future (e.g. optimization of external receiver responsivity, optical and electrical crosstalk suppression, improved fibre/chip coupling through integration of a spot size transformer, and improved packaging).

Acknowledgments

This work was partly supported by the EC (ACTS 065/BLISS), the German Ministry of Education and Research, and the Senate of Berlin (Photonik II). We thank B. Borchert and his team at Siemens, Munich, for providing 1.3 µm laser layer structures, E. Pawlowski at HHI for AR coating of the PICs, and P. Devoldere, M. Morin, G. Térol, and J.-P. Defars at CNET/France for performing the system experiments.

References

[1] J.A. Quayle (Ed.), Full Services Access Network Requirement Specification, http://www.labs.bt.com/profsoc/access/atlanta.html.

[2] W. Warzanskyj et al., Proc. Full Services Access Networks Conf., London, 1996.

[3] OITDA News Lett., 1997.02.10, no. 2.

[4] M. Hamacher et al., Proc. 24th Europ. Conf. on Optical Communication (ECOC'98), 20.-24.09.1998, Madrid, ThA07, pp. 639-640.

[5] M. Hamacher, H. Heidrich and R. Kaiser, HHI Report '97, pp. 85-92.

[6] T.L. Koch and U. Koren, IEEE J. Quant. Electron., vol. 27, no. 3, pp. 641-653, 1991.

M. MÖHRLE, A. SIGMUND,
F. REIER, W. REHBEIN,
R. STEINGRÜBER, H. ROEHLE
AND S. SCHELHASE

INTEGRATABLE HIGH-POWER 1.55 µM INGAASP-INP RIDGE WAVEGUIDE DFB LASERS

Abstract

High-power single-mode 1.55 µm DFB lasers are key components in optical signal processing. At HHI ridge waveguide (RW) type DFB lasers are favoured as transmitters in a variety of different photonic application specified integrated circuits (PHASICS) for optical networks. The main objective of this activity was to develop high power InGaAsP-InP SL RW DFB lasers suitable for monolithic integration into PHASICS. Through optimization of the heterostructure design, RW DFB lasers with single-mode CW output powers of more than 40 mW at 200 mA drive current could be realized.

1. Introduction

The implementation of photonic integrated circuits for WDM telecommunication applications requires the integration of high performance 1.55 µm DFB lasers [1, 2]. To simplify the fabrication technology involved, the use of ridge-waveguide (RW) type lasers appears to be more advantageous than the use of buried heterostructure (BH) lasers, considering that the former needs only two epitaxial steps. However, the high power performance of RW lasers is generally limited by lateral mode instability, leading to undesirable lasing action of a second lateral mode at higher injection currents. The main reason for this behaviour is lateral current spreading in the waveguide layer under the ridge [3, 4, 5]. Another issue for RW lasers relates to the relatively high value of the series resistance due to the small width of the ridge. High values of the series resistance cause excessive heating of the active layer at high injection currents and therefore result in lower output power.

The application of integrated WDM light sources in optical communication systems, e.g. DFB laser arrays or DFB lasers integrated with a combiner network [2], requires the fabrication of devices with emission wavelengths in accordance with the ITU wavelength standard. To keep production costs low, a high yield of devices meeting these wavelength specifications is needed. One way to increase the allowed fabrication tolerances is to use the heat sink temperature as a tuning parameter for wavelength adjustment. To this end DFB lasers are required which are capable of delivering large optical output power over a wide temperature range.

For fabrication of high-power DFB lasers at high yields it is also essential to relax the requirements on the epitaxy-related reproducibility of the exact gain peak wavelength $\lambda_{gain\ peak}$ of the layer structure. The impact of the detuning parameter λ_{DFB}-$\lambda_{gain\ peak}$ on the DFB laser performance is therefore of special interest.

2. Device structure design

In a first step the InGaAsP-InP SL MQW heterostructure was optimized with respect to low threshold current density and high optical output power. The structures were grown by low-pressure (LP) MOVPE. The best values were obtained with an active layer consisting of six 1% compressively strained InGaAsP quantum wells separated by 0.3% tensilely strained InGaAsP barriers (λ_g=1.28 µm). Figure 1 shows the dependence of the threshold current density on the inverse cavity length.

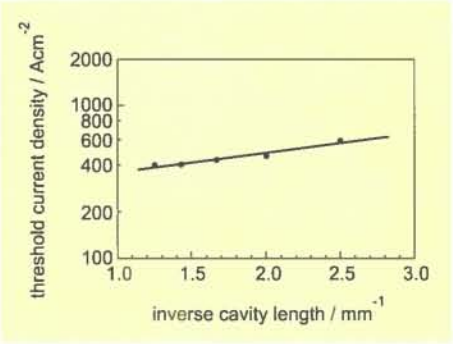

Fig. 1: Threshold current density as a function of the cavity length for InGaAsP-InP SL MQW lasers with 6 quantum wells.

It can be seen that the optimized heterostructure has low values for the threshold current densities for all cavity lengths. The extrapolated threshold current density for infinite cavity length

amounts to 280 Acm^{-2} for the complete structure and to 47 Acm^{-2} for a single quantum well.

To suppress the lasing action of the second lateral mode at high injection currents in RW structures, three different measures can be taken: firstly, by employing a low p-doping level in the p-side waveguide layer, the lateral current spreading under the ridge can be minimized; secondly and thirdly, by using an appropriate waveguide design or small ridge widths, the guiding of the second lateral mode can be weakened. However, the use of small ridge widths leads to unwanted high values for the series resistance. Therefore the maximum ridge width providing lateral single mode emission should be used to obtain maximum CW output power performance of the DFB lasers.

Experimental investigations of the lateral single mode behaviour carried out on ridge waveguide lasers with different stripe widths and different waveguide designs revealed that a combination of all three measures is needed to guarantee stable lateral single mode behaviour.

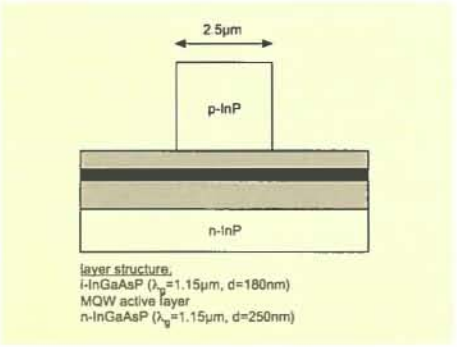

Fig. 2: Heterostructure parameters of the optimized RW laser structure (i = not intentionally doped, n = n-doped, p = p-doped, λ_g= bandgap, d = layer thickness).

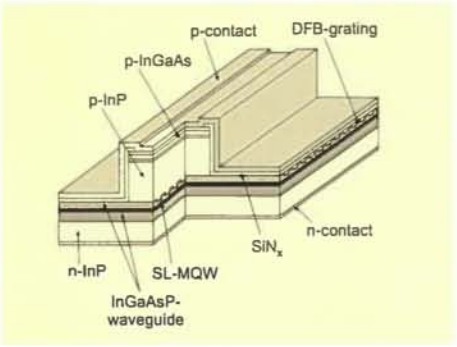

Fig. 3: Schematic cross section of a completed DFB RW laser.

Figure 2 shows a schematic cross section of the optimized ridge waveguide structure.

The upper waveguide layer is not intentionally doped in order to reduce lateral current spreading. The guiding of the second lateral mode is reduced by using an asymmetric waveguide design and a stripe width of 2.5 µm. RW DFB lasers with the described optimized heterostructure design were fabricated using the following technological steps.

The DFB gratings, including a built-in $\lambda/4$ phase shift, were defined by electron beam exposure and etched using a standard CH_4/H_2 reactive ion etching process on the p-side waveguide layer. The coupling coefficient was adjusted to about $30cm^{-1}$. In a second MOVPE growth step the wafers were overgrown with a p-InP cladding layer and a p-InGaAs cap layer. After deposition of the stripe contact metallization, the ridges were formed using reactive ion etching and a subsequent wet etching procedure. Thereafter the ridges were covered with a plasma-deposited SiN_x-layer. On top of the ridge a contact window was opened again using reactive ion etching, followed by the deposition of the p-contact metallization using a sputtering process. Thinning the wafer to a thickness of about 100 µm and deposition of the n-contact metallization completed the fabrication process. Laser devices 400 µm long were cleaved and mounted junction side up on copper heatsinks. Both facets of the DFB lasers were AR coated. Figure 3 shows a schematic cross section of the completed DFB RW laser.

3. Output power

To evaluate the fabrication tolerances concerning the spectral position of the DFB wavelength relative to the gain-peak wavelength, we investigated λ_{DFB} lasers with various grating periods realized simultaneously on the same wafer. The DFB wavelength λ_{DFB} at threshold and a heatsink temperature of 20°C was detuned from the gain-peak wavelength $\lambda_{gain\ peak}$ by -4 nm (structure 1), +5 nm (structure 2) and +14 nm (structure 3), respectively. Fig. 4 shows the temperature dependence of the CW output power behaviour of these DFB lasers between 15°C and 50°C. Each data point represents a typical mean value obtained from about 10 nominally identical DFB laser elements.

The largest optical output power of about 36 mW is achieved with structures 1 and 2 at 20°C. However, all three struc-

tures give output powers of more than 25 mW for temperatures between 15°C and 35°C, and at 50°C values of about 18 mW are achieved at 200 mA driving current.

It should be noted that the side-mode suppression ratio was more than 40 dB in all three structures for all investigated temperatures.

Selected DFB lasers showed output powers even greater than 40 mW at 20°C and 200 mA driving current. Fig. 5 shows the current-dependent output power, the voltage characteristic and the optical spectra of these lasers.

The side-mode suppression is greater than 50 dB. The achieved high output power is to our knowledge the highest value reported for 1.55µm λ/4 phase-shifted InGaAsP-InP RW DFB lasers with both facets AR coated.

4. Fabrication tolerances

The fabrication tolerances to achieve a high yield of high power DFB lasers meeting the ITU specification can be estimated if we know the temperature dependence of the output power (Fig. 4) together with the experimentally evaluated temperature dependence of the DFB wavelength position of $\Delta\lambda_{DFB}$ (T) = 0.1 nm/K. From the fact that the DFB lasers with λ_{DFB}-$\lambda_{gainpeak}$ detunings of -4 nm, +5 nm and +14 nm exhibit similar output power performances (Fig. 4), it can be inferred that the epitaxy wavelength tolerance of the laser heterostructure stack, as indicated by the photoluminescence wavelength, amounts to at least λ_{DFB}-$\lambda_{gainpeak}$ = ±9 nm.

The maximum deviation of the absolute DFB wavelength $\lambda\Delta_{DFB}$ induced by processing uncertainties that can be compensated for by an appropriate adjustment of the heatsink temperature is summarized in table 1. If the required maximum output power is less than 18 mW a deviation of the DFB wavelength of 3.5 nm can be compensated using the complete heatsink temperature range between 15°C and 50°C. For a maximum output power of 25 mW the tolerable deviation is reduced to about 2 nm.

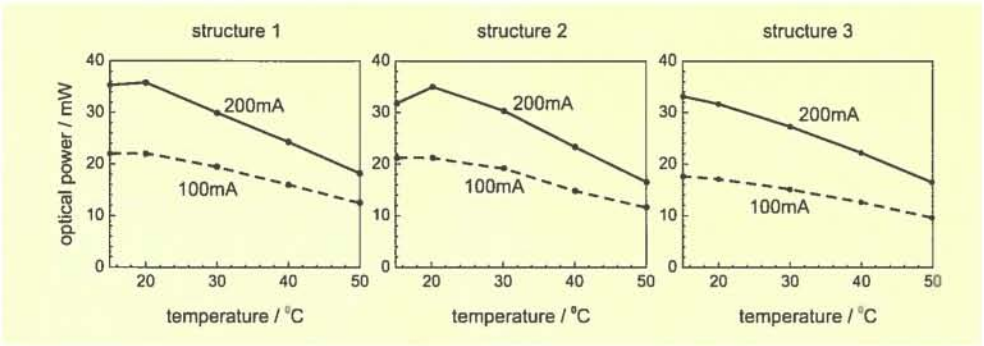

Fig. 4:
CW output power of DFB lasers with λ_{DFB}-$\lambda_{gain\ peak}$ detuning of -4 nm (structure 1), +5 nm (structure 2) and +14 nm (structure 3) at heatsink temperatures between 15°C and 50°C.

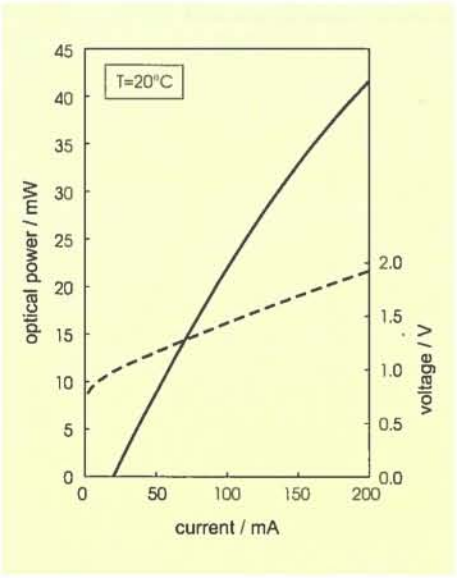

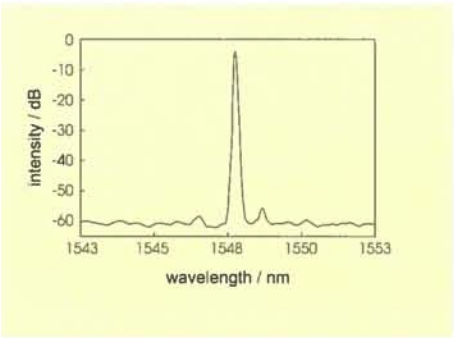

Fig. 5:
Output power, voltage characteristic and optical spectrum of high performance DFB lasers.

Required output power at = 200 mA [mW]	Allowed deviation of the DFB wavelength $\Delta\lambda_{DFB}$ [nm]	Minimum required heatsink temperature range [°C]
≤18	3.5	15-50
≤25	2	15-35

Table 1: Deviation of the DFB wavelength that can be compensated for by tuning the heatsink temperature.

5. Aging tests

To confirm the reliability of the developed high performance DFB lasers we are presently performing aging tests on the devices. During these tests the lasers are operated at 300 mA driving current at an environmental temperature of 70°C.

6. Conclusions

Optimized InGaAsP-InP RW DFB lasers show excellent output power performance in a temperature range between 15°C and 50°C. We have demonstrated that the use of these lasers allows the compensation of the inevitable wavelength deviations (up to 3.5 nm) due to fabrication tolerances by adjustment of the heatsink temperature without losing the good power performance.

The epitaxy wavelength tolerance for high output power was found to be about ±9 nm. Hence the developed integratable RW DFB lasers are well suited for the realization of low cost integrated WDM devices.

References

[1] R. Kaiser, M. Hamacher, H. Heidrich, P. Albrecht, W. Ebert, R. Gibis, H. Künzel, R. Löffler, S. Malchow, M. Möhrle, W. Rehbein and H. Schroeter-Janßen, **"Monolithically integrated transceivers on InP: The development of a generic integration concept and its technological challenges"**, 10th International Conference on Indium Phosphide and Related Materials 98, Ibaraki, Japan, pp. 431-434.

[2] F. Fidorra, M. Möhrle, W. Rehbein, F. Reier, A. Sigmund, R. Stenzel and H. Venghaus, **"Integrated WDM transmitter"**, 24th European Conference on Optical Communication 1998, Madrid, paper TuB08.

[3] M. Aoki, M. Kamori, T. Tsuchiya, H. Sato, K. Nakahara and K. Uomi, **"InP-based reversed-mesa ridge-waveguide structure for high-performance long-wavelength laser diodes"**, IEEE J. Selected Topics in Quantum Electron., vol. 3, pp. 672-682, Apr. 1997.

[4] M.-C. Amann and B. Stegmüller, **"Threshold current analysis of InGaAsP-InP ridge-waveguide lasers"**, IEE Proceedings, vol. 133, pp. 341-348, Dec. 1986.

[5] S.Y. Hu, D.B. Young, A.C. Gossard and L.A. Coldren, **"The effect of lateral leakage current on the experimental gain/current-density curve in quantum-well ridge-waveguide lasers"**, IEEE J. Quantum Electron., vol. 30, pp. 2245-2250, Oct. 1994.

UMBACH, TH. ENGEL AND H.-G. BACH

WITH CONTRIBUTIONS FROM G. G. MEKONNEN, W. SCHLAAK, A. SEEGER, R. STEINGRÜBER, C. SCHRAMM, G. JACUMEIT, W. PASSENBERG, G. UNTERBÖRSCH AND W. EBERT

TECHNOLOGY OF INP-BASED 1.55 µM ULTRAFAST PHOTORECEIVER OEMMICS AND APPLICATION TO 40 GBIT/S RECEIVERS

Abstract

Ultrafast photoreceivers will be needed for future long-haul communication systems operating at bit rates of 40 Gbit/s and for broadband mobile access systems using 38 or 60 GHz carrier frequencies. In this context an integration concept that allows independent device optimization for InP-based OEMMICs for the 1.55 µm wavelength regime is demonstrated. Two different types of photodetectors (PDs), a waveguide-integrated PIN-PD and a top-illuminated MSM PD, each with bandwidths as high as 70 GHz, have been fabricated together with HEMTs with transit frequencies up to 90 GHz. The application to a 40 Gbit/s photoreceiver and its characterization for high bit rate TDM systems are reported.

1. Introduction

The speed requirements of optoelectronic components are rapidly approaching the millimetre-wave regime:

- Time division multiplexing (TDM) systems at bit rates of 40 Gbit/s and beyond are being developed for optical communication networks. Such high transmission rates will be required to serve the bandwidth demand that is predicted for the near future because of the explosive increase of multimedia applications.
- In order to provide mobile access to such broadband services (up to 155 Mbit/s), current research concentrates on the development of fibre-fed cellular networks operating at millimetre-wave frequencies in the 38 GHz and 60 GHz regions.

To solve the challenging task of building optoelectronic components capable of operation at millimetre-wave frequencies, photonic device technologies are merging with the techniques of microwave monolithic integration, leading to OEMMICs (optoelectronic microwave monolithic integrated circuits).

For this purpose, In-Ga-Al-As-P/InP has proven to be a well suited material system. Ultrafast photodetectors for the long wavelength regime 1.3 µm to 1.55 µm are realized by using InGaAs absorption layers, while the excellent material properties, such as high mobility and carrier saturation velocity, make high electron mobility transistors (HEMTs), lattice matched to InP, the ideal candidates for the highest-speed electronics. The monolithic integration of these devices, together with passive components such as MIM capacitors, resistors and coplanar waveguides, is made possible by the availability of semi-insulating substrates and epitaxial layers. An integration concept and a fabrication technology for monolithically integrated high-speed and high-frequency photoreceivers based on InP technology has been developed [1].

In this report, we start with the description of a set of discrete devices and present a general integration concept for ultrafast photoreceiver circuits. In the second part a monolithic InP-based photoreceiver OEMMIC for $\lambda = 1.55$ µm is presented. Its optoelectronic conversion capabilities up to 50 Gbit/s with RZ and NRZ PRBS data streams are demonstrated. The applications of narrow-band photoreceivers in the 38 GHz and 60 GHz regimes [2, 3] is presented elsewhere in this annual report.

2. Ultrafast optoelectronic and electronic devices on InP

A set of devices for the millimetre-wave regime has been developed based on the InP material system for use in coplanar waveguide circuits, including two different types of ultrafast photodetectors, the HEMT, and passive millimetre-wave components. As ultrafast photodetectors for 1.55 µm, both a waveguide-integrated PIN PD (p-i-n photodetector, shown in Fig. 1) and a top-illuminated MSM PD (metal-semiconductor-metal photodetector, shown in Fig. 2) were successfully fabricated. Both devices used an InP-based MOVPE layer stack.

In general, there are advantages and disadvantages of these two concepts (top

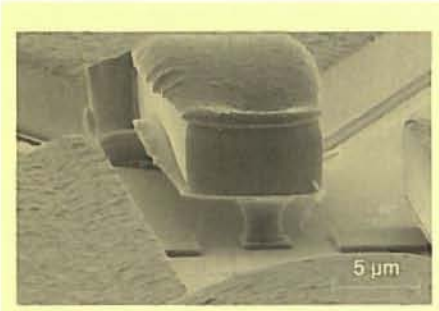

Fig. 1:
SEM picture of a waveguide-integrated PIN PD showing air bridge connection to the active area.

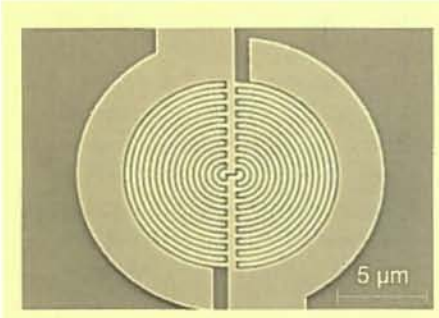

Fig. 2:
SEM micrograph of a top-illuminated MSM PD with 0.2 µm interdigitated electrodes.

illumination and waveguide integration). A top-illuminated photodetector needs a less complicated layer stack and fabrication process as compared to the waveguide-integrated solution. However, at millimetre-wave frequencies the bandwidth-to-trade-off of top-illuminated photodetectors becomes a serious limitation, whereas the waveguide-integrated photodetector with evanescent field coupling of the light offers the possibility of enhancing the transit-time-limited electrical bandwidth by reduction of the absorption layer thickness, but without decreasing the responsivity.

For operation in the millimetre wave range, the MSM PD needs a sub-half micrometre interdigitated electrode structure, which requires advanced lithography techniques such as electron-beam writing. The PIN PD requires a well controlled process step for diffusion of p-doped zones into the layer stack. The series resistance has to be minimized and low-field regions have to be avoided by an appropriate fabrication process. The MSM PD offers a lower intrinsic capacitance, which leads to a higher RC frequency limit than for the PIN PD. On the other hand, the curved electric field lines in the MSM PD lead to longer transit times for the same thickness of the absorption layer.

Accordingly, the top-illuminated MSM PD achieves a 3 dB bandwidth of 70 GHz [4] and a 0.08 A/W responsivity, whereas the waveguide-integrated PIN PD has a responsivity of 0.35 A/W, a bandwidth of 70 GHz and excellent high-power-handling capabilities [5].

The HEMT is made of a lattice-matched InAlAs / InGaAs / InP layer stack grown by MBE. In order to achieve transit frequencies f and maximum frequencies of oscillation f_{max} beyond 100 GHz and 200 GHz, respectively, the gate length of the HEMTs has been reduced to the sub-quarter-micrometre range. This was achieved by developing a reproducible electron-beam lithography process and subsequent recess etching. As a result the fabrication of trapezoidal 0.25 µm gates with excellent uniformity and reliability has been achieved. Furthermore, the fabrication of 0.2 µm mushroom-shaped gates led to f_T/f_{max} of 90/180 GHz. Figure 3 shows a microphotograph of the cross section of a mushroom gate, while Fig. 4 shows a completed HEMT structure.

Coplanar waveguides (CPW) with sufficiently thick metallization are used as low loss and low dispersion interconnections for millimetre-wave signals, leading to transmission losses of less than 0.22 dB/mm (at 38 GHz, 50Ω). The MIM capacitors and NiCr resistors were designed for minimal perturbation of the CPW geometry.

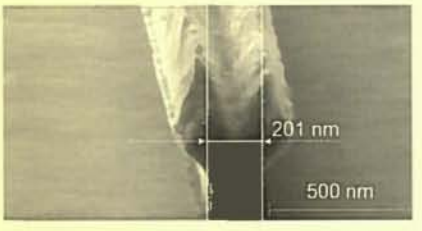

Fig. 3:
SEM picture showing the cross section of a 0.2 µm mushroom-shaped HEMT gate.

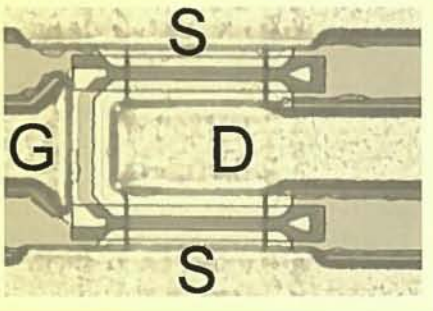

Fig. 4:
Microphotograph of an InAlAs/InGaAs HEMT in a U-type double gate formation.

3. Integration concept

The main advantages of monolithic integration as compared to hybrid solutions are increased device uniformity, lower production costs and, especially for ultrafast applications, reduced parasitics. However, the performance of integrated devices must not be degraded due to the integration process itself. The key issue for a successful realization of OEMMICs is therefore to combine devices that individually offer state-of-the-art performance. This can only be achieved if the integration concept allows the separate optimization of each device without reducing the performance of the other constituents. Hence, the integration concept presented here is based on separate layer stacks for the photodetector (PIN PD or MSM PD) and the high-electron mobility transistor (HEMT).

Following this concept, a basic integration process was developed that is suited for fabricating either PIN HEMT or MSM HEMT photoreceiver OEMMICs. The integration schemes of the two types of photoreceiver OEMMICs are shown in Fig. 5. The process consists of an MOVPE growth of the photodetector and waveguide layers and an MBE regrowth of the HEMT layers, taking advantage of the rather low growth temperature of MBE. For the waveguide-integrated photodetector the MBE regrowth takes placeon the waveguide layer. Therefore the waveguide material has to be semi-insulating, which is accomplished by the use of Fe doping.

Several process steps, such as the deposition of metallization or SiNX layers, are used for multiple purposes and for different devices of the OEMMIC, thus significantly reducing the processing effort.

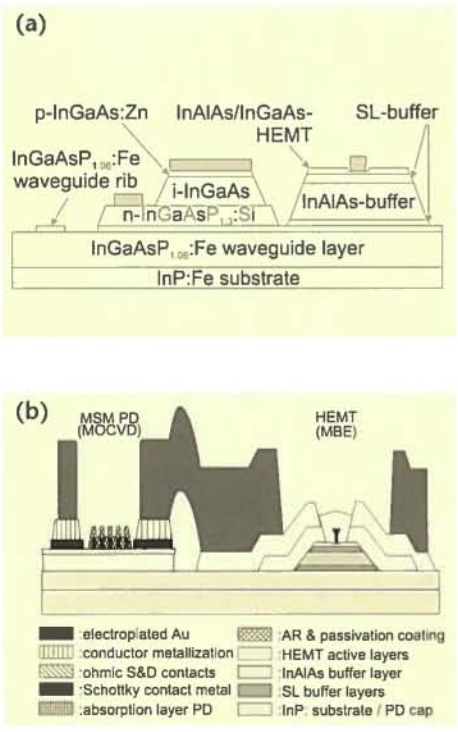

4. Fabrication technology

For the PIN-HEMT integration the waveguide and PIN PD layers are grown in one run by MOVPE comprising Fe-doped InGaAsP (λ_{gap} = 1.05 µm) waveguide slab and rib layers, an InGaAsP (λ_{gap} = 1.3 µm) n-doped contact layer and an undoped InGaAs absorption layer, capped by an InP etch stop layer. Alternatively, for the MSM HEMT integration, a stack consisting of a 50 nm InP:Fe cap layer, a 200 nm InGaAs:Fe active layer and a 300 nm InP:Fe buffer layer is grown by MOVPE on a semi-insulating InP:Fe substrate.

In both cases the HEMT mesas are formed by MBE regrowth of an InAlAs/InGaAs lattice-matched layer stack and subsequent selective wet chemical etching. The waveguide and photodetector mesas are built by wet chemical and reactive ion etching steps.

For the PIN PD, Zn diffusion from the gas phase is used to form the p-type region and a self-aligned etching of the active layer is used. For the MSM PD the interdigitated electrodes (0.2 µm minimum finger width and spacing) are written in a two-layer resist by e-beam lithography, followed by the evaporation and lift-off of a 110 nm Pt/Ti/Pt/Au layer stack.

The subsequent MMIC processing includes the formation of the NiCr resistors and MIM capacitors, passivation and the metallization for the conductors and air bridges. It starts with the formation of ohmic source and drain contacts and n-type ohmic contacts of the PIN PD using alloyed Ge/Ni/Ge/Ni/Au. Coplanar integrated resistors are fabricated by co-evaporation of Ni and Cr. Two different e-beam gate processes have been established. Quartermicrometre trapezoidal gates were fabricated to achieve high process yield. Alternatively, mushroom-shaped gate electrodes with lengths from 0.18 µm to

Fig. 5:
(a) Integration scheme of a PIN HEMT photoreceiver (Au-plated interconnect layers not shown).
(b) Integration scheme of the MSM HEMT photoreceiver.

0.22 µm were fabricated. For this purpose we employ a three-layer resist, followed by the evaporation and lift-off of a 375 nm Pt/Ti/Pt/Au layer stack.

Silicon nitride is deposited in a PECVD reactor, and serves variously as an antireflection coating in the MSM HEMT process, as passivation for the HEMTs, and as the insulator for the MIM capacitors. An evaporated Ti/Au layer forms the ground planes and interconnections. Finally a gold electroplating process is employed to build air bridges.

Based on this general OEMMIC fabrication process, a library of automated parametric layout generators for all the devices has been implemented in the MENTOR Graphics ICgraph environment. This drastically reduces the effort needed for mask design. For the circuit design of the OEMMICs, equivalent circuit models of the devices have been developed using the HP EEsof libra microwave design environment. Apart from different types of HEMTs (e.g. as in Fig. 4) and photodetectors, a variety of passive devices and coplanar waveguide elements is included in the library. Some examples are given in Fig. 6.

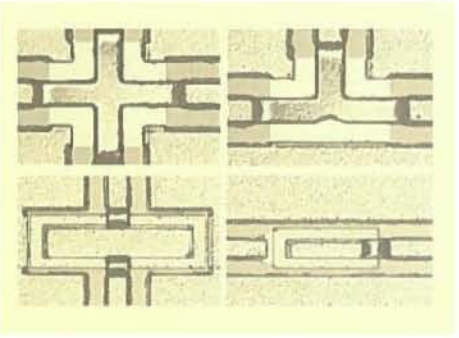

Fig. 6: Top left: CPW X-junction. Top right: CPW T-junction. Bottom left: CPW termination capacitor. Bottom right: CPW coupling capacitor.

5. 40 Gbit/s broadband photoreceiver OEMMIC

The fabrication process described above was applied to the realization of broadband photoreceiver OEMMICs to be used in 40 Gbit/s TDM systems [6]. In order to achieve a flat transfer function and a small group delay variation, a travelling wave amplifier (TWA) design was preferred. Circuit simulations of the receiver transimpedance revealed that, by scaling down the HEMT gate length from 0.6 µm to approximately 0.2 µm and by appropriately matching the gate line termination resistance, a considerable increase of the bandwidth from 28 GHz to more than 42 GHz could be obtained. At the same time the flattened transfer characteristic of the transimpedance vs frequency curve is preserved [7].

The integrated photoreceiver was characterized up to 50 GHz by heterodyne measurements of the power transfer function at a wavelength of 1.55 µm. The frequency response is shown in Fig. 7a, and corresponds to an amplifier gain of about 8 dB with respect to the power delivered from the PIN PD. The observed 3 dB bandwidth exceeds 35 GHz, achieved in the presence of some undulations of the transimpedance Z_T. The distributed amplifiers themselves even show a transimpedance cut-off frequency in the range of 38-42 GHz with an amplitude ripple of Z_T of only ±1 dB in the passband (Fig. 7b). This proves that the properties of the fabricated HEMTs and passive components are accurately described by our circuit simulation library. The high bandwidth (up to 37 GHz) of the photoreceivers makes them suitable for optical data reception at bit rates up to 50 Gbit/s, as will be shown in the following sections.

The measurement setup for generating and detecting 40 Gbit/s RZ data signals comprises a laser pulse source (LKF Advanced Optics, hybrid mode-locked diode laser) with FWHM ≈ 3 ps and 10 GHz repetition rate. The RZ pulses are modulated by a 10 Gbit/s bit pattern generator and then optically multiplexed to obtain a 40 Gbit/s RZ data stream. The averaged optical input power was -3 dBm. The PIN TWA receiver OEMMIC was biased at a drain voltage of 2 V (I_d =106 mA) and a 2 V photodiode reverse voltage. The average photodiode current was 130 µA. Figure 8 shows the electrical output signal (inverted) after converting the optical RZ input stream. The electrical RZ signal reaches zero level within the 25 ps bit period and has a well opened eye of approximately 35 mV_p output value. This eye pattern quality is maintained up to approximately 500 mV_p output voltage, so that the receiver OEMMIC could drive any following digital decision circuitry.

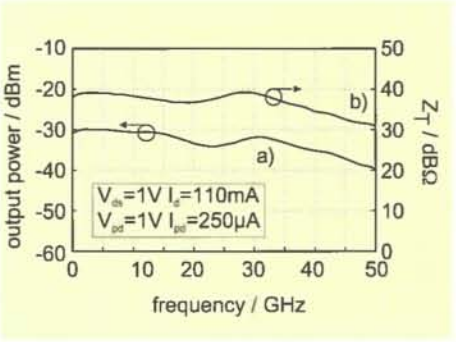

Fig. 7:
(a) Heterodyne measurement of the frequency response of the receiver OEMMIC at λ = 1.55 µm.
(b) Transimpedance of the integrated amplifier.

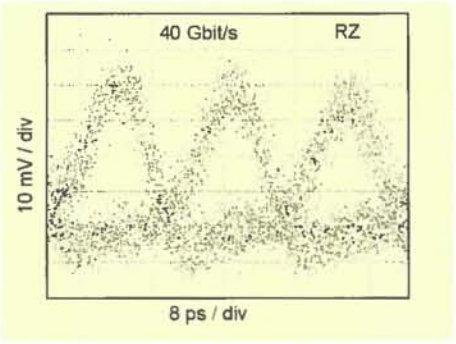

Fig. 8:
Measured 40 Gbit/s RZ eye pattern of the PIN TWA photoreceiver OEMMIC (inverted output).

6. Derivation of eye pattern from heterodyne-measured frequency characteristics

For predicting the eye pattern behaviour of photoreceiver OEMMICs and of packaged modules for various codings (e.g. RZ or NRZ) and at arbitrary bit rates, a procedure was established that is based solely on a heterodyne measurement of the magnitude of the optoelectronic power transfer function.

For applying FFT and IFFT convolution methods, the phase of the transfer function is required. It was proved using the circuit simulator that the integrated TWA behaves approximately as a minimum phase system in the relevant frequency range up to 50 GHz. This means that the phase $\theta(\omega)$ can be calculated from the magnitude $H(\omega)$ by means of the Hilbert transform. $H(\omega)$ is extended beyond 50 GHz with a decay of -140 dB/dec, as known from circuit simulation.

However, the variation of the group delay $\tau_g = -d\theta/df$ (-360°) is more relevant than the phase information. We proved that the group delay obtained by differentiating the phase information is almost equal to the original group delay, which was directly calculated using the circuit simulator for reference. Now, with the measured magnitude $H(\omega)$ and the phase information of our OEMMICs and modules, the receiver output bit pattern can be calculated by standard convolution methods. One example is given in Fig. 9, which shows the synthesized 40 Gbit/s RZ-coded output eye pattern of our receiver OEMMIC. This calculated eye pattern is closely comparable to the measured one (Fig. 8).

For ETDM system applications, the photoreceiver conversion properties of NRZ-coded signals is of special interest. Fig. 10 shows the simulated NRZ eye pattern of our photoreceiver OEMMIC at a bit rate of 50 Gbit/s, using the same evaluation procedure as before. The eye pattern appears well opened, so that there is sufficient reserve for the operation of future pig-tailed modules containing these devices at 40 Gbit/s.

7. Conclusions

A general integration concept for the fabrication of ultrafast InP-based OEMMICs is presented. This comprises either MSM PDs with 0.2 µm finger spacings or waveguide-integrated PIN PDs, both with bandwidths of 70 GHz, together with InAlAs / InGaAs HEMTs with 0.2 µm gate lengths and passive millimetre-wave components.

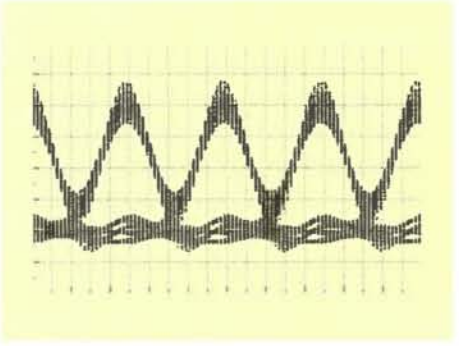

Fig. 9:
40 Gbit/s RZ eye pattern (1024 bit) of the photoreceiver OEMMIC, as deduced from the magnitude of the heterodyne-measured frequency characteristics, assuming a minimum phase system (noise neglected).

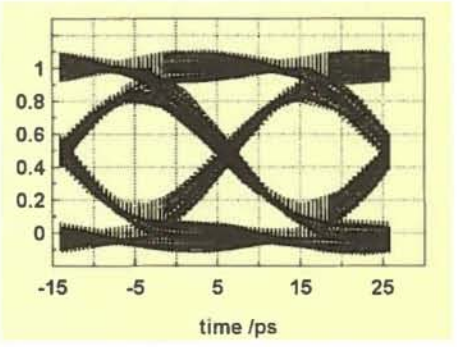

Fig. 10:
50 Gbit/s NRZ eye pattern (1024 bit) of the photoreceiver OEMMIC, as deduced from the magnitude of the heterodyne-measured frequency characteristics, assuming a minimum phase system (noise neglected).

A consistent concept of device libraries employed during mask-layout and device modelling has led to a straightforward and reliable design process for the OEMMICs. The fabrication process is applied to a 40 Gbit/s broadband photoreceiver and to 38 GHz and 60 GHz narrow-band photoreceivers. Broadband 1.55 µm photoreceiver OEMMICs with flattened transfer characteristics of the integrated amplifier transimpedance up to 37 GHz have proved to be suitable for 50 Gbit/s transmission systems using an NRZ coding format.

Acknowledgments

The authors thank V. Breuer of the Institute for Microwave Technology, TU Berlin, for noise measurements on HEMTs.

The work concerning the MSM PD activities was carried out in collaboration with the group of Prof. Bimberg from the Institute for Solid State Physics, TU Berlin. Th. Engel is funded by the NaFöG program of the Senate of Berlin.

The authors would like to thank S. van Waasen and R. Bertenburg from FG HLT-GH-Duisburg for TWA design and fruitful discussions. This joint work was funded by the German BMBF and the Senate of Berlin under the PHOTONIK II program.

References

[1] A. Umbach, S. van Waasen, U. Auer, H.-G. Bach, R. M. Bertenburg, V. Breuer, W. Ebert, G. Janssen, G. G. Mekonnen, W. Passenberg, W. Schlaak, C. Schramm, A. Seeger, F.J. Tegude and G. Unterbörsch, **"Monolithic pin-HEMT 1.55 µm photoreceiver on InP with 27 GHz Bandwidth"**, Electron. Lett., vol.32, 23, pp. 2142-2143, 1996.

[2] Th. Engel, A. Strittmatter, W. Passenberg, A. Umbach, W. Schlaak, E. Dröge, A. Seeger, R. Steingrüber, G. G. Mekonnen, G. Unterbörsch, H.-G. Bach, E. H. Böttcher and D. Bimberg, **"Narrow-band photoreceiver OEIC on InP operating at 38 GHz"**, IEEE Photon. Technol. Lett., vol. 10, no. 9, pp. 1298-1300, 1998.

[3] Th. Engel, A. Strittmatter, W. Passenberg, A. Seeger, R. Steingrüber, G.G. Mekonnen, G. Unterbörsch and D. Bimberg, **"Design, fabrication and characterization of narrow-band photoreceiver OEICs based on InP"**, IEEE LEOS'98 Annual Meeting, Orlando, USA, paper TuJ1, 1-4 December 1998.

[4] E. Dröge, E. H. Böttcher, D. Bimberg, O. Reimann and R. Steingrüber, **"70 GHz InGaAs metal-semiconductor-metal photodetectors for polarisation-insensitive operation"**, Electron. Lett., vol.34, no.14, pp. 1421-1422, 1998.

[5] G. Unterbörsch, D. Trommer, A. Umbach, R. Ludwig and H.-G. Bach, **"High-power performance of a high-speed photodetector"**, Proc. 24th Europ. Conf. on Optical Communication (ECOC'98), Madrid, Spain, ISBN 84-89900-15-9, vol. 1, pp. 67-68, 1998.

[6] S. van Waasen, A. Umbach, U. Auer, H.-G. Bach, R. M. Bertenburg, G. Janssen, G.G. Mekonnen, W. Passenberg, R. Reuter, W. Schlaak, C. Schramm, G. Unterbörsch, P. Wolfram and F.J. Tegude, " **27 GHz bandwidth high speed monolithic integrated optoelectronic photoreceiver consisting of a waveguide fed photo-diode and an InAlAs/InGaAs-HFET-traveling wave amplifier"**, IEEE J. Solid State Circuits, vol. 32, no. 9, pp. 1394-1401, 1997.

[7] H.-G. Bach, W. Schlaak, G.G. Mekonnen, R. Steingrüber, A. Seeger, Th. Engel, W. Passenberg, A. Umbach, C. Schramm and G. Unterbörsch, **"50 Gbit/s InP-based photoreceiver OEIC with gain flattened transfer characteristics"**, Proc. 24th Europ. Conf. on Optical Communication (ECOC '98), ISBN 84-89900-15-9, vol. 1, pp. 55-56, Madrid, Spain, 1998.

B. KUHLOW AND
G. PRZYREMBEL

AWG-BASED DEVICE FOR A WDM OVERLAY PON

Abstract

A novel concept has been developed for overlaying a power-splitting PON in one wavelength band with a WDM PON in another wavelength band. Two versions of such a device for different broadcast wavelengths have been realized in silica technology. Eight channels of a WDM band around 1.55 µm wavelength with 200 GHz spacings are overlayed on a 1 to 8 power split broadcast signal at a wavelength of either 1.31 µm or 1.50 µm. The key component is a 2-band MUX device that relies on a specially designed arrayed waveguide grating (AWG) integrated with a 1 to 8 power splitter ahead of it.

1. Introduction

The upgrade of an existing passive optical network (PON) for broadcast applications (e.g for CATV) with broadband interactive services by employing high density wavelength division multiplexing (WDM) represents an attractive way of adding additional features to the access network and of exploiting more of the huge optical fibre capacity. For a WDMPON with well defined wavelength channels, the broadcast signal and the WDM channels can be distributed over the same optical network, each using separate wavelength bands.

We have realized such a WDMPON device that allows the overlaying of a WDM network on a broadcast network [1]. This device distributes the light broadcast signal from one input port evenly to N output ports, either at 1.31 µm or at 1.50 µm, and overlays N demultiplexed WDM channels in the 1.55 µm band. The device functionality is shown in the block diagram in Fig. 1.

The key component is an arrayed waveguide grating (AWG) for multiplexing two or more wavelength bands or broadcast wavelengths (2-band WDM MUX) with low loss and low crosstalk. This solution is very flexible and can easily be adapted to different network demands. It offers a wide choice of broadcast and WDM wavelengths, an easy way to increase the channel numbers, and even the possibility of overlaying additional wavelength bands with special features.

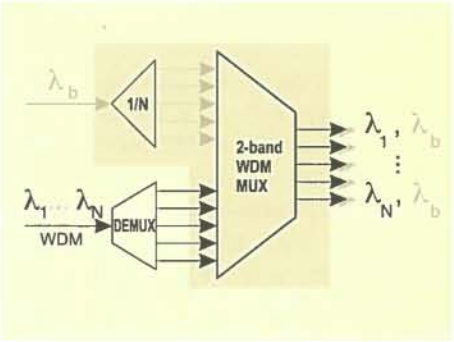

Fig. 1:
Basic function block of a WDM broadcast MUX system, including 1/N power splitter, WDM demultiplexer (1 × N – DEMUX), and 2-band WDM multiplexer (2N × N – MUX).

Some integrated WDMPON devices have already been reported for specific wavelength band separations. One solution, which enables an eight channel 1.31 µm broadcast with a 1.55 µm WDM overlay, uses individual coarse wavelength selective 1×2 couplers in each path, but waveguide crossings are inevitable [2]. Another solution that is suitable for much closer wavelength bands uses a special AWG with a chirped grating [3].

Our concept can be adapted to a wide span of band separations $\Delta\lambda_{band}$. The main topic to be reported here is this new 2-band MUX device in combination with the 1/N distribution function shown in the shaded block of Fig.1. However, the 8-channel AWG DEMUX with 200 GHz channel spacing, which is incorporated in both devices, but not directly connected on the wafer, will not be described in detail here. The two demonstrated devices, one designed for the 1.31 µm broadcast wavelength and one for 1.50 µm, consist of special 2-band MUX AWGs [4, 5]. Each of these overlays eight distributed broadcast channels with eight individual WDM channels in the 1.55 µm band. The device for the 1.31 µm broadcast wavelength uses a low order MUX AWG (m=3) in S-bend geometry, whereas the one for the 1.50µm broadcast wavelength uses the more compact standard AWG geometry [6].

2. Design

The device design is based on planar silica technology with $\Delta n = 0.7\,\%$ and with $6 \times 6\ \mu m^2$ cross sections for the single mode channel waveguides used. The design for the 2-band MUX AWG makes use of the two basic properties of an AWG spectrometer, namely the imaging property between input and output and the wavelength-dependent shift of the images.

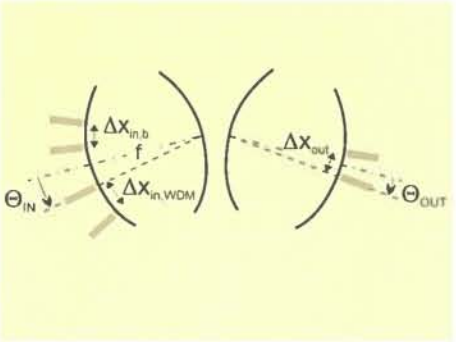

Fig. 2: Schematic illustration of MUX AWG slab regions, showing input/output waveguide angles Θ according to equation 1, slab focal length f, and waveguide pitches Δx for the broadcast and WDM combs.

The AWG behaviour is described by equation (1), where Θ_{in} and Θ_{out} represent the angles between slab center and the attached input/output waveguides, as shown in Fig. 2.

$$\Theta_{IN} = \frac{m}{n_s d}\left\{\lambda - \lambda_C\left[1 + \frac{1}{n_c}\frac{dn_c}{d\lambda}(\lambda - \lambda_C)\right]\right\} - \Theta_{OUT}$$

In this equation, m is the grating order, λ_c the design centre wavelength and d the grating pitch. Also, n_s and n_c are the effective refractive indices at λ_c of the slab and grating waveguides, respectively. This equation also takes into account the chromatic material dispersion by a linear fit of n_c around λ_c (given in square brackets). The input/output waveguide positions are $x = \Theta f$ with slab focal length *f*.

The two different MUX AWGs require either λ_c = 1430 nm and a centre-to-centre band gap of $\Delta\lambda_{band}$ = 240 nm, or λ_c = 1525 nm and $\Delta\lambda_{band}$ = 50 nm, respectively. We have chosen a grating order of m = 3 in one case, yielding FSR ≈ 357 nm, and of m = 14 in the other case, yielding FSR ≈ 100 nm. These choices allow the implementation of several input channels in both bands, each without overlap.

The pitch Δx_{out} of the 6 µm wide output waveguides in both MUX devices was chosen to be 20 µm. This value guarantees a sufficiently low crosstalk. A value of $dn_c/d\lambda = 0.016\ \mu m^{-1}$ for the silica material dispersion was taken into account. Furthermore, a 1:1 image formation system was taken as the basis of the design, which means that input and output focal lengths f are equal. The m = 3 MUX AWG has f = 4.5 mm and a pitch of d = 12.8 µm between the 120 grating waveguides, resulting in an AWG dispersion of $d\lambda/dx$ = 1.3 nm/ µm and a corresponding gap between the two main wavelength axes at the AWG input of 180 µm. Similarly, the m = 14 MUX AWG with f = 3.25 mm and d = 8.6 µm between the 120 grating waveguides yields an AWG dispersion of $d\lambda/dx$ = 0.27 nm/ µm and a corresponding gap at the input of 180 µm.

The two waveguide combs consisting of eight waveguides each are attached at the input slab region. Pairs from each comb are exactly imaged to their output waveguide counterparts. Eight input waveguides fed from the output of a DEMUX AWG are implemented to deliver the wavelength channels $\lambda_1 - \lambda_8$ in the 1.55 µm band at 200 GHz channel spacing, and another 8 waveguides are implemented to deliver the broadcast channels at λ_b.

The ability to distribute the broadcast signal at wavelength λ_b equally among the eight channels was achieved by an additionally attached 1/8 power splitter ahead of the MUX AWG input. At this point we tested two different structures for a power splitter with different bandwidths and different excess losses.

For the low order AWG (Fig. 3) we attached an MMI structure with hyperbolic horn at the MUX input. It embeds the eight input waveguides that are provided for λ_b at the slab interface. A broadcast signal around 1.31 µm wavelength fed into this horn diverges along the widening horn, with a nearly rectangular intensity profile covering all eight inputs, and ac-

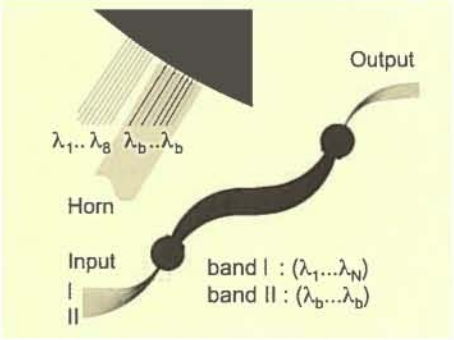

Fig. 3: AWG layout of the two band 8 channel MUX AWG (1.31/1.55 µm) in S-bend geometry, and enlarged view of the slab input region showing the two waveguide combs, one for the broadcast wavelength λ_b with embedded horn and one for the WDM channels $\lambda_1 - \lambda_8$.

cordingly exciting all eight output waveguides at nearly uniform powers. This splitterstructure proves to be very wavelength tolerant, but is associated with higher losses since a large part of the power, which falls outside the waveguides, is lost. A more promising solution from the point of view of losses is to integrate a star coupler instead, although this would be much less wavelength tolerant. Such a star coupler was provided in front of the high order AWG (m = 14).

The pitch of the input waveguides is $\Delta x_{in} = \Delta x_{out} + (dx/d\lambda)\,\Delta\lambda$. Therefore the pitch $\Delta x_{in,b}$ of the broadcast waveguides, all carrying the same wavelength λ_b, is the same as for the output waveguides (20 µm). However, the pitch of the WDM input waveguides $\Delta x_{in,WDM}$ delivering $\lambda_1 - \lambda_8$ with $\Delta\lambda = 1.6$ nm (200 GHz) varies. $\Delta\lambda$ is positive if the WDM wavelengths run in the same direction as the AWG dispersion, otherwise it is negative. For the low order MUX AWG we chose negative $\Delta\lambda$, resulting in a WDM input pitch of $\Delta x_{in,WDM} \approx 19$ µm, whereas for the high order MUX AWG it was chosen positive, giving a WDM input pitch of $\Delta x_{in,WDM} \approx 26$ µm.

3. Experiment

First devices were fabricated on a SiO_2/Si wafer purchased from PIRI Corporation. The WDM DEMUX in both devices is an 8-channel 200 GHz AWG for the 1.55 µm band with a flat top design using MMI input sections [7]. An increased 3 dB bandwidth of about 105 GHz and an insertion loss of 8 to 10 dB was achieved.

The 2-band MUX device exhibits the desired gate property for the 8 WDM channels with 200 GHz (1.6 nm) channel spacing via corresponding input/output ports 1/1´ – 8/8´. In contrast to a conventional N × N AWG, the transmission curves for the 8 paths are not centred at the same wavelength, but are intentionally shifted 200 GHz with respect to each other, in order to be most transparent to the WDM comb. This shift was realized by adapting the waveguide pitch as described above.

Figure 4a shows the measured transmission characteristic as a function of wavelength for the WDM channels of the 1.31/1.55 µm WDMPON device. The bold curves hold for the correctly associated input/output ports N/N´, whereas the dashed curves are measured for input ports one lower in index than the output ports, thus yielding the nearest neighbour crosstalk values. The 3 dB working range in each WDM channel is about 1 THz (8 nm). An insertion loss of 4 dB, including fibre-waveguide coupling, was achieved, and the crosstalk is in the region of -25 dB.

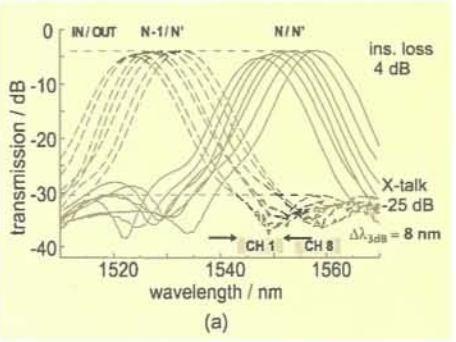

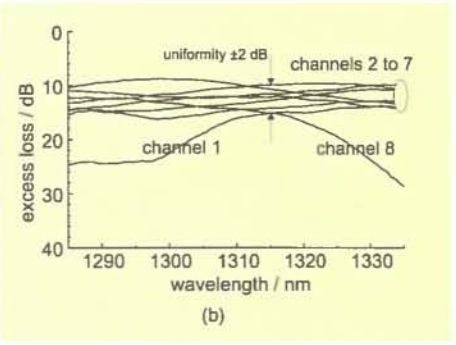

Fig. 4:
(a) Measured transmission spectra of the MUX AWG (1.31/1.55 µm) in the 1.55 µm WDM band.
(b) Measured excess loss of the distributing system for the broadcast wavelength λ_b around 1.31 µm.

Figure 4b shows the distribution behaviour for the broadcast wavelength around 1.31 µm. An average loss of 10 dB is measured, in addition to the 9 dB theoretical splitting loss of the 1 to 8 power splitter. If the loss of 4 dB mentioned above for pure AWG imaging is subtracted, we obtain a distribution penalty of 6 dB for the horn structure, with a power uniformity of ±2.5 dB. The window for the broadcast band is more than 50 nm wide, apart from the two outer ports 1´and 8´, which are not well covered by the slightly undersized horn.

Figure 5a shows the measured transmission characteristic as a function of wavelength for the WDM channels of the 1.50/1.55 µm WDMPON device. The 3 dB working range in each WDM channel is 250 GHz (2 nm). An insertion loss of 3.5 dB was achieved, including fibre-waveguide coupling. The crosstalk behaviour of the MUX device was less than -23 dB.

Figure 5b shows the distribution property

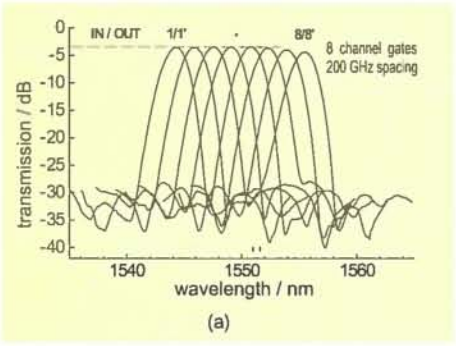

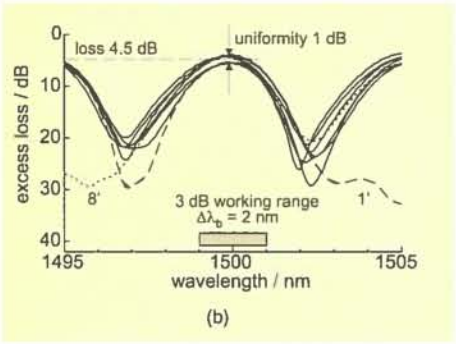

Fig. 5:
(a) Measured transmission spectra of MUX AWG (1.50/1.55 µm) in the 1.55 µm WDM band.
(b) Measured excess loss of the distributing system for the broadcast wavelength λ_b around 1.50 µm.

at the 8 output ports of the MUX for the common wavelength around 1.50 µm, which is launched into the star coupler input. An average loss of 4.5 dB is measured at 1.500 µm in addition to the 9 dB theoretical splitting loss of the 1 to 8 power splitter. If we subtract the loss of 3.5 dB for pure AWG imaging, a distribution penalty of 1 dB is obtained, with a power uniformity of ± 0.5 dB. The 3 dB working range in the broadcast band is again 250 GHz (2 nm). Considering that there is a temperature shift of about 1.3 GHz/°C for silica, all devices are relatively temperature tolerant, as generally required for PON applications.

Acknowledgments

The authors would like to acknowledge W. Fürst for the CAD processing of the masks and R. Steingrüber for writing the e-beam masks. This work was financially supported by the BMBF and the State of Berlin.

References

[1] U. Hilbk, Th. Hermes, J. Saniter and F.-J. Westphal, **"High capacity WDM overlay on a passive optical network"**, Electron. Lett., vol. 32, pp. 2162-2163, 1996.

[2] Y.P. Li, L.G. Cohen, C.H. Henry, E.J. Laskowski and M.A. Cappuzzo, **"Demonstration and application of one monolithic two-PONs-in-one device"**, Proceedings ECOC'96, TuC.3.4.

[3] M. Zirngibl, C.R. Doerr and C.H. Joyner, **"Demonstration of a splitter/router based on a chirped waveguide grating router"**, IEEE Phot. Technol. Lett., vol. 10, no. 1, pp. 87-89, 1998.

[4] G. Przyrembel et al., **"Multichannel 1.3 µm / 1.55 µm AWG multiplexer/ demultiplexer for WDM-PONs"**, Electron. Lett., vol. 34, no. 3, pp. 263-264, 1998.

[5] B. Kuhlow et al., **"AWG based device for a WDM overlay PON in the 1.5 µm band"**, to be published in IEEE Photon. Technol. Lett.

[6] H. Takahashi et al., **"Transmission characteristic of arrayed waveguide N × N wavelength multiplexer"**, J. Lightwave Technol., vol. 13, no. 3, pp. 447-455, 1995.

[7] M.R. Amersfoort et al., **"Passband broadening of integrated arrayed waveguide filters using multimode interference couplers"**, Electron. Lett., vol. 32, no. 5, pp. 449-451, 1996.

E. PAWLOWSKI, M. FERSTL
AND W. FÜRST

DIFFRACTIVE OPTICAL ELEMENTS FOR MULTIPURPOSE OPTICAL INTERCONNECTS

Abstract

Various types of diffractive optical elements (DOE_s), in the form of Fresnel zone lenses (FZL_s), phase correcting elements, beam deflection elements, zero order gratings and polarization elements, have been realized for optical interconnects.These elements exhibit large diffraction efficiencies and good optical qualities for practical use. Several elements were implemented in various systems.

1. Introduction

Interest in diffractive optical elements for optical interconnects, optical imaging, optical data storage, laser machining and optical sensors has grown rapidly in recent years. DOEs are smaller and lower in size and weight than conventional optical elements. The functionality of several different optical components can be combined in one diffractive optical element, giving reduced system complexity. DOEs are usually optimized for a particular wavelength, but combinations of refractive and diffractive elements can reduce chromatic aberrations of refractive components over a wide wavelength region.

Our fabrication processes are based on computer-aided design (CAD), electron-beam writing, ion-beam sputter deposition (IBSD), ion-beam etching (IBE), reactive ion etching (RIE) [1,2] and a novel phase/amplitude mask photolithographic technique (patent pending [3, 4]). The fabrication techniques are adapted from microelectronic technology. The design of the DOEs is based on scalar theory, ray trace calculations, and on the electromagnetic theory of gratings (for elements with structures near the resonance region, where the grating period and the wavelength are of the same order of magnitude) [5-7]. With modern CAD tools, various DOEs can be combined to carry out complex optical tasks.

In order to reduce optical losses, crosstalk and optical feedback between different opticl components, we coated the DOE_s with AR coatings [8, 9]. The reflection of these elements was optimized using an angular spectrum approach. A minimum reflectivity as low as $1x10^{-4}$ was realized using in situ controlled multilayers of TiO_2 and SiO_2.

2. DOEs for laser collimators and light collectors for mobile communication systems

One factor that limits the reliability of laser collimators is the mechanical stability and the wavelength variations of the laser diodes. The wavelength variations are caused by thermal effects of the source and by the finite bandwidth of the laser. To realize a collimator with stable characteristics, it is advantageous to use a hybrid combination of refractive and diffractive optical elements.

Accordingly, a multilevel phase corrector was fabricated for a refractive lens. The hybrid optical element collimates the light from a laser diode (Fig. 1) with wavefront aberrations smaller than l/20 (rms). Large diffraction efficiencies were achieved by approaching the kinoform profile using binary mask coding and a multi-level step approximation. For a phase element with L levels the diffraction efficiency is given by $\eta = [\sin(\pi/L)/(\pi/L)]^2$. This equation indicates that a perfect rotationally symmetric element of eight levels should achieve an efficiency of 95 %. The measured transmission efficiency of the complete collimator was greater than 90%.

We have developed a focussing lens with large numerical aperture and large diameter to collect the light from an indoor LAN base station. The element was designed on

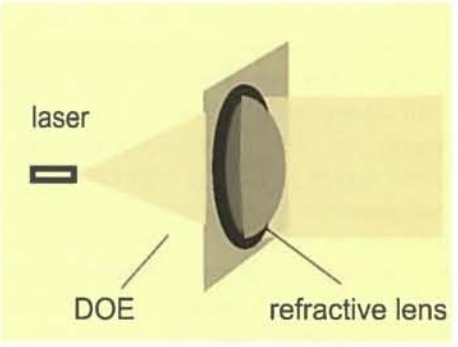

Fig. 1: Hybrid laser collimator lens.

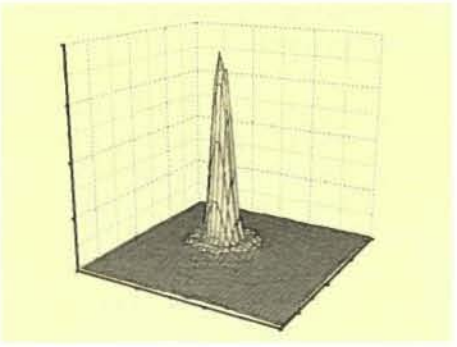

Fig. 2: (a)Transmission microphotograph of an eight-level FZL. (b) PSF of a silicon FZL.

the basis of a Fresnel zone lens (FZL) structure, where the element has rotational symmetry with a diameter of 48 mm and a focal length of 30 mm. The zone radius r_m is given in the non-paraxial domain by $r_m = [2m\lambda f + (m\lambda)^2]^{1/2}$, where m is the zone index number, λ is the illumination wavelength and f is the focal length. The phase profile in each zone was approximated by a discrete multi-level step profile.

The electromagnetic theory calculations reveal that large refractive index differences between the DOE material and the adjacent medium move the resonance region towards smaller grating periods. Therefore, the efficiency of diffractive optical elements with a large refractive index should be larger than for elements with a small refractive index.

We used silicon as a large refractive index material (n=3.4), which is transparent for wavelengths above 1.1 µm. The indoor LAN works at 1.55 µm. Fig. 2a shows a transmission-microscope image from the centre of the eight-level FZL. Due to the light absorption in the visible wavelength region, we observed the different phase levels as grey levels. The depth of the FZL was about 0.6 µm. The incoherent impulse response of a FZL with a circular limiting lens aperture is a so-called sombrero function: $\mathrm{somb}(r) = 2\,J_1(\pi r)/(\pi r)$. We measured the point spread function (PSF) with an expanded laser beam and an IR camera. Fig. 2b shows a representative example of the measured intensity distribution in the focal plane (PSF) for an AR-coated 8-level Fresnel zone lens with F/number = 0.625, fabricated for the wavelength of 1.55 µm.

3. DOEs as beam deflectors for optical interconnects

Deflection elements are key components of optical interconnects. Especially for laser applications, where the wave nature of light becomes noticeable, DOEs have large advantages. DOEs are attractive elements due to their small volume, low weight and large functionality. For a large deflection efficiency it is necessary to concentrate all the light into one diffraction order. To obtain such a condition we have fabricated blazed gratings with a newly developed oblique sputtering technique [10]. In comparison with other techniques, this technique is very attractive due to the very simple fabrication process and the realization of smooth grating profiles. A simple computer simulation routine was used to optimize the sputtering process.

Fig. 3b shows a SEM photograph of a blazed grating fabricated with the oblique sputtering method. The fabrication process of the elements is described in the following.

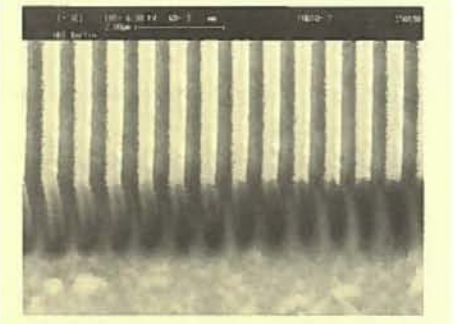

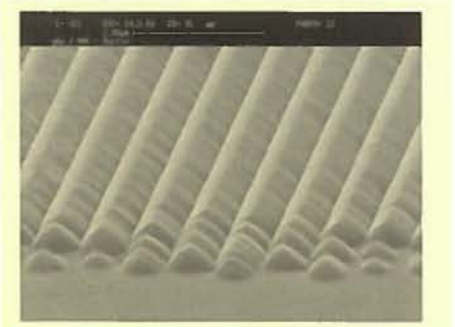

Fig. 3: SEM photographs of cleaved gratings: (a) Binary sputtered by IBSD; (b) Blazed grating realized by oblique sputtering, Λ=760 nm.

The blaze was realized by oblique sputtering, at an angle of 45° to 70° of TiO_2 or silicon over the prestructured binary grating shown in Fig. 3a. The sputtering rate was 10 nm/min at an ion beam energy of 1000 eV. For our element we chose a grating period of Λ=760 nm. The depth was determined to be 0.62 µm, close to the theoretical value of 0.67 µm. At such conditions the higher orders become evanescent and the first order efficiency is improved. Our measurements revealed that nearly all the light is deflected into the first order. The radiation efficiency of the DOE can exceed 90 % when the coupling angle in the air is about 20°.

4. DOEs as polarization elements

Diffractive optical elements with feature sizes smaller than the wavelength are of particular interest for laser applications and laser systems. Resonance-domain DOEs with feature sizes in the sub-micrometre range are strongly polarization dependent, which means that the phases as well as the efficiencies of the diffracted orders depend on the polarization of the incident light [11]. With the aid of optimization methods such as simulated annealing [12], large diffraction efficiencies for both polarization modes can be obtained. Due to the progress of micro-fabrication technologies, such structures with typical grating periods well below one micrometre became fabricable. Using direct e-beam writing combined with successive reactive ion etching, we realized high frequency gratings that work as polarization elements, such as polarizing beam splitters or phase retarders. The polarizing gratings that we fabricated in quartz glass for the wavelength of 650 nm exhibited large diffraction efficiencies for both polarizations:

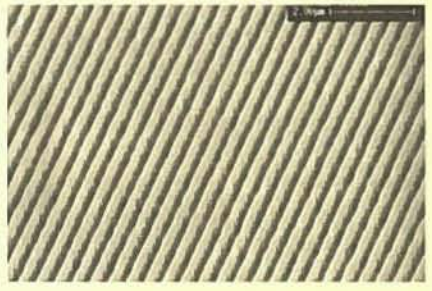

Fig. 4:
High frequency grating (RIE-etched in quartz glass).

$TE_1 > 70\%$ and $TM_0 > 90\%$. A SEM view of such a binary grating is shown in Fig. 4. The line width of this polarization selective grating was about 170 nm and the aspect ratio was about five.

5. Conclusions

We have designed and developed various DOEs. We have developed simple processing techniques to easethe manufacture of special DOEs. These processes are suitable for various optical materials and critical structural dimensions.

The realization of DOEs with diffraction efficiencies of more than 90 % of the predicted theoretical values has been demonstrated. The spot intensity distributions of the realized FZLs are symmetrical and the measured full-width at half-maximum (FWHM) intensities are close to the diffraction-limited values, indicating good optical performance.

Our measurements and experiments show that the efficiencies and optical performances of the DOEs make them suitable for application in various optical systems.

Acknowledgment

This work was performed by the HHI and supported by grants from the German Ministry for Education, Science, Research and Technology (BMBF) and from the State of Berlin. The responsibility for the contents rests exclusively with the authors.

References

[1] M. Ferstl, Proc. EOS Topical meeting on Diffractive Optics, pp. 210-211, 1997.

[2] M. Ferstl, OSA Techn. Digest Ser., vol. 10, pp. 167-69, 1998.

[3] E. Pawlowski, patent application: DE 195 02 624.1, 1996.

[4] E. Pawlowski et al., Pure and Applied Optics, vol. 6, no. 6, pp. 655-662, 1997.

[5] E. Noponen et al., J. Opt. Soc. Am. A., vol. 10, no. 3, pp. 434-443, 1993.

[6] R. Petit, Springer Verlag Berlin, 1980.

[7] T. K. Gaylord et al., Proc. IEEE, vol. 73, pp. 894-937, 1985.

[8] E. Pawlowski et al., Opt. Eng., vol. 33, no. 11, pp. 3537-3546, 1994.

[9] M. Ferstl et al., Proc. SPIE, vol. 1992, pp. 90-101. 1993.

[10] E. Pawlowski et al., OSA Techn. Digest Ser., vol. 10, pp. 56-58, 1998.

[11] D. Dias et al., Annual Report 1996/1997, Institute for Applied Optics, University of Darmstadt, pp. 54-55, 1998

[12] H. Haidner, Opt. Comm., vol. 130, p. 219, 1996

TH. ENGEL, G. GROSSKOPF,
G. G. MEKONNEN, D. ROHDE,
M. ROHDE AND
G. UNTERBÖRSCH

HYBRID AND MONOLITHIC INTEGRATED OPTIC/MILLIMETRE-WAVE CONVERTERS FOR 60 GHZ RADIO-OVER-FIBRE SYSTEMS

Abstract

Hybrid and monolithic integrated optic/millimetre-wave converters at $\lambda = 1.55\,\mu m$ were developed on the basis of detailed microwave simulations, and were investigated experimentally. Both converters working near 60 GHz had spectral responsivities of about 1 A/W.

1. Introduction

The generation and transmission of millimetre-wave radio signals by optical means is a cost-effective solution for picocellular broadband mobile communication systems.

The use of optical heterodyne techniques for optical millimetre-wave generation in a base station has been successfully demonstrated [1]. A main advantage of this approach is that millimetre-wave oscillators and modulators are then not necessary. Optic/millimetre-wave converters (OMC) having a high responsivity at millimetre-wave frequencies are key components of such systems. The prerequisites are reliable, low-cost OMCs. The OMC usually consists of a photodetector followed by an electrical amplifier. At the HHI successful fabrications of such OMCs have been achieved, using both hybrid integration [1] and completely monolithic integration, [2, 3].

2. Hybrid optic/millimetre-wave converter

The hybrid converter module (Fig. 2) consists of a removable mounting carrier made of gold plated brass, on which the photodetector and amplifier chips, as well as the fibre and a coaxial V-connector, are mounted.

The commercially available photodetector chip (New Focus) contains a back-illuminated InGaAs Schottky photodiode with an active area diameter of 12 µm and a coplanar bias-T. The GaAs-based MMIC amplifier chips [6] were designed for the V-band, working in a 50 Ω environment. One amplifier (type 1) covers the upper part of the V-band while the other (type 2) of similar design covers the lower part The amplifiers are fabricated in a microstrip structure (size 4.2 mm×1.8 mm) containing four GaAs pseudomorphic heterojunction field effect transistor (PMHFET) stages on a 100 µm substrate. The total amplifier gain is about 20 dB, so that each of the stages has only a moderate amplification, thus leading to an oscillation-insensitive device. Equal chip heights allowed the bond wire lengths to be minimized. The interconnection between the amplifier output and the coaxial connector was made by using a short piece of semi-rigid coaxial line, which has inner conductor dimensions fitting the V-connector.

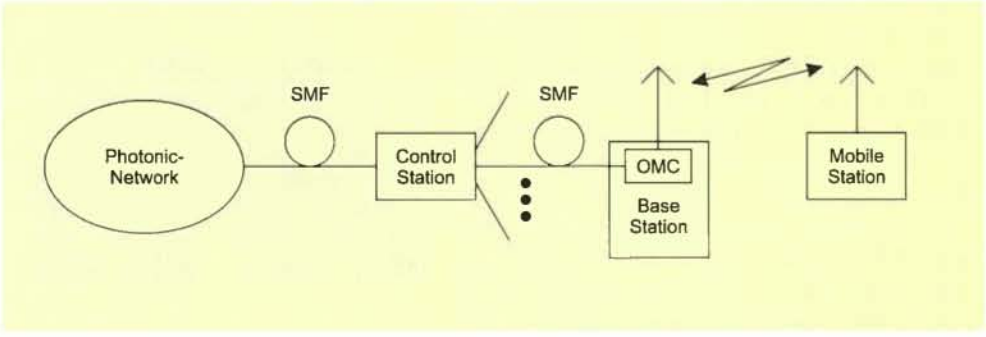

Fig. 1:
Network architecture of a mobile and photonic network (OMC: Optic/Millimetre-Wave Converter. SMF: Single Mode Fibre).

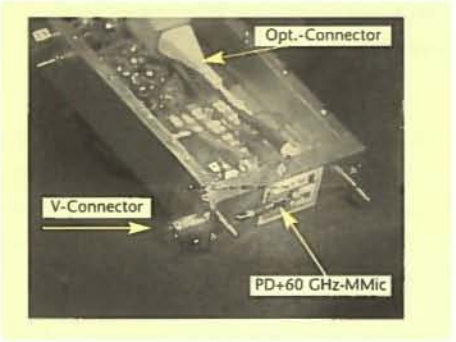

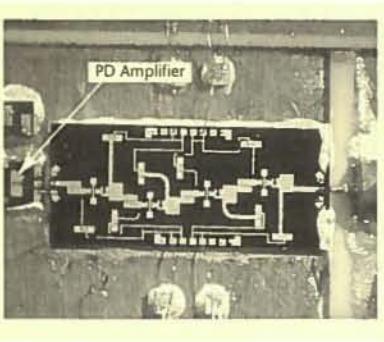

Fig. 2:
(a) Photograph of the V-band optic/millimetre-wave converter module (hybrid version). (b) Photodiode and amplifier chips.

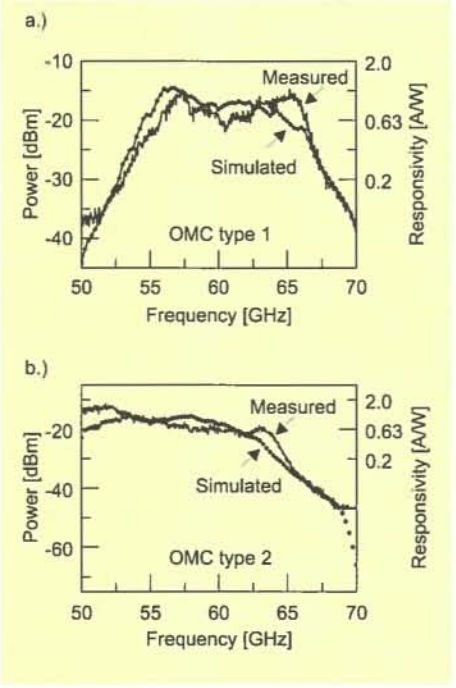

Fig. 3:
Simulated and measured frequency responses of the complete hybrid optic/millimetre-wave converter modules.

3. Simulation and characterisation of the hybrid OMCs

Modelling of the photodiode was done with an RF circuit that was fitted to the measured S-parameter electrical response and to the opto-electronic response. The simulation of the whole OMC was carried out using SUPERCOMPACT 6.5. The photodiode model was combined with the measured S-parameter data sets of the MMIC amplifier chips. Bond wire influences were included as additional serial inductances. Due to the small size of the mounting area of the millimetre-wave circuit, there was no need to take cavity resonances into account.

The frequency responses of the complete OMC modules (Fig.3), which were mainly determined by the MMIC amplifier characteristics, were measured using the optical heterodyne technique. The optical input powers of the two optical waves were both -3 dBm, and the photodiode bias voltage was -4V. The sensitivities of the modules were found to be approximately 1 A/W. The OMC type 1 was also tested in two-channel data transmission experiments at 2×155 Mbit/s [7].

4. Monolithic integrated optic/millimetre-wave converter (OEIC)

The design, modelling and characterisation of ultra-high-frequency narrow-band photoreceiver OEICs based on InP, for applications as OMCs, is presented. A detailed description of the fabrication technology and the integration scheme of the OEICs can be found elsewhere in this annual report. The recently fabricated 60 GHz OEIC chip (Fig.4) consists of a top-illuminated 0.2 µm feature size MSM PD with integrated bias-T and a three-stage coplanar narrow-band amplifier using 0.2 µm mushroom-gate HEMTs with f_T and f_{max} values of 90 GHz and 200 GHz, respectively [2]. It was fabricated by modifying and improving the fabrication techniques used for an OEIC working in the 38 GHz regime [3], which was based on a 0.3 µm feature size MSM PD and HEMTs with 0.26 µm trapezoidal gates.

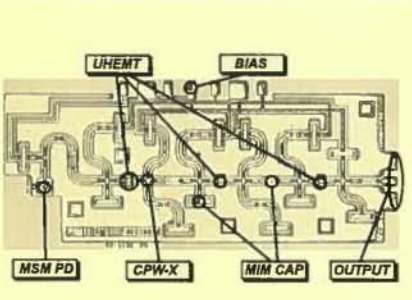

Fig. 4:
Photograph of the 60 GHz OEIC showing its main components. The chip size is 2.5 mm × 1.1 mm.

5. Design and modelling of the OEICs

The photodetector and the amplifier that compose the OEICs have been designed as separate building blocks working in a 50 Ω environment. The detector building block (DBB) consists of the MSM PD and a coplanar bias-T. It includes coplanar waveguides (CPW), a coplanar T-junction and metal-insulator-metal (MIM) capacitors, which reactively match the MSM PD to an impedance of 50Ω over the frequency range of interest. In this range a reactive peaking behaviour could be observed [5], resulting in about 4 dB of additional gain compared to that of a discrete MSM PD in a 50 Ω environment.

The three stage HEMT amplifier building block (ABB) consists of CPWs with an impedance of 50Ω, coplanar X-junctions, MIM capacitors, NiCr resistors and HEMTs. Each stage includes two coplanar networks for narrow-band reactive matching of the HEMT impedances between the stages, and also of the amplifier inputs and outputs. NiCr resistors are used to obtain amplifier stability. The ends of the CPW lines were shorted by coplanar integrated MIM capacitors coupled to the ground plane. The cascaded stages are coupled by inline MIM capacitors. The 38 GHz and 60 GHz OEICs share a uniform modelling and mask layout concept, based on a device library. Equivalent circuits of all devices have been added to the HP EEsof libra microwave circuit design environment. These models correspond directly to a library of mask layout generators for the devices, which have been introduced into the Mentor ICgraph environment [4].

The library of equivalent circuits includes an illumination-sensitive noise model for the MSM PD (Fig. 5a), a small-signal noise model for the HEMT (Fig. 5b), a large-signal HEMT model, and models for the coplanar junctions and the coplanar integrated MIM capacitors.

6. Characterisation of the OEICs

The frequency response of the fabricated OEIC chip was obtained by on-wafer characterization using a heterodyne measurement setup at $\lambda = 1.55$ µm. A responsivity of about 3.5 A/W in the narrow band is obtained for the 38 GHz OEIC, while a responsivity of 0.9 A/W at the 57 GHz centre frequency is obtained for the first 60 GHz OEIC (Fig. 6).

Compared to a discrete MSM PD, the entire insertion gain for the 38 GHz OEIC is about 27 dB, which is composed of 23 dB gain due to the three-stage amplifier and about 4 dB gain caused by the reactive peaking of the bias-T. For the first 60 GHz OEIC the entire gain is about 18 dB, which could probably be increased by further improvements of the non-ideal HEMT properties, which in part also led to a deviation from the intended working frequency of 60 GHz.

Modelling of the noise behaviour for the 38 GHz OEIC results in an estimate of -40 dBm for the output noise power when the noiseless optical input power is 0 dBm, and an estimated signal-to-noise ratio (SNR) of 38 dB at 0dBm optical input power (Fig. 7). The noise equivalent power (NEP), which is the lowest possible optical input power allowing signal detection, was found to be -21dBm. From large signal simulations, a 1 dB compression point for an optical input power level of about +6.5 dBm and a first order intercept point of about +11.5 dBm can be estimated, resulting in a maximum working range from -21 dBm to +6.5 dBm for the optical input power.

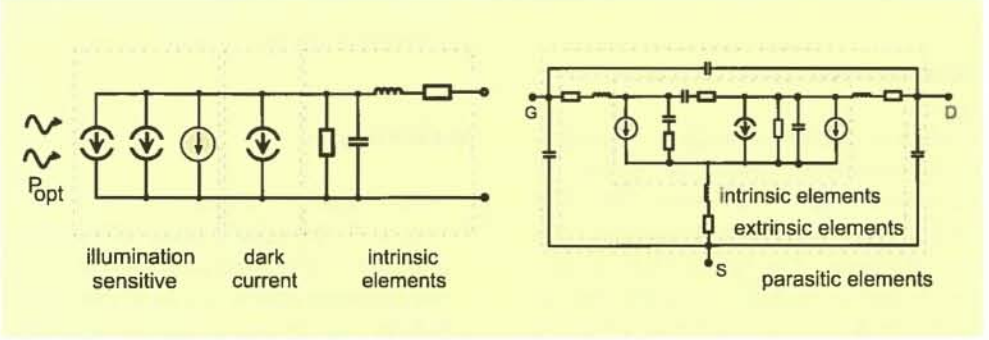

Fig. 5:
(a) Illumination-sensitive noise model of the MSM PD.
(b) Small-signal noise model of the HEMT.

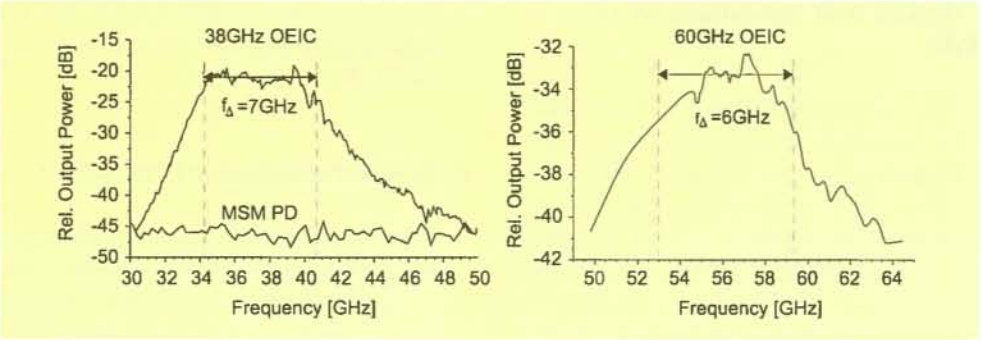

Fig. 6: Measured frequency responses of the OEICs working in the 38 GHz and 60 GHz regions.

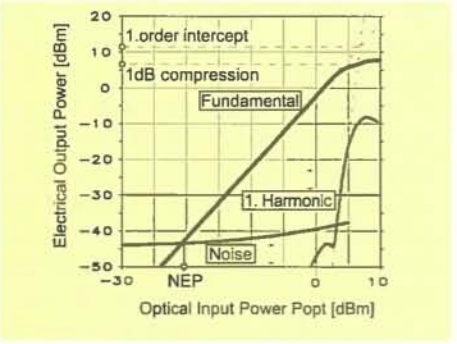

Fig. 7: Large-signal behaviour and noise characteristics of the 38 GHz OEIC.

7. Comparison of hybrid and monolithic OMC

The main advantage of the hybrid OMC is that photodetectors and amplifiers based on different fabrication technologies can be chosen independently for their performance and costs. However, the mounting technology is very complex due to the need for exact positioning of the chips relative to each other. Also, the RF interconnection is critical, since changing the bond wire lengths leads to a significant change in their inductances, which degrades the reproducibility of the opto-electric transfer function. On the other hand, the fixed design of the PD-to-amplifier interconnection in a monolithic OMC allows the introduction of additional gain in the OEIC by a reactive matching technique [5].

8. Conclusions

We reported the simulation, realization, and experimental results of V-band optic/millimetre-wave converters with high sensitivities of about 1 A/W working in the 60 GHz range. The hybrid OMC module was tested successfully in experiments for mobile multi-channel communications [7].

The recently introduced 60 GHz OEIC was shown to be an attractive alternative to the hybrid type, especially because of its reliable optimized power transfer from the photodetector to the amplifier.

Acknowledgments

The development of the hybrid OMC and parts of the work concerning the OEICs were carried out under the national research project Photonik II, which was supported by the German Federal Ministry of Education, Science, Research, and Technology (BMBF) and by the State of Berlin.

The authors would like to thank Dr. U. Guettich of DASA (Daimler-Benz Aerospace Ulm) for providing the amplifier chips, Dr. M. Martin of the Hahn-Meitner Institut Berlin for extracting intrinsic elements of the photodiode, which were essential for the simulation, and Dr. Schlechtweg and Dr. Rosenzweig of IAF (Institute for Applied Solid State Physics Freiburg) for their support during the S-parameter measurements of the photodiode chips. Th. Engel is the recipient of a doctoral scholarship funded by the NaFöG program of the Senate of Berlin. The work on the OEIC was carried out in collaboration with A. Strittmatter, E. Dröge, Dr. E. H. Böttcher and Prof. Dr. D. Bimberg of the Institute of Solid State Physics at the Technical University of Berlin.

References

[1] R.-P. Braun, G. Grosskopf, D. Rohde and F. Schmidt, **"Low phase noise millimeter-wave generation at 64 GHz and data transmission using optical side band injection locking"**, IEEE Photonics Technology Letters,

vol. 10, no. 5, pp. 728-730, May 1998.
[2] Th. Engel, A. Strittmatter, W. Passenberg, A. Seeger, R. Steingrüber, G.G. Mekonnen, G. Unterbörsch and D. Bimberg, **"Design, fabrication and characterization of narrow-band photoreceiver OEICs based on InP"**, IEEE LEOS'98 Annual Meeting, 1-4 December 1998, Orlando FL, USA, paper TuJ1.

[3] Th. Engel, A. Strittmatter, W. Passenberg, A. Umbach, W. Schlaak, E. Dröge, A. Seeger, R. Steingrüber, G.G. Mekonnen, G. Unterbörsch, H.-G. Bach, E.H. Böttcher and D. Bimberg, **"Narrow-band photoreceiver OEIC on InP operating at 38 GHz"**, IEEE Phot. Tech. Lett., vol. 10, no. 9, Sept. 1998, pp. 1298-1300.

[4] Th. Engel, G. G. Mekonnen, A. Umbach, V. Breuer, H.-G. Bach, E. H. Böttcher and D. Bimberg, **"Design and modeling of narrow band InP-photoreceiver OEICs based on HEMTs and MSM photodetector"**, 22nd Workshop on Compound Semiconductor Devices and Integrated Circuits (WOCSDICE'98), Zeuthen, Germany, May 24-27, 1998.

[5] Th. Engel, E. Dröge, G. Unterbörsch, E.H. Böttcher and D. Bimberg, **"Reactive matching of millimetre-wave photodetectors using coplanar waveguide technology"**, IEE Electron. Lett., vol. 34, no. 17, 1998, pp. 1690-1691.

[6] U. Güttich, A. Plattner, W. Schwab, I. Telliez, S. Tranchant, P. Savary, P. Bourne-Yaonaba, B. Byzery, E. Delhaye, C. Cordier and M. Chelouche, **"60 GHz GaAs MMIC technology for a high data rate mobile broadband demonstrator"**, Digest, Intern. Microwave Symp. (IEEE MTT-S), San Francisco, USA, June 1996, vol. 2, pp. 495-498.

[7] R.-P. Braun, G. Grosskopf, R. Hentges, D. Rohde, M. Rohde and F. Schmidt, **"Transmission experiments with optically generated carriers in the 60 GHz region"**, submitted to Wireless Communications, Kluwer Academic Press.

M. FERSTL AND
R. STEINGRÜBER

COMMERCIAL FABRICATION OF MICRO-STRUCTURES AND MICRO-OPTICAL ELEMENTS FOR RESEARCH AND INDUSTRIAL APPLICATIONS

Abstract

Micro-structures and micro-optical components have been fabricated commercially for customers in research and industry, mostly small and medium sized enterprises. The palette of elements that we realized, mainly in quartz glass and silicon, includes binary gratings, high frequency gratings (with feature sizes down to 100 nm), microlenses (refractive and Fresnel zone lenses), lens arrays, and special computer-generated diffractive optical elements. The fabrication techniques, the specifications of the optical structures and some applications are presented.

1. Introduction

Refractive and diffractive micro-optical elements, key components for systems and devices where small dimensions and compactness are demanded, play an important role in a broad variety of applications. They are successfully exploited in fields such as optical sensor systems, optical communications, metrology, and medicine, to name but a few. Refractive elements, consisting of macroscopic surface-relief structures, have properties that are not wavelength dependent, apart from those related to material dispersion. In contrast, diffractive optical elements (DOEs), which use diffraction principles, require coherent, monochromatic light (usually laser beams). DOEs have simple two-level or multilevel surface profiles ("binary optics") or continuous microreliefs, with typical feature sizes down to the micrometre and submicrometre range.

A diffractive optical element is in general a complex pattern of micro-structures that can modulate and transform light in a predetermined way. For example the beam of a laser can be transformed into a ring of dots as shown in Fig.1. With these computer-generated DOEs a laser beam can be shaped into any intensity pattern, such as dot arrays, lines, circles, arrows, etc., including arbitrary patterns designed to the customer's requirements. Other better known examples of diffractive optical elements are Fresnel zone lenses (FZLs), used for collimating or focussing purposes, and

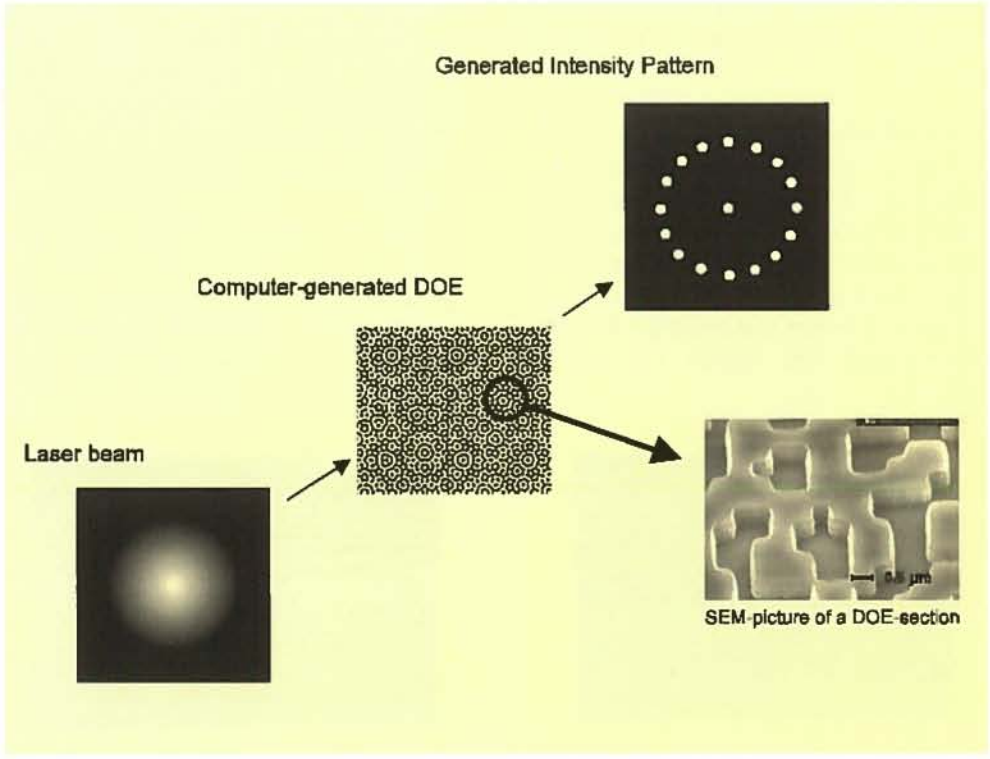

Fig. 1: Transformation of a laser beam into a dot ring pattern by use of a computer-generated DOE.

linear gratings (binary, sinusoidal, triangular,...), which are commonly employed for beam splitting or beam deflection.

Replication technologies, such as injection moulding, hot embossing, UV embossing or casting, offer the possibility of low-cost mass production of micro-optics, which is of great importance for industrial applications.

2. Realized micro-optical elements

Novel micro and nanotechnologies, similar to those known in the semiconductor industry, are exploited for the fabrication of micro-optical elements to the customer's requirements. As we are well equipped with modern computer-aided design tools, an e-beam writer (Leica), mask aligners (SUESS) and dry etching facilities (mainly reactive ion etching – RIE), we are able to realize micro- and sub-micro-structures, chromium masks, and refractive and diffractive optical elements of high optical quality [1]. As a research institute we also have the flexibility to produce elements in small numbers at affordable prices, even one-off items.

Various refractive and diffractive lenses and lens arrays were fabricated in quartz glass and silicon for optical interconnection and free space applications, mainly for the wavelengths 633 nm and 1.5 µm, as follows:

• Refractive lenses

Refractive spherical and cylindrical lenses were realized by melting photoresist cylinders and bars, respectively. Microlens arrays of more than 32,000 spherical lenslets with circular and square apertures of about 30 µm in diameter and cylindrical lenses of 50 µm width were realized. Typically the focal lengths were in the range of a few hundred micrometres. Figure 2a shows an array of spherical microlenses, each of 100 µm focal length.

• Fresnel zone lenses

Many various FZLs, with focal lengths ranging from 400 µm to 22.8 mm, and with various apertures from 200µm to 2 mm, were fabricated. The on-axis and off-axis FZLs intended for collimating, focussing and deflecting purposes were realized in quartz glass [2]. These lenses, whose smallest feature size was about 0.6 µm, were approximated by up to 16 phase levels, using multiple steps of photolithographic mask t and anisotropic RIE. Thus diffraction efficiencies (the proportion of the incoming intensity which is concentrated in the focus) of about 94% could be achieved.

One possibility of avoiding alignment errors, which result in a decrease of the diffraction efficiency [3], is to directly write, using an e-beam, the appropriate structure into resist and to analog transfer this polymer mask into the substrate. In this way FZLs of 150 µm in diameter and with an F-number of about F=0.4 were realized in silicon for 1.5 µm wavelength (Fig. 2b).

• Linear gratings

A large palette of linear binary gratings, designed mainly for beam deflection and beam splitting purposes, were structured in quartz glass, SiO_2, Si and resin, with grating periods down to the micrometre range. Figure 3a shows a linear grating etched in quartz glass, with a grating period of 1 µm and a line width of about 200 nm. The etch depth is about 1 µm, which results in an aspect ratio of about 5. The SEM picture reveals that we get steep sidewalls and smooth surfaces – the roughness determined with a surface profiler wasbelow 2 nm.

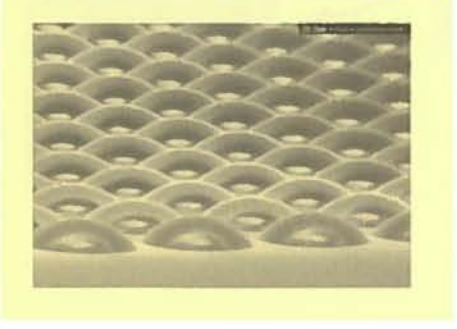

Fig. 2: SEM views of: (a) Microlens array fabricated in quartz glass; (b) An eight-level FZL directly etched in silicon.

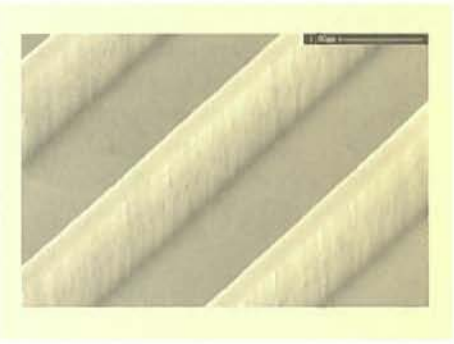

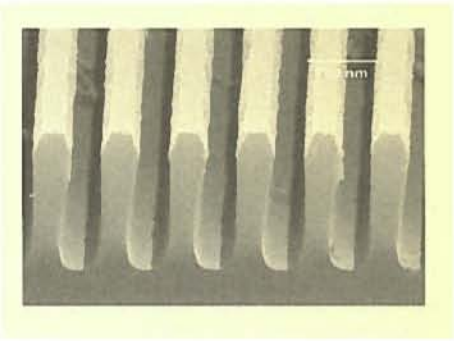

Fig. 3:
Binary gratings in quartz glass:
(a) Beam splitter;
(b) Polarization-selective element.

We also realized high frequency gratings with periods as low as 200 nm. In order to get such a high resolution, these small structures were first written in PMMA by e-beam. In Fig. 3b a polarization beam splitter, with a line width of 380 nm and an etch depth of 1.7 µm, is shown. Additional sinusoidal and trapezoidal gratings with continuous surface profiles and periods down to 0.5 µm were produced in silicon by variable dose e-beam writing and successive RIE.

A sophisticated grating design was exploited to realize a special multilayer dielectric diffraction grating that served as a wavelength selective resonator mirror in a Nd:YAG laser [4].

• Computer-generated DOEs

Various binary computer-generated DOEs have been fabricated in quartz glass for the visible wavelength region, mainly for beam shaping and beam splitting purposes, but also for the generation of predetermined intensity patterns (e.g. spirals, arrows, company logos...). The calculation of the design data for these computer-generated (CG) elements was performed by our competent local partner "Holographie Design Berlin GbR".

A CG-DOE that generates a circle of dots with a dot in the centre (as in Fig. 1) has been fabricated for application in a non-contact IR thermometer, in which it is used to indicate the measuring spot on the target at all distances. To keep the production costs as low as possible, these elements served as masters for replication in PMMA using injection moulding.

Another beam splitting element designated for the use in a measuring instrument was created to split a laser beam into a ring of 40 dots of equal intensities. The efficiency of this element was about 70 % and the intensity deviations of the single dots were well below the required 3 %.

3. Fabrication techniques

The design data that describe the DOEs – given by the phase function or as graphic (pixel or bitmap) files – are translated into a binary amplitude or intensity code that results either in patterns of opaque chromium and clear regions on a photomask (for lithographic pattern transfer), or in modulation of the e-beam intensity in

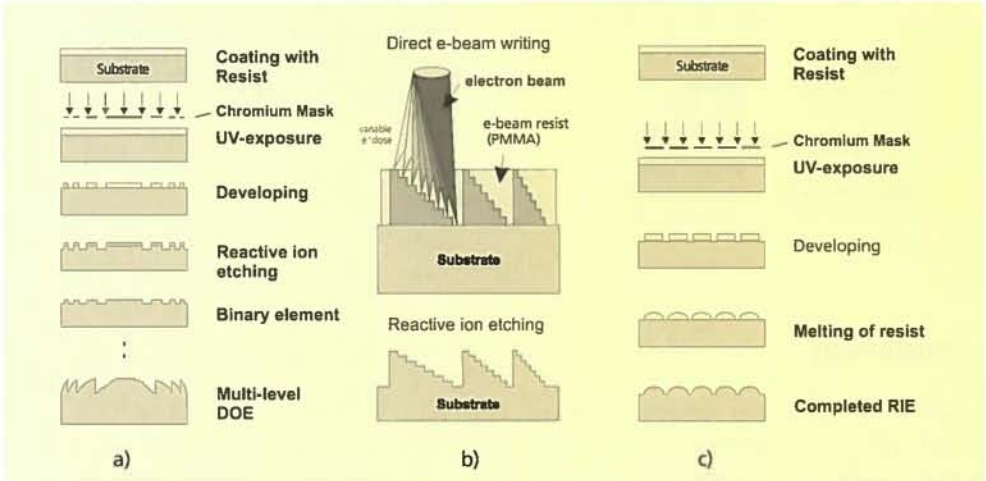

Fig. 4:
Fabrication methods.

a direct-write technique. Two methods are employed for transferring the DOE structures into the substrate:

(a) Binary optics technology, which uses multiple steps of repeated pattern transfer by photolithography and successive RIE (Fig. 4a).

(b) Analog reactive ion etching of a polymer mask which has been preshaped by direct electron-beam writing (Fig. 4b).

The refractive lenses are fabricated by heating the patterned photoresist above the melting point. During the thermal reflow process the resist forms a nearly spherical surface, which is transferred into the substrate by RIE (Fig. 4c). The anisotropic etching required for all of these optical components is performed in a conventional parallel plate reactor operated at radio frequency.

4. Performance

A short overview of our performance, including some characteristic data, is given in Fig. 5.

As micro-optical elements come in a variety of configurations, materials, specification tolerances etc., we also offer consulting services and engineering assistance to customers.

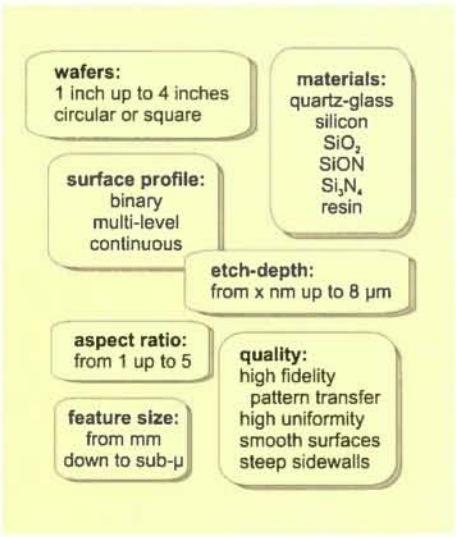

Fig. 5: Characteristic data.

5. Conclusions

Advanced fabrication capabilities, combined with our experience in micro-fabrication, enable us to produce a variety of micro-structures and optical elements, including refractive and diffractive lenses, microlens arrays, beam splitters, beam shapers, spot array generators, binary gratings, high frequency gratings, etc. These are of high optical quality and may be realized in quartz glass, silica or silicon.

Acknowledgment

This work was supported by the German Federal Ministry for Education, Science, Research and Technology and by the State of Berlin. The responsibility for the contents rests exclusively with the authors.

References

[1] M. Ferstl, **"Reactive ion etching: a versatile fabrication technique for micro-optical elements"**, OSA Technical Digest Series, 1998, vol.10, pp. 167-169.

[2] M. Ferstl and A.-M. Frisch, **"Static and dynamic Fresnel zone lenses for optical interconnections"**, Journal of Modern Optics, 1996, vol. 43, pp.1451-1462.

[3] M. Ferstl, B. Kuhlow and E. Pawlowski, **"The effect of fabrication errors on multilevel Fresnel zone lenses"**, Optical Engineering, 1994, 33(4), pp. 1229-1235.

[4] H.-J. Rostalski, J. Guhr, B.H. Kleemann, J. Elscher, G. Schmidt, M. Ferstl, E. Pawlowski, R. Steingrüber, G. Bostanjoglo and R. Motzkus, **"Use of a multilayer dielectric diffraction grating as resonator mirror of a neodymium-doped yttrium aluminium garnet laser"**, Journal of Modern Optics, 1998, vol. 45, no. 7, pp. 1523-1535.

H. BOCHE, T. KUHWALD AND
M. SCHUBERT

CONSTRAINED BEAM FORMING FOR LINEAR ANTENNA ARRAYS

Abstract

Antenna arrays are expected to increase the overall system performance (bit error rate and user capacity) of future mobile communication systems through the use of spatial filtering. The expected performance increase depends on how accurately the beam pattern can be adapted to the changing user distribution. In this contribution a new beam forming algorithm is presented and a performance estimate is given.

1. Introduction

In recent years there has been an increasing demand for new heterogeneous broadband mobile communication services and applications. Given the limited spectrum available for high data rate communication among an increasing number of cellular subscribers, it is generally expected that the deployment of smart antennas will increase the overall system capacity and performance. Smart antennas will not only increase the antenna gain, but also reduce interference and delay spread by means of spatial filtering, and thus enhance the properties of the mobile radio channel for high data rate communication.

While the use of smart antennas is generally anticipated in emerging communication systems like UMTS/IMT2000, the design of the Integrated Broadband Mobile System (IBMS) [1] is based entirely on Smart Antenna technology, which provides a flexible and adaptive means of using more bandwidth-efficient modulation techniques. This gives an effective tradeoff between mobility and data rate and utilizes the system resources more efficiently.

Smart antennas increase the system capacity in several ways. While spatial separation of different users can be used to support an increasing number of users in the same frequency band (SDMA), spatial filtering also effectively reduces the interference due to multipath propagation and multiuser access (SFIR). By decreasing the influence of multipath propagation, spatial filtering also reduces delay spread and Doppler spread, thus improving the overall channel characteristics and resulting in more benign communication channels (SFCI).

The performance increase to be expected when using smart antennas depends greatly on how accurately the interference pattern can be reduced while still maintaining a maximum gain in the direction of the signal of interest (SINR). In this paper a new constrained beam former (CB) is introduced and compared with other existing beam forming algorithms.

2. Signals and beam pattern

When a signal $x(t)$ arrives at an antenna array it will reach the antenna elements at different times (Fig. 1).

For very small signal variations over the maximum delay τ, we may assume that the signal is approximately constant as the wave front passes the array and can thus

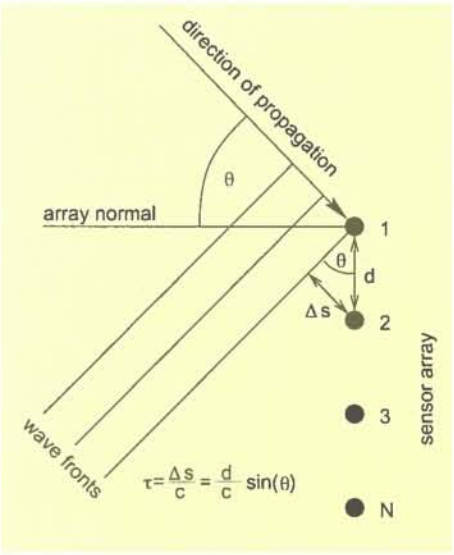

Fig. 1:
Antenna array with incident wave front.

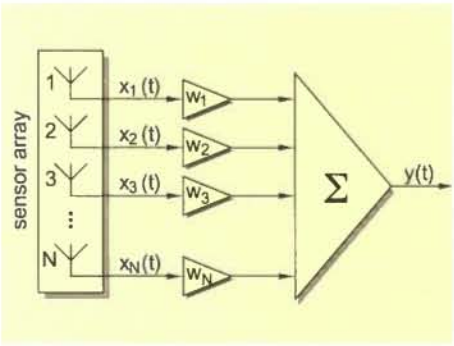

Fig. 2:
Narrow band beam forming receiver.

be considered to be a narrow band signal. In this case the delay is described by a simple phase factor, $x(t-\tau)=x(t)\cdot e^{-j2\pi f_0 \tau}$.

Fig. 2 shows a narrow band beam former. The individual signals are weighted by complex factors wl, $1 \le l \le N$, and added to give the received signal $y(t)$.

Due to constructive and destructive interference the amplitude of the received signal depends on the angle of arrival θ. For linear arrays the beam pattern (transfer function of the beam former) can be described by

$$H(e^{j\Omega}) = \frac{y(t)}{x(t)} = \sum_{l=1}^{N} w_l \cdot e^{j(l-1)\Omega}, \text{ with } \Omega = -\frac{2\pi d}{c} \sin\theta.$$

Fig. 3: **Zero beam pattern for an antenna array with N=16 elements.**

By properly choosing the weights W_l the beam pattern can be formed in such a way that signals from a desired direction will be received with a large amplitude, while at the same time signals from as many as $N-1$ other directions (e.g. the directions of disturbing signals) can be suppressed.

3. Constrained beam former

For a constrained beam former the weights w_l must be calculated so that the beam pattern will have given amplitudes at fixed points Ω_l. In the following various beam forming algorithms [2,3] are presented.

3.1 Bartlett beam former

The Bartlett beam former generates a simple phased array with a maximum antenna gain in direction Ω_*. The only constraint is this main beam direction. It is not possible to predefine the sidelobes or points where the beam pattern is equal to zero. Thus this beam former is not suitable for SDMA.

3.2 Zero beam former

The zero beam former generates a beam pattern which is equal to zero at $N-1$ predefined points Ω_l. Furthermore, a direction Ω^* where the beam pattern will reach $H(e^{j\Omega^*})=1$ may be predefined.

Based on these constraints a basic polynomial of degree N-1 can be formulated as

$$H_*(e^{j\Omega}) = \prod_{l=1}^{N-1} (e^{j\Omega} - e^{j\Omega_l}).$$

The beam pattern can be described as

$$H(e^{j\Omega}) = H_*(e^{j\Omega}) / H_*(e^{j\Omega_*}).$$

A possible beam pattern is shown in Fig. 3 Note that the direction of the main beam cannot be controlled. Furthermore, the beam pattern can reach very large amplitudes outside the given constraints.

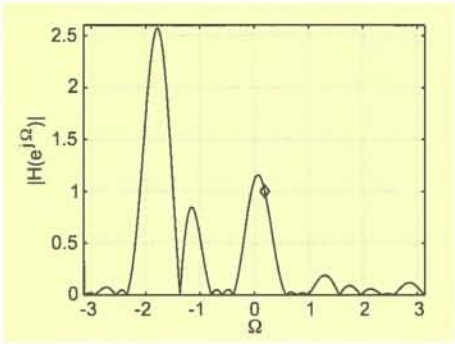

3.3 Zero beam former with derivative control

The construction of the beam pattern is done in the same way as the zero beam former with the predefinition of zeros Ω and the desired main beam direction Ω_*. To reduce the variations near Ω_* the following additional constraint is imposed:

$$dH(e^{j\Omega}) / d\Omega \Big|_{\Omega=\Omega_*} = 0.$$

However, this constraint does not enforce a global maximum at Ω_* – instead, it is often a turning point. The direction of the main beam still cannot be controlled and the beam pattern can reach very large amplitudes outside the given constraints.

3.4 Beam former with minimized power

Now we present a new beam former that allows both the main beam and a designated number of zeros to be predefined. The constraints can be formulated as follows:

a) Main beam directed to the desired signal at direction of arrival (DoA) Ω_*.

b) Zeros for m disturbing signals with DoAs Ω_l.

c) The power has to be minimal:

$$p = \frac{1}{2\pi} \int_{-\pi}^{\pi} \left| H(e^{j\Omega}) \right|^2 d\Omega = \text{minimal}.$$

The minimization ensures that the amplitude of the beam pattern outside the desired direction is limited (Fig. 4).

This leads to a beam pattern with a maximum directivity $D=1/p$ as shown in Fig. 5. The directivity strongly influences the SIR

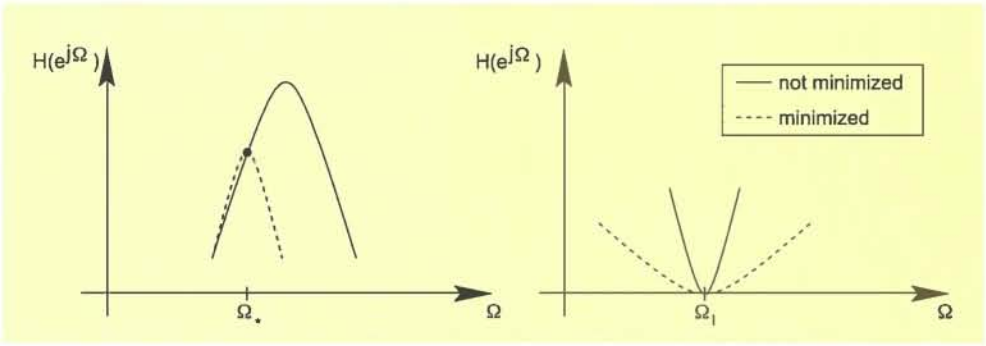

Fig. 4:
Results of minimizing at the maximum (left) and at zero (right).

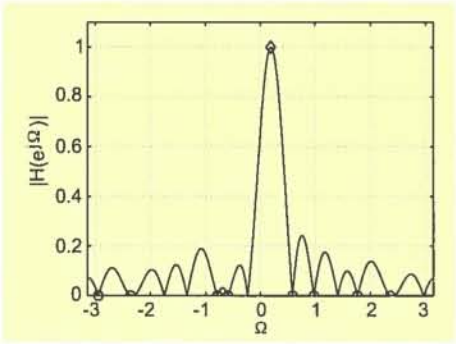

Fig. 5:
Beam pattern for an antenna array with N=16 elements.

and therefore the achievable bit error rate (BER). An approximation for the BER of CDMA systems with smart antennas was presented in [4]:

$$P_b = \Phi\left(\sqrt{\frac{3DM}{K-1}}\right), \text{ with } \Phi = \frac{1}{\sqrt{2\pi}}\int_{\chi}^{\infty}\exp\left(\frac{-\tau^2}{2}\right)d\tau,$$

where K is the number of users in a cell and M is the spreading factor. This estimate shows that the directivity D of an antenna array directly influences the achievable BER of a CDMA system. Because of the maximized directivity the new beam former achieves the best possible performance enhancement in CDMA systems with smart antennas.

4. Conclusions

In this paper we have presented a new constrained beam forming algorithm. While existing beam formers only provide direction control of the zeros or of the main beam, this beam former allows both. Furthermore, the number of constrained zeros in the beam pattern is arbitrary. The generated beam pattern for an ideal 16 element array with given constraints is shown. With this algorithm an optimized beam pattern can be formed allowing SDMA, and it also gives minimum BER in CDMA systems.

5. Acknowledgments

The work presented here was performed in cooperation with the Technical University of Ilmenau. It is supported by the German Federal Ministry of Education, Science, Research, and Technology (BMBF).

References

[1] M. Bronzel, D. Hunold, G. Fettweis, T. Konschak, T. Dölle, V. Brankovic, H. Alikhani, J.-P. Ebert, A. Festag, F. Fitzek and A. Wolisz, **"Integrated broadband mobile system (IBMS) featuring wireless ATM"**, Proc. of the ACTS Mobile Communications Summit '97, pp. 641-646, October 7-10, 1997, Aalborg, Denmark.

[2] L. C. Godara, **"Application of antenna arrays to mobile communications, Part I: Performance, improvement, feasibility and system considerations"**, Proceedings of the IEEE, vol. 85, no. 7, pp. 1029-1060, July 1997.

[3] L. C. Godara, **"Application of antenna arrays to mobile communications, Part II: Beam-forming and direction of arrival considerations"**, Proceedings of the IEEE, vol. 85, no. 8, pp. 1193-1245, August 1997.

[4] J. C. Liberti and T. S. Rappaport, **"Analytical results for capacity improvements in CDMA"**, IEEE Transactions on Vehicular Technology, vol. 41, no. 3, August 1992.

H. BOCHE AND E. JUGL

EVALUATION OF THE SYSTEM CAPACITY OF MOBILE COMMUNICATION SYSTEMS ALLOWING FOR MOBILITY

Abstract

The system capacity of mobile communication systems can be increased by applying sectorization of radio cells and by exploiting quiet voice periods. However, assessments of the capacity gains that can be achieved by these means have been too optimistic. In our work we have found some restrictions of the sectorization gain caused by the mobility behaviour of the subscribers and by soft handoff. A more realistic mobility model was developed which allows for local as well as temporal properties.

1. Introduction

Since the number of mobile subscribers has been rising steadily in recent years, mobile communication is clearly of great importance. Because of the large number of mobile subscribers to be expected in the near future, a proper evaluation of the system capacity of the upcoming mobile communication systems is very important. Third and fourth generation mobile communication systems will support a large number of mobile subscribers as well as higher data rates than current systems. Because of higher data rates the carrier frequencies are increasing – e.g. 2 GHz for the Universal Mobile Telecommunications System (UMTS), and inhouse systems with up to 60 GHz are under consideration. This leads to smaller cell sizes. Hence, when evaluating the performance and capacity of these systems, the mobility behaviour of the subscribers must be considered.

A typical estimate of the system capacity without allowing for mobility aspects, similar to those found in the literature, will be given in the following. In 1993 the Code Division Multiple Access (CDMA) air interface of Qualcomm was adopted as the North American digital cellular standard IS-95. Initial estimates of the capacity gain ranged up to about 20 times the capacity of the analogue Advanced Mobile Phone Service (AMPS). But the capacity of this system was overestimated, as will be explained in the following.

By applying CDMA technology, each subscriber is allowed to use the whole available bandwidth of the system. To distinguish the subscribers, they are each assigned a code sequence. The maximum number of subscribers k_U (corresponding to the capacity) per radio cell can be calculated in a simplified manner from the formula [1]

$$k_U = \frac{\frac{W}{R}}{\frac{E_b}{I_0}} \frac{G_V \cdot G_A}{1+F}$$

where E_b/I_0 is the ratio of bit energy to interference power density and W/R is the ratio of bandwidth to data rate (processing gain). The term F allows for the interference of other radio cells ($F \approx 0{,}6$ according to Viterbi). The factor G_V is the gain achieved by applying voice activity detectors ($G_V \approx 2{,}67$ according to Brady [2]).

We have shown that this gain is valid only for a large number of active subscribers. The capacity gain achieved by sectorization of the radio cells is captured by the factor G_A, which was set to the number of sectors in [1]. But in [3, 4] it was shown that this gain is not constant over time and will vary very strongly as a function of the mobility behaviour of the subscribers. Consequently, realistic mobility models are needed to specify the movement of the subscribers.

2. Restrictions of the sectorization gain

As mentioned previously, the gain achieved by sectorization of the radio cells is captured by the factor G_A, which in the literature is often set to the number of sectors n. However, this assumption is valid only if all subscribers are distributed uniformly among the sectors. But under realistic circumstances this can never be guaranteed – in fact, the sectorization gain is a stochastic function of time. Thus, a mean value can be determined. Restrictions of the sectorization gain arise from the following facts:

1. To improve the signal quality during a handoff procedure, soft handoff is applied, e.g. as in the IS-95 standard. Thus, during

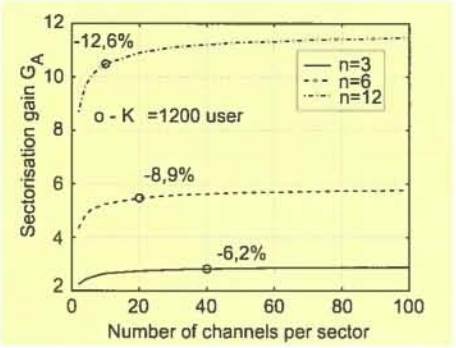

Fig.1: G_A as a function of the number of channels per sector, but not allowing for soft handoff.

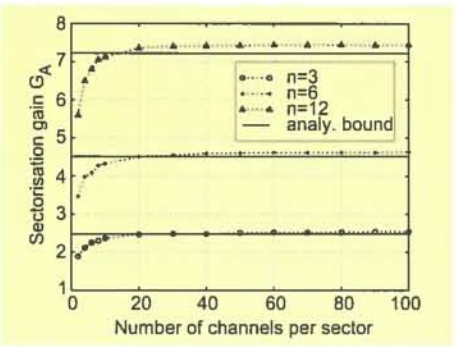

Fig. 2: G_A as a function of the number of channels per sector, allowing for soft handoff and mobility. The analytical bound is also shown.

a handoff a subscriber is connected to two base stations at the same time. Therefore, the capacity gain is reduced, and a simple analytical bound is proposed. A distinction must be made between soft handoffs at cell level and sector level.

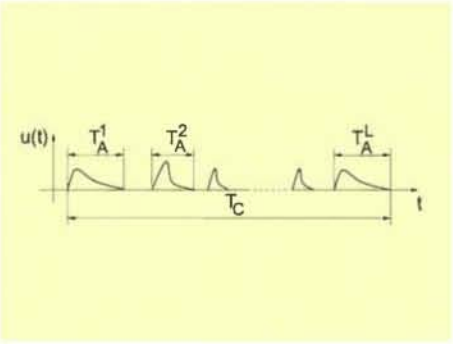

Fig. 3: Active periods T_A^k of a voice signal $u(t)$ with call holding time T_C.

2. A further limitation is caused by the mobility behaviour of the subscribers, which causes an inhomogeneous distribution of the subscribers among the sectors. For first estimates of this sectorization gain, mobility was modelled as Brownian motion based on an equidistant grid pattern. The number of subscribers is assumed to be constant in the cell cluster.

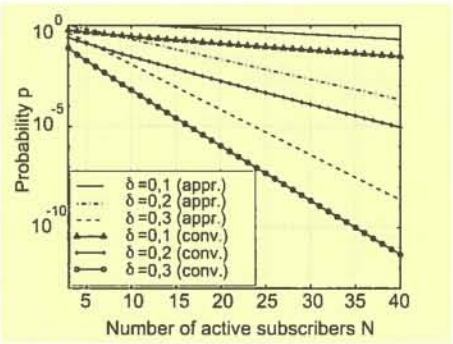

Fig. 4 : Comparison of the analytical estimate with results obtained from N -fold convolution.

The simulation results in Fig. 1 for the mean sectorization gain are obtained by averaging over10 realizations, but ignoring soft handoff. It can be seen that the sectorization gain is higher the more logical channels per sector are used, and consequently the larger the number of subscribers. The theoretical gain limit $G_A = n$ will be reached for an infinite user population. The results show that a higher degree of sectorization has a negative effect on reduces the sectorization gain.

In Fig. 2 the results are compared with the analytical bound, which provides a good estimate of G_A for more than 20 channels per sector. Details of the simulation as well as the parameters can be found in [4].

3. An analytical estimate of the voice activity gain

Since voice consists of a sequence of active periods T_A^k and quiet periods, the transmission of such quiet periods should be avoided by means of voice activity detection (see Fig. 3).

Consequently, the transmitted amount of data can be reduced or the capacity of the system can be increased. By employing statistical multiplexers, there may be more connections available than there are physical channels. Many investigations of the duration of these active and quiet periods have appeared in the literature, especially those of Brady [2, 5]. The active period fits an exponential distribution reasonably well.

However, the duration of the quiet periods is not as well approximated by the exponential distribution [5], although this is still a reasonable approximation and often employed in the literature. Brady found that the voice signal is intermittent with a duty factor of approximately $\alpha = 3/8$. Consequently, the capacity can be increased by a factor G which is inversely proportional to α [1, 6, 7].

In the following some shortcomings of the model given above will be discussed. This model says that, regardless of the number of active subscribers, a capacity gain of $G_V = 1/\alpha$ is available. However, this statement holds only for a large number of active subscribers. Also, the mean active time T_l will not be the same for each subscriber l but can vary from one subscriber to another. Thus, by having N active subscribers there is a non-negligible probability that the mean active time during a time unit T is greater than the mean value αT. This reduces the capacity gain. Furthermore, a free time slot may not coincide with the active period of a subscriber – it is a matter of luck as to whether a time slot is free or not.

If we assume a uniform distribution (probability density function $f(t)$) of the mean active time T_l, since no preferred durations exist, the following analytical estimate for the probability that the norm of the difference from the mean value αT is greater than a small value δ is obtained [8, 9]:

$$\Pr\left(\left|\frac{1}{N}\sum_{l=1}^{N} T_{A_l} - \alpha T\right| > \delta\right) < 2e^{\frac{\delta^2 N}{\sinh(1)-1}}.$$

In Fig. 4 this analytical estimate and the results obtained by means of N-fold convolution of the probability density function $f(t)$ are compared for different δ. It is seen that the analytical estimate is an upper bound which is easy to apply and very fast, and which seems to be appropriate for fundamental considerations.

4. Mobility modelling

We have proposed a new mobility model which allows for preferred directions of movement [10-12]. It is also possible to choose a certain divergence from the preferred direction. This way typical topologies such as shopping streets and campus areas can be modelled. Within a certain region several areas with different mobility parameters are defined, as follows:

- Approximate preferred direction of movement α, $0° \le \alpha < 360°$
- Divergence σ from the preferred direction, $0 \le \sigma \le 1$
- Mean velocity v_{mean}
- Standard deviation of the velocity v_{dev}
- Probability p of staying in this area at initialization.

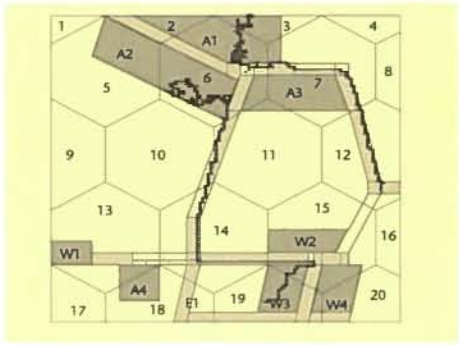

Fig. 5: Test environment: Campus area, 650x650 metres, 20 hexagonal radio cells with radius R =115 metres, random movement of two subscribers (movement from W3 to A2 and from E2 to A1).

In Fig. 5 an example for the implementation of a real environment is given (the campus area of the Technical University of Ilmenau).

Areas marked with "A" represent workplaces and areas marked with "W" represent residences. The light grey areas illustrate street segments. If they are marked with "E", subscribers may stay within these segments at the beginning of the movement. If a subscriber is located within a street segment, his movement is well defined. On the other hand, if he is located in a building, some divergence of the movement may be allowed for. A further assumption is that the velocity of the subscribers is a Gaussian process with minimum velocity equal to zero.

It is also possible to simulate the movement of the subscribers at specific times, e.g. in the mornings when people move from their residences to their workplaces or lecture halls. As a result of our simulations we found that short travel lengths as well as short cell residence times will occur very frequently in reality, which further affects performance evaluations.

5. Conclusions

We have shown that the mobility behaviour of the subscribers has a substantial impact on performance and capacity of mobile communication systems. Especially in environments with few subscribers, a substantial loss of the capacity gain due to sectorization of the radio cells was detected. Furthermore, we have demonstrated that the gain due to voice activity detectors will be smaller than suggested in the literature. Finally, a more realistic mobility model was proposed which allows for local as well as temporal details. The results obtained will influence further performance evaluations.

Acknowledgments

The work presented here was performed in cooperation with the Technical University of Ilmenau. It is supported by the German Federal Ministry of Education, Science, Research and Technology (BMBF).

References

[1] A. H. M. Ross and K. S. Gilhousen, **"CDMA technology and the IS-95 North American standard"**, The Mobile Communications Handbook (J. D. Gibson, ed.), pp. 430-448, CRC Press, Inc., 1996.

[2] P. T. Brady, **"A statistical analysis of on-off patterns in 16 conversations"**, Bell Syst. Tech. J., vol. 47, pp. 73-91, January 1968.

[3] H. Boche and T. Ferchland, **"Bewertung des Sektorisierungsgewinns bei CDMA-Verfahren"**, Proc. 43rd International Scientific Colloquium, Ilmenau, September 1998.

[4] E. Jugl and H. Boche, **"Limits of sectorization gain caused by mobility and soft handoff"**, accepted for publication in: Electronics Letters, 1999.

[5] P. T. Brady, **"A model for generating on/off speech patterns in two way conversations"**, Bell Syst. Tech. J., vol. 48, pp. 2445-2472, 1969.

[6] K. S. Gilhousen, I. M. Jacobs, R. Padovani, A. J. Viterbi, L. A. Weaver, Jr. and C. E. Wheatley III, **"On the capacity of a cellular CDMA System"**, IEEE Transactions on Vehicular Technology, vol. 40, pp. 303-312, May 1991.

[7] A. J. Viterbi, CDMA Principles of Spread Spectrum Communication, Addison Wesley Publishing Company, 1995.

[8] H. Boche and E. Jugl, **"An analytical appraisal concerning the gain by using voice activity detectors"**, Preprint, Heinrich-Hertz-Institut für Nachrichtentechnik Berlin GmbH and Technische Universität Ilmenau, 1998.

[9] H. Boche and E. Jugl, **"Analysis of factors to increase the capacity of CDMA based mobile communication systems"**, Preprint, Heinrich-Hertz-Institut für Nachrichtentechnik Berlin GmbH and Technische Universität Ilmenau, 1998.

[10] E. Jugl and H. Boche, **"A new mobility model for performance evaluation of future mobile communication systems"**, accepted for publication in: Proc. ICC'99, Vancouver, June 1999.

[11] H. Boche and E. Jugl, **"Analyse vom ETSI Indoor Mobilitätsmodell zur Evaluierung von UMTS"**, Proc. DFG-Workshop **"Indoor-Mobilkommunikation"**, Kassel, October 1998.

[12] H. Boche and E. Jugl, **"Extension of ETSI's mobility models for UMTS in order to get more realistic results"**, Proc. UMTS Workshop, Günzburg, November 1998.

V. JUNGNICKEL,
C. V. HELMOLT, TH. HAUSTEIN
AND U. KRÜGER

SPACE DIVERSITY CONCEPTS FOR WIRELESS INFRARED COMMUNICATION

Abstract

A closed system concept for wireless infrared (IR) communication in an indoor environment is presented, based on the optical space diversity technique. The transmitter and receiver consist of a lens in combination with a diode laser array and a photodiode array, respectively. This is a very flexible hardware configuration, and it is easily adapted to supply broadband and narrowband services to a number of mobile users. At low data rates, reliable access to the network and the voice service is made possible by using the diffuse, multi-path light propagation inside the room. At higher data rates, however, a directed line-of-sight link is established in order to overcome the bandwidth constraints of the diffuse channel.

1. Introduction

In the future wireless information infrastructure, a single base station must provide a number of services that may differ markedly from each other in terms of their data rates. Network access and voice require relatively small bandwidths, but video and data transfer rates are much higher.

In the Integrated Broadband Mobile Communication System (IBMS), which is currently being developed in the ATMmobil joint project funded by the German Ministry of Science and Technology, the space diversity technique is the key to providing higher bandwidth services from a single base station and for increasing the number of users who can be connected simultaneously. In principle, the more bandwidth required by a user, the more the link is directed towards the user [1].

For radio frequency transmissions, tracking of the user is performed by an intelligent ("smart") antenna, and the directional gain of the antenna is used to compensate for the reduced receiver sensitivity at higher bandwidths. Beam steering requires individual driving of the array antenna elements in both amplitude and phase. This is a big challenge, since real time signal processing is needed to distinguish between the different users [2].

The wireless IR channel is a promising alternative to radio transmission, and is especially suited for indoor applications. Also, space diversity offers a variety of benefits for IR technology. This becomes evident when the different broadband wireless IR concepts are compared.

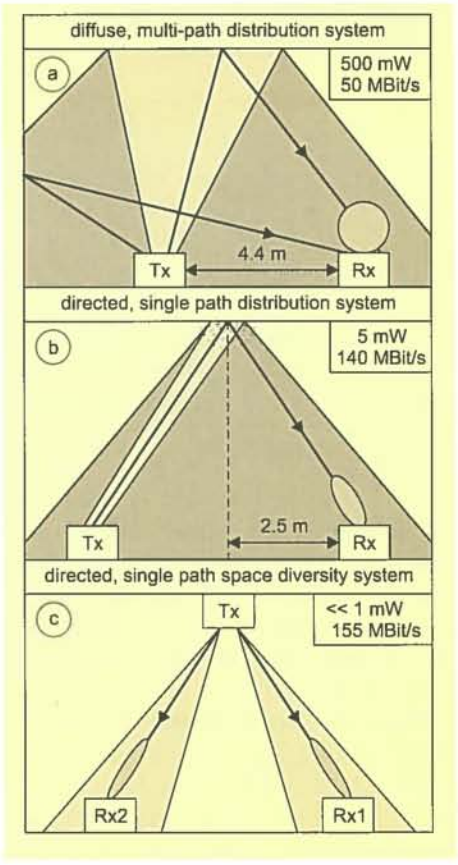

Fig. 1:
Comparison of different system concepts for broadband wireless infrared transmission.
(a) Diffuse system with non-directed links.
(b) Directed system based on spot diffusing.
(c) Space diversity system.

In the diffuse IR system the bandwidth is limited by the delay spread due to the multiple signal paths. A critical bit rate times distance product of 260 Mbit·m/s was derived by Gfeller et al. [3], and a data rate of 50 MBit/s over a distance of 4.4 m has been demonstrated by Kahn and Barry [4], who measured a bit error rate of 10^{-7} at 475 mW transmitter power (see Fig. 1a).

When using directed receivers (Figs. 1b, 1c), much less of the background light is picked up, and the transmitter power can be markedly reduced. In a recent

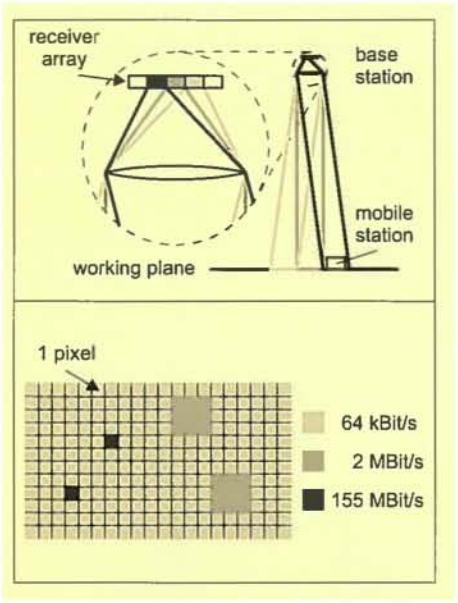

Fig. 2:
Top: Principle of optical space diversity using an array and a lens. Bottom: For the lower bit rate services a number of adjacent pixels is combined. This increases the field of view of the receiver.

140 MBit/s experiment using directed transmitters and receivers (Fig. 1b), an optical power of only 5 mW was sufficient to reach an error rate of better than 10^{-9}. Due to diffuse reflection at the ceiling, the collimated upward beam creates a wide downward radiation cone, and beam expansion sets a lower limit to the link budget. At 2 m below the ceiling an area of roughly 20 m^2 is illuminated, and a lens 5 cm in diameter was used to collect part of this light at the receiver. With reasonable effort using a single collimated beam and an avalanche photodiode receiver, eye-safe operation of this system seems to be possible only at long wavelengths ($\lambda \approx 1550$ nm) [5].

When the system can take advantage of space diversity (Fig. 1c), only a small sector is actually illuminated by a narrow beam. Beam expansion is then less critical, and the transmitter power can be further reduced. One implication that will be stressed in more detail below is that, by matching the sector size to the eye safety regulations, the space diversity concept might also allow directed links at near infrared wavelengths ($\lambda \approx 850$ nm).

2. System concept

The basic concept of an optical space diversity system is shown in Fig. 2 (top). The optical base station is located at the ceiling looking down to a number of mobile stations in the cell. The base station receiver consists of a lens and a photodiode array. Since the lens projects a small image of the cell onto the array, each pixel in the array is responsible for one sector in the cell. All pixels can be addressed individually, and an additional switch matrix allows the arbitrary combination of adjacent pixels. The transmitter consists of a lens and an array of diode lasers. In this way, each sector gets a beam of its own. In principle, the same hardware is used in the mobile unit.

This is a simple but very flexible hardware configuration. When a user requests the highest data rate service, for instance, a single pixel is reserved for that user (Fig. 2, bottom). Any motion in the cell must be tracked by switching the signal from pixel to pixel. Because of the small pixel size, the transmitter and receiver characteristics have a relatively narrow cone, and a directed link is established between the base station and the user (Fig. 3c). Of course, this link is sensitive to shadowing and blocking, and the user's degree of mobility is small.

At medium data rates, the demand for increased mobility is satisfied by combining a number of adjacent pixels. The number of

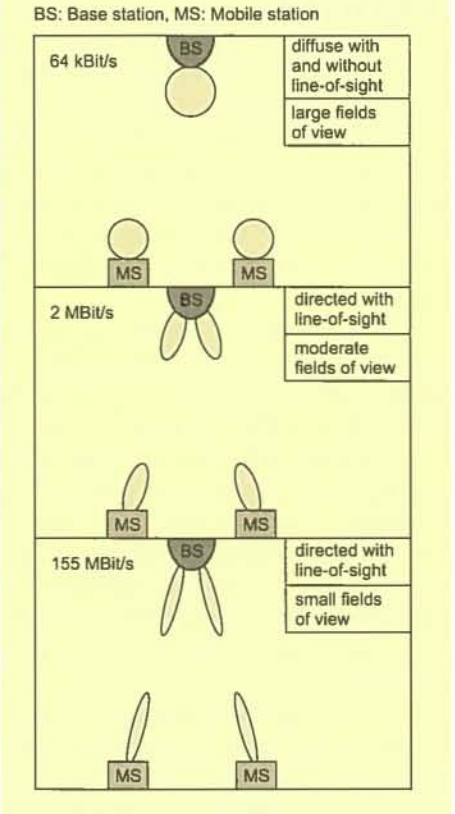

Fig. 3:
Fields of view of the base station and the mobile station at different data rates. (a) Low data rate and high mobility. (b) Moderate data rate and medium mobility. (c) High data rate and low mobility.

handover events is then reduced, and a wider cone is generated at the transmitter and receiver (Fig. 3b). Although mobility is increased, the link is still susceptible to blocking.

For the network access channel and the low bit rate services such as voice and email, all residual pixels in the array are combined. The transmitters and receivers then have wide cones (Fig. 3 a). When the line of sight is blocked, the information can still be transmitted via the various non-direct paths inside the cell, which occur because of the multiple diffuse reflections in the room. Hence the basic services are reliably supported.

Obviously, a single hardware configuration using arrays and lenses can support narrow bandwidth services with high mobility as well as broadband services with low mobility. As in radio frequency transmission, beam shaping and steering is performed by array techniques, but in optics no additional signal processing is necessary to distinguish between the different users. This is performed by the lens and the right selection and combination of the pixels.

3. Eye safety and feasibility

As already mentioned, in a space diversity system the total transmitter power can be much lower than in a distribution system, and the sector size can be matched to the maximum permissible exposure (MPE) that is defined in IEC 825-1 [6].

The MPE is measured 10cm from the source by using apertures of 7mm and 3.5mm diameter at $\lambda \approx 850$ nm and $\lambda \approx 1550$ nm, respectively. The light is emitted from a small pixel, and the maximum power of this point source is 0.25 mW (at 850 nm) and 10 mW (1550 nm), respectively. (Absorption of the longer wavelength IR light in the cornea and the aqueous humour is responsible for the large differences in these figures.)

When the measurement configuration in IEC 825-1 is projected onto the working plane as indicated in Fig. 4, the minimum diameter of one sector at this power level can be calculated. At a distance of 2m, the resulting sector diameters work out to be 14cm (at 850 nm) and 7cm (1550 nm).

Of course, the eye safety limit at 1550 nm is less stringent, and a less sensitive receiver would be required. But with current technology, reliable vertical cavity surface emitting laser (VCSEL) diode arrays, which find a promising application in the scenario described above, are only available in the short wavelength region [7]. Therefore, it is interesting to check the power budget that is available at 850 nm.

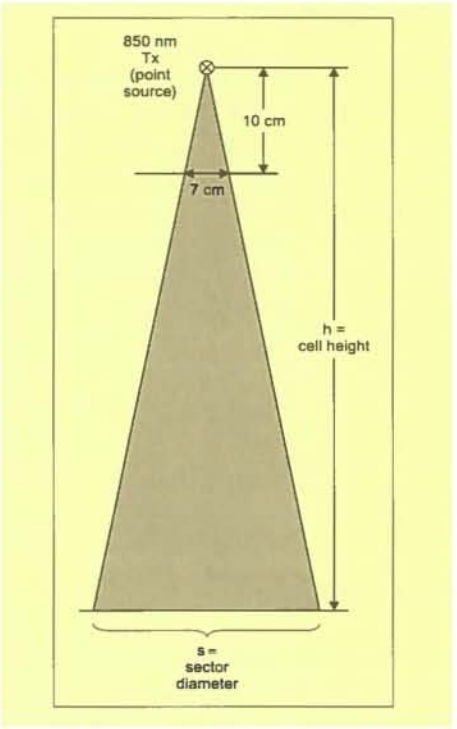

Fig. 4:
The sector size can be derived from the rule for eye safety measurements.

On the array an image of the total $5 \times 5\,m^2$ cell is present. At a reasonable array size of $1 \times 1\,cm^2$, a reduction ratio of 500:1 therefore is required. When the distance is about 2m, an imaging lens with a focal length f=4 mm is required. Since the aperture of a glass lens is never larger than its focal length, a beam expansion loss of at least 31 dB is calculated from the areas of the lens and the sector. At 850nm and -6 dBm transmitter power, a minimum receiver sensitivity of -37 dBm is therefore required.

For 155 MBit/s and direct detection, this is known to be possible only with an avalanche photodiode (APD) receiver. Presently, silicon APD arrays, which are used in the near IR, are readily available components [8]. The optical space diversity concept which is described above is hence expected to be feasible at 850 nm.

4. Conclusions

A new concept for the simultaneous support of narrowband and broadband services to a large number of mobile users in an indoor environment has been presented. It is based on VCSEL arrays and photodiode arrays. At low data rate services there is no limit to mobility, but at higher bandwidths a directed line-of-sight link is required. The space diversity concept allows for a further reduction of the transmitter power compared to the distribution system. The feasibility of the concept at short wavelengths (850 nm) has been checked.

Acknowledgment

This work was supported by the German Ministry for Education, Science, Research and Technology as part of the ATM*mobil* Project under contract No. 01 BK 611/3.

References

[1] M. Bronzel, D. Hunold, G. Fettweis, T. Konschak, T. Dölle, V. Brankovic, H. Alikhani, J.-P. Ebert, A. Festag, F. Fitzek and A. Wolisz, **"Integrated broadband mobile system (IBMS) featuring wireless ATM"**, ACTS Mobile Communication Summit '97, pp. 641-646, Aalborg, Denmark, October 7-10, 1997.

[2] M. Bronzel, D. Hunold, J. Jelitto, N. Lohse and G. Fettweis, **"Unterstützung variabler Datenraten durch den Kapazitätsgewinn adaptiver Antennen"**, ITG-Diskussionssitzung **"Systeme mit intelligenten Antennen"**, University of Kaiserslautern, December 5, 1997.

[3] F.R. Gfeller and U.H. Bapst, **"Wireless in-house data communication via diffuse infrared radiation"**, Proc. IEE, vol. 67, no. 11, pp. 1474-1486, 1979.

[4] J.M. Kahn and J.R. Barry, **"Wireless infrared communications"**, Proc. IEEE, vol. 85, no. 2, pp. 265-298, 1997.

[5] V. Jungnickel, C. v. Helmolt and U. Krüger, **"WireLAN: A broadband wireless IR LAN architecture compatible with the Ethernet protocol"**, Proc. 24th European Conference on Optical Communication, vol. 1, pp. 367-368, Madrid, Spain, 1998.

[6] DIN EN 60825-1:1994, **"Sicherheit von Lasereinrichtungen"**, Teil 1: Klassifizierung von Anlagen, Anforderungen und Benutzer-Richtlinien, VDE-Verlag, Berlin, 1997.

[7] K.J. Ebeling, R. Michalzik, R. King, P. Schnitzer, D. Wiedemann, R. Jäger, C. Jung, M. Grabherr and M. Miller, **"Applications of VCSEL for optical interconnects"**, Proc. 24th European Conference on Optical Communication, vol. 3, pp. 29-31, Madrid, Spain, 1998.

[8] http://www.egginc.com.

K.-O. VELTHAUS, U. TROPPENZ AND B. HÜTTL

ELECTROLUMINESCENT DISPLAY DEVELOPMENT AT HHI

Abstract

New results and recent developments in the field of inorganic thin film EL (TFEL) are reported. Emphasis is given to the development of the efficient blue-green emitter SrS:Ce. Several demonstrators have been realized with this new material using the 'colour by white' approach. A fully transparent display is also described.

Research activities and cooperative activities demonstrate successful research work and the perspective for advanced new display types.

1. Introduction

Electroluminescent (EL) displays are all-solid-state devices and major contenders for rugged, flat panel information displays. They have several inherent advantages such as wide viewing angle, high contrast and high temperature range, making them an obvious solution for industrial and automotive demands. In addition, micro displays on silicon substrates offer the prospect of new solutions for rugged, lightweight, high-resolution mobile displays.

So far the blue colour component has been the main problem for full colour EL applications, and this is still an issue. So far the most promising candidate for a blue emitter has been SrS:Ce. This alkaline-earth sulphide shows an efficient broad emission in the blue-green region with the possibility of filtering out the primary blue, e.g. by using dye filters.

Because colour filtering is needed in any case, SrS:Ce was combined with ZnS:Mn to get a broad band white spectrum from which all three primary colours can be filtered out. Since there is no need to pattern the phosphor itself, this 'colour by white' concept is a simple and cheap process technology similar to the well known monochrome ZnS:Mn. Consequently, it is expected that this concept will yield the first competitive commercially available full colour EL display products in the near future.

2. 'Colour by white' approach

Figure1 shows the simple setup for the 'colour by white' approach. The structure is inverted compared to the conventional one. Hence the light is not outcoupled through the substrate but through the opposite side, where filters are mounted in order to subtractively generate the proper pixel colour. Only the light emitting layer and the colour filters have to be adapted to the particular application. In addition, the inverted structure is characterized by a very high contrast in ambient light. This is due to the low reflectivity molybdenum electrode and the use of colour filters.

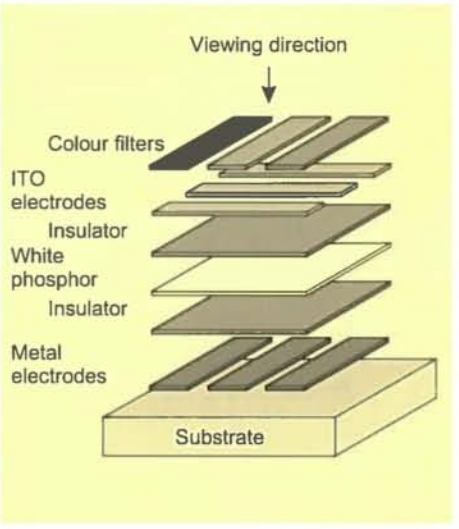

Fig. 1:
Inverted display structure for the 'colour by white' concept.

3. SrS:Ce, Ag, Mn electroluminescent material

Many laboratories have been investigating SrS:Ce in the last few years by employing different deposition techniques (e.g. e-beam evaporation and CVD). This research shows that the behaviour of this phosphor material depends strongly on the deposition method, the preparation conditions and the use of co-activator materials, as is well known from the powder phosphor research. At HHI a multi-source reactive evaporation method has been established for the preparation of this material. This is a very flexible method for evaluating different doping materials in a wide concentration range. Within 4 years the luminance and efficiency of SrS:Ce EL devices have been increased at HHI by

almost a factor of three up to 2 lm/W, while at the same time achieving a deeper blue emission and greatly improved aging behaviour.

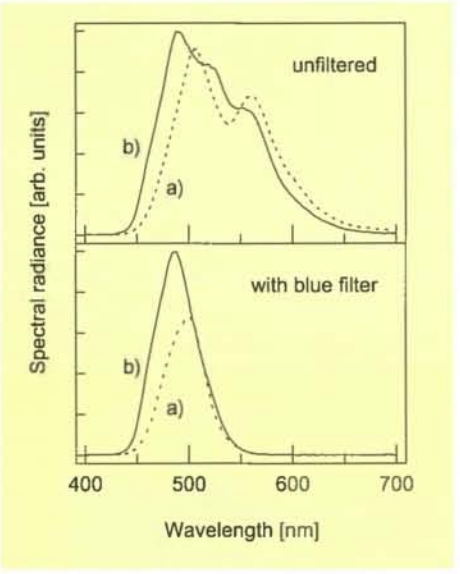

Fig. 2: Comparison of the blue filtered and the unfiltered emission spectra of: (a) conventional SrS:Ce, Mn, and (b) SrS:Ce, Ag, Mn.

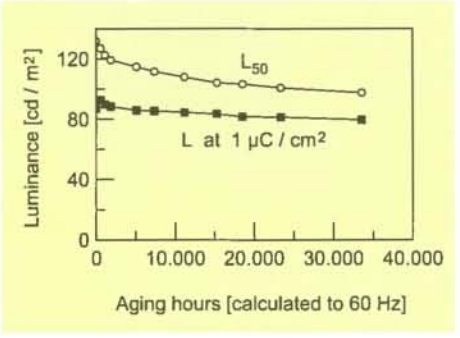

Fig. 3: Aging behaviour of the new SrS:Ce, Ag, Mn EL device. Luminance measured at L_{50} and at a transferred charge of 1µC/cm².

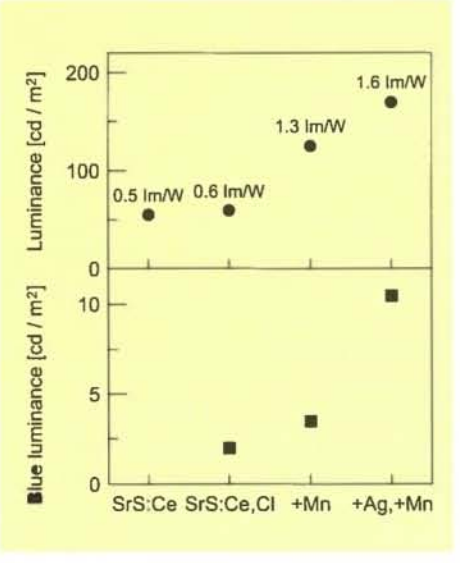

Fig. 4: Improvement of the primary SrS:Ce luminance and efficiency (upper part) and increase of the filtered blue component (bottom part) due to defect engineering with different codoping materials.

In this context manganese has been found to improve the crystal quality of the SrS:Ce film, and therefore to enhance the luminance and efficiency of the EL device.

In addition, silver Ag^{1+} has been introduced as a new charge compensating material for the Ce^{3+} luminescent centre. The silver codopant is responsible for a remarkable increase of the blue luminance, due to a blue shift of the emission spectrum accompanied by a higher absolute spectral radiance in the blue [1].

This situation is shown in the top part of Fig. 2, where the unfiltered emission of the novel SrS:Ce, Ag, Mn TFEL device with a dominant wavelength of λ_{dom} = 500.2 nm is compared with that of a conventional SrS:Ce, Mn sample (λ_{dom}=511.6 nm). The blue-filtered spectra are also shown in the bottom part of Fig. 2. The new material exhibits an enhanced radiance measured through a blue filter of more than 40% compared to the conventional process. Fairly good colour coordinates of x=0.10 and y=0.26 at the high luminance level L_{50} (measured at 50 V above the threshold) of more than 25 cd/m² at 60 Hz driving frequency have been achieved. The corresponding efficiency for the filtered blue emission is 0.2 lm/W.

The dense film structure, in which no pinholes could be detected, the co-doped silver, and the good crystal quality seem to be responsible for the very good aging behaviour achieved by this new SrS process. For illustration, the aging characteristics of an unsealed SrS:Ce, Ag, Mn device are shown in Fig. 3. The accelerated aging has been performed at 2 kHz for more than 1000 hours. Since time scales approximately proportional to the driving frequency, this corresponds to more than 34,000 hours at a 60 Hz display frequency. After that time the luminance L_{50} is still 74% of the initial value. Moreover, this is without significant change of the threshold voltage. At a fixed transferred charge of 1 µC/cm² the aging is only 10%, which shows the stable quantum efficiency and the potential of the phosphor itself.

In the last few years the most important blue part of the emission spectrum could be improved by a factor of 4. The given luminance values in the bottom part of Fig. 4 correspond to the mathematically filtered blue component that meets the EBU colour standard for CRT monitors. The

results achieved at HHI with SrS:Ce EL devices actually showed the highest luminance and efficiencies ever reported.

4. HHI – Partner in an ESPRIT project

Because of these encouraging results, the HHI and the company Planar are evaluating SrS:Ce films in hybrid device structures. This means that HHI is preparing the blue emitter SrS:Ce and Planar is preparing the other thin films for a 'colour by white' display. This combined research is carried out in an ESPRIT project of the European Community called ELDISP. The objective of this project is the development of next generation colour EL displays for industrial and specific consumer applications and to develop the technology and pilot manufacturing capacity for the production of these new displays.

The hybrid structure with the blue emitter made by HHI shows a 3 times higher efficiency for the filtered blue emission and better CIE colour coordinates than the Planar samples. Hence prototype displays are being constructed using the HHI process. The format will be a 5" QVGA display with a resolution of 320×240 colour pixels.

5. Demonstrators realized at HHI

In order to demonstrate the research results, we succeeded in fabricating various prototypes. For a 'colour by white' prototype we combined the developed SrS:Ce, Ag, Mn material with the well known ZnS:Mn. This combination is currently the best choice for the colour by white concept.

The demonstrator has been built with an active area of 3"×3" and a resolution of 128 ×128 pixels. The achieved luminance for the 3 primary colours red (R) green (G) and blue (B) are measured through Fuji-Hunt colour filters. We did not use structured filters, but measured the areal luminance values with special filter plates one after the other. The achieved luminance values are shown in the following table:

Colour	Luminance (cd/m^2)	Colour coordinates CIE 1936
Red	65	(0.63; 0.36)
Green	196	(0.34; 0.59)
Blue	40	(0.1; 0.3)
Blue	21	(0.12; 0.25)

These luminance values would lead to a mixed white emission of 70 cd/m^2, allowing for the fill factor of a fully structured RGB panel. The efficiency of the primary broadband emission is about 3 lm/W.

Another demonstrator with the same dimensions, but built first with ZnS:Mn, makes use of the unique advantages of EL displays compared to those of all other technologies. By replacing the metal electrode by an additional ITO electrode, a transparent emissive display with a transmission of 90 % can be realized.

This opens up novel possibilities for electronic imaging, since several stacked viewing planes can be realized. One promising application is in cars, where a cockpit with conventional instrumentation can be upgraded for GPS and other alphanumeric or graphic information by mounting a transparent display in front of the other instruments. This design, patented by Bosch (Germany), displays only the conventional instrumentation if digital information is not required. But if navigation, for example, is needed, a different plane – the transparent EL display – lights up in front of the instrument panel.

This demonstrator is actually built as a monochrome version, but work is under way to extend it to a full colour version.

6. Micro displays – the Planar/DARPA project

Active Matrix Electroluminescence (AMEL) technology is produced by the integration of IC and thin film EL technologies on a silicon wafer to produce a very small, very high resolution display. The AMEL device is realized by fabricating the electronic circuitry for the display on an IC wafer and then by overlaying a thin film, light-emitting EL structure on top of the IC to produce a fully integrated emissive display [2].

The AMEL device structure overcomes the size limitations of traditional TFEL technology by integrating the driver electronics onto the wafer, which forms the substrate for the AMEL device. Using this approach, the manufacturer Planar has demonstrated AMEL displays with a resolution of 2000 lines per inch (lpi) in display formats of both 640×480 and 1280× 1024. The first AMEL devices were monochrome displays but recent work has resulted in the development of colour AMEL displays. The single colour (usually yellow) phosphor in the monochrome device is replaced by a broad band 'white phosphor' which allows the primary red, green and blue colours to be obtained by filtering.

The HHI is involved in the phosphor development for these displays in a DARPA-sponsored project. In particular, the new SrS:Ce, Ag, Mn phosphor developed at HHI is under investigation. The delivered films yield twice the luminance and better colour coordinates than the SrS:Ce material used by Planar.

One example of target applications for these AMEL displays is lightweight display glasses. With integrated magnifying optics, the displays can show a large virtual image with high resolution in a rugged and very mobile setup. These display glasses are thought to be the ideal solution for new mobile broadband telecommunication systems working with the new UMTS standard, because the killer application for this new generation of mobile telecommunication systems will be the Internet rather than speech as we find it today.

7. New blue emitter – SrS:Cu, Ag

With the very recent introduction of SrS:Cu, Ag as a new blue-emitting electroluminescence phosphor material [3], there is now a second candidate for the blue emission beside SrS:Ce which could meet the requirements for a full colour EL display. The emission spectra of these two materials are shown in Fig. 5. The new material yields a much deeper blue emission and should therefore be the better choice.

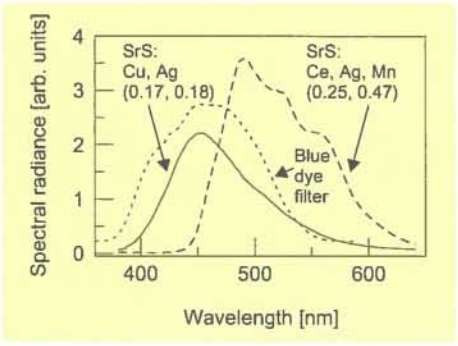

Fig. 5: Comparison of the emission spectra of SrS:Ce, Ag, Mn and the new SrS:Cu, Ag.

However, the SrS:Cu, Ag so far reported has been prepared by sputter deposition and subsequent post annealing at about 830° C. Standard substrate glass like Corning 7059 or 1737 is not capable of meeting these high temperature requirements, and available glass ceramics, for example, are too expensive to be used for direct view displays.

Actually, a new deposition process which works at preparation temperatures of only about 600° C has been developed at HHI. The results were published as a late news item at the EL workshop in Bend (USA) [4]. The HHI is still the only research group that has reported the successful development of such a low temperature deposition process.

This new process still needs further development, but promises the possibility of a new full colour EL display with similar coordinates to those of the standard television set.

8. Conclusions

Dramatic improvements of the blue-green emitting material SrS:Ce have been achieved. Due to its very good results and leading research activities in this field, the HHI is involved in additional projects for the European Community and the US Planar/DARPA.

The HHI has succeeded in fabricating demonstrator displays using the 'colour by white' approach for a full colour display and ZnS:Mn for the fully transparent version.

The new SrS:Cu, Ag phosphor offers the prospect of full colour displays that will equal the colour quality of CRT monitors.

Furthermore, EL technology has some inherent special properties that open the vista of new generations of displays for new emerging markets, such as transparent displays or rugged micro displays.

Acknowledgments

The authors wish to thank the German Ministry for Education, Science, Research and Technology for support under contract 01 BK 520/3. Furthermore the assistance of the colleagues of the EL research team at HHI is gratefully acknowledged.

References

[1] K.-O. Velthaus, B. Hüttl, U. Troppenz, R. Herrmann and R. H. Mauch, Digest of Technical Papers, 1997 SID Int. Symp., Boston, 1997, p. 411.

[2] R.Tuenge et al., Digest of Technical Papers, 1998 SID Int. Symp., Anaheim, 1998, p. 949.

[3] S.-S. Sun, E. Dickey, J. Kane and P. Niel Yocom, Conference Record of the Int. Display Res. Conf., Toronto, 1997, p. 301.

[4] K.-O. Velthaus, B. Hüttl, U.Troppenz, T. Gaertner and G. Bilger, Extended Abstracts 9th Int. EL Workshop on Inorganic and Organic EL, Bend, 1998, p. 231.

J.-R. OHM, W. LIEBSCH,
B. MAKAI, K. MÜLLER, D. ZIER
AND T. SIKORA

MPEG-7 SEARCH ENGINE FOR IMAGE AND VIDEO DATABASE RETRIEVAL APPLICATIONS

Abstract

This contribution reports on an implementation of a search engine for visual information retrieval that has been developed at HHI in the context of the forthcoming MPEG-7 standard. The system supports similarity-based retrieval of visual (image and video) data along feature axes such as colour, texture, shape, geometry and motion. The descriptors for these features have been developed in such a way that invariance against common transformations of visual material (e.g. filtering, contrast/ colour manipulation, resizing etc.) is achieved. They are also matched to human perception properties. Furthermore, they have been designed to allow a fast, hierarchical search procedure in which the inherent search mechanisms of database systems can be employed. This is important for distributed client-server applications, where pre-selection should be performed at the database side. Database interfaces have been implemented in a platform-independent way based on the SQL standard.

1. Introduction

Visual-feature based search and retrieval of images and videos in databases (archives) is a technique that has attracted considerable research interest in recent years [1][2][3]. The demand for visual content description in networks (broadcast and Internet) is also rising quickly due to the worldwide exponential growth of available visual items. Visual information not only enhances the value of textual information, but also opens up new horizons if it is possible to categorize and index the content in an appropriate way. Textual key words alone are definitely not sufficient for this purpose, since they are not adequate to meet the levels of perception and abstraction inherent in visual information.

To meet this challenge, the ISO Moving Pictures Experts Group (MPEG) has started a standardization activity for a 'Multimedia Content Description Interface', called MPEG-7, that shall provide a standardized feature description for audiovisual data [4]. The meaning of 'features' in this sense is very broad, and can include elements of high-level descriptions (e.g. authoring information, scripting information, narrative relationships between scenes), mid-level descriptions (e.g. semantic categories of objects or subjects present within a scene), or low-level descriptions (e.g. signal-based features like colour, texture, geometry, motion of scene or camera).

Of course, low-level description categories can be transformed into higher level ones by setting specific rules, and qualitative separation of these categories is not always straightforward. The work reported in this contribution concentrates on the example of low-level descriptions; in this case, automatic extraction of features from the data is usually possible, and the definition of matching criteria for similarity-based retrieval using a specific feature type is more or less unique.

To obtain optimum results, the feature descriptions that characterize the visual data should be closely related to the retrieval algorithms used to search the databases, broadcast streams or networks. Even though many visual search engines already exist, these are mostly dedicated systems, and it is impossible to perform a net-wide search to retrieve visual data with some predefined features from different database sources. With multimedia content spreading over the worldwide computer networks, the use of distributed systems becomes necessary.If retrieval of data is supposed to be a de-coupled process, a normative feature description as planned by MPEG-7 is required.

2. MPEG-7 description concept

It is not the intention of MPEG-7 to standardize either the feature extraction or the search/retrieval algorithms, which may be differently optimized for specific applications. Nevertheless, it is clear that the features described relate to some feature extraction mechanisms, and that the structure of a normative feature description has

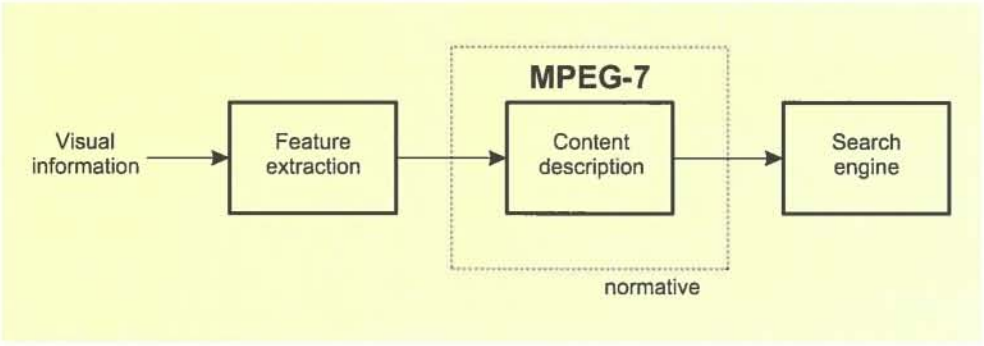

Fig. 1: MPEG-7 processing chain.

a large impact on the non-normative search algorithm that uses this description for retrieval purposes. The basic chain of MPEG-7 processing is illustrated in Fig. 1.

The MPEG-7 description will consist of description schemes (DS) and descriptors (D), which are instantiated as descriptor values. Furthermore, it is planned to create a description definition language (DDL) that will allow the definition of new description schemes and descriptors for specific applications [5]. The whole description will be encoded in such a way that efficient storage and transmission are possible.

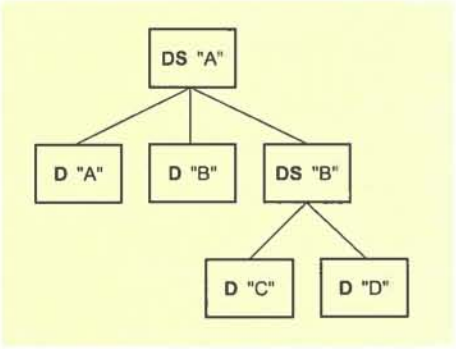

Fig. 2: Example of a simple MPEG-7 description scheme structure.

In this paper we concentrate on the optimization of description scheme structures, so that they can be used in an efficient way for distributed applications. A description scheme is generally a combination of one or more subordinate descriptor(s) and/or description scheme(s). An example is illustrated in Fig. 2, where the **DS** 'A' at the top level is a combination of the **D**s "A" and "B", and **DS** "B", which again is a combination of **D**s "C" and "D". Multiple nesting of DSs shall be possible. Each descriptor usually characterizes one single feature of the content. The associated descriptor value can be either a scalar or a vector, depending on the nature of the descriptor.

3. Visual feature description and content retrieval

Figure 3 shows an example for the structure of a description scheme characterizing the visual features of an 'image object', which may be a still image, a keyframe from a video, a single segment of an image or keyframe, or any other (rectangular or arbitrarily shaped) visual content item. This DS can again be a sub-description of a higher-level DS in MPEG-7, e.g. for the purpose of shot description within a video scene.

Detailed insight is given here only into the colour feature description, although similar sub-trees have also been developed for texture and contour. The use of colour histograms is very efficient for describing the colour features of visual items. For this purpose we use a transformation of the colour into the HSV (Hue, Saturation, Value) space. It is known that differences in HSV space approximately coincide with the human perception of colour differences. The HSV space is quantized, and the frequency of occurrence of the quantized colours is calculated. Comparison of the histograms of two visual items is performed by calculating the sum of absolute differences (SAD). This descriptor is capable of finding images of similar colour with a high accuracy, but the matching function requires a considerable number of comparisons, so that there is no straightforward way of performing fast retrieval from large databases.

The SAD criterion used in histogram comparison is also not usually supported by the selection mechanisms of conventional database systems. Hence, we implemented in addition a very simple descriptor for characterization of the dominant colours. This is based on a clustering procedure, wherein the geometry of each

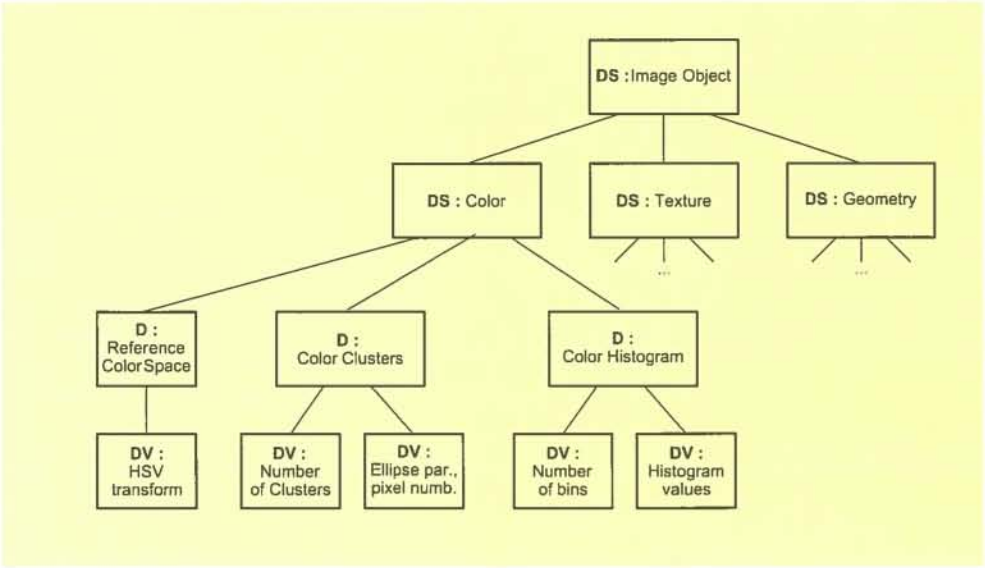

Fig. 3:
Hierarchical structure of an image object DS based on colour, texture and geometry descriptors.

cluster is described by the moments of an ellipsoid, and the number of pixels within the cluster is an additional parameter. This descriptor is used for comparisons in the first stage of a coarse-to-fine procedure. It requires only numerical comparisons, and uses the pre-selection mechanisms of a remote database server system. The complete histogram data have to be retrieved only for those items that pass the pre-selection tests, and are then compared by the histogram method in the search engine residing at the client.

In a distributed system, where data are located on a remote server, proper organization and pre-selection of the description data are of high importance to facilitate an efficient search. This aspect is discussed in the following section.

4. Retrieval in a client/server environment

For audiovisual data search and retrieval, a search engine needs flexible access to the feature description resources. This means that, for specific search tasks, only particular subsets of the feature representation data are needed. This can easily be achieved if not only the visual content items, but also the MPEG-7 description data, are themselves organized as items in the database. Only the structure of the organization (which specifies, for example, which descriptor values can be found in particular fields of a data table) needs to be made available in an initial descriptor table, which is an entry point to the database. The AV data to which the description

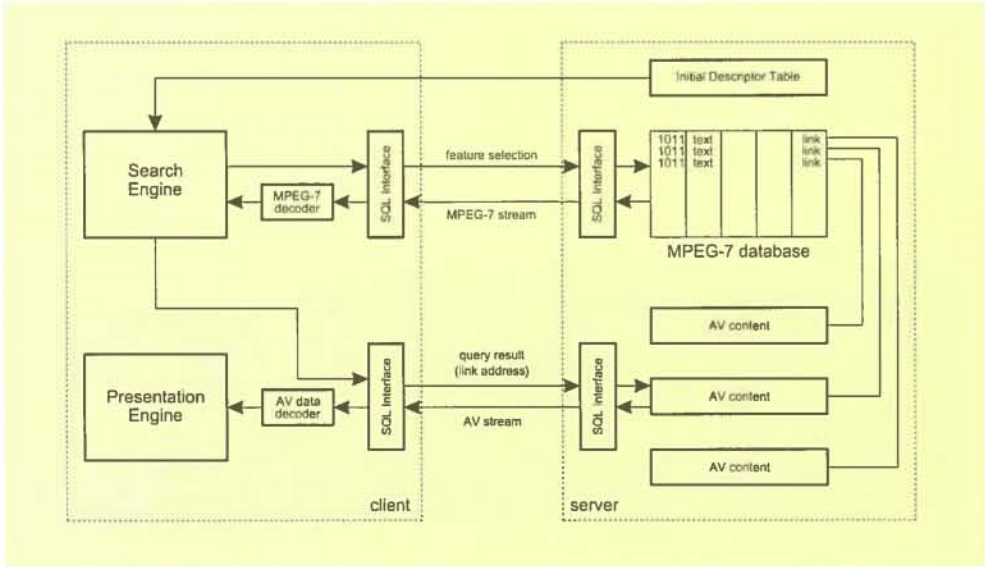

Fig. 4:
Configuration of a client-server architecture in visual data retrieval.

is related need not necessarily be stored in the same database – it is sufficient that the description holds a link to the real location.

The search engine situated at the client can then access via the database interfaces any descriptor values associated with any AV object in any set of data. Since the Structured Query Language (SQL) [6] is a very common interface supported by most database systems, we have used it for this purpose. The configuration is illustrated in Fig. 4.

5. Implementation

The concepts elaborated in this contribution have been implemented in a visual data search engine developed at HHI. For platform independence, the system's core parts – presentation, user interactivity and database interfaces – were realized in JAVA. For database interfacing, we have used the JAVA Database Connectivity (JDBC) Tools, which allow the implementation of a database-independent SQL interface. The user interface is also of great importance in the realization. The search engine's basic visible desktop includes only the most relevant setting capabilities, such as data management and the selection of basic features for a specific query. Users with more skills can also use finer settings for better search results (e.g. they may adjust the weightings of the available texture descriptors). The search can be performed both on still images and on key frames from video sequences. The presentation interface also contains a video player.

Figure 5 shows a retrieval result in which the 10 images shown at the right are the results in ranked order of a query that started with the image in the left box as a reference.

6. Conclusions

A normative description of visual features, as will be defined in MPEG-7, is needed to achieve interoperability between visual information systems (e.g. storage of visual content in distributed databases), to achieve automatic acquisition from visual sensors of all kinds, and to handle the visual information flood on the Internet or broadcast channels. Such a description will not only assist humans in the search and retrieval of visual information, but will also enhance automated systems (e.g. surveillance systems in which specific procedures are triggered if a certain status of the visual scene is recognized by feature classification, or automatic capturing by smart cameras).

A distributed configuration imposes additional requirements on the content-based search, especially with respect to data organization and the structure of feature descriptions. In this context we have tested different descriptors that can be used in a coarse-to-fine search strategy, with initial searching done at the server end in order to speed up the query and avoid unnecessary transmission of feature data. The communication between the search engine and the database can be organized in a very efficient way using existing interconnection standards such as SQL. For multi-tier systems, e.g. simultaneous linking with several databases or connection with intelligent agents, an object-oriented approach like CORBA would be more convenient.

So far we have limited our efforts to the lower level description of image content and to architectures where there is a one-to-one connection between a database and a search engine. It is expected that in future the use of distributed components, such as intelligent agent technology resident on the network, as well as the use of 'learning' search technologies that better model the human visual recognition

Fig. 5: Retrieval result with the HHI search engine.

system, can help to build better systems, which also imply automatic classification of higher-level visual features.

Acknowledgment

This work was supported by the German Federal Ministry of Education, Research, Science and Technology under grant 01 BN 702.

References

[1] J.R. Smith and S.-F. Chang, **"VisualSeek, a fully automated content-based image query system"**, Proc. Int. Conf. on Image Proc. (ICIP), Lausanne, 1996.

[2] J.R. Bach et al., **"The Virage image search engine, an open framework for image management"**, Proc. Storage and Retrieval for Image and Video Databases, SPIE, vol. 2670, pp. 76-87, 1996.

[3] W. Niblack et al., **"The QBIC project, querying images by content using colour, texture and shape"**, Proc. Storage and Retrieval for Image and Video Databases, SPIE, vol. 1908, pp. 173-187, 1993.

[4] ISO/IEC/JTC1/SC29/WG11, MPEG-7 **"Context and Objectives"**, document no. N2460, Atlantic City, Oct. 1998.

[5] ISO/IEC/JTC1/SC29/WG11, MPEG-7 **"Requirements Document"**, document no. N2461, Atlantic City, Oct. 1998.

[6] ISO/IEC 9075:1992, **"Information Technology – Database Languages – SQL."**

S. RENAULT, O. STACHEL AND S. PASTOOR

CREATING A NEW GENERATION OF MULTIMEDIA COMPUTER INTERFACES

Abstract

In this paper a new kind of computer interface allowing 3D visualization and eye-controlled interaction is proposed. In order to explore the advantages and limitations of the concept, a prototype system has been set up.The testbed includes a visual operating system for integrating novel forms of interaction. The paper outlines an anticipated scenario for future multimedia applications and reviews the new operating system, and also gives preliminary results of user testing.

1. Introduction

Rapid progress in the enabling technologies has provided the basis for universal data and communication networks such as the Internet. Standardization allows the exchange of various types of information (e.g. JPEG for still images, MPEG for motion sequences, and HTML for complex hypermedia objects), so that increasingly powerful networked multimedia systems become available. The end users are confronted with a range of new possibilities such as access to huge external data bases delivering information for daily use or for entertainment (encyclopedic information, video games, video-on-demand), access to numerous transactional services (home banking, home shopping), teleworking, and video communication.

In combination with common application programs for editing text, graphics and spreadsheets, the new functionalities constitute a novel field of interaction characterized by two principles:

1.The first principle is the hypermedial structure of the new media, meaning that the data and services available are distributed over nodes connected via direct links forming open, non-hierarchically structured networks. This allows free, non-linear access – users may select any entry point and each node will offer various alternatives for navigation.

2. The second principle is the availability of multiple types of media objects. Apart from visualizing static types of information (text, graphics), the user interface will simultaneously present dynamic, time-based data such as animations, motion pictures and sound. This applies both to the retrieved media objects as well as to the control elements used for their manipulation (e.g. to select, position, zoom or edit the information objects and to address the various peripheral devices).

Although empirical results on usability aspects of such complex systems are sparse, there is increasing evidence that some general problems are inherent in the concept, including:

- The risk of disorientation ('getting lost in hyperspace'). Major causes of disorientation include inadequate representation of the sources of information and of the available processing possibilities, of the current location in the network and of the path leading to this location, of the available backward and forward options, and of the ways to change between various procedures (such as reading versus editing and navigation by exploring versus specific search).
- Problems caused by cognitive overhead due to non-linear access to the media. Any jump between nodes will interrupt reading and the user may be required to adapt to new functionalities.
- Possible psychological problems resulting from the integration of video communications, including the loss of psychological distance in a sensorically rich communications environment (intrusive social presence) and the loss of domain control (merging of the privately and publicly accessible spheres). Hence, in order to avoid negative emotional reactions (frustration, helplessness), the user interface should offer methods for sovereign control and management of video communications.

2. Interactions in 3D

Considering the user demands for quick cognitive orientation, sovereign management, and personal control, the following solutions are conceivable:

• 3D representation of tools, applications and media objects. Menus and icons could be placed on the surface of 3D objects, such as cylinders or cubes, and animated when selected by the user. Thus it will be possible to keep the essential functional elements (tools) permanently present. Moreover, a 3D display gives room to clearly arrange objects in the depth dimension. All in all, this would allow a more efficient use of the limited display area available.

• Functional placement in depth. Discrete depth layers could be connected with functional attributes so that, when users place information objects in a special layer, this will cause a special action. For domain control, documents placed at a certain depth layer could be accessible or not accessible (visible or invisible) to other users, for example. Also, the size of an object (full screen vs reduced size vs minimized) could depend on the depth layer selected. An intelligent interface agent could automatically select special depth layers to place various types of information objects according to user-defined rules (e.g. according to subject, context, relevance to the current situation, and type of data), with the possibility of automatically rearranging the display when the user changes criteria.

• Intuitive direct manipulation. By sensing the user's head position, a simple head movement could temporally open the view of a data object hidden behind a visually overlapping foreground object (look-around function). Simultaneously, a gaze tracker could evaluate the user's point of fixation. Looking at a formerly hidden object could pull it closer to the user making its contents easier to read. Moreover, the gaze tracker could adjust the process of image rendering so that only the object being looked at would appear in full focus – objects out of the user's gaze would be temporarily considered unimportant and therefore shown out of focus, helping them to fade from the viewer's perception and attention (active accentuation, mimicking the limited depth of focus range of the human eye).

• Non-command interaction. Being aware of the user's current actions and taking the situational context into account, the computer should be able to interpret the user's intentions and to optimally adapt to the user's goals. Hence, a non-command interface could significantly relieve users of 'routine' actions in controlling the computer, giving them the freedom to fully concentrate on the task at hand, rather than on how to operate the computer. Through sensing the user's intentions and by representing the media objects in 3D, it should be possible to make interaction with a computer more human-like.

In order to investigate the advantages and limitations of this concept, a testbed has been set up. The core element is a novel visual operating system which supports both a 3D graphic user interface and new kinds of interaction in 3D. The system includes a 3D display and senses the user's head location and gaze direction without making the user wear glasses or other encumbering devices [1].

3. Visual operating system

The developed visual operating system (VOS) is based on the concepts of both object-oriented programming (in terms of adaptation and the use of already available program functions) and visual programming (in terms of the display of software modules). This means that users can use a graphic editor to create and 'program' their entire environment and applications by simply linking appropriate software modules together. Compared to conventional visual programming tools, the proposed system builds on the advantages of 3D visualization, allowing a clearly structured representation of the interconnected program modules. The operating system runs on a Silicon Graphics Onyx computer and uses the virtual reality software dVS by Division Ltd as a basis for generating 3D graphics and for implementing user interactions.

The operating system subdivides all user-accessible software modules into three levels of complexity, comprising primitives as the smallest accessible units (basic arithmetic or graphic functions), components, and large-scale applications (aggregations of lower-level modules), respectively. The graphic representations of primitives (called gadgets) can be used to visually add animation, sound or database queries to a module, for example. The gadgets are stored in the basic library of the VOS and can easily be modified in order to change their visual appearance, without changing

their particular functionality. Fig. 1 shows represen tations of a gadget used for scrolling the visible part of a text document.

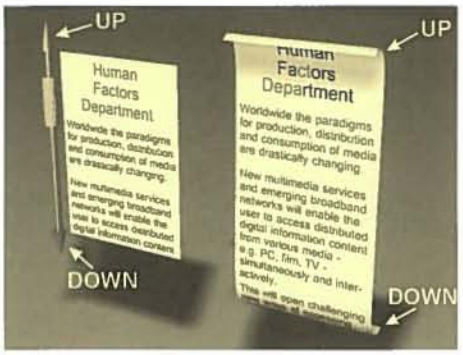

Several gadgets may be combined in order to form a component, which can then be used in various applications. In order to form larger software entities from lower-level modules, a module may have 'docks' that can be visually connected via a pipeline in order to enable the exchange of information packages between the modules (Fig. 2). This means that a network of interconnected software modules can easily be created, tested and modified step by step in order to ultimately create a rather complex application program.

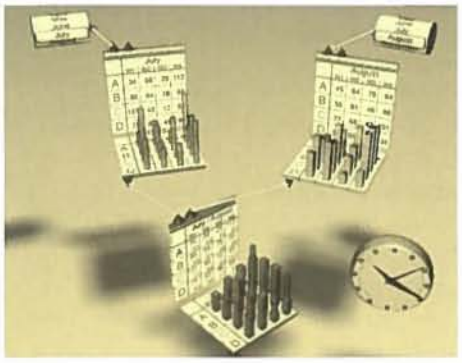

In order to get a clearly structured representation of complex programs, users can apply a 'zoom-out' function. In this way components can be compiled to form an aggregation where only the external docks are visible and the inner network is hidden. It is also possible to zoom in to view the large number of primitives and components forming the network of software modules in an application program.

When talking of 'users' in the framework of the proposed operating system, it should be noted that traditional differences between software developers and end users are intentionally diminishing. Future end users should have the possibility of setting up their own individually tailored application programs. Instead of using a huge monolithic program with a multitude of possibly never used functions, end users should be allowed to combine software modules from different suppliers according to their particular needs. The VOS aims at making interchangeable software components applicable to end users whilst providing an easy-to-use, clearly structured visual interface and intuitive manipulation and interaction techniques.

Fig. 1:
The appearance of a basic gadget is easily adapted to the user's preference without changing its functionality (e.g. scrolling the content of a text document could be either with a conventional scroll-bar or a papyrus-scroll metaphor).

4. Application scenario

The boxes shown in Fig. 3 have icons of frequently used applications or tools mapped onto their surfaces. Our application scenario includes an interface that allows the computer to detect the viewing position and gaze direction of the user [2]. By changing the viewing position (head movement), the user sees the tool boxes from different perspectives. The tool boxes change their perspectives overproportionally, so that it is possible for the user to make each side of the surface visible by small head movements.

Now imagine that the user is looking at one of the application icons (e.g. a spreadsheet application). Since the computer knows the user's gaze point, an 'event' is triggered, starting an animation primitive that magnifies the fixated icon for feedback and improved visibility. If the user continues looking at the magnified icon (e.g. for 150 ms, as proposed in [3]), thus signalling an increased interest in this particular item, the interface agent will instance the corresponding program (in this example a spreadsheet application). A sequence of visual interactions will allow the user to select and visualize numerical data in a 3D bar diagram.

In the example shown in Fig. 2, some data from the months of July and August are displayed on a weekly basis. Looking at the corresponding input and output docks of the spreadsheets will create pipelines and display a combined presentation of the data. Meanwhile, the operating system will automatically re-position the applications within the limited 3D display volume

Fig. 2:
The user-accessible software modules provide synapses (docks). Pipelines between the docks enable the transfer of information and allow the user to create complex applications (in this example a multi-dimensional spreadsheet) by visually connecting the docks of basic components.

to optimize visibility. The position and size of a graphic element can also be manually relocated by drag-and-drop operations with a conventional 2D input device, such as a mouse. In this case, the user's gaze selects the object to be moved in predefined planes.

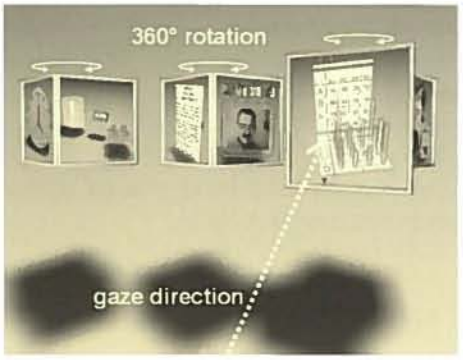

Fig. 3:
Toolboxes showing icons of applications or documents. The icons change perspective in response to the user's head movements and react when the user looks at a particular icon, e.g. by launching the relevant application program.

Fig. 4 shows an implementation of a Web browser. Glancing at a hypertext item will automatically download the hyperlinked document. The previously loaded documents will move backwards, thus indicating the search path to the current document. Looking at a background document will in turn move it closer to the user so that it becomes easily readable. Changing the viewing position by moving the head visualizes hidden documents and thus helps the user keep track when browsing the Web.

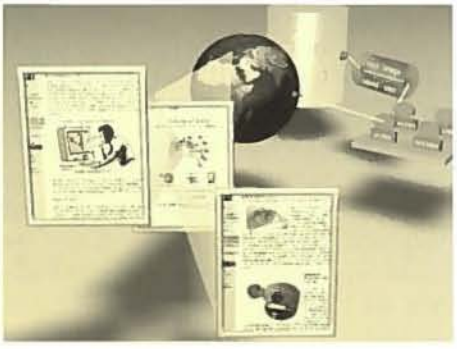

Fig. 4:
Implementation of a Web browser.

5. Results and conclusions

Testing in our lab and at an exhibition indicated that most users were impressed by the 3D presentation and the possibility of communicating with the computer by simply looking at the object of interest or by changing the viewing position. Critical remarks concerned the design of the graphic elements (some were too small for easy gaze interaction in our initial setup) and the delay due to the various interprocess communications. Immediate feedback of initiated actions seems to be indispensable for avoiding visual stress. A fixed dwell time, however, does not seem to be the optimal solution, since it appeared to be too long for certain applications and users and too short for others. Moreover, any action launched by the agent but not desired by the user (due to misinterpretation of the user's behaviour) should preferably be reset by the agent (trivial undo, based on monitoring the user's immediate actions). Sensitive actions like the deletion of a file should rely on unambiguous confirmation by the user.

A critical issue in the concept of the use of gaze direction for interactions is the fact that human eyes are normally used as input organs and not for manipulation tasks [4]. It was often mentioned that intolerable eye strain occurred when the eyes were used for manipulating graphical objects, e.g. in drag-and-drop operations. On the other hand, pointing operations are very easily performed by looking at the corresponding icons. If the icons are sufficiently large, eye pointing seems to be significantly faster and easier than mouse pointing. Obviously, it would be preferable to combine gaze-controlled pointing with another modality (such as speech input) in order to specify the action desired [4].

3D displays allow image presentation at a distance in front of the screen where the displayed objects are within reach and where binocular depth perception outperforms any other depth cue. Therefore, direct manipulation of a virtual 3D object through hand gestures may be another useful interaction modality for a range of applications.

Acknowledgments

This work was supported by grants from the German Ministry for Education, Science, Research and Technology.

References

[1] S. Pastoor and J. Liu, **"Head and gaze controlled interactions with a 3D multi-**

media computer", Annual Report 97, 105-110, HHI Berlin, 1998.

[2] J. Liu, "Determination of the point of **fixation in a head-fixed coordinate system"**, Proc. of the 14th ICPR, Brisbane, Australia, 1998.

[3] R.J.K. Jacob, **"Eye movement-based human-computer interaction techniques: toward non-command interfaces"**, Advances in Human-Computer Interaction, Vol. 4, Ablex Publishing Co., Norwood, N.J., 1993.

[4] A.J. Glenstrup and T. Engell-Nielsen, **„Eye Controlled Media: Present and Future State"**, Thesis, University of Copenhagen, Denmark, 1995.

J. LIU, D. PRZEWOZNY AND S. PASTOOR

OBJECT AND DEPTH LAYERING OF IMAGES FOR MULTIMEDIA APPLICATIONS

Abstract

This paper describes a new algorithm for stereo image segmentation. The key idea is based on the combined evaluation of various image features such as pixel-based luminance/colour distributions, object contours and disparity information. The segmentation results were used to interpolate intermediate views for an interactive autostereoscopic display and to synthesize images with a variable depth of focus.

1. Introduction

Numerous applications in the field of digital image processing require reliable and effective segmentation techniques, e.g. low-bitrate coding (MPEG-4), content description and retrieval (MPEG-7), and image synthesis for multi-view displays. The overall goal is to detect the enclosing boundaries of the various objects found in a natural scene in order to decompose the scene into its constituent parts. Generally, the level of detail depends on the requirements of the particular application and should be a variable parameter in the segmentation procedure.

This paper focusses on a special application where more than one camera captures the scene, so that stereo information is available for segmentation. The application aims at interpolating intermediate views (views from virtual camera positions located between the real cameras). Moreover, selected depth layers should be blurred in order to produce an artificial depth-of-focus effect [1]. For this purpose, the scene has to be decomposed into objects at distinct depth layers (a layered representation).

Although extensive research has been done in this area, a universal and common solution has yet to be found. Recent approaches suggest exploiting multiple sources of information and combining the various segmentation results [2] [3]. We have developed a hybrid approach that combines the results obtained from grey value image analysis and stereo analysis at intermediate stages in a new cooperative procedure.

Our approach uses three cameras arranged, for example, around a display used for video communications. Two cameras placed one above the other at one side of the display form a stereo unit with a rather short baseline (8 cm). The third camera is placed on the other side of the display, thus providing a large baseline (48 cm). This unsymmetrical arrangement has the advantage that a course disparity map is easily estimated using the two closer cameras, whereas more accurate depth estimates are obtained from a camera pair with a large baseline.

In the first stage, one image (Image 2 in the system diagram shown in Fig. 1) is segmented based on the grey level information, and disparities are estimated from the short-baseline stereo-camera images. In this stage, grey-level segmentation and disparity estimation are performed independently. In the following stage, errors occurring in the grey-level segmentation are corrected by considering the results obtained from disparity estimation, and vice versa. After that, the large-baseline stereo images are evaluated in the same cooperative manner in order to refine the disparity estimates and segmentation results.

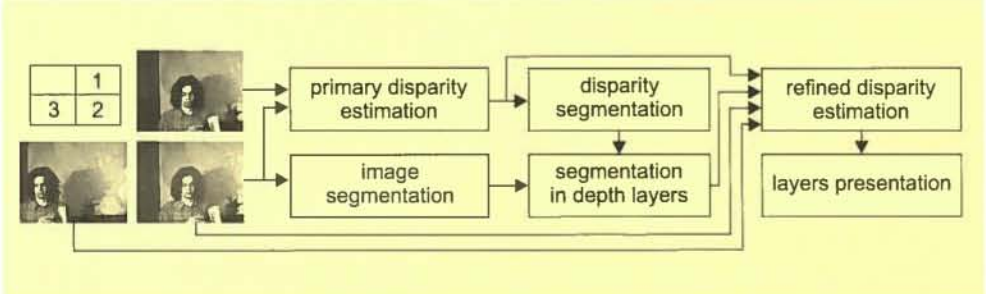

Fig. 1:
Scheme of the hybrid segmentation algorithm.

2. Image segmentation

For grey-level segmentation of Image 2, a region growing technique is applied [4]. In order to speed up the algorithm a simple one-dimensional technique is applied. The grey-level information of the image is analyzed line by line, grouping pixels into regions according to their grey-level distribution. Parallel to the line-by-line analysis, the same process runs over the image row by row. Under ideal conditions, both analysis tasks should yield identical region boundaries. However, due to image noise and surface characteristics of the objects, the results are usually different. As various segmentation algorithms will yield the same or similar segmentation results only at true region boundaries, both region growing results are checked in the following step in order to find overlapping and corresponding region boundaries. The same algorithm used for grey levels (luminance) could also be applied to the colour components (UV channels) when colour images were available. Separating the two-dimensional region growing algorithm into two one-dimensional processes simplifies implementation and speeds up computation. The process is illustrated in Fig. 2.

To overcome the over-segmentation problem, various post-processing techniques are applied for merging smaller regions into bigger ones. For this purpose, edges are extracted. Features such as the luminance and colour distribution in each region, the characteristics of the boundary, and the size and form of the regions are taken into consideration. Weak regions (having luminance or colour distributions similar to their neighbours, or low boundary gradients) and very small or thin regions are eliminated and allocated to the neighbour with the nearest luminance/colour distribution. This step usually yields reliable and precise segmentation results at true object boundaries. Strongly textured objects, however, are usually over-segmented.

3. Disparity segmentation

Disparity estimation based on hierarchical block matching is first carried out on the two closer stereo images. One of the stereo images (Image 2) is divided into regular blocks, and feature points (Moravec points) in each image block are detected. In the global matching step, disparity values are determined for the feature points. In our approach a significant modification has been introduced: instead of calculating the luminance/colour differences between the two points under consideration and their surroundings, differences of the gradient of the luminance/colour levels between the two images are calculated. The pixel gradient is defined as the sum of the two gradients in the north-east and south-east directions. The two points with the smallest gradient difference between each other and their surroundings are registered as corresponding points. This makes the matching process insensitive to luminance/colour deviations between different camera images. The subsequent local matching step is carried out in the same way as described in [5], by evaluating the global matching results and the image gradient information. A dense disparity map is obtained by this local matching procedure.

As opposed to luminance/colour image segmentation, the disparity map provides highly reliable results for strongly textured objects. Unreliable disparity estimates occur mainly near object boundaries. This is an effect of half-occlusions occurring at

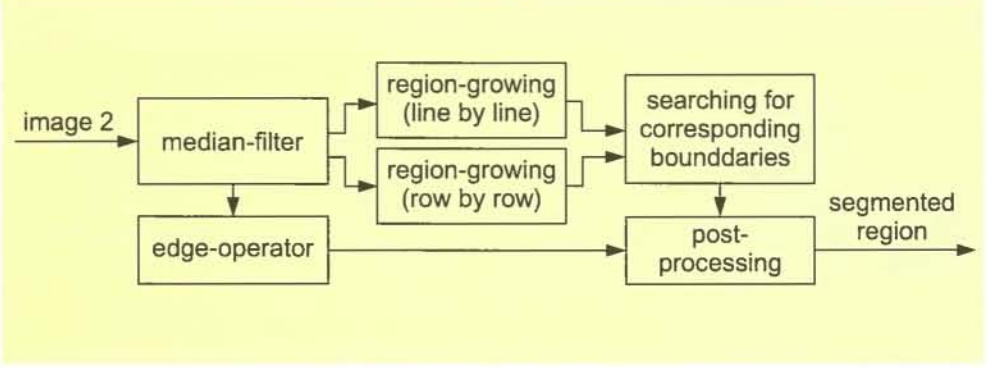

Fig. 2: Intensity-based image segmentation.

depth discontinuities (depth jumps). Again, the region growing technique as described in Section 2 is applied to the disparity map in order to segment the disparity values into regions.

4. Combination and refinement

The segmentation results obtained in the luminance/colour image and disparity segmentation processes are analyzed in order to refine the disparity estimates and to decompose the disparity map into discrete depth layers. For this purpose, objects with the same or similar disparity values are grouped together. The region boundaries should correspond to the real object boundaries at depth jumps.

In view of the fact that disparity segmentation yields reliable results within objects with strong textures, whereas luminance/colour-based segmentation usually provides exact results at true object boundaries, the following rules for the combination of the two segmentation results are applied:

1. Region boundaries obtained with luminance/colour-based segmentation are eliminated if they are located within one segmented disparity region.
2. Holes in disparity regions that do not cross luminance/colour boundaries are eliminated.
3. Disparity boundaries are substituted by their corresponding luminance/colour boundaries if both boundaries are partly overlapping and/or have partly similar courses.
4. When a disparity boundary intersects a luminance/colour segmented region, the disparity boundary is accepted (the same is applied in the reverse case).

Rules (1) and (2) overcome the over-segmentation problem, both in luminance/colour-based and disparity-based segmentation. Rule (3) utilizes the advantages of image segmentation to correct 'vague' disparity boundaries,whereas rule (4) avoids the possibility that two objects lying at different depth layers but having low luminance/colour differences are grouped into one segment.

After that, the segmented disparity regions are divided into depth layers and the disparity distribution at each depth layer is analyzed. Wrong and uncertain disparity values are eliminated. An improved and reliable disparity map based on the closer stereo image pair is now obtained.

However, this disparity map possesses very low resolution in depth due to the short baseline of the two cameras. In order to improve the disparity estimates and to allow motion parallax over an extended range of head movements, a large baseline is required (e.g. by using cameras 2 and 3 in Fig. 1).

Knowing the primary disparity information, stereo analysis with the large baseline camera pair is significantly simplified. In our approach, the local range for searching corresponding points is dynamically adapted to the primary disparity values without restricting the possibly large disparity values caused by the large baseline. The matching process is significantly speeded up. Primary disparity boundaries suggest possible depth jumps where occlusions may occur. Such hints make it possible to detect significant depth jumps and to determine occluded regions for a large camera baseline. More accurate disparity values are available after this step.

5. Results and conclusions

The algorithm was implemented and tested on real scenes. Original camera images are given in Fig. 1 (a black/white image sequence) and Fig. 5 (a colour image sequence). Figure 3 shows segmentation results at different processing stages. After the luminance/colour based segmentation, about 20-30 regions still remain (Fig. 3a). Over-segmentation occurs particularly in the background, where the image is split into many small regions due to the strong texture. As opposed to the luminance/colour segmentation, the disparity-based segmentation process yields considerably fewer regions (about 10-15 regions, Fig. 3b). The flat background is mainly segmented into one region, and most regions represent the real object with depth jumps. The segmented region boundaries, however, do not correspond exactly with the real object boundaries. Application of the described combination rules gives the segmented regions shown in Fig. 3c.

Figures 4 and 6 show the layered representation of the two scenes. In the first

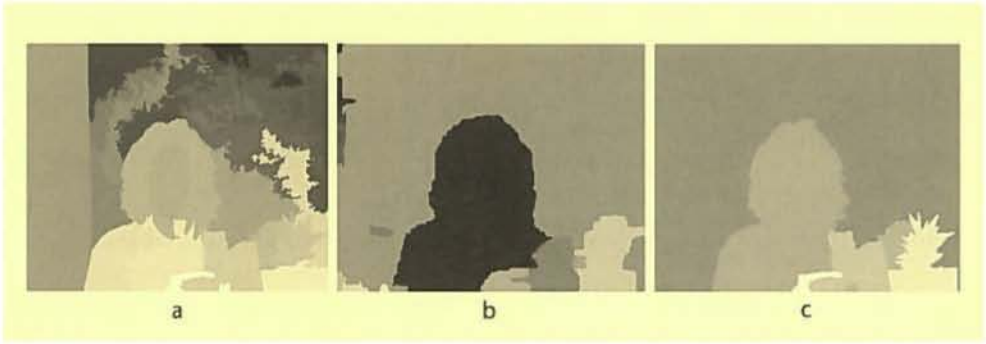

Fig. 3:
Segmented regions of: (a) the grey-level image, (b) the disparity map, and (c) the combined segmentation.

Fig. 4:
Layered representations (a) – (e) and intermediate view (f).

Fig. 5:
Original stereo images.

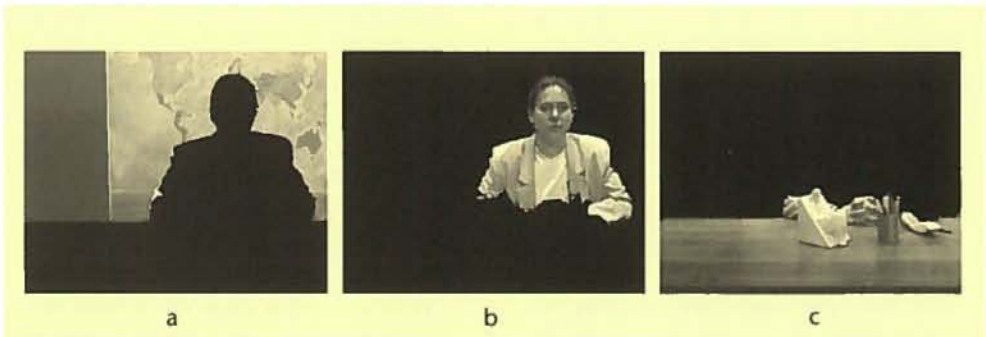

Fig. 6:
Layered representations of the image.

example, the complete scene is decomposed into five depth layers (Figs. 4a-4e). Fig. 4f shows a synthesized view for an intermediate position between image 2 and image 3. In the second example, the scene is decomposed into three layers (Fig. 6).

When running on a dual-board PC (400 MHz), the computation time is about 30 seconds for a black/white image triple and 50 sec for a colour image triple (image resolution 720×578). The novel part of the algorithm is the hybrid use of multiple image processing results to achieve a reliable decision process for robust segmentation. Very different image analysis techniques are combined into one system, and each is supplied with feedback from the other. The disadvantages of each technique are compensated by the advantages of the other.

Acknowledgments

This work was supported by grants from the German Ministry for Education, Science, Research and Technology.

References

[1] S. Pastoor and J. Liu, **"Head and gaze controlled interactions with a 3D multimedia computer"**, Annual Report, Heinrich-Hertz-Institut, 1997.

[2] D. Tzovaras, N. Grammalidis and M. G. Strintzis, **"Object-based coding of stereo image sequences using joint motion/disparity compensation"**, IEEE Trans. Circuit and Systems for Video Technology, vol. 7, no. 2, April 1997.

[3] G. Xu, **"A unified approach to image matching and segmentation in stereo, motion, and object recognition via recovery of epipolar geometry"**, Journal of Computer Vision Research, Fall 1997, vol. 1, no. 1, The MIT Press.

[4] I. Pitas, **"Digital Image Processing Algorithms"**, Prentice Hall, 1993.

[5] E. Izquierdo, **"Stereo Matching for Enhanced Telepresence in Three-Dimensional Videocommunications"**, IEEE Trans. on CSVT, vol. 7, no. 4, Aug. 1997.

R. BUSS, J. FABER,
L. MÜHLBACH AND D. RUSCHIN

USABILITY ENGINEERING AT HHI

Abstract

Usability is increasingly acknowledged by manufacturers and service providers as a factor that affects the uptake of new telecom products and services. Considering the importance of usability, HHI has conducted Usability Engineering and Human Factors research for many years. The paper outlines the HHI approach, which is oriented towards both applications and basic research. The Usability Engineering approach is presented in principle, complemented by examples of basic research and user-centred design projects.

1. Introduction

The acceptance as well as the frequency of use of telecom products and services depends on various variables, such as to what extent the product is known by the end users, the accessibility of the product, the need for the product, the costs, the attitude of the end users towards new media, and the usability of these products and services. Frequently used synonyms for usability are user friendliness, ease of use, or quality of use.

Currently there are several definitions of usability which stem from international standards organizations (e.g. ISO [1,2], ETSI [3]), national standards organizations (e.g. ANSI) or usability experts (e.g. Nielsen, 1993 [4]; Dumas and Redish, 1993 [5]; Redmond-Pyle and Moore, 1995 [6]).

Usability is defined by ISO 9241/11 (1992) [2] as the "extent to which a product can be used by specified users to achieve specified goals with effectiveness, efficiency and satisfaction in a specified context of use".

The ISO usability components are defined as follows:

- Effectiveness: "The accuracy and completeness with which specified users can achieve specified goals in particular environments".
- Efficiency: "The resources expended in relation to the accuracy and completeness of the goals achieved".
- Satisfaction: "The comfort and acceptability of the work system to its users and other people affected by its use".

The ETSI [3] definition of usability mainly adopts the ISO [2] definition, but excludes monetary costs (included in the definition of Efficiency by ISO 9241/11 [2]). Other definitions (e.g. Nielsen, 1993 [4]) include such dimensions as learnability or memorability of system features as main components of usability. Another concept introduced by ETSI [3] is the flexibility of a system, i.e. the degree to which usability is maintained when user category, task, or environment are varied.

Apart from some differences in their definitions of usability, all experts apparently would consider a system usable if it can be used with success, ease, and fun. This can be regarded as the core intension of the various definitions of usability. Finally, it is to be stressed that although the concept of usability is not defined uniformly, its practical value is doubtless. The existing concepts help to focus attention on attributes of use that are relevant from the users' perspective and that have an effect on the acceptance of telecom products and services.

2. Usability Engineering – concepts and methods

Usability Engineering describes an approach that is performed as part of the product and service development process. The related term "user (or human) centred design" emphasises the continuous involvement of users during all phases of the development process. No matter which term is used, most human factors experts agree on the many activities necessary to establish the usability of telecom products and services. One proposal to arrange the activities is contained in ISO/DIS 13407 [1] and shown in Figure 1.

According to ISO, to ensure usability one has to:

1. Understand and specify the context of use.
2. Specify the user requirements and organizational requirements.
3. Produce design solutions.
4. Evaluate designs against requirements.

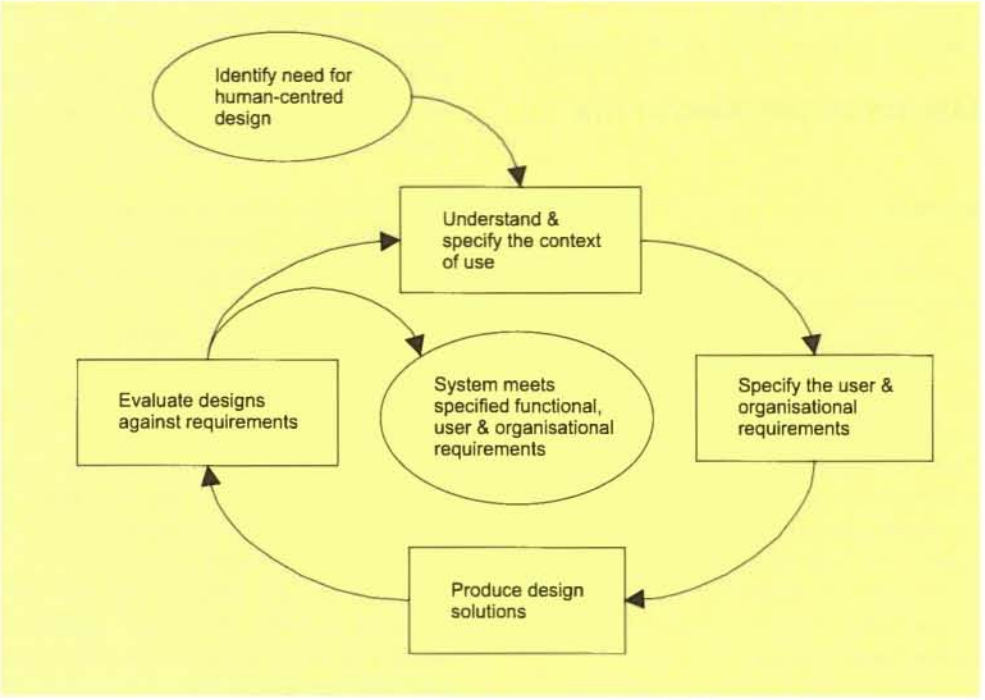

Fig. 1: Usability Engineering in ISO/DIS 13407 [1], there called "human-centred design activities".

The context of use should be described in terms of

- The characteristics of the intended users – habits, skills, knowledge, physical attributes.
- Features of the tasks performed by the users in the domain considered – task goals, task frequency, etc.
- Characteristics of the environment of use – hardware, software, materials to be used, attributes of the physical environment, etc.

The specification of user and organizational requirements encompasses statements on:

- Financial restrictions.
- Relevant statutory or legislative requests.
- Demands for cooperation and communication between users and other relevant parties.
- Requirements for the well-being of the users that are relevant, for instance, to their safety, health and motivation.

Methods used for specifying the context of use and the user/organizational requirements encompass brainstorming, group discussions, observation, focus groups, interviews, document analysis, task analysis, etc. On the basis of the requirements analysis, design solutions are produced, which can be tested by means of simulations, models, or mock-ups.

The evaluation process aims at assessing whether user and organizational objectives have been met and at developing proposals for improvement. Various methods can be considered for usability evaluation. In user tests mainly performance (objective) and attitude (subjective) measures are obtained. This can be accomplished by using techniques such as thinking aloud, questionnaires, audio and video recording, or interviews. Expert evaluations are appropriate when the task is to test whether the design of products and services corresponds to relevant Human Factors findings, standards or features known from "best practice" solutions. Methods used here include cognitive walkthrough, heuristic evaluation, and list checking. Which methods are the most appropriate under the given circumstances depend on cost/benefit considerations or on anticipated consequences of overlooking usability faults.

Usability Engineering, or the human-centred design process, is a multi-disciplinary approach involving programmers, system analysts, application domain specialists, user interface designers, human factors and ergonomics experts, managers, purchasers and, last but not least, the end users.

3. Usability Engineering approach at HHI

The Usability Engineering approach at the HHI is twofold. On the one hand, products and services are developed (usually in cooperation with manufacturers or

service providers) and evaluated according to the usability engineering and user-centred design methods described above. On the other hand, various projects were and are dedicated to the "generic feature approach", i.e. are aimed at establishing values or ranges of system variables that can be considered to enhance usability, or that can at least guarantee a sufficient degree of usability. The methods adopted in these projects are mainly those of experimental or social psychology or of psychophysics.

Of particular importance are the synergetic effects that come with this approach. The results of the basic research oriented projects are fed directly into the more application oriented projects. These results are also contributions to international standardization bodies such as ETSI and ITU-T, and are components of consultancy services that HHI provides (e.g. the USINACTS Web services). The application oriented projects, in turn, very often reveal gaps of human factors or usability knowledge and thus lead to new basic research aimed at tackling the issues that have turned out to be of major relevance.

4. Human factors research – the basis of Usability Engineering

Usability Engineering derives design specifications from data on the requirements of the user and his organization as well as on the intended context of use. Not all of the features of a usable product or service need to be based on requirements captured during the development of the actual product. Usually some of the features can be considered generic for a whole class of similar products and are already known to be required to make the product usable. Examples are features such as a certain display resolution or certain input devices. Note that knowledge of generic features can help to simplify user validation. One of the benefits from generic features is that less attention needs to be paid to those features during the testing phase.

The determination of generic features is an important branch of the Human Factors research within HHI. A generic features approach seeks to provide a mapping between user requirements and system parameters. Research in the field of new and advanced telecommunication systems based on the generic features approach starts from the likely user requirements and then designs and evaluates the usability of a range of possible solutions. The features of the best solutions found will then be recommended, and perhaps even standardized for future use.

To give an example for this approach, it is known that if nonsense syllables were transmitted over an audio system humans could still understand about 90% of these syllables, even if the transmission bandwidth were restricted to 3.5 kHz. Since this is enough for a near perfect recognition of natural language, given the requirement of verbal communication effectiveness, a bandwidth of 3.5 kHz or more can be considered a generic feature of audio systems.

Over the last two decades a number of studies have been undertaken in the Human Factors department aimed at developing the specifications for future telecom services and products, following a generic features approach as described above. Major activities focused on enhanced TV, videotelephony, videoconferencing, and multimedia information retrieval.

Some of the many findings are:

- That more accurate colour reproduction can be achieved by coding and transmitting image colours in the form of CIELAB components [9].
- Image flipping in autostereoscopic systems only remains undetectable if the aspect presented to the viewer's eye changes ten or more times as the viewer moves through a distance equal to the distance between his eyes [10].
- For apparent eye contact in videotelephones, the angle between the gaze direction and the camera axis must not exceed 7.5° [11].
- The standard viewing distance for wide screen displays should be 3 times the display height [12].
- Audio rendering in videoconferences should be stereophonic [13].
- The acquisition of competencies in various domains can be facilitated or even enabled by the use of moving pictures [14].

5. Development of usable telecom products and services

Practical knowledge about all phases of an approach now called Usability Engineering was first acquired in a cooperative projectwith the German Federal Employment Institute (1981-1986), in which a career information system was developed that allowed access to information on 150 vocational training programs. The system was supposed to support young people in their choice of occupation. It was realized in various versions that were compared in experimental user tests. Finally a version proved to be satisfactory that:

- Offered an orientation on the capability and the limitations of the system.
- Assisted its users to state more precisely their often vague and ambiguous information needs.
- Presented the information in the resolution, order and media (text, stills, moving pictures) that were requested by the user.
- Supplied an overview of those attributes of the vocational training programs on which information was requested by the user ('dialogue history') and also of those attributes that additionally might be interesting, although the user did not think of them ('recommendations').

In a final field trial the system proved to be at least equivalent to a traditional local career information system supplying information in the form of printed material, slides and videotapes. Beyond that it was found that the electronic system was preferred by a substantial proportion of users.

During the development of the system various research gaps were identified. One of these led to a HHI research project (see above) concerning the question of what types of task learning are facilitated, or even enabled, by the use of moving pictures.

Efforts of HHI to transfer research results to industry started about three years ago. So far twelve application projects have been conducted on behalf of service providers and manufactures. Mostly the tasks were to evaluate existing prototypes of services and terminals according to usability criteria.

However, on some occasions the Human Factors Department cooperated during the design phase, e.g. of a telelearning service. This service allows access to information and training programs supplied by more than 20 providers. It presents information in various fields such as politics, economics and computers, it offers the possibility of joining professional training programs and language courses, and also assists the users with do-it-yourself activities. HHI contributed to the specification of the interface layout and of service functionalities. With regard to the latter, special attention was paid to functions that facilitate both an efficient information retrieval (search functions) and online communications (chat program). Additionally, HHI was asked to evaluate the service prior to its public introduction. This was done by user tests. Here various usability defects were identified that led to recommendations for improvement of the service.

Another contract required the evaluation of a service that allows online travel bookings offered within interactive videotext and the WWW. The task was to explain why almost no one was willing to use this booking service. The HHI expert evaluation revealed various defects in the interface design and in the organization of the user-service interaction. Problems in controlling the highly sensitive online booking and payment processes could be explained. Also, the information available on the offered travels proved to be unsatisfactory.

A final illustration concerns a video telephone terminal intended to serve as a component of a videoconference system. Results of the generic feature approach, including outcomes of other HHI projects (see above), were used to evaluate the prototype, and human factors layout guidelines were adapted to this application. Various defects were identified in both the interface design and the terminal functions. For instance, it was found that important functions that allow ordinary telephony in a user-friendly manner were not implemented.

6. Conclusions

Usability Engineering provides a systematic way not only for improving quality but also for reducing development costs. Both increasing competition in the field of telecommunications as well as cost pressures have led to a growing interest in

usability by manufacturers and service providers. In the last few years a number of companies have established their own usability labs, but others chose and will continue to choose to cooperate with specialized companies or institutes such as HHI to design and evaluate their products.

Research in the field of generic human factors problems, however, is rarely conducted by privately owned companies. Due to its pre-competitive nature and the benefits to be expected for the general public, this type of research will be a continuing activity in the HHI Human Factors department.

Topics to be addressed in the future include the satisfactory reproduction of motion parallax in imaging systems, the recording and display of haptic information, the visualization of virtual environments, and intelligence in user interfaces.

Acknowledgments

The work described here has been supported by the European Commission (ACTS program), by the German Federal Ministry of Education, Research, Science and Technology, and by the DTAG.

The responsibility for the contents rests exclusively with the authors.

References

[1] ISO/DIS 13407, **"Human-Centred Design Processes for Interactive Systems,"** 1997.

[2] ISO/FDIS 9241-11, **"Ergonomic Requirements for Office Work with Visual Display Terminals (VDTs)"** – Part 11: Guidance on Usability, 1992.

[3] ETSI DTR/HF 3001, **"Guide for Usability Evaluations of Telecommunications Systems and Services"**, 1993.

[4] J. Nielsen, **"Usability Engineering"**, Academic Press (AP Professional), 1993.

[5] J.S. Dumas and J.C. Redish, **"A Practical Guide to Usability Testing"**, Ablex Publishing Corporation, 1993.

[6] D. Redmond-Pyle and A. Moore, **"Graphical User Interface Design and Evaluation (Guide) – A Practical Process"**, Prentice Hall, 1995.

[7] C. Smith and T. Mayes, **"Telematics Applications for Education and Training – Usability Guide"**, The European Commission, 1995.

[8] M. Maguire, **"RESPECT User Requirements Framework Handbook"** – Version 2.21, RESPECT Consortium, 1997.

[9] R. Schäfer and P. Kauff, **"HDTV colorimetry and gamma considering the visibility of noise and quantization errors"**, SMPTE Journal, vol. 96, no. 9, pp. 822-833, 1987.

[10] S. Pastoor, **"3D-television: A survey of recent research results on subjective requirements"**, Signal Processing, Image Communication, vol. 4, no. 2, pp. 21-32, 1991.

[11] L. Mühlbach, B. Kellner, A. Prussog and G. Romahn, **"The importance of eye contact in a videotelephone service"**, Proc. 11th International Symposium on Human Factors in Telecommunications, Cesson Cevigne, France, 9-13 September, 1985.

[12] M. Wöpking, **"Subjective assessment of 3D vs 2D presentation of motion pictures for large screen home television"**, Proc. 1st International Symposium on 3-D Images, Paris, 1991.

[13] L. Mühlbach, **"User-friendly videotelephone terminals"**, Proc. 12th International Symposium on Human Factors in Telecommunications, The Hague, Netherlands, May, 1988.

[14] J. Faber, T. Meiers, D. Ruschin and K. Titze, **"Multimedia für den Erwerb von Kompetenzen: Nutzen von Bewegtbildern?"**, Nachrichtentechnische Zeitung (ntz) Telekommunikation + Informationstechnik, 1 (1996), pp. 16-21.

R. ERNST, U. HÖFKER,
H. KRAHN, R. SCHÄFER,
P. STAMMNITZ AND M. TALMI

HIPEG AND HIBOX – DVB COMPLIANT COMPONENTS FOR REAL TIME DECODING OF MPEG-2 COMPRESSED HDTV SIGNALS

Abstract

This paper describes one of the world's first single chip HDTV decoders realizing the Main Profile@High Level of MPEG-2, called HiPEG. This chip was designed by HHI as part of the European ACTS project CINENET, and is manufactured by Fujitsu using their advanced 0.35 micrometre technology. It is also built into a DVB-compliant HDTV decoder box, called HiBOX. This unit accepts MPEG-2 transport streams and is therefore compliant with all Digital Video Broadcasting (DVB) transmission systems, including DVB-S for satellite, DVB-C for cable and DVB-T for terrestrial transmission. HiBOX has been demonstrated together with real time DVB-T transmission on various occasions in Europe, South America and Asia.

1. Introduction

High Definition Television has suffered from a lack of interest for some years, especially in Europe. Nevertheless, HDTV technology has been used for some niche applications and, due to the ongoing discussions in the US and the recent decision by Japan to introduce digital HDTV in the year 2000, interest is growing again in Europe. Recently HDTV also became an important issue within the European DVB project, since the acceptance of the DVB standards outside Europe, especially DVB-T, is highly dependent on their suitability for HDTV transmission. As a result, the DVB project included several HDTV formats in its completed "Implementation Guidelines for the Use of MPEG-2 Systems". Also, successful DVB-T transmissions of HDTV were carried out in Australia at the end of 1997.

In the meantime, the European ACTS project CINENET was carried out after a two-year development of DVB-compliant cable and satellite transmission systems and high performance projectors for electronic cinemas using HDTV technology. Successful and very impressive live transmissions over satellite and cable were demonstrated to the public in December 1997[1]. For this project, one of the world's first single chip MP@HL HDTV decoders based on the MPEG-2 standard was developed at HHI. This chip, called HiPEG, is manufactured by Fujitsu using their advanced 0.35 micrometre technology. It supports all HDTV formats defined by DVB, as well as all 18 ATSC formats. Furthermore, outputs up to XVGA resolution are available.

Additionally, HiBOX, an integrated HDTV decoder box that is fully DVB compliant has been developed. It consists of a single board, called HiBOARD, that carries six main building blocks: the systems demultiplexer, the audio surround sound decoder, the video decoder, a microcontroller, a DVB Common Interface, and the D/A converters for video and audio. These elements give an MPEG-2 decoder box with the following key features:

- Demultiplexing of transport stream data up to 280 Mbit/s
- Decoding of video data streams up to 80 Mbit/s and up to high level resolution (1920×1152 pixels).
- Decoding of multichannel surround sound (MPEG-2 Surround Sound or AC3).
- Flexible control of demux and decoders to support various system configurations.
- Digital and analogue outputs for audio and video, and digital output for data.
- Conditional access to encrypted MPEG-2 transport streams.

2. HiPEG – a single chip MPEG-2 decoder

HiPEG is a single chip that decodes MPEG-2 video data with the maximum allowed picture size at HDTV resolution. It decompresses the compressed data and produces synchronized digital output, ready for digital-to-analogue conversion. The chip is programmable and supports various input/output formats. It is thus ideal for online set-top box decoders for cable, satellite, or terrestrial broadcasts, and for offline applications such as DVD or hard disk systems.

The Input Stream Handler (ISH) receives encoded MPEG-2 bitstreams as Transport Stream (TS), Packetized Elementary Stream (PES) or Elementary Stream data (ES). The TS packets are unpacked to PES, whereas PES and ES are bypassed. For TS inputs the ISH performs PID-directed packet filtering, unpacking, PCR extraction, packet-loss detection and error-code insertion. For PES/ES error code, insertion is controlled by an external signal. PES/ES data are then stored n an external SDRAM FIFO (vbv_buffer) A FIFO controller (Fifocon) handles read/write actions, computes addresses and generates full/empty flags. Buffer size and flags are programmable. An arbitration unit (Arbiter) organizes the sequence of read and write requests. A general and simplified description of the data flow in HiPEG is as follows (refer to Fig. 1).

In the first step, PES/ES data are read from the external SDRAM FIFO and transmitted to the Packetized Elementary Stream Handler (PESH). This unit either unpacks PES to ES data or bypasses ES data to its output. In the case of PES the time stamps PTS/DTS are extracted for the synchronization of the decoding process. The Variable Length Decoder (VLD) decodes the ES data and generates control information from the bitstream according to the MPEG video bitstream syntax and tables. Control information included in the various fields of the video bitstream is extracted as far as required and sent to the Dequantizer (Deq) and the Macroblock Controller (MBC).

The Timing unit controls the correct timing of the decoding process, as this is essential for audio/video synchronization. In the case of TS inputs, the Program Clock Reference PCR is received from the ISH and the Presentation/Decoding Time Stamp PTS/DTS is received from the PESH. Both values are used to compute the start time of the decoding process. In the case of PES +PCR inputs, the PCR is delivered using the microcontroller bus via Init, whereas for ES inputs the value of vbv_delay is used for synchronization.

The Dequantizer performs zigzag scanning and inverse quantization on a block-by-block basis. Saturation and (IDCT) oddificationis included in this unit. The output coefficients are sent to the Inverse Discrete Cosine Transformation unit (IDCT).

The Macroblock Controller (MBC) receives all necessary picture and mac roblock control information from the bitstream and computes all necessary control information (e.g. motion vectors) on a macroblock-by-macroblock basis for the motion compensation back end of the decoder. Before macroblock based motion compensation takes place, the Inverse Discrete Cosine Transformation (IDCT) computes the frequency-to-spatial transformation on a block-by-block basis and passes the results to the back end. The Infor-

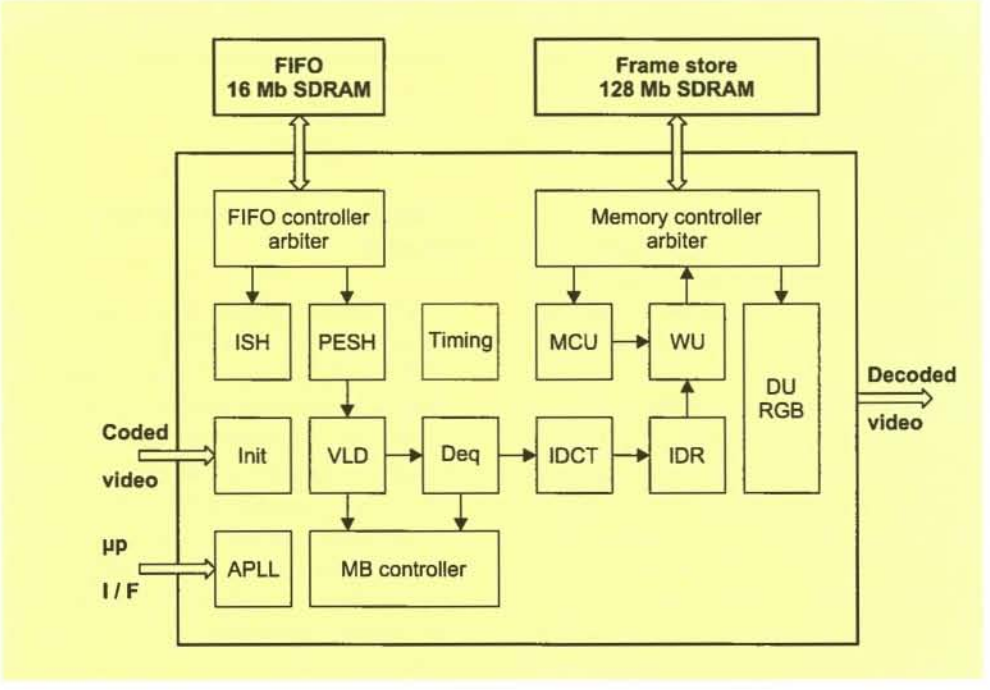

Fig. 1: Block diagram of HiPEG.

mation Data Receiver (IDR) stores and reorders the IDCT output for motion compensation. Motion vectors sent by the MBC address memory locations in the external frame store. Thus, the Motion Compensation Unit (MCU) performs motion vector based address computation, half-pel interpolation and interpolation of forward and backward reference macroblocks. The result of this process is stored in an on-chip macroblock memory.

The Weighting Unit (WU) combines IDCT data (via IDR) with MCU data to interpolate the resulting reconstructed macroblock and stores it in the external frame store. This frame store is built up from an internal Memory Controller (MemCon) and an external SDRAM bank. Four frames (Actual, I-Picture, P-Picture, and Output) are located in this memory for interpolation, reconstruction and output. In a similar way to the FifoCon, the MemCon handles all three requests and produces command sequences for the SDRAMs. The Display Unit (DU) takes the decoded data from the SDRAM and prepares the data for output to a display. The major functions of this unit are the interpolation of 4:2:2 data from the (decoded) 4:2:0 data, the interfacing of digital YUV/RGB in the CCIR or HDI schemes, external synchronization, and some picture editing capabilities. Progressive output and the interlace-to-progressive transformation are also supported, as well as YCr Cb and RGB outputs.

The main features of HiPEG, which requires a 3.3 V voltage supply and dissipates about 2.5 W power, can be summarized as follows:

- Single-chip MPEG-2 HDTV video decoder
  - Supported profiles and levels: MP@ML, MP@H-14 and MP@HL
  - Decodes images up to 1920/1125/60/2:1 and 1920/1125/30/1:1
  - Supports all 18 ATSC formats and all DVB formats
  - Decodes I, P and B frames
  - General purpose interface for initialization and control
  - Self initialization

- Input interfaces
  - Supported input interfaces:
    - MPEG-2 Transport Stream (TS):
    - DVB-SPI Interface, EN 50083-9
    - MPEG-2 Packetized Elementary Stream (PES): Synchronous/ Asynchronous
    - MPEG-2 Elementary Stream (ES): Synchronous/Asynchronous
  - Input clock frequency up to 20.0 MHz
  - Input data rate up to 160.0 Mb/s

- Output interfaces
  - TV: ITU-R BT.601/656
  - H-14: Modified ITU-R BT.601/656 (Lum and Chrom parallel, 54.0 MHz)
  - HDTV: ITU-R BT.709/1120

- Progressive output up to XVGA resolution
  - 4:2:0 to 4:2:2 to 4:4:4 conversion
  - Digital YCr Cb/RGB outputs
  - 3:2 pull-down supported

Only by using an ASIC technology like the 0.35 µm Gate Array CE61 allows the integration of complex functions such as an HDTV decoder together with a display processor on a single chip. To achieve the required decoding performance, HiPEG runs with an internal clock speed of 108 MHz. The memory bottleneck has been overcome by an interface to the external SDRAM memory that runs at the same frequency and with a bus width of 64 bits. This achieves a theoretical bandwidth of 864 Mb/s, which is needed for storing reference pictures, but it also increases the requirements for the PCB layout.

The next generation of the HiPEG family, called HiPEG+, combines the HiPEG chip with the transport stream demultiplexer. Subsequently the audio decoder and additional features, such as On-Screen Display, Picture-in-Picture etc., will be added.

3. HiBOX – A DVB-compliant HDTV decoder box

As well as an evaluation system for the HiPEG chip, HHI also developed a complete HDTV set-top box based on it, called HiBOX, which is fully DVB compliant. Apart from the power supply and connectors, it consists of a just single board, called HiBOARD. This main board contains six blocks, which manage the signal processing, starting from the MPEG-2 transport stream layer and ending at the analogue streams for presentation. Figure 2 gives a

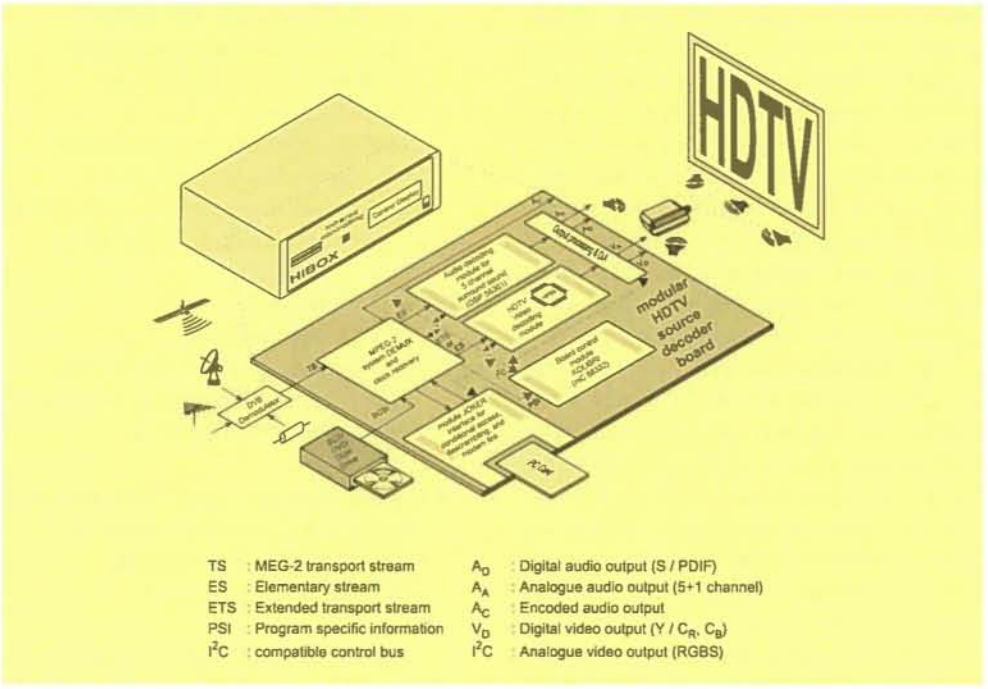

Fig. 2: HiBOX – a DVB-compliant high level source decoding box.

simplified overall view of the configuration and interfaces of HiBOX.

The following main blocks have been implemented [2]:

- System demultiplexer including system time clock recovery.
- HDTV video decoding module using HiPEG.
- Audio surround sound decoding module.
- Output processing including D/A conversion for video and audio.
- Board control module KOLIBRI.
- Module Joker for Conditional Access, system test and backup.

The main functions of the MPEG-2 System Demux are to recover the System Time Clock (STC, 27 MHz) using the Program Clock Reference (PCR), and to analyze the Program Specific Information (PSI), which is necessary for defining the demultiplexing procedure. Furthermore, the system Demux has a SCSI interface to handle external stream storage devices, including stream rate recovery.

HiBOX accepts MPEG-2 Transport Streams as input signals, which can be fed in either by the DVB Common Interface, where Conditional Access and descrambling can be implemented, or by a DVB Professional Interface. The output processing unit manages the video and audio interfacing according to several ITU-R standards. The control unit is used to load or modify system parameters and for diagnostics. If external system control over an RS232 connection is not availble, the system can be configured via an infrared remote control, which triggers the software running on the control unit.

4. Real time demonstrations of HiPEG and HiBOX

Currently there is a remarkable world wide interest in HDTV broadcast services. Therefore HiBOX and HiPEG have been demonstrated at various exhibitions in 1998. In total there were five opportunities to demonstrate the exceptional capabilities of HiBOX:

ECMAST '98, Berlin, 26-28 May 1998. For the first time in Europe a live DVB-T transmission of HDTV was demonstrated. MPEG-2 decoding was performed with HiBOX, which had been connected to a professional DVB-T demodulator. Furthermore MPEG-2 encoded stereo was presented on a standard 100 Hz consumer TV in combination with shutter glasses.

DVB-T Seminar, Hong Kong, 24. July 1998. This seminar was the second in a series of three on the three digital terrestrial systems. The first seminar dealt with the Japanese ISDB-T system, and there was a third seminar on the American ATSC system scheduled for September. The

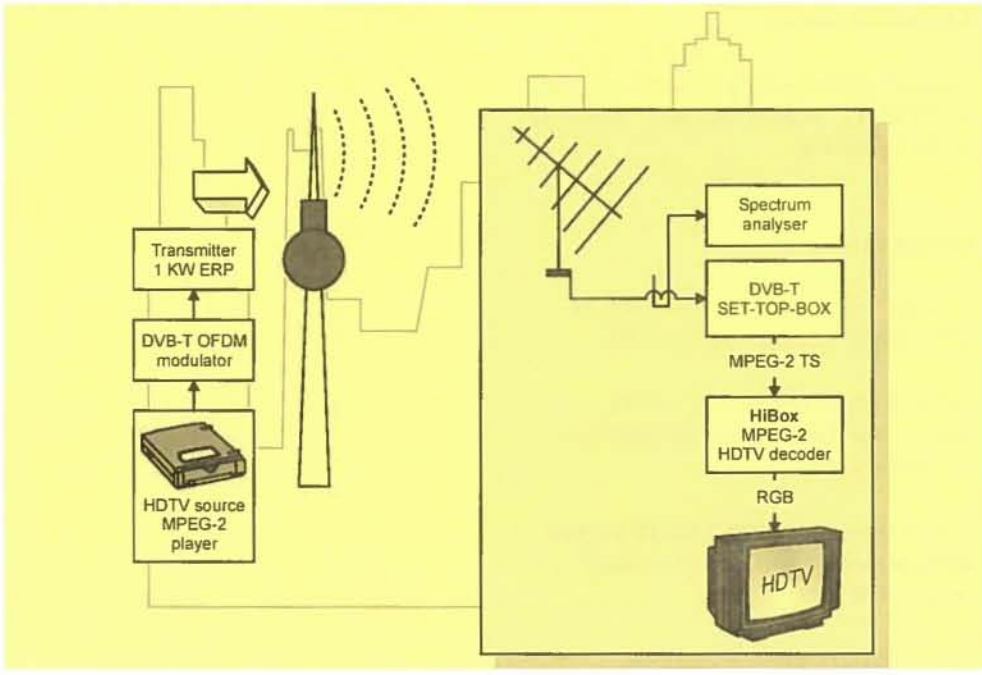

Fig. 3:
First terrestrial HDTV transmission demonstrated using HiBOX and HiPEG at ECMAST 98 in Berlin.

highlight of this seminar was a live DVB-T transmission of High Definition TV decoded by HiBOX and displayed with a projector on a large screen [3].

IBC '98, Amsterdam, 11-15 September 1998. HiBOX was demonstrated at the DVB booth. An MPEG-2 encoded HDTV film produced by DVB was transmitted from a local TV tower, received by a professional DVB-T receiver and decoded by HiBOX [4].

Caper '98, Trade Show, Buenos Aires, Argentina, 28. September-1.October, 1998. Argentina had begun with the evaluation of Digital Terrestrial Television Broadcasting (DTTB) systems from Europe and America from the point of view of their HDTV capabilities. This was one of the fundamental criteria for the system selection. The demonstrations in Buenos Aires showed the DVB-T system operating in real time and delivering HDTV signals decoded by HiBOX. During the same show the American ATSC system was demonstrated at a booth opposite the DVB presentation [5].

Electronica 98, Munich, 10-13 November 1998. In cooperation with Fujitsu, the manufacturer of HiPEG, HiBOX was presented to demonstrate the capabilities of HiPEG to the public. Fujitsu has announced the follow-up product HiPEG+, which is currently being developed by HHI's spin-off company MikroM.

5. Conclusions

In this paper a complete decoder unit called HiBOX for decoding compressed HDTV signals according to the MPEG-2 MP@ML standard has been presented. This decoder box is built around HiPEG, one of the world's first single chip HDTV video decoders for image resolutions up to 1152 lines × 1920 pixels. This chip is very flexible and supports all TV and HDTV formats defined by DVB and by the ATSC. HiBOX is fully DVB compliant and can decode compressed HDTV signals transmitted via satellite (DVB-S), cable (DVB-C) or terrestrial transmitters (DVB-T).

HiBOX is based on a modular concept and is therefore very flexible in its applications and configurations. It has all the necessary hardware components for conditional access and descrambling. Both stereo audio and five channel surround sound are supported. The box can also be used for stereo TV by changing the video module and decoding and synchronizing two separate MPEG-2 encoded video scenes (representing a left and a right view of a stereo pair).

The system has been tested with over-the-air transmission of HDTV and stereo TV signals using DVB-T modems on various occasions in Europe, South America and Asia.

Acknowledgment

Parts of the work were carried out under the CINENET project AC 062, which is funded by the EU.

References

[1] ACTS Project CINENET, Final Report 1998, AC062 AES DNS DS P 321-B1.

[2] HHI Product Information, HiBOX – MPEG-2 High Level Source Decoder Box, September 1998.

[3] DVB News 4.2, **"DVB-T HDTV presentation in Hong Kong a great success"**, August 1998.

[4] U. Höfker, H. Krahn, R. Schäfer, P. Stammnitz and M. Talmi, **"HiPEG – a single chip MPEG-2 HDTV decoder and HiBOX, a DVB compliant HDTV decoder box"**, Proc. IBC'98, Amsterdam, 11-15 September 1998, pp. 185-189.

[5] DVB Press Release, First Live HDTV Demonstrations in Argentina, September 28th, 1998.

P. KAUFF, J.-R. OHM,
S. RAUTHENBERG AND
O. SCHREER

MPEG-4 SERVICES USING VIRTUAL 3D ENVIRONMENTS

Abstract

The MPEG-4 standard is almost complete and will soon be released. In addition to increased compression efficiencies for a wide range of storage and transmission applications, MPEG-4 will in particular offer advanced content-based functionalities for interactive services. Against this background the paper presents implementations of two interactive MPEG-4 services using virtual 3D environments in combination with the streaming of real time data. It also presents an approach to the advanced representation of natural video objects in virtual worlds.

1. Introduction

Anticipating the rapid convergence of the telecommunications, computer and TV/film industries, and following on the successes of digital television, interactive graphic applications and the World Wide Web, the Moving Pictures Experts Group (MPEG) of the international standards body ISO/IEC initiated its MPEG-4 phase in 1994. The mandate is to specify a compression standard for the representation of audio-visual information in multimedia environments [1][2]. Meanwhile the MPEG-4 standard has achieved the mature status of a Final Draft International Standard (FDIS), and the first version of the official International Standard (IS) will be released early in 1999, followed by an extended second version one year later [3].

In view of the versatile requirements of multimedia, MPEG-4 envisages the support of a wide range of bit rates and functionalities as well as increased coding efficiency. One outstanding feature is the philosophy of considering scenes as compositions of several audio-visual objects (AVOs). For this purpose MPEG-4 supports various kinds of natural and synthetic AVOs such as conventional video (i.e. sequences of rectangular frames), arbitrarily shaped video objects, still images, panoramic images (sprites), 2D and 3D computer graphics, textural and graphical media data, graphical 3D models of human faces and bodies, 2D meshes, and synthetic or natural sound, speech or music [7].

In an MPEG-4 system these AVOs are encoded separately by using dedicated tools for each AVO type. Hence, a particular scene is transmitted as a multiplex of individual AVO streams, and the final assembly of the scene occurs at the receiver. This is achieved by a compositor which is available at the MPEG-4 terminal and which interprets a special scene description language called BIFS (Binary Format for Scenes) – usually in combination with some user interaction [3] [7].

Within this framework, the paper describes two concrete application scenarios for interactive MPEG-4 services using virtual 3D worlds [4]. The first application is explained in section 2. It encompasses a complete client-server configuration of a virtual 3D shop where AVOs can be streamed on demand and displayed in real time as integrated components of a 3D BIFS scene [5]. The second application follows in section 3 and is a video conference system where several participants can meet in a virtual 3D meeting room. Both scenarios have been implemented as prototypes in cooperation with Deutsche Telekom Berkom GmbH (DTAG/BERKOM).

In addition, section 4 discusses a possible extension of these developments towards an advanced multi-view representation of video objects in virtual 3D worlds, the so-called Incomplete 3D representation format [6].

2. The virtual shop

Figure 1 outlines a complete server-client configuration that has been developed at HHI in cooperation with DTAG/BERKOM in order to demonstrate the benefits of MPEG-4 and the AVO and BIFS structures for interactive services using virtual 3D worlds [5]. In this prototype of an MPEG-4 application, a user can start the service at a client by using existing Internet browsers. After down-loading a 3D BIFS scene of a virtual shop from a media server via TCP/IP, the user can 'walk' through the virtual shop. During this user navigation

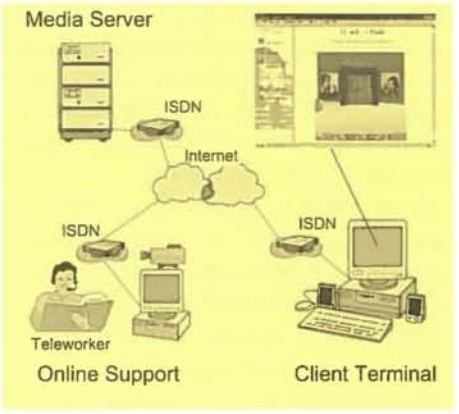

Fig. 1: Outline of the 'Virtual Shop'.

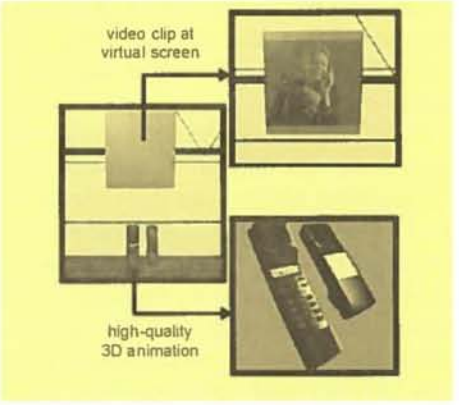

Fig. 2: Retrieval of 3D and AV data.

Fig. 3: Connection to online support.

the visualization of the scene is achieved by a high-speed software render engine working near real time without hardware support (e.g. 15 fps for scenes with 16000 triangles and 8000 vertices).

While browsing, the user can inspect the exposed products by retrieving associated AVO information from the media server as shown in Fig. 2. He or she has the choice of retrieving two different kinds of data: either additional graphical 3D BIFS data for advanced wire-frame animation of the selected product, or an informative audio-visual clip that is displayed on a virtual screen. In the latter case natural audio-visual data are loaded via RTP/UDP/IP, decoded on the fly in real time by a fast MPEG-4 software decoder, and streamed as synchronized real time data into the virtual 3D world.

If all the retrievable information does not satisfy the user, he or she has the further option of connecting to a teleworker of an online support service for further advice. After establishing this link, the teleworker appears as an arbitrarily shaped video object in the 3D world, as illustrated in Fig. 3. The user can now ask individual questions and the teleworker will answer them in real time via the audio-visual connection, while being integrated into the virtual 3D world.

3. The virtual meeting point

The virtual meeting point is a video conference application that again takes advantage of the AVO and BIFS structures of MPEG-4. In contrast to conventional multipoint conference systems based on the ITU-T H.32X standards, which display the participants in separate rectangular windows, the MPEG-4 conference integrates all participants into a shared virtual environment where, for example, they may be sitting around a common synthetic table (Fig. 4).

As for the virtual shop, a prototype of the virtual meeting point was developed in cooperation with DTAG/BERKOM. A first version of the system was demonstrated at the MINT Symposium in November 1998 in Berlin. It consists of up to three MPEG-4 terminals and an additional multi-point control unit (MCU) that manages all control tasks (e.g. by BIFS update if a new participant joins the meeting) and transcodes for backward compatibility to conventional H.32X terminals. Unicast and multicast

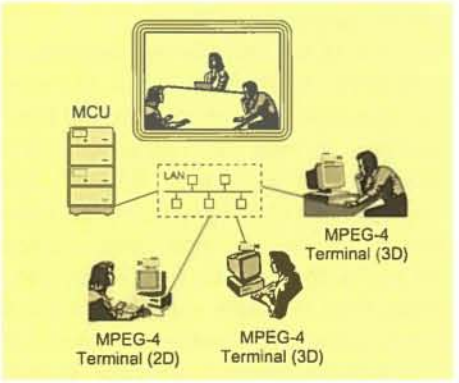

Fig. 4: Outline of the 'Virtual Meeting Point'.

configurations as well as a combination of both are also supported.

As the Delivery Multimedia Integration Framework (DMIF) of MPEG-4 Version 1 does not allow multicast configurations [7], a proprietary encapsulation of elementary streams in RTP/UDP packets on top of IP-multicast was implemented [8]. Existing H.323 stacks and T.120 data channels are used for call control, conference management and data exchange [9]. However, an upgrade to a system layer that is more compliant with MPEG-4 will be implemented during a follow-up project in 1999, as soon as multicast over IP is supported by the DMIF of MPEG-4 Version 2 [10].

One terminal of the MPEG-4 conference runs several processes in parallel: multiple video/audio decoders, online capture of the participant's video, real time video segmentation against a known background, and real time video and audio encoders. In addition, each terminal performs the composition of the virtual scene, including synchronized rendering of all the AVOs. Table 1 shows details of a complexity measure for these parallel processes, which all run in software without any dedicated hardware.

Processing Step	Time [ms]
3D Compositor	≈ 60
Segmentation	18
MPEG-4 Video Encoder (QCIF@12.5 Hz)	16
MPEG-4 Video Decoder (QCIF@12.5 Hz)	6
G.723 Encoder	3
G.723 Decoder	< 1

Table 1: Complexity measures (Pentium II, 400 MHz)

Due to this fairly high computational load, interoperability with less well equipped terminals is an important issue for the conference system. It can therefore be operated at different complexity levels depending on the computing power of particular devices (e.g. a full-featured 3D composition with up to three conference participants with a dual processor PC or, for a single processor terminal, a reduced 2D composition where up to three participants are displayed in a static scene provided by the MCU).

4. Multiview extension

One crucial limitation of the above application scenarios is the representation of natural video objects as 2D textures, which do not allow perspective adaptation to the user's 3D viewpoint. To overcome this restriction, a new technique called Incomplete 3D (I3D) representation for video objects has been developed at HHI [6]. It can be used whenever an object is captured by two or more cameras. In this case, a common texture surface is extracted from all available camera views, and the depth information is coded in an associated disparity map, as shown in Fig. 5b. This I3D representation can be encoded like an arbitrarily shaped MPEG-4 video object, where the disparity map is transmitted as an assigned auxiliary component – an extension of the MPEG-4 grey-level shape syntax [6] [12].

Since the I3D texture surface contains all information available from two or more synchronously operating cameras, alternative views of the video object can be synthesized from the texture surface. For this purpose, the disparities are scaled according to the desired viewpoint, and a disparity-controlled projection is performed. Basically, the original left and right camera views, and also any views from positions on the axis between the two cameras, can be reconstructed (see Fig. 6).

One benefit of I3D is its low complexity and high stability compared to algorithms using complete 3D wire frames. In particular, the synthesis of the viewpoint-adapted video object is quite simple and requires a very low and constant CPU time – an important aspect in combination with applications like the virtual shop or the virtual meeting point in which the software 3D render engine, the real time segmentation and the MPEG-4 encoders and decoders already require a huge amount of CPU time (see Table 1). It is therefore intended to integrate this I3D technique into the prototypes during a follow-up project, again planned in cooperation with DTAG/BERKOM GmbH for 1999.

A further important advantage of I3D is that it fits very well into the plane-oriented structure of the MPEG-4 video syntax [7]. Therefore, following the I3D proposal, one of the extensions most likely to be included in MPEG-4 Version 2 is the inclusion of

so-called multiple auxiliary components, which can be used to add the disparity map for I3D, as described above [12]. Other useful examples of auxiliary components are depth or surface orientation maps, which are needed as side information for advanced mixing processes in professional post-production systems [13][14].

5. Conclusions

MPEG-4 is a multimedia standard of ISO/IEC that offers some new and outstanding features. Through its generalized scene description language (BIFS), MPEG-4 enables flexible composition of 2D and 3D scenes and integrates multiple natural and synthetic audio-visual data into this framework. It supports algorithms, tools and profiles for the efficient coding of different kinds of natural and synthetic video, sound and speech data as well as for the flexible representation of audio-visual data at terminals. MPEG-4 allows user interaction with audio, video and graphical objects, and it supports streaming of real time data. MPEG-4 aims at a wide range of bit rates between 10 kbit/s and 10 Mbit/s, it offers various types of content-based functionality, and it serves a large field of multimedia applications.

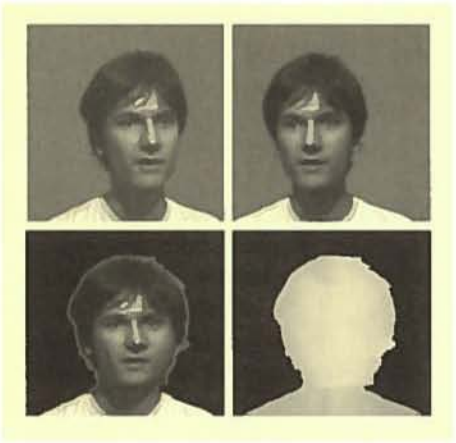

Fig. 5: Examples of I3D analysis for test sequence Man. (a) Left and right original images. (b) Texture and disparity map.

Fig. 6: Synthesis examples at different views for test sequence Man.

Several example applications for complete MPEG-4 systems, such as the virtual shop from section 2 or the virtual meeting point from section 3, have already been developed and have been successfully demonstrated. Real time implementations of key components, such as software encoders and decoders or compositors, as well as the real time segmentation of natural video objects, have been implemented and can be used for further developments. As MPEG-4 Version 1 is focussed on low bit rate coding in error prone environments, it will find its first applications in mobile radio and the Internet [1][2]. However, taking into account the extensions envisaged in MPEG-4 Version 2, it can be expected that high quality applications such as the professional production of multimedia documents at shared interactive platforms will follow later on [12].

Acknowledgments

This work was supported by the Ministry for Education, Science, Research and Technology of the Federal Republic of Germany under Grant No. 01 BN 701. The two applications were developed in cooperation with DTAG/BERKOM (Contract Nos. 4160/65183, 4160/75182 and E100150198).

References

[1] T. Sikora and L. Chiariglione, **"MPEG-4 and its potential for future multimedia service"**, Proc. IEEE ISCAS`97 Hong Kong, Juni 1997.[2] R. Schäfer, **"MPEG-4 – a new compression standard for interactive applications and services"**, HHI Report 97, Selected Achievements, Electronic Imaging,

pp. 111-118, 1998.
[3] ISO/IEC/MPEG-98, **"MPEG-4 Overview"**, Requirements Group, Document N2459, Oct. 1998.

[4] P. Kauff, J.-R. Ohm, S. Rauthenberg and T. Sikora, **"The MPEG-4 standard and its application in virtual 3D environments"**, Proc. 42nd Asilomar Conference, Monterey, Nov. 1998.

[5] S. Rauthenberg, S. Kruse, A. Graffunder and J. Johann, **"An MPEG-4 demonstrator for interactive services in virtual environments"**, Proc. PCS'97, Berlin, Sept. 1997.

[6] J.-R. Ohm and K. Müller, **"Incomplete 3D – multiview representation of video objects"**, IEEE Trans. CSVT, Special Issue SNHC, 1998.

[7] ISO/IEC/MPEG-98, Text of ISO/IEC FDIS 14496-1-6, MPEG Systems, Audio, Video and DMIF Group, Documents N2501 to N2506, Oct. 1998.

[8] H. Schulzrinne, **"RTP: A transport protocol for real-time applications"**, RFC 1889, Jan. 1996.

[9] ITU-T, Recommendation T.120, July 1996.

[10] ISO/IEC/MPEG-98, DMIF ISO/IEC 14496-6 Extensions Amd1 for Version 2 WD 4.0, MPEG DMIF Group, Document N2480, Oct. 1998.

[11] J.-R. Ohm, Report from Multiview CE M1, MPEG-4 Document M3640, July 1998.

[12] P. Kauff and J. Figue, Contributions from NEMESIS to MPEG-4 Studio Profile, MPEG-4 Document M3739, July 1998.

[13] P. Kauff and J. Figue, **„On the Use of an MPEG-4 Studio Profile for Professional Post-Production"**, MPEG-4 Document M4095, Oct. 1998.

Communications and Events

PUBLICATIONS*

Photonic Networks

C. Baack, **Anmerkungen zum Internet von Morgen (Keynotes on the internet of tomorrow)** (invited), Münchner Kreis, in: Das Internet von Morgen (The internet of tomorrow), Nov. 1998, Proc. in press.

H.-G. Bach, D. Hoffmann and H.G. Weber, **Progress in 40 Gbit/s TDM techniques,** HHI Annual Report 1997, pp. 55-60, Feb.1998.

H.-G. Bach, W. Schlaak, G.G. Mekonnen, R. Steingrüber, A. Seeger, Th. Engel, W. Passenberg, A. Umbach, C. Schramm and G. Unterbörsch, **50 Gbit/s InP-based photoreceiver OEIC with gain flattened transfer characteristics,** Proc. 24th Europ. Conf. on Optical Communication (ECOC '98), Madrid, Spain, Sept. 20-24, 1998, vol. 1, pp. 55-56.

E.-J. Bachus, K. Habel, K.-D. Langer, W. v. Reden, J. Schneider, J. Vathke and C.M. Weinert, **Physical layer aspects for a nationwide WDM network,** Proc. European Conf. on Networks & Optical Communications (NOC '98), Manchester, U.K., June 23-25, 1998, vol. 3, pp. 235-242.

S. Bauer-Gogonea[1], S. Bauer[1] and W. Wirges, **Pulsed electrothermal technique for the characterization of dielectric films,** Proc. SPIE Dielectric and Related Phenomena, (Bielsko-Biola, Poland) Sept. 98, in press.

S. Bauer-Gogonea[1], Z.Y. Cheng[3], W. Wirges, S. Bauer[1], R. Gerhard-Multhaupt[2] and D.K. Das-Gupta[4], **Dielectric investigation of thermally-induced chromophore degradation in nonlinear optical polymer electrets,** IEEE Transactions on Dielectrics and Electrical Insulaters, Feb. 1998, vol. 5, pp. 21-25.

E.H. Böttcher[5], E. Dröge[5], D. Bimberg[5], A. Umbach, H. Engel and M. Collischon[6], **Polarization dependence of the response of micrometer and submicrometer InGaAs metal-semiconductor-metal photodetectors,** IEEE Photon. Techn. Lett., vol. 9, June 1997, pp. 809-811.

D. Breuer, H. J. Ehrke, F. Kueppers, R. Ludwig, K. Petermann, H.G. Weber and K. Weich, **Unrepeatered 40 Gbit/s RZ single channel transmission at 1.55um using various fiber types,** IEEE Photon. Techn. Lett. vol. 10, no. 6, Jan. 1998, pp. 822-824.

A. Buxens[7], A.T. Clausen[7], H. N. Poulsen[7], K. S. Jepsen[7], K. E. Stubkjaer[7], C. Bornholdt, O. Brox, M. Möhrle and B. Sartorius, **40 to 10 Gbit/s demultiplexing using a self-pulsating DFB laser for clock recovery,** Proc. 24th Europ. Conf. on Optical Communication (ECOC '98), 20-24 Sept. 1998, Madrid, Spain, vol. 1, pp. 507-8.

C. Caspar, H.-M. Foisel, R. Freund[9] and B. Strebel, **4-channel 10 Gbit/s transmission over 15 wavelength selective crossconnect paths and 1175 km dispersion compensated standard single-mode fiber links,** OFC '98, San Jose, USA, Feb. 22-27, Techn. Dig. vol. 2, paper ThP3, pp. 327-329.

C. Caspar, H.-M. Foisel[9], L. Molle and B. Strebel, **4 x 2.5 Gbit/s, NRZ transmission experiments over transparent crossconnects with opto-electronic frequency converters and dispersion compensated standard single-mode fibre links,** OECC '98, Chiba, Japan, July 12-16, Techn. Dig., pp. 426-427.

C. Caspar, H.-M. Foisel[9], R. Freund[9] and B. Strebel, **4-channel 10 Gbit/s transmission over 15 wavelength selective crossconnect paths and 1175 km dispersion compensated standard single-mode fiber links,** Photon. Technol. Lett., Oct. 1998, vol. 10, no. 10, pp. 1479-1480.

Z.Y. Cheng[3], S. Yilmaz, W. Wirges, S. Bauer-Gogonea[1] and S. Bauer[1], **Temperature-domain analysis of primary and secondary dielectric relaxation phenomena in a nonlinear optical side-chain polymer,** J. Appl. Phys., vol. 83, no. 6, June 1998, pp. 7799-7807.

S. Diez, U. Feiste, R. Ludwig and H.G. Weber, **Characterization of an all-optical gain-transparent SLALOM-switch,** Optical Amplifiers and Their

* If titles are given bilingually the communication is in German. The list of footnotes is on page 184.

Applications (OAA '98), Vail (Colorado), USA, July 27-29, 1998, Techn. Digest, paper TuD9, pp. 151-154.

S. Diez, E. Hilliger, R. Ludwig and H.G. Weber, **Characterization of interferometric switching devices for ultrafast all-optical signal processing,** Techn. Digest Ultrafast Phenomena, Garmisch-Partenkirchen, Germany, July 12-17,1998, pp. 96-97.

S. Diez, R. Ludwig, E. Patzak and H.G. Weber, **Novel gain-transparent SOA-switch for high bit rate OTDM-add/drop-multiplexing,** Proc. 24th Europ. Conf. on Optical Communication (ECOC '98), Madrid, Spain, Sept. 20-24, 1998, vol. 1, pp. 461-462.

S. Diez, R. Ludwig and H.G. Weber, **All-optical switch for TDM and WDM/TDM systems demonstrated in a 640 Gbit/s demultiplexing experiment,** Electron. Lett., vol. 34, no. 8 (1998), pp. 803-805.

S. Diez, R. Ludwig and H.G. Weber, **Gain-transparent SOA-switch for high bitrate add/drop multiplexing,** Photon. Techn. Lett. (in press).

S. Diez, C. Schmidt, R. Ludwig, H. G. Weber, T. Ducellier[12] and P. Doussière[12], **Effect of birefringence in a bulk semiconductor-optical amplifier on four-wave mixing,** IEEE Photon. Technol. Lett., vol. 10, no. 2 (1998), pp. 212-214.

S. Diez, C. Schmidt, R. Ludwig, H. G. Weber, K. Obermann[5], S. Kindt[5], I. Koltchanov[5] and K. Petermann[5], **Four-wave mixing in semiconductor optical amplifiers for frequency conversion and fast optical switching,** IEEE JSTQE, Nonlinear Devices for All-Optical Signal Processing, vol. 3, no. 5, (1998), pp. 1131-1145.

S. Diez, R. Ludwig and H. G. Weber, **A Novel SOA-based switching device for high-speed, high contrast, all-optical demultiplexing,** The Rank Prize Funds, Proc. Symposium on Ultrafast Photonic Processing and Networks, Grasmere, England, 20th to 23rd April 1998.

S. Diez, R. Ludwig and H.G. Weber, **High-speed all-optical signal processing by switching devices based on semiconductor optical amplifiers** (invited), Proc. LEOS 1998 Annual Meeting Orlando (FL), USA, Dec.1-4, 1998, vol.2, pp. 401-402.

S. Diez, C. Schmidt, D. Hoffmann, C. Bornholdt, B. Sartorius, H.G. Weber, L. Jiang[13] and A. Krotkus[14], **Simultaneous sampling of optical pulse intensities and wavelengths by four-wave mixing in a semiconductor optical amplifier,** Appl. Phys. Lett., vol. 73, no. 26, pp. 3821-3823.

E. Dröge[5], E.H. Böttcher[5], D. Bimberg[5], O. Reimann[11] and R. Steingrüber, 70 GHz **InGaAs metal-semiconductor-metal photodetectors for polarisation-insensitive operation,** Electron. Lett., vol. 34, July 1998, pp. 1421-1422.

E. Dröge[5], E.H. Böttcher[5], S. Kollakowski[5], A. Strittmatter[5], D. Bimberg[5], O. Reimann[11] and R. Steingrüber, **78 GHz distributed InGaAs MSM photodetector,** Electron. Lett. (1998), vol. 34, no. 23, p. 2241.

E. Dröge[5], E.H. Böttcher[5], S. Kollakowski[5], A. Strittmatter[5], O. Reimann[11], R. Steingrüber, A. Umbach and D. Bimberg[5], **Distributed MSM photodetectors for the long-wavelength range,** Proc. 24th Europ. Conf. on Optical Communication (ECOC '98), Madrid, Spain, Sept. 20-24, 1998, vol. 1, pp. 57-58.

E. Dröge[5], E.H. Böttcher[5], S. Kollakowski[5], A. Strittmatter[5], O. Reimann[11], R. Steingrüber, A. Umbach and D. Bimberg[5], **Distributed millimeter-wave InGaAs metal-semiconductor-metal photodetector,** Proc. Intern. Topical Meeting on Microwave Photonics (MWP '98), New Jersey, USA, Oct. 12-14, 1998, TuD1, pp. 173-176.

E. Dröge[5], E.H. Böttcher[5], S. Kollakowski[5], A. Strittmatter[5], O. Reimann[11], R. Steingrüber, A. Umbach and D. Bimberg[5], **Distributed MSM photodetectors for the long-wavelength range,** Proc. 24th Europ. Conf. on Optical Communication (ECOC '98), Madrid, Spain, Sept. 20-24, 1998, vol. 1, pp. 57-58.

R. Eggemann and E. Patzak, **Operation, administration and maintenance (OAM)**

in photonic networks, HHI Annual Report 1997, pp. 69-74, Feb.1998.

A. Ehrhardt[10], C. Caspar, H.-M. Foisel[10] and B. Strebel, **4000 km 2.5 Gbit/s single channel laboratory and 245 km 4x2.5 Gbit/s field transmission experiment of chirped WDM signals over dispersion compensated standard single-mode fibre trunks,** Proc. MMET '98, Kharkov, Ukraine, June 2-5, 1998, vol. 2, pp. 911-913.

A. Ehrhardt[10], C. Caspar, H.-M. Foisel[10], B. Strebel and C.M. Weinert, **8x2.5 Gbit/s 2340 km transmission experiments over a replica of the Berlin-Darmstadt field transmission line,** Proc. 24th Europ. Conf. on Optical Communication (ECOC '98), Madrid, Spain, Sept. 20-24, 1998, vol.1, pp. 277-278.

M. Eiselt, R. Schnabel and E. Dietrich, **Polarisation insensitive frequency converter with the capability of chirp removal,** IEEE Photon. Technol. Lett., vol.10, no.1, Jan. 1998, pp. 63-65.

T. Elsässer[15], R.A. Kaindl[15], S. Lutgen[15], M. Wörner[15], A. Hase and H. Künzel, **Ultrafast coherent and incoherent dynamics of intersubband excitations in quasi-two-dimensional semiconductors,** Proc. SPIE Photonic West '98, (San Jose, USA), Jan. 24-30, 1998, vol. 3277, pp. 2-9.

Th. Engel, G.G. Mekonnen, A. Umbach, V. Breuer[5], H.-G. Bach, E. H. Böttcher[5] and D. Bimberg[5], **Design and modeling of narrow band InP-photoreceiver OEICs based on HEMTs and MSM photodetector,** Proc. 22nd Workshop on Compound Semiconductor Devices and Integrated Circuits, (WOCSDICE '98), Zeuthen, Germany, May 24-27, 1998, pp. 93-94.

Th. Engel, A. Strittmatter[5], W. Passenberg, E. Dröge[5], A. Umbach, W. Schlaak, R. Steingrüber, A. Seeger, G.G. Mekonnen, G. Unterbörsch, H.-G. Bach, E.H. Böttcher[5] and D. Bimberg[5], **Narrow band photoreceiver OEIC on InP operating at 38 GHz,** IEEE Photon. Techn. Lett., vol. 10, Sept. 1998, pp. 1298-1300.

Th. Engel, A. Strittmatter[5], W. Passenberg, E. Dröge[5], A. Umbach, W. Schlaak, R. Steingrüber, A.Seeger, G.G. Mekonnen, G. Unterbörsch, H.-G. Bach, E.H. Böttcher[5] and D. Bimberg[5], **38 GHz narrow band photoreceiver OEIC with MSM photodetector and HEMT amplifier,** Proc. 24th Europ. Conf. on Optical Communication (ECOC '98), Madrid, Spain, Sept. 20-24, 1998, vol. 1, pp. 63-64.

Th. Engel, A. Strittmatter[5], W. Passenberg, A. Seeger, R. Steingrüber, G.G. Mekonnen, G. Unterbörsch and D. Bimberg[5], **Design, fabrication and characterization of narrow band photoreceiver OEICs based on InP,** Proc. 11th Annual Meeting Lasers and Electro-Optical Society (LEOS '98), Orlando, USA, Dec. 1-4, 1998, paper TuJ1.

Th. Engel, E. Dröge[5], G Unterbörsch, E.H. Böttcher[5] and D. Bimberg[5], **Reactive matching of millimeter-wave photodetectors using coplanar waveguide technology,** IEEE Electron. Lett., Aug. 1998, vol. 34, no. 17, pp. 1690-1691.

U. Feiste, R. Ludwig, E. Dietrich, S. Diez, H. J. Ehrke, D. Razic and H.G. Weber, **40 Gbit/s transmission over 434 km of standard fiber using polarisation independent Mid-Span-Spectral Inversion,** Proc. 24th Europ. Conf. on Optical Communication (ECOC '98), Madrid, Spain, Sept. 20-24, 1998, postdeadline paper, vol. 3, pp. 115-117.

M. Ferstl, **Reactive ion etching: a versatile fabrication technique for micro-optical elements,** Diffractive Optics and Micro-Optics, (Kailua-Kona, USA), June 8-11, 1998, in: OSA Techn. Dig., 1998, vol. 10, pp.167-169.

F. Fidorra, D. Franke, M. Möhrle, W. Rehbein, A. Sigmund, R. Stenzel, H.Venghaus, M. Weickhmann[8], M. Töpfer[8], M. Schmidt[8] and H. Reichl[5], **Thermal crosstalk of integrated multiwavelength transmitters,** Proc.16th IEEE International Semicond. Laser Conf., Nara, Japan, Oct. 1998, TuE28, pp. 149-150.

F. Fidorra, M. Möhrle, W. Rehbein, F. Reier, A. Sigmund, R. Stenzel and H. Venghaus, **Integrated WDM Transmitter,** Proc. 24th Europ. Conf. on Optical Communication (ECOC '98), Madrid, Spain, Sept. 20-24, 1998, vol.1, pp. 207-208.

U. Fischer, K. Peters, D. Pech and Th. Eckhardt, **Faser-Chip-Koppelmodule für die optische Nachrichtentechnik (Fiber chip coupling modules for optical networks),** in: "Position & Bewegung" Ausg. 26, Informationszeitschrift Physik Instrumente (PI) GmbH, April 1999, in press.

D. Franke, F.W. Reier and N. Grote, **Post-growth Zn diffusion into InGaAs/InP in a LP-MOVPE reactor,** Proc. 9th Intern. Conf. on Metal Organic Vapour Phase Epitaxy (IC MOVPE IX), La Jolla, USA, May, 30-June 4, 1998, in: J. Crystal Growth, vol. 195 (1998), pp. 112-116.

R. Freund[9], C. Caspar, H.-M. Foisel[10], B. Strebel, C.M. Weinert, N. Hanik[10] and W. Reimer[16], **Numerical Analysis of Transparency Limitations in optical Core Networks and Verification by Experiment,** Proc. Internationales Wissenschaftliches Kolloquium (IWK '98), Ilmenau, Germany, 21.-24. Sept. 1998.

N. Grote, **Mit Laserlicht um die Welt (Laser light connecting the world),** Spektrum der Wissenschaft, no. 2, Feb. 1998, pp. 75-78.

M. Hamacher, H. Heidrich and R. Kaiser, **Photonic application specified integrated circuits (PHASICs) for photonic networks,** HHI Annual Report 1997, pp. 85-92, Feb. 1998.

M. Hamacher, H. Heidrich, R. Kaiser, P. Albrecht, W. Ebert, D. Franke, G. Jacumeit, S. Malchow, W. Rehbein, H. Schroeter-Janßen and R. Stenzel, **Monolithically integrated 1.5 5m/1.3 5m transceiver modules for full-duplex operation,** OFC/IOOC '99, accepted.

M. Hamacher, H. Heidrich, R. Kaiser, P. Albrecht, W. Ebert, S. Malchow, M. Möhrle, W. Rehbein, H. Schroeter-Janßen and R. Stenzel, **Full-duplex WDM-transceiver-PICs,** Proc. 24th Eur. Conf. on Optical Communications (ECOC '98), Madrid, Spain, 1998, ThA07, pp. 639-640.

S. Herbst[17], Th. Hermes and P. Meissner[17], **Theoretical investigation of the sensitivity of a direct WDM-system with a frequency selective optical receiver and optical preamplifier,** Journal of Optical Communications, vol. 19 (1998), no. 5, pp. 162-168.

E. Hilliger, S. Diez and H. G. Weber, **Indirekte Bestimmung von SLALOM-Schaltfenstern (Indirect determination of SLALOM switching windows),** Frühjahrstagung der Deutschen Physikalischen Gesellschaft, paper Q 3.4, Konstanz, Germany, March 1998, p. 172.

G. Jäger[18], I. Stegeman[18], S. Yilmaz, W. Brinker, W. Wirges, S. Bauer-Gogonea[1], S. Bauer[1], M. Ahlheim[19], M. Stähelin[19], B. Zysset[19], F. Lehr[19], M. Deimeer[20] and M.C. Flipse[20], **Poling and characterization of polymer waveguides for modal dispersion phase-matched second-harmonic generation,** J. Opt. Soc. Am. B, vol. 15, no. 2, Febr. 1998, pp. 781-788.

O. Kahle[21], U. Wielsch[21], H. Metzner[21], J. Bauer[21], C. Uhlig[21] and C. Zawadzki, **Glass transition temperature and thermal expansion behaviour of polymer films investigated by temperature variable spectroscopic ellipsometry,** in: Thin Solid Films, 1998, vol. 313-314, pp. 803-807.

R.A. Kaindl[15], S. Lutgen[15], M. Wörner[15], T. Elsässer[15], B. Nottelman[22], V.M. Axt[22], T. Kuhn[22], A. Hase and H. Künzel, **Ultrafast dephasing of coherent intersubband polarizations in a quasi-two-dimensional electron plasma,** Phys. Rev. Lett., vol. 80, p. 3575, 1998.

R. Kaiser, M. Hamacher, H. Heidrich, P. Albrecht, S. Ebert, H. Künzel, R. Löffler, S. Malchow, W. Rehbein and H. Schroeter-Janßen, **Monolithically integrated transceivers on InP: the development of a generic integration concept and its technology challenges** (invited), Proc. 10th Intern. Conf. on Indium Phosphide and Related Materials (IPRM '98), Tsukuba, Japan, May 11-15, 1998, IEEE, 98H36129, WA4-1, pp. 431-434.

N. Keil, **Polymeric integrated optical waveguide devices for signal processing in optical networks** (invited), Proc. Intern. Symp. on Image Processing Molecular Systems (IPMS '98), Tsukuba, Japan, March 9-10, 1998, Conf. Dig., pp. 14-17.

N. Keil, **Research on photonic devices and related technologies at HHI** (invited), Proc. Intern. Symp. Photoreaction Control and Photofunctional Materials (PCPM '98), Tsukuba, Japan, March 9-10, 1998, Conf. Dig., pp. 75-78.

N. Keil, W. Wirges, H.H. Yao, S. Yilmaz and C. Zawadzki, **Integrated optical switching devices for telecommunications made of plastics,** Proc. Photonic Switching Session (PIT '98), London, UK, Sept. 14-16, 1998, Conf. Dig., pp. 11-17.

N. Keil, H.H. Yao and C. Zawadzki, **Polymeric optical space switches** (invited), Proc. Integrated Photonics Research '98, (Victoria, Canada), March 30 - April 2, 1998, Conf. Dig., ITuL2-1, pp. 353-355.

A. Krotkus[14], D. Hoffmann, R. Ludwig and S. Diez, **Optical sampling technique for fast electro-optic devices,** Electron. Lett., vol. 34, Sept. 17, 1998, no.19, pp.1877-1879.

B. Kuhlow and G. Przyrembel, **Integrated multichannel 1.3 µm/1.55 µm AWG MUX/DEMUX for WDM-PONs,** Proc. Optical Fiber Communication Conf. (OFC '98), San Jose, USA, Febr. 22-27, 1998, OSA Techn. Dig., vol. 2, TuN2, pp. 77-78.

H. Künzel, **Selective MOMBE: Improved fabrication technology for PHASICs,** HHI Annual Report 1997, pp. 93-96, Feb.1998.

H. Künzel. P. Albrecht, S. Ebert, R. Gibis, P. Harde, R. Kaiser, H. Kizuki[23] and S. Malchow, **MOMBE growth of semi-insulation GaInAsP (λg = 1.05 µm): Fe optical waveguides for integrated photonic devices,** Appl. Phys. Lett., vol. 72, p. 3050, 1998.

H. Künzel, S. Ebert, R. Gibis, P. Harde, R. Kaiser, H. Kizuki[23] and S. Malchow, **MOMBE grown GaInAsP (λg = 1.05/1.15 µm) waveguide for laser integrated photonic ICs,** J. Crystal Growth, vol.188, p. 281, 1998.

H. Künzel, S. Ebert, R. Gibis, R. Kaiser, H. Kizuki[23] and S. Malchow, **Laser/waveguide integration utilizing selective area MOMBE regrowth for photonic IC applications,** Proc. 10th Intern. Conf. on Indium Phosphide and Related Materials (IPRM '98),Tsukuba, Japan, May 11-15, 1998, IEEE Catalog ThP-15, pp. 571-574.

H. Künzel, S. Ebert, R. Gibis, R. Kaiser, H. Kizuki[23], S. Malchow and G. Urmann, **Selective MOMBE growth of InP-based waveguide/laser butt-joints,** J. Crystal Growth, vol. 192, p. 56, 1998.

K.-D. Langer, **Technische Entwicklungen in der Telekommunikation im Jahr 1997 (Technical advances in telecommunications 1997),** Jahrbuch Telekommunikation und Gesellschaft 1998, Prof. H. Kubicek et al. (Ed.), R. v. Decker's Verlag Heidelberg, pp. 445-453.

R. Ludwig, S. Diez, A. Ehrhardt, L. Küller, W. Pieper and H. G. Weber, **A tunable femtosecond modelocked semiconductor laser for applications in OTDM-systems,** IEICE Trans. Electron., vol. E81-C, no. 2 (1998), pp. 140-145.

R. Ludwig, S. Diez and H. G. Weber, **A novel all-optical switch for demultiplexing in OTDM-systems demonstrated in a 640 Gbit/s WDM/TDM experiment,** Optical Fiber Communication Conference 1998, OFC '98, postdeadline paper PD22 (1998).

S. Lutgen[15], R.A. Kaindl[15], M. Wörner[15], T. Elsässer[15], A. Hase and H. Künzel, **Ultrafast heating and cooling of electron plasmas in GaInAs/AlInAs quantum wells after intersubband excitation,** Solid State Commun., vol. 106, pp. 425-429, 1998.

L. Mörl, C. Bornholdt, D. Hoffmann, K. Matzen, G.G. Mekonnen and F.W. Reier, **A travelling wave electrode Mach-Zehnder 40 Gb/s demultiplexer based on strain compensated GaInAs/AlInAs tunnelling barrier MQW structure,** Proc. 1998 Intern. Conf. InP and Related Materials, Tsukuba, Ibaraki, Japan, 1998, pp. 403-406.

K. Mueller[24], N. Hanik[10], A. Gladisch[10], H.- M. Foisel[10] and C. Caspar, **Application of amplitude histograms for quality of service measurements of optical channels and fault ildentification,** Proc. 24th Europ. Conf. on Optical Communication (ECOC '98), Madrid, Spain, Sept. 20-24, 1998, vol. 1, pp. 707-708.

G. Nachtwei[25], A. Weber[25], H. Künzel, J. Böttcher, O. Jaschinski[26], **Fermi surfaces of InGaAs/InAlAs superlattices with thin δ-doped barriers,** J. Appl. Phys., vol. 84, p. 383, 1998.

H.-P. Nolting, R. März, **Optical filter,** Encyclopedia of Electrical and Electric Engineering, John Wiley and Sons, NY, Feb. 99, www.wiley.com/ee/engineering.

H.-P. Nolting, W. v. Reden, S. Diez, **COST 240 Book on Photonic Devices for Telecommunications,** Springer Vlg., XXXIII, ISBN number: 3-540-64318-4, Nov. 1998.

E. Pawlowski, M. Ferstl, H. Hellmich, B. Kuhlow, G. Przyrembel, C. Warmuth and J.R. Salgueiro[27], **Novel multichannel WDM-PON demultiplexer using an AWG and diffractice optical elements,** Diffractive Optics and Micro-Optics, (Kailua-Kona, USA), June 8-11, 1998, in: OSA Techn. Dig., vol. 10, pp. 56-58, 1998.

W. Pieper, R. Ludwig, C.M. Weinert, B. Kuhlow, G. Przyrembel, M. Ferstl, E. Pawlowski and H.G. Weber, **4-channel × 40 Gbit/s unrepeatered OTDM-transmission over 100 km standard fiber,** IEEE Photon. Technol. Lett., vol. 10, no. 3, March 1998, pp. 451-453.

G. Przyrembel, B.Kuhlow, E. Pawlowski, M. Ferstl, R. Steingrüber, W. Fürst and H. Ehlers, **Multichannel 1.3 µm/1.55 µm AWG multiplexer/demultiplexer for WDM-PONs,** Electron. Lett., Febr. 1998, vol. 34, pp. 263-264.

R. Riemenschneider[17], J. Peerlings[17], J. Pfeiffer[17], A. Dehe[17], A. Vogt[17], P. Meißner[17], H.L. Hartnagel[17], N. Chitica[28], J. Daleiden[28], K. Streubel[28], H. Künzel, W. Görtz[29], **Mechanical-optical analysis of InP-based Bragg membranes for selective tunable WDM receivers,** Proc. SPIE Photonic West '98, (San Jose, USA), vol. 3276, 1998.

Th. Rosin, C. Bornholdt, D. Hoffmann and R. Burghardt, **Opto-electronic packaging for broadband high speed (40 Gb/s) optical demultiplexer chip,** Proc.11th Annual Meeting Lasers and Electro-Optical Society (LEOS '98), Orlando, USA, Dec. 1-4, 1998, vol. 2, pp. 386-387.

H.-J. Rostalski[30], J. Guhr[30], B.H. Kleemann[30], J. Elscher[31], G. Schmidt[31], M. Ferstl, E. Pawlowski, R. Steingrüber, G. Bostanjoglo[32] and R. Motzkus[32], **Use of a multilayer dielectric diffraction grating as resonator mirror of a neodymium-doped yttrium aluminium garnet laser,** J. Modern Optics, 1998, vol. 45, pp. 1523-1535.

J. Saniter and F.-J. Westphal, **Transponders for WDM systems,** HHI Annual Report 1997, pp. 81-83, Feb.1998.

B. Sartorius, C. Bornholdt, O. Brox, H.J. Ehrke, D. Hoffmann, R. Ludwig, and M. Möhrle, **All-optical clock recovery module based on a self-pulsating DFB laser,** Electron. Lett. 1998, vol. 34, no. 17, pp. 1664-65.

B. Sartorius, C. Bornholdt, O. Brox, H.J. Ehrke, D. Hoffmann, R. Ludwig and M. Möhrle, **System performance of an all-optical clock recovery module,** Proc. 24th Europ. Conf. on Optical Communication (ECOC '98), 20-24 Sept. 1998, Madrid, Spain, pp. 505-506.

B. Sartorius, C. Bornholdt, O. Brox, M. Möhrle, P. Brindel[33], O. Leclerc[33] and E. Desurvire[33], **Analysis and compression of pulses emitted from an all-optical clock recovery module,** Electronics Letters, vol. 34, no. 24, pp.2344-2345.

W. Schlaak, **40 Gigabit pro Sekunde (40 G/bit per second),** Technik & Gesellschaft, 3/1998, pp. 22-23.

W. Schlaak, G.G. Mekonnen, W. Passenberg, R. Steingrüber, A. Seeger, Th. Engel, A. Umbach and H.-G. Bach, **InP-HEMT based integration of distributed amplifiers for 40 Gbit/s photoreceivers,** Proc. 22nd Workshop on Compound Semiconductor Devices and Integrated Circuits, (WOCSDICE '98), Zeuthen, Germany, May 24-27, 1998, pp. 80-81.

R. Steingrüber and S. Ullerich, **Grey-tone lithography and dry etching technique for the fabrication of integrated spot size converters,** Proc. Intern. Conf. Micro- and Nanoengineering '98, (Leuven, Belgium), Sept. 22-24, 1998.

B. Strebel, C. Caspar, H.-M. Foisel and R. Freund[9], **Experimentelle und theoretische Untersuchung der Signalausbreitung in WDM Netzen (Experimental and theoretical examination of signal propagation in WDM networks),** MMONT '98, Günzburg, Germany, March 4-6, 1998, p. 55.

B. Strebel, C. Caspar, R. Freund[9], **Loop experiments and simulations for the wavelength division multiplex network signal path,** Photonics China, Conference PC06, Beijing, China, Sept. 16-19, 1998, Proc. SPIE vol. 3552.

B. Strebel and B. Kuhlow, **Application of wavelength multiplexers in WDM networks,** HHI Annual Report 1997, pp. 61-67, Feb. 1998., HHI Annual Report 1997, pp. 61-67, Feb. 1998.

D. Trommer, M. Arps, J. Kreissl, R. Steingrüber, W. Ebert and H. Venghaus, **Polarisation insensitive meander-type wavelength demultiplexer with large tuning range,** Proc. 24th Europ. Conf. on Optical Communication (ECOC '98), Madrid, Spain, Sept. 20-24, 1998, vol.1, pp. 113-114.

D. Trommer, M. Arps, R. Steingrüber, W. Ebert and J. Kreissl, **Polarisation insensitive WDM channel dropping filter with large tuning range,** Proc. 10th Intern. Conf. on Indium Phosphide and Related Materials (IPRM '98), (Tsukuba, Japan), May 11-15, 1998, post-deadline paper, FB3-4, pp. 7-8.

Trommer, A. Umbach and G. Unterbörsch, **InGaAs photodetector with integrated biasing network for mm-wave applications,** Proc. 10th Intern. Conf. on Indium Phosphide and Related Materials (IPRM '98), (Tsukuba, Japan), May 11-15, 1998,TuP-52, pp. 276-279.

A. Umbach, G. Unterbörsch, R.-P. Braun and G. Großkopf, **Stable optical source and high-speed photodetector used for remote fiber-optic 64 GHz mm-wave generation,** Proc. Optical Fiber Communication Conf. (OFC '98), San Jose, USA, Febr. 22-27, 1998, Techn. Dig. paper ThB3, pp. 260-261.

G. Unterbörsch, D. Trommer, A. Umbach, R. Ludwig and H.-G. Bach, **High-power performance of a high-speed photodetector,** Proc. 24th Europ. Conf. on Optical Communication (ECOC '98), Madrid, Spain, Sept. 20-24, 1998, vol.1, pp. 67-68.

H. Venghaus, **Optoelectronic and optical devices and circuits,** in: V. Jung und H.-J. Warnecke (Eds.), Handbuch für die Telekommunikation, Berlin, Springer, 1998, chapter 2.1.2.

G. Walf, **Bericht von der 24. European Conference on Optical Communication 1998 in Madrid (Report on 24th European Conference on Optical Communication 1998 at Madrid),** ITG Rundbrief, Informationstechnische Gesellschaft im VDE, vol. 23, Dec. 1998.

G. Walf, **Bericht über die OFC '98 Optical Fiber Communication Conference (Report on OFC '98 Optical Fiber Communication Conference)** San Jose, California, Feb. 22-27, 1998, Laser und Optoelektronik, vol. 30 no. 4, Aug. 1998, pp. 30-35.

H.G. Weber, S. Diez, H.J. Ehrke, U. Feiste, R. Ludwig, E. Patzak and C. Schmidt, **All-optical semiconductor switching devices for applications in time division multiplexing transmission systems,** NATO Advanced Research Workshop, Kiryat Anavim (Israel), Oct. 19-21, 1998, pp. 29-30.

H.G. Weber, R. Ludwig, S. Diez, W. Pieper, H. J. Ehrke and C.M. Weinert, **All-optical 40 Gbit/s transmission technology,** International Topical Workshop on Contemporary Photonics Technologies, CPT '98, Tokyo, Japan, Jan. 12-14, 1998, Techn. Digest, pp. 41-44.

C.M. Weinert, C. Caspar, H.-M. Foisel and B. Strebel, **Influence of laser linewidth on optical fiber transmission: modelling and measurement,** Integrated Photonics Research '98, Victoria, Canada, March 30-April 1, 1998, Technical Series, vol. 4, pp. 145-147.

C.M. Weinert, C. Caspar, H.-M. Foisel, B. Strebel and E.-J. Bachus, **Einfluss von**

Transmittereigenschaften auf die optische Signalausbreitung: Experimente und numerische Simulation (Influence of transmitter properties on the propagation of optical signals: experiments and numerical simulation), Proc. MMONT '98, Günzburg, Germany, 4.-6. March 1998, p. 19.

C.M. Weinert, C. Caspar, H.-M. Foisel[10], B. Strebel, L. Molle, **Modellierung von Transpondern im optischen Netz: Experiment und Simulation (Modelling of transponders in an optical network: experiment and simulation)** Proc. 43rd Intern. Scientific Coll., IWK '98, Ilmenau, Germany, Sept. 21-24, 1998, vol.1, pp. 110-114.

C.M. Weinert, C. Caspar, H.-M. Foisel[10], B. Strebel and L. Molle, **Numerical simulation of optical transmitters and optoelectronic transponders in optical networks,** Proc. Scientific Computing in Electrical Engineering (SCEE '98), Berlin, Germany, Sept. 30-Oct. 2, 1998, pp. 46-47.

C.M. Weinert, B. Strebel and R. Freund, **Numerical simulations of optical paths and verification by experiment,** HHI Annual Report 1997, pp. 75-79, Feb. 1998.

W. Wirges, H.H. Yao, S. Yilmaz, C. Zawadzki and N. Keil, **Low-loss polymer waveguide with high thermal stability,** Proc. Micro Systems Technologies '98 (Potsdam, Germany), Dec. 1-3, 1998, pp. 71-76.

H.H. Yao and N. Keil, **Design and simulation of polymer thermo-optic waveguide switches,** Proc. Micro Systems Technologies '98 (Potsdam, Germany), Dec. 1-3, 1998, pp. 95-100.

Mobile Broadband Systems

H. Boche, **An extension of the final value theorem of the Z-transform and applications,** Proc. of the IASTED '98 Intern. Conf. Modelling and Simulation, Pittsburgh (USA), 1998, pp. 109-111.

H. Boche, **Anwendbarkeit der Shannon-Zahl zur Bewertung von Mobilfunksystemen (On the use of the Shannon number for the investigation of mobile communications systems),** Proc. 43rd Intern. Scientific Coll., IWK '98, Sept. 1998, Ilmenau, D, vol. 1, pp. 32–37.

H. Boche, **Approximation of linear time varing systems with applications to the simulation of mobile radio channels,** Proc. 9th Intern. Symp. on System-Modelling-Control, Zakopane, Poland, 1998, 8 pages, CD-ROM.

H. Boche, **Approximierbarkeit der Hilbert-Transformation mittels konjugierter Shannonscher Abtastreihen und Anwendungen für die analytischen Signale (On the approximation of the Hilbert transform with conjugate Shannon sampling series with applications for analytic signals),** accepted at ZAMM 1998, Zeitschrift für Angewandte Mathematik und Mechanik.

H. Boche, **Divergenzverhalten mehrdimensionaler Shannonscher Abtastreihen (On the divergence behaviour of multidimensial Shannon sampling series),** manuscripta mathematica, vol. 95, 1998, pp. 137-147.

H. Boche, **Energy stable time continuous linear systems,** accepted at AEÜ 1999.

H. Boche, **Estimation of the peak value of oversampled bandlimited signals,** accepted at AEÜ, 1999.

H. Boche, **Iteratives Verfahren für die Rekonstruktion bandbegrenzter Signale mit Anwendungen auf das Sample-and-Hold-Verfahren (An iterative algorithm for the reconstruction of bandlimited signals with applications for sample-and-hold-circuits),** Electrical Engineering, Springer Verlag, 1998, vol. 81, no. 1, pp. 35-40.

H. Boche, **Mathematische Untersuchungen zum idealen Tiefpaß (On the behaviour of the ideal low pass),** accepted at Rostocker Mathematisches Kolloquium 1999.

H. Boche, **On the behavior of the ideal low pass (time continuous),** accepted at AEÜ 1999.

H. Boche, **On the input-output map of energy-stable systems,** Journal of Electrical Engineering, 1998, vol. 49, no. 3-4, pp. 101-102.

H. Boche, **Stable models for mobile radio channels,** Proc. of the IASTED '98 Intern. Conf. Modelling and Simulation, Pittsburgh (USA), 1998, pp. 347-351.

H. Boche, **Untersuchungen zu den optischen Systemen zur Ermittlung der Fourier-Transformation und der Hilbert-Transformation (Characterization of optical systems for the calculation of the Hilbert transform and the Fourier transform),** Acta Polytechnica Scandinavica, Applied Physics Series, no. 219, 1998, pp. 1-31.

H. Boche, **Untersuchungen zum Verhalten des Hardy-Littlewood Maximaloperators und des Poissonschen Integrals für VMO-Funktionen (On the behaviour of the Hardy-Littlewood maximal operator and the Poisson integral for VMO-functions),** accepted at Illinois Mathematical Journal, 1999.

H. Boche, **Untersuchungen zur abgeschnittenen Hilbert-Transformation von BMO-Funktionen und VMO-Funktionen (Investigation of the behaviour of the finite Hilbert transform for BMO-functions and VMO-functions),** accepted at Bulletin of the Belgian Mathematical Society Simon Stevin, 1999.

H. Boche, **Verhalten der Cauchy-Transformation und der Hilbert-Transformation für auf dem Einheitskreis stetige Funktionen (On the behaviour of the Cauchy-transform and the Hilbert transform for continuous functions on the unit disk),** accepted at Numerische Mathematik, 1999.

H. Boche, **Verhalten der Lagrangeschen Interpolationspolynome für die Disk-Algebra (On the behaviour of the Lagrange interpolation polynomial for the disk-algebra),** accepted at Numerische Mathematik, 1999.

H. Boche, **Zerlegung von LTI-Systemen und eine vollständige Charakterisierung der Systeme vom Faltungstyp (Structure of LTI-systems and complete characterization of the systems of convolution type),** Electrical Engineering, Springer Verlag, 1998, vol. 81, no. 1, pp. 21-26.

H. Boche, **Zum Verhalten der Autokorrelationsfunktion zeitdiskreter Funktionen (On the behaviour of the autocorrelationfunction for time discrete functions),** accepted at Zeitschrift für Angewandte Mathematik und Mechanik (ZAMM), 1999.

H. Boche and T. Ferchland[34], **Wechselwirkungen zwischen den Nyguist-und Butzer-Bedingungen bei der Konstruktionvon Abtastreihen (Relations between the Nyquist- and Butzer conditions for the construction of sampling series),** Proc. 43rd Intern. Scientific Coll., IWK '98, Sept. 1998, Ilmenau, D, vol. 1, pp. 503-508.

H. Boche and M. Jugl[16], **Analyse von ETSI's Mobilitätsmodellen für Indoor-Mobilfunksysteme (Analysis of ETSI's mobility models for indoor mobile communications systems),** DFG Schwerpunktprogramm Indoor-Mobilkommunikation, Proc. in preparation.

H. Boche and E. Jugl[16], **A new mobility model for Performance Evaluation of future mobile Communication Systems,** accepted at ICC '99.

H. Boche, T. Kuhwald[16] and M. Schubert, **Ein neuer Beamforming-Algorithmus für Indoor-Anwendungen (Beamforming optimization for indoor applications of antenna arrays),** DFG-Schwerpunktprogramm Indoor-Mobilkommunikation, Proc. in preparation.

H. Boche and M. Protzmann, **Behavior of the hard-limiter for bandpass signals and possibilities of signal reconstruction,** Proc. of the Intern. Conf. on Telecommunications ICT '98, Chalkidiki (Greece), 1998, 6 pages, CD-ROM.

H. Boche and M. Protzmann, **Cell loss recovery algorithms for voice and implementations for third generation mobile telecommunication systems,**

Proc. of the First Annual UCSD Conf. on Wireless Communications, San Diego, USA, 1998, CD ROM.

H. Boche and M. Protzmann, **Ein Konvergenzbeweis für den Algorithmus von Papoulis- und Gerchberg (Covergence proof for the algorithm by Papoulis and Gerchberg),** Frequenz 52 (1998) pp. 175-182.

H. Boche and M. Protzmann, **Generalized kernels for reconstructing irregularly sampled bandlimited signals,** in: AEÜ 1998, pp. 81-86.

H. Boche and M. Protzmann, **Oversampling and limitation of signals,** accepted at IEEE Transactions on Circuits and Systems, 1999.

H. Boche and M. Protzman, **Oversampling and reconstruction of lost values of speech signals,** Proc. Intern. Conf. Signal Processing and Communications (IASTED '98), Canary Islands (Spain), 1998, 6 pages, CD-ROM.

H. Boche and M. Protzmann, **Problemspezifische Algorithmen für die Signalrekonstruktion (Design of algorithms for the signal reconstruction),** 43rd Intern. Scientific Coll., IWK '98 Sept. 1998, Ilmenau, D, Proc. vol.1, pp. 497-502.

H. Boche and M. Protzmann, **Überabtastung und Rekonstruktion verlorener Werte bandbegrenzter Signale (Oversampling and reconstruction of lost values of bandlimited signals),** accepted at Zeitschrift für angewandte Mathematik und Mechanik (ZAMM), 1999.

H. Boche, M. Protzmann and H. Schreiber[34], **Precise determination of required oversampling for simulation of communication systems,** Proc. Intern. Conf. on Telecommunications (ICT '98), Chalkidiki (Greece), 1998, 6 pages, CD-ROM.

H. Boche and G. Reißig[34], **An extension of Sandberg's representation theorem for linear time-continuous systems,** Proc. of the 9th Intern. Symp. on System-Modelling-Control, Zakopane, Poland, 1998, CD-ROM, 8 pages.

H. Boche and G. Reißig[34], **Eine notwendige und hinreichende Bedingung für die energetische Stabilität von zeitvarianten zeitkontinuierlichen Systemen (A necessary and sufficient condition for the stability of time variant time continuous systems),** Proc. Informations- und Mikrosystemtechnik, Magdeburg, 1998, pp. 411-418.

H. Boche and H. Schreiber[34], **Faltungseigenschaften von Signalen mit endlicher Energie und Beziehungen zum Verhalten des idealen Tiefpasses (On the convolution of signals with finite energy and relations to the behaviour of low pass),** J. of Electrical Engineer., Nov. 1998. vol. 81, no.4, pp. 263-270.

H. Boche and H. Schreiber[34], **On the time-frequency duality fotime-variant linearchannels,** Proc. Intern. Conf. Signal Processing and Communications (IASTED '98), Canary Islands (Spain), 1998, 6 pages CD-ROM.

H. Boche and H. Schreiber[34], **Stabilitätsnachweis für zeitdiskrete zeitvariante Systeme (On the stability of time variant time continuous systems),** Proc. 43rd Intern. Scientific Coll. (IWK '98) Sept. 1998, Ilmenau, D, vol.1, pp. 521-526.

H. Boche and M. Schubert, **Beamforming von Antennenarrays mit Interpolationsverfahren (Beamforming for linear antennas arrays with interpolation methods),** Proc. 43rd Intern. Scientific Coll. (IWK '98), Sept. 1998, Ilmenau, D, vol. 1, pp. 56-61.

H. Boche and M. Schubert, **Beamforming von linearen Antennen-Arrays mit Interpolationsverfahren (Beamforming for linear antennas arrays with interpolation methods)** accepted at Frequenz, 1999.

R.-P. Braun[10], **Fibre radio systems, applications and devices,** Proc. 24th Europ. Conf. on Optical Communication (ECOC '98), Madrid, Spain, Sept. 20-24, 1998, Tutorial ThA08.

R.-P. Braun[10] and G. Grosskopf, **Optical feeding of base stations in millimetre-wave mobile communications** (invited), Proc. 24th Europ. Conf. on Optical

Communication (ECOC '98), Madrid, Spain, Sept. 20-24, 1998, paper ThC01.

R.-P. Braun[10], G. Grosskopf, H. Heidrich, C. v. Helmolt, R. Kaiser, K. Krüger, U. Krüger, D. Rohde, F. Schmidt, R. Stenzel and D. Trommer, **Optical microwave generation and transmission experiments in the 12 and 60 GHz region for wireless communications,** IEEE Microwave Theory and Techniques, vol. 46, no. 4, April 1998, pp. 320-330.

R.-P. Braun[10], G. Grosskopf, R. Hentges, D. Rohde, M. Rohde and F. Schmidt, **Transmission experiments with optically generated carriers in the 60 GHz-region,** Wireless Communications, Kluwer Academic Press 1999, accepted.

R.-P. Braun[10], G. Grosskopf, D. Rohde and F. Schmidt, **Optical millimeter-wave systems for broadband mobile communications, devices and techniques** (invited), Proc. Intern. Zurich Seminar on Broadband Communications - Accessing, Transmission, Networking -, ETH-Zürich, Switzerland, Febr. 1998, pp. 51-58.

R.-P. Braun[10], G. Grosskopf, D. Rohde and F. Schmidt, **Low phase noise millimeter-wave generation at 64 GHz and data transmission using optical side band injection locking,** IEEE Photonics Techn. Lett., vol. 10, no. 5, May 1998, pp. 728-730.

R.-P. Braun, G. Großkopf, D. Rohde, F. Schmidt, D. Trommer, A. Umbach and G. Unterbörsch, **Bidirectional broadband mobile communications at 60 GHz using optical sideband injection locking,** HHI Annual Report 1997, pp. 97-103, Feb. 1998.

R.-P. Braun[10], G. Grosskopf, D. Rohde, F. Schmidt and G. Walf, **Fiber optic millimeter-wave generation at 64 GHz and spectral efficient data transmission for mobile communications,** Conf. on Optical Fiber Communication (OFC '98), San Jose, CA, USA, Febr. 1998, paper TuC4.

T. Ferchland[34] and H. Boche, **Bewertung des Sektorisierungsgewinns von CDMA-Systemen (Calculation of the sectorization gain for CDMA-based mobile communications systems),** Proc. 43rd Intern. Scientific Coll., IWK '98 Sept. 1998, Ilmenau, D, vol. 1, pp. 127-132.

G. Großkopf, **Multichannel Data Transmission with Optically Generated Carriers in the 60 GHz-Band,** Proc. Eurescom "Triban" Workshop, Nov. 1998, Bern, CH.

V. Jungnickel, C. v. Helmolt and A. Can, **Fast word synchronisation for mobile optical communication,** Proc. 43rd Intern. Scientific Coll., IWK '98, Sept.1998, Ilmenau, D, vol. 1, pp. 104-109.

V. Jungnickel, C. v. Helmolt and U. Krüger, **A broadband wireless infrared LAN architecture compatible with the ethernet protocol,** Electron. Lett., vol. 34 (1998), pp. 2371-2372.

V. Jungnickel, C. v. Helmolt and U. Krüger, WIReLAN: **A broadband wireless IR LAN architecture compatible with ethernet protocol,** Proc. 24th Europ. Conf. on Optical Communication (ECOC '98), Madrid, Spain, Sept. 20-24, 1998, vol. 1, pp. 367-368.

R. Maerz[35], T.M. Almeida[36], C. v. Helmolt, B. v. Canegem[37], B. Hein[29], M. Bischoff[38], M. Lehdorfer[38], W. Muellner[39], M. Rasztovits-Wiech[40], D. Werner[41] and P. Kuindersma[42], **Photonet: Field trial demonstrating WDM cross-connected networks** (invited), Conf. PC06, Proc. Intern. Symposium on Lasers, Optoelectronics and Microphotonics, Sept. 98, Beijing, China, SPIE vol. 3552, pp. 24-30.

W. Mathis[43] and H. Boche, **Faltungseigenschaften der zeitdiskreten Signale mit endlicher Energie (Behaviour of the convolution of time discrete signals with finite energy),** Proc. Informations- und Mikrosystemtechnik, Magdeburg, 1998, pp. 449-456.

G. Reißig[34] and H. Boche, **A normal form for implicit differential equations near singular points and its applications,** Proc. Informations-und Mikrosystemtechnik, Magdeburg, 1998, pp. 419-425.

G. Reißig[34] and H. Boche, **Straightening out trajectories near singular points of implicit differential equations,** Proc. 9th International Symposium on System-

Modelling-Control, Zakopane, Poland, 1998, CD-ROM, 8 pages.

C.G. Schäffer[44], R.-P. Braun[10], G. Grosskopf and F. Schmidt, **Compensation of fiber dispersion in an optical mm-wave system in the 60 GHz-band,** IEEE MTT-S Intern. Microwave Symp. (IMS '98), Baltimore, Maryland, USA, June 7-12, 1998, paper Th3C6.

C.G. Schäffer[44], R.-P. Braun[10], G. Grosskopf, F. Schmidt, and M. Rohde, **Microwave multichannel system with a sideband injection locking scheme in the 60 GHz-band,** Microwave Photonics, MWP '98, Princeton (NJ), USA, Oct. 12-14, 1998, p. 67.

A. Umbach, G. Unterbörsch, R.-P. Braun[10] and G. Grosskopf, **Stable optical source and high-speed photodetector used for remote fiber-optic 64 GHz mm-wave generation,** Conf. on Optical Fiber Communication, OFC '98, San Jose, CA, USA, Febr. 1998, paper ThB3.

G. Unterbörsch, Th. Engel, D. Rohde, M. Rohde[45], D. Bimberg[5] and G. Grosskopf, **Hybrid and monolithic integrated optic/millimeter-wave converters for 60 GHz radio-over-fiber systems,** OFC '99 accepted paper.

Electronic Imaging Technology for Multimedia

A.A. Alatan[46], L. Onural[46], M. Wollborn[47], R. Mech, E. Tuncel[46] and T. Sikora, **Image sequenceanalysis for emerging interactive multimedia services - the European COST211ter framework** (invited), in: Representation and Coding of Images and Video I, Special Issue in IEEE Transactions on Circuits and Systems for Video Technology, vol. 8 (Nov. 1998), no. 7, pp. 802-813.

I. Benjes[26], D. Hepper[48], T. Herfet[49] and T. Meiers, **Stationäre Multimedia-Endgeräte und Benutzerschnittstellen (Stationary multimedia terminals and user interfaces),** Der Fernmelde-Ingenieur, Sonderausgabe anläßlich des Symposiums "Multimedia-Kommunikation auf Netzen und Endgeräten", Berlin, 26. Nov. 1998, pp. 75-94

R. Börner, **Vier autostereoskopische Einpersonen-Monitore mit Trackingsystemen (Four autostereoscopic single user monitors with tracking systems),** Fernseh- und Kinotechnik, 52. Jg. Nr. 12/1998, pp. 747-751.

B. Duckstein, **Autostereoskopische Displays mit Linsenrastern (Autostereoscopic displays with lenticular screens),** DER FAVORIT, alpha CAM, periodical company journal, no. 5, 6/98, p. 6.

M. Hagemeister and T. Weber[50], **Fernsehen wie im Kino (Television like cinema),** Technik & Gesellschaft, Forum des VDI Berlin-Brandenburg, vol. 6, 1998, pp. 16-17.

G. Heising, D. Marpe, and H.L. Cycon[51], **A wavelet-based video coding scheme using image warping prediction,** Proc. IEEE Intern. Conf. on Image Processing, Chicago, IL, USA, Oct. 4-7, 1998.

U. Höfker, H. Krahn, R. Schäfer, P. Stammnitz and M. Talmi, **HIPEG – A single chip MPEG-2 HDTV decoder and HIBOX – a DVB compliant HDTV decoder box,** Proc. IBC '98, (Amsterdam, NL), Sept. 11-15,1998, pp. 185-189.

B. Hüttl, U. Troppenz, S. Richter and K.-O. Velthaus, **The potential of SrS:Ce^{3+} aselectroluminescence phosphor,** Extended Abstracts of the 9th Intern. Workshop on Inorganic and Organic Electroluminescence/4th Intern. Conf. on the Science and Technology of Display Phosphors, (Bend, USA), Sept. 1998, pp. 335-338.

E. Izquierdo, **Stereo image analysis for multi-viewpoint telepresence applications,** Image Communication, vol. 11, no. 3, Jan. 1998, pp. 231-254.

E. Izquierdo, **Disparity/segmentation analysis: Matching with adaptive windows and depth driven segmentation,** Trans. on CSVT, Special Issue on Image and Video Processing for Emerging Interactive Multimedia Services, to be published in Febr. 99.

E. Izquierdo and X. Feng, **Image-based 3D modelling of arbitrary natural objects,** Proc. VLBV Workshop, Urbana (IL), USA, Oct. 1998, pp. 109-112.

E. Izquierdo and S. Kruse, **Image analysis for 3D modelling, rendering and virtual view generation,** Computer Vision and Image Understanding, Special Issue on Computer Vision Applications for Network-Centric Computing, vol. 71, no. 2, Aug. 1998, pp. 231-253.

P. Kauff, J.-R. Ohm, S. Rauthenberg and T. Sikora, **The MPEG-4 Standard and its applications in virtual 3D environments** (invited), Proc. 32nd Asilomar Conf. on Signals, Systems and Computers, Monterey, USA, Nov. 1998, vol. 1, pp. 104-107.

P. Kauff and K. Schüür, **Shape-adaptive DCT with block-based DC-separation and DDC-correction,** IEEE Trans. CSVT, vol. 8, no. 3, June 1998. pp. 237-242.

J. Kreissl, U. Troppenz, B. Hüttl, L. Schrottke and C. Fouassier[52], **Electron-paramagnetic-resonance and photoluminescence studies of chromium in SrS,** Appl. Phys. Lett., vol. 72 (1998), pp. 1232-1234.

W.-M. Li[53], M. Ritala[53], M. Leskelä[53], R. Lappalainen[53], J. Jokinen[53], E. Soininen[54], B. Hüttl, E. Nykänen[53] and L. Niinistö[53], **Elemental characterization of electroluminescent SrS:Ce thin films,** J. Appl. Phys., vol. 84, no. 2, 1998, pp 1029-1035.

J. Liu, **Determination of the point of fixation in a head-fixed coordinate system,** Proc. 14th Intern. Conf. on Pattern Recognition (ICPR '98), Aug. 16-20, 1998, Brisbane, Australia, pp. 501-504.

J. Liu and D. Przewozny, **Stereo image segmentation using hybrid analysis techniques,** Proc. Workshop on Non-Linear Model Based Image Analysis (NMBIA), Glasgow, UK, July 1-3 Juli, 1998, pp. 33-38.

J.R. Ohm, **Format conversion for multimedia terminals,** HHI Annual Report 1997, pp. 119-129, Feb.1998.

J.-R. Ohm et al., **Der MPEG-4 Multimediastandard und seine Anwendungen im MINT-Projekt (The MPEG-4 multimediastandard and its applications in the MINT project),** Der Fernmeldeingenieur, 52. Jg., 11/12 '98, pp. 43-64.

J.-R. Ohm, K. Grüneberg, E. Hendriks[55], E. Izquierdo, D. Kalivas[56], M. Karl, D. Papadimatos[57] and A. Redert[55], **A realtime hardware system for stereoscopic videoconferencing with viewpoint adaptation,** Signal Processing: Image Communication, Special Issue on 3D Technology 14 (1998), pp. 147-171.

J.-R. Ohm, E. Izquierdo and K. Müller, **Systems for disparity-based multiple-view nterpolation** (invited), Proc. IEEE Intern. Symp. on Circuits and Systems, Monterey, CA, USA, June 1998.

J.-R. Ohm and K. Müller, **Incomplete 3D for multiview representation and synthesis of video objects,** Proc. ECMAST '98, Berlin, May 1998, pp. 26-41.

J.-R. Ohm, K. Müller and S. Ekmekci, **Incomplete 3D - A new technique for multiview data representation,** Proc. IEEE 10th IMDSP Workshop, Alpbach, July 1998, pp. 311-314.

S. Pastoor and J. Liu, **Head and gaze controlled interactions with a 3D multimedia computer,** HHI Annual Report 1997, pp. 105-110, Feb. 1998.

S. Pastoor, J. Liu and S. Renault, **An experimental multimedia system allowing 3-D visualisation and eye-controlled interaction without user-worn devices,** IEEE Transactions on Multimedia, vol. 1, no. 1, to be published in March 1999.

S. Richter and R.H. Mauch, **Output characteristics and optical efficiency of SrS:Ce and ZnS:Mn thin film electroluminescent devices,** J. Appl. Phys., vol. 83, no. 10, 1998, pp. 5433-5441.

R. Schäfer, **Drahtlose Interaktivität: Interaktive Multimediadienste erobern den Mobilfunk (Wireless interactivity:**

Interactive multimedia services are conquering mobile communication), Proc. Online '98, Düsseldorf, 18.2.1998.

R. Schäfer, **Entwicklungstendenzen bei der digitalen Quellcodierung: MPEG-4 und danach (Development tendencies in digital source coding: MPEG-4 and after)** (invited), Proc. 2. ITG-Fachtagung Codierung für Quelle, Kanal und Übertragung, RWTH Aachen, 3.-5.3.1998.

R. Schäfer, **MPEG-4: A multimedia compression standard for interactive applications and services** (invited), Electronics Communication Engineering Journal, Dec. 1998, vol. 10, no. 6, pp. 253-262.

R. Schäfer, **MPEG-4 – A new compression standard for interactive applications and services,** HHI Annual Report 1997, pp. 111-118, Feb. 1998.

R. Schäfer, **Multimediakommunikation auf Integrierten Netzen und Terminals – das MINT-Projekt präsentiert seine Ergebnisse (Mulitimedia communication on integrated networks and terminals – results of the MINT project),** Der Fernmeldeingenieur, Heft 11&12, Dec. 1998, pp. 5-9.

R. Schäfer (Ed.), **Multimediakommunikation auf Netzen und Terminals (Multimedia communication on networks and terminals),** special issue of "Der Fernmeldeingenieur", Dec. 1998, pp.1-9.

R. Schäfer (Ed.), **Themenheft ECMAST '98 (Special Issue ECMAST '98),** Fernseh- und Kinotechnik, Heft 12/98, p. 713.

R. Schäfer, C. Fehn and A. Smolic, **MPEG-4 transmission over wireless networks** (invited), Proc. EUSIPCO '98, Rhodes, Greece, Sept. 8-11, 1998, pp. 245-248.

R. Schäfer and D. Hutchison (Eds.), **Multimedia applicatons, services and techniques - ECMAST '98,** Lecture notes in: Computer Science 1425, Springer Verlag, 1998, ISBN 3-540-64594-2.

T. Sikora, **An overview to MPEG video standards,** invited tutorial at NATO Seminar, Toskana, Italien, July 1998.

T. Sikora, **Experiments on Wiener filter design for optimal image interpolation in multiresolution coding schemes,** accepted for publication in: IEEE Trans. on Circuits and Systems for Video Technology.

T. Sikora, **Intelligente Multimedia-Suchmaschinen für das Internet – der MPEG-7 Standard (Intelligent multimedia search engines for the internet – the MPEG-7 standard)** (invited), Münchner Kreis, in: Das Internet von Morgen (The internet of tomorrow), Nov. 1998, Proc. in press.

T. Sikora, **MPEG video coding standards** (invited), to be published in: Compressed Video Over Networks, Ed. Reibman and Sun, McGraw Hill, 1999.

T. Sikora, J. Brailean[58] and Y. Itoh[59] (Eds.), **Error robustness and error resilience in mobile video communications,** Special Issue in Signal Processing: Image Communications, Elsevier, in press.

T. Sikora and K. Brandenburg[60], **MPEG-4 audio and video – an overview,** invited tutorial at IEEE International Conference on Acoustics, Speech & Signal Processing, ICASSP '98, Seattle, Washington, USA, May 1998.

T. Sikora and T. Ebrahimi[61], **MPEG-4 videocoding standard for multimedia applications,** invited tutorial at ICIP, USA, Oct. 1998.

T. Sikora, J. Ostermann[62] and M. Etoh[63] (Eds.), **Shape coding for future multimedia applications,** Special Issue in Signal Processing: Image Communications, Elsevier, to be published in June 1999.

T. Sikora, S. Panchanathan[64], M.-T. Sun[65] and K.N. Ngan[66] (Eds.), **Representation and coding of images and video I,** Special Issue in IEEE Transactions on Circuits and Systems for Video Technology, vol. 8 (Dec. 1998), no. 7.

T. Sikora, S. Panchanathan[64], M.-T. Sun[65] and K.N. Ngan[66] (Eds.), **Representation and coding of images and Video II,** Special Issue in IEEE Transactions on Circuits and Systems for VideoTechnology, in press, to be published in Jan. 1999.

T. Sikora, S. Panchanathan[64], M.-T. Sun[65] and K.N. Ngan[66] (Eds.), **Segmentation, description and retrieval of video content,** Special Issue in IEEE Transactions on Circuits and Systems for Video Technology, Oct. 1998.

A. Smolic, J.-R. Ohm and T. Sikora, **Object-based global motion estimation using a combined feature matching and optical flow approach,** Proc. VLBV '98, Urbana, IL, USA, Oct. 1998, pp. 165-168.

A. Smolic, K. Rümmler, J.-R. Ohm, R. Schäfer and S. Bauer, **MPEG-4 video transmission over DAB/DMB: Joined optimization of encoding and format conversion,** 5th Intern. Workshop on Mobile Multimedia Communication, Berlin, Germany, Oct. 12-14, 1998, pp. 83-94.

A. Smolic and T. Sikora, **Real-time estimation of long-term 3D motion parameters for SNHC face animation and model-based coding applications,** accepted for publication in: IEEE Trans. on Circuits and Systems for Video Technology, Jan. 1999.

U. Troppenz, B. Hüttl, P. Kratzert S.-S. Sun[67], U. Storz, D. Tuenge[67] and K.-O. Velthaus, **Photoluminescence and electroluminescence studies on Cu and Ag doped SrS ACTFEL device,** extended abstracts of the 9th Intern. Workshop on Inorganic and Organic Electroluminescence/4th Intern. Conf. on the Science and Technology of Display Phosphors (Bend, USA), Sept. 1998, pp. 187-190.

K.-O. Velthaus, **Progress of electroluminescence display development at HHI,** Intern. Conf. on Displays and Vacuum Electronics (Garmisch-Partenkirchen, Germany), April 1998, ITG-Fachbericht, vol. 150, pp. 93-98.

K.-O. Velthaus, B. Hüttl, U. Troppenz, T. Gaertner and G. Bilger, **Late-news-paper: Low-temperature deposition for SrS:Cu,Ag EL-phosphor,** extended abstracts of the 9th Intern. Workshop on Inorganic and Organic Electroluminescence/4th Intern. Conf. on the Science and Technology of Display Phosphors (Bend, USA), Sept. 1998, pp. 231-234.

K.-O. Velthaus, **Neue Entwicklungen auf dem Gebiet der anorganischen Dünnschicht-Elektrolumineszenz (New developments in the area of anorganic thin-film electroluminescence),** Proc.13. Electronic Displays-Conf. (Berlin, Germany), Nov. 1998, pp. 100-105.

REPORTS

P. Albrecht, M. Hamacher, H. Heidrich, D. Franke, G. Jacumeit, R. Kaiser, R. Löffler, S. Malchow, W. Rehbein, H. Schroeter-Janßen, R. Stenzel and D. Trommer, **Integration technology: Frequency selective tunable receiver OEICs based on InP for OFDM systems,** Final Report on BMBF Research Project (PHOTONIK II), grant no. 01 BP 440/4, Sept. 1998.

H.-G. Bach, G.G. Mekonnen, W. Passenberg, W. Schlaak, C. Schramm, A. Seeger, R. Steingrüber, H. Engel, A. Umbach, G. Unterbörsch, S. van Waasen[68], R.M. Bertenburg[68] and F.J. Tegude[68], **Höchstfrequente Empfänger OEIC´s auf InP-Basis (High-speed receiver OEICs on InP),** Final Report on Research Project 01 BP 431/7, HHI, Berlin, Nov. 1998.

A. Chiari[69], S. Pastoor and R. Sand[70], **Stereoscopic television – Standards, technology and signal processing,** COST 230 Project, Final Report, June 1998.

B. Duckstein and H. Röder, **Studie für Mannesmann VDO AG zu einem Kfz-Display – erster Teil (Study for Mannesmann VDO AG on a display for automobiles – 1st section),** Confidential Report, 4/98.

Faber, R. Buß, F. Sniehotta and R. Sniehotta, **Gestaltung und Evaluierung des Global Learning Basissystems nach Kriterien der Usability (Design and evaluation of the global learning system according to criteria of usability),** Final Report on evaluation contract I with the Deutsche Telekom AG, HHI Berlin, Febr. 1998

J. Faber, R. Buß, B. Quante and R. Sniehotta, **Gestaltung und Evaluierung des Global Learning Basissystems nach Kriterien der Usability (Design and eva-**

luation of the global learning system according to criteria of usability), Final Report on evaluation contract II with the Deutsche Telekom AG, HHI Berlin, June 1998

H. Heidrich, M. Hamacher and R. Kaiser, **Monolithically integrated 1.5 µm/1.3 µm Transceivers,** contribution in the Final Report on ACTS Research Project ACTS Broadband Lightwave Sources and Systems (BLISS), activity 5.2 (OEICs for access networks), grant no. AC065, Nov. 1998.

A. Hutter, S. Bauer, U. Benzler, M. Köhler, R. Rauschert and A. Smolic, **Proposal for simple visual composition profiles and levels,** ISO/IEC JTC1/SC29/WG11 MPEG98/3172, San Jose, USA, Febr. 1998.

P. Kauff, M. Zhou, K. Schüür and A. Smolic, **Results of mini experiment (SM2) for arbitrary shaped texture,** ISO/IEC JTC1/SC29/WG11 MPEG98/3291, Tokyo, Japan, March 1998.

H. Künzel, **Flächenselektive MOMBE für die Laser/Wellenleiter Integration (Selective area MOMBE for laser/waveguide integration),** Final Report on Research Project PHOTONIK II (01 BP 469/9), 9/1998.

O. Machui, **Autostereoscopic Displays. Entwicklung von autostereoskopischen Multimedia Displays (Autostereoscopic displays. Development of autostereoscopic multimedia displays),** Presentation of research results in the Internet, www.hhi.de/at/3D_displays.

L. Mühlbach, **Telepräsenz am Arbeitsplatz (Telepresence at the workplace),** Final Report on Research Project 01 BK 408/7, HHI, Berlin, Nov. 1998.

H.-P. Nolting and C.M. Weinert, COST 239 Report on **Optical Transparent Networks,** Nov. 1998.

S. Rauthenberg, U. Kowalik, S. Kruse and D. Schneeweiß, **Virtueller T-Punkt mit Online-Fachberatung im Internet (Virtual T-Point with online support in the internet),** Final Report on R&D contract with T-BERKOM, No. 4160/75182, July 1998.

T. Sinnig and H. Röder, **Untersuchungen zum Übersprechen bei Linsenrasterbildschirmen (Research in crosstalk in displays with lenticular screens),** Report for Carl Zeiss, Oberkochen, Germany, 6/98.

A. Smolic, F. Bunjamin and K. Rümmler, **Complexity Analysis of Format Conversion Algorithms,** MEDEA M4M project report, Doc. No. M4M-WP2-035, Munich, Germany, March 1998.

A. Smolic, F. Schweitzer and K. Rümmler, **Evaluation of MPEG-4 coding at 1 Mbit/s with different frame sizes,** MEDEA M4M project report, Doc. No. M4M-WP2-035, Munich, Germany, March 1998.

A. Smolic, F. Schweitzer and K. Rümmler, **Evaluation of channel formats and format conversion algorithms for BISMC,** MEDEA M4M project report, Doc. No. M4M-WP2-046, Berlin, Germany, June 1998.

B. Stabernack and C. Stoffers, **Complexity analysis – comparison of the Momusys and the HHI MPEG4 video decoder,** MEDEA M4M project report, Doc. No. M4M-WP3-035, Munich, Germany, March 1998.

T. Tekin and M. Schlak, **Monolithically integrated Mach-Zehnder interferometer a an add/drop multiplexer,** contribution in the Final Report on ACTS Research Project ACTS Broadband Lightwave Sources and Systems (BLISS), activity 6.2 (SOAs), grant no. AC065, Nov. 1998.

G. Walf, J. Saniter and F.-J. Westphal, **OFDM-LAN mit optischer Filtertechnik (OFDM-LAN with optical filters),** Final Report on research project 01 BP 437/2, Sept. 1998.

1 University of Linz, A
2 University of Potsdam, D
3 University of Puerto Rico, USA
4 University of Wales, UK
5 Technical University Berlin, D
6 University of Erlangen-Nürnberg, D
7 Technical University Kopenhagen, DK
8 Fraunhofer Institut IZM, Berlin, D
9 VPI, Berlin, D
10 Deutsche Telekom AG, Berlin, D
11 Technical University Cottbus, D
12 Alcatel, Marcoussis, F

13 MIT, Cambridge, (MA), USA
14 Semiconductor Physics Institute, Vilnius, LIT
15 Max-Born-Institut, Berlin, D
16 Technical University Ilmenau, D
17 Technical University Darmstadt, D
18 CREOL Univ. of Florida, USA
19 Sandoz Optoelectronics, F
20 AKZO Nobel, NL
21 FhG-IZM, Teltow, D
22 University of Münster, D
23 Mitsubishi, Osaka, J
24 Humboldt Universität Berlin, D
25 MPI-FKF-Stuttgart, D
26 Technical University Braunschweig, D
27 University de Santiago de Compostela, E
28 KTH, Stockholm, S
29 Deutsche Telekom AG, Darmstadt, D
30 Berliner Institut f. Optik, D
31 Weierstraß-Institut f. Angewandte Stochastik, Berlin, D
32 Laser Medizintechnik, Berlin, D
33 Alcatel, Marcoussis, F
34 Technical University Dresden, D
35 Siemens AG, München, D
36 INESC, Aveiro, P
37 University of Gent, B
38 Siemens AG Wien, A
39 Post&Telekom Austria, Wien, A
40 Technical University Wien, A
41 Lucent Technologies, Nürnberg, D
42 Uniphase Netherlands B.V., Eindhoven, NL
43 Technical University Magdeburg, D
44 FH Lübeck, D
45 DeTeWe AG Berlin, D
46 Bilkent University, Ankara, TR
47 University of Hannover, D
48 Deutsche Thomson-Brandt GmbH, Hannover, D
49 Grundig AG, Fürth, D
50 MAZ Brandenburg GmbH, Werder, D
51 FHTW Berlin, D
52 CNRF, Bordeaux, F
53 Helsinki University of Techniques, SF
54 Planar International, Espoo, SF
55 Technical University Delft, NL
56 Intracom, Athen, GR
57 University of Patras, GR
58 Motorola, Chicago (IL), USA
59 Sharp, Tokyo, J
60 Fraunhofer Institut f. Mikroelektronik, Erlangen, D
61 EPFL, Lausanne, CH
62 AT&T Bell Labs, Holmdel (NJ), USA
63 Sony, Tokyo, J
64 Arizona State University, USA
65 University of Washington, Seattle (WA), USA
66 University of Western Australia, Perth, AUS
67 Planar America, Beaverton (OR), USA
68 Universität-GH Duisburg, D
69 Fondazione Ugo Bordoni, Rome, I
70 IRT München, D

PATENT APPLICATIONS

D. Rohde, Ch. Fröhlich, **Anordnung für die Feinjustage einer Lichtleitfaser-Chip-Kopplung (Arrangement for fine positioning a fibre-to-chip-coupling),** 198 02 173.9

R. Ludwig, St. Diez, **Vorrichtung zum Schalten und Abtasten von getakteten optischen Datensignalen (Device for switching and sampling of optical data signals),** 198 05 413.0

G. Przyrembel, B. Kuhlow, **Vorrichtung zum Überlagern optischer Signale mit unterschiedlichen Wellenlängen (Device for superposition of optical signals from different wavelength bands),** 198 06 371.7

R. Börner, **Vorrichtung zur stereoskopischen Wiedergabe von Bildern (Device for stereoscopic reproduction of images),** 198 08 558.3

S. Pastoor, J. Liu, **Vorrichtung zum Verfolgen von Augentranslationen (Device for tracking eye translations),** 198 10 728.5

F. Fidorra, M. Möhrle, H. Venghaus, **Monolithisch integriertes Laserarray (Monolithically integrated laser array),** 198 15 567.0-33

J. Vathke, **Anordnung zur Strahlführung achssymmetrisch einfallender Lichtstrahlen (Free space fabric using micromachined light beam deflectors),** 198 18 706.8

L. Mörl, D. Hoffmann, **Verfahren zur Herstellung integrierter elektro-optischer Wellenleiterbauelemente (Method**

for the fabrication of integrated electro-optic waveguide devices), 198 20 165.6

M. Hamacher, H. Heidrich, R. Kaiser, M. Möhrle, R. Stenzel, D. Trommer, **Monolithischer Photonik-IC zur schmalbandigen Erzeugung optischer Signale bei Frequenzen im Millimeter-Wellenband (Monolithic photonic integrated circuit for generation of optical narrow-band signals in the mm-wave-band),** 198 20 166.4

K. Talmi, S. Pastoor, **Vorrichtung zum Aktivieren von objektbezogenen Schaltflächen (Device for activating object-related control buttons),** 198 24 451.7

R. Steingrüber, R. Kaiser, **Anordnung zur Herstellung vertikaler Strukturen in Halbleitermaterialien (Arrangement for fabrication of vertical profiles in semiconductor Materials),** 198 33 756.6

S. Pastoor, A. Simon, **Vorrichtung zur Erzeugung farbiger dreidimensionaler Bilder (Device for Reproduction of 3-D Color Images),** 198 33 528.8

V. Jungnickel, C.v. Helmolt, A. Can, **Vorrichtung zur Worttaktregeneration bei einer Datenübertragung mittels Pulslagenmodulation (Device for the recovery of the word clock at a data transmission using pulse position modulation),** 198 37 324.4

H. Bünning, **Quasi-Rechteck-Filter (Quasi-rectangular filter),** 198 40 697.5

C. Baack, K.-O. Velthaus, H. Venghaus, **Tragbares multifunktionales Breitbandkommunikationsgerät (Portable multifunctional broadband communication device),** 198 44 301.3

K.-O. Velthaus, **Elektrolumineszenz-Display (Electroluminescence display),** 198 44 302.1

U. Höfker, Ch. Weissig, M. Thomeczek, P. Stammnitz, **Interaktives Multimedia-Card-Modul (Interactive multimedia card module),** 198 47 071.1

K. Peters, **Einrichtung und Verfahren zum Ankoppeln eines faserförmigen Lichtwellenleiters an ein optisches Bauelement (Device and method for coupling an optical fiber waveguide to an optical device),** 198 52 843.4

H. Boche, M.J. Bronzel, Th. Kuhwald, **Verfahren und Anordnung zur Erzeugung vorgegebener Richtcharakteristiken (Procedure and system for the calculation of beam patterns),** 198 58 951.4

E. Pawlowski, **Optischer Abtastkopf für Datenspeicherplatten (Optical pick-up for data disks),** 198 60 563.3

Th. Rosin, **Verfahren und Vorrichtung zum Ausgleichen von Nichtparallelitäten zwischen benachbarten Flächen zweier Körper (Procedure and device for compensating non-parallelism between neighbouring surfaces of two bodies),** 198 60 566.8

AWARDS

W. Blohm, **ITG-Preis 1998** for the paper "Lightness determination at curved surfaces with applications to dynamic range compression and mode-based coding of facial images", IEEE Trans. On Image Processing 6 (1997), no. 8, pp. 1129-1138.

C. Caspar, H.-M. Foisel, L. Molle and B. Strebel, **Paper Award OECC '98** for paper no. 112, "4 x 2.5 Gbit/s, NRZ transmission experiments over transparent crossconnects with opto-electronic frequency converters and dispersion compensated standard single-mode fibre links", OECC '98, Chiba, Japan, July 12-16, Techn. Dig., pp. 426-427.

S. Diez, **The Rank Prize Funds,** best contributed paper entitled "A Novel SOA-based switching device for high-speed, high contrast, all-optical demultiplexing" at Symposium on Ultrafast Photonic Processing and Networks, Grasmere, England, 20th to 23rd April 1998.

K.-O. Velthaus, B. Hüttl, U. Troppenz, R. Herrmann and R.H. Mauch, **Best**

Student Paper Award for "New deposition process for very blue and bright SrS:Ce, CI TFEL Devices", SID International Symposium 97, Boston (USA).

C. Warmuth, **Studienförderpreis SS 98 der Heraeus-Stiftung** im Fach Physik für besonders gute Diplomabschlüsse und einer Verkürzung der Studiendauer (awarded for outstanding Diplomas in Physics in a short study time).

M. Zhou, **Urtel Preis der FKTG** for the Doctorate Theses "Optimisation of MPEG-2 Encoding".

DOCTORATE THESES

H. Boche, **Approximation in Komplexen (Approximation in the Couplex Domain)**, TU Berlin, Fachbereich 3 (Mathematik), Prof. Pommerenke.

S. Richter, **Räumliches Abstrahlverhalten und optische Auskopplung von Dünnschichtstrukturen mit Luminophoren aus SrS:Ce und ZnS:Mn (Spatial emission characteristics and optical outcoupling of thin film luminescent structures based on SrS:Ce and ZnS:Mn)**, Universität Potsdam, Mathematisch-Naturwissenschaftliche Fakultät, Prof. Mikelskis.

S. Schelhase, **Selektive metallorganische Molekularstrahlepitaxie von InP und GaInAs für Heterobipolartransistor-Anwendungen (Selective metal organic molecular beam epitaxy of InP and GaInAs for heterojunction bipolar transistor applications)**, TU Berlin, Fachbereich 12 (Elektrotechnik), Prof. Wagemann.

DIPLOMA THESES

A. Al Bozbek, **Untersuchungen zum Einbauverhalten von Beryllium in AlInAs für p-modulations-δ-dotierte AlInAs/GaInAs Mehrfachquanten topfstrukturen (Investigation of the incorporation behaviour of beryllium in AlInAs for p-modulation-δ-doped AlInAs/GaInAs multiple quantum wells)**, TU Berlin, Fachbereich 4 (Physik). Supervisor at HHI: H. Künzel.

K. Biermann, **Molekularstrahl-Epitaxie und Materialuntersuchungen von GaAsSb und AlAsSb Schichten, gitterangepaßt auf InP-Substrat (Molecular beam epitaxy and characterization of GaAsSb and AlAs Sb layers grown lattice-matched on InP substrates)**, Universität Erlangen-Nürnberg, Fachbereich Physik. Supervisor at HHI: H. Künzel.

A. Can, **Analyse von Kanalmodellen für UMTS (Analysis of channel models for UMTS)**, TU Berlin, Fachbereich 12 (Elektrotechnik). Supervisor at HHI: H. Boche.

M. Doulis, **Gestaltung eines autostereoskopischen Bildschirms (Design of an autostereoscopic display)**, Hochschule für Gestaltung, Technik und Wirtschaft, Pforzheim, Fachbereich Industrial Design. Supervisor at HHI: R. Skerjanc.

C. Fehn, **Vergleichende Untersuchung von Bewegungsschätzverfahen für die modellbasierte Codierung von Bildtelefon-Videosequenzen (Comparative study of global motion estimation techniques for the model-based coding of video telephone sequences)**, Universität Dortmund, Fakultät für Elektrotechnik, Lehrstuhl für Nachrichtentechnik. Supervisors at HHI: T. Sikora, A. Smolic.

X. Feng, **3D-Modellierung von Objekten in stereoskopischen Bildsequenzen (3D-modelling of objects in stereoscopic image sequences)**, TU Berlin, FB 13 (Informatik). Supervisor at HHI: J.-R. Ohm.

J. Freydank, **Implementierung eines MPEG-4 Shapedecoders (Implementation of an MPEG-4 shapedecoder)**, TU Berlin, Fachbereich 12 (Elektrotechnik). Supervisors at HHI: B. Stabernack, M. Talmi.

Ch. Günter, **Schnittstellenwandler mit FPGA-Design (FPGA design of an interface adapter)**, Technische Fachhochschule Berlin, Fachbereich 12 (Elektrotechnik), Studiengang Nachrichtentechnik. Supervisor at HHI: K. Grüneberg.

E. Hilliger, **Interferometrische Schalter mit Halbleiterlaserverstärkern (Interferometric switching devices based on semiconductor optical amplifiers),** TU-Berlin, Fachbereich 4 (Physik). Supervisor at HHI: H.G. Weber.

D. Iskandar, **Herstellung integrierter, wellenlängenselektiver Photodetektoren für Empfangswellenlängen von λ = 1,3 mm und λ = 1,55 mm (Production of integrated wavelength selective photodetectors for the reception wavelength of λ = 1,3 mm and λ = 1,55 mm),** TU Berlin, Fachbereich 12 (Elektrotechnik). Supervisor at HHI: M. Hamacher.

K. Matzen, **Untersuchungen zur Optimierung eines auf Indiumphosphid basierenden integriert-optischen Demultiplexers für Datenraten bis 40 Gbit/s (A study to optimize an integrated optical demultiplexer based on InP and operated at 40 Gbit/s),** Technische Fachhochschule Berlin. Supervisor at HHI: L. Mörl.

W. Metze, **Objektorientierter Entwurf einer Benutzerschnittstelle für ein multimediales, diensteübergreifendes Kommunikationsgerät für den TV-Dienst (Object-oriented design of a user interface for a cross-service multimedia communication device for the TV-service),** TU Berlin, Fachbereich 13 (Informatik). Supervisor at HHI: Th. Meiers.

J. Naujocks, **Simulation eines Powerline-Übertragungssystems unter MATLAB/SIMULINK (Simulation of a powerline communication system using MATLAB/SIMULINK),** Fachhochschule Hamburg, Fachbereich Elektrotechnik/Informatik. Supervisor at HHI: K.-D. Langer.

C. Oberreich, **Auswertung der Program Specific Information innerhalb eines MPEG-2 Transport Stream Demultiplexers (Evaluation of the program specific information within a MPEG-2 transport stream demultiplexor),** TU Berlin, Fachbereich 12 (Elektotechnik). Supervisor at HHI: K. Grüneberg.

J. Päßler, **Implementierung einer MPEG-2 Transportstrom Analysesoftware (Implementation of an MPEG-2 transportstream analysis software),** TU Berlin, Fachbereich 12 (Elektrotechnik). Supervisors at HHI: B. Stabernack, M. Talmi.

M. Phong, **Segmentierung von Bildsequenzen mit einem merkmalsorientierten Verfahren (Segmentation of image sequences using feature-based algorithms),** TU Berlin, Fachbereich 13 (Informatik). Supervisor at HHI: J.-R. Ohm.

L. Prüßner, **Analyse, Implementierung und Optimierung von MPEG-4 Decoderalgorithmen auf dem RISC VLIW DSP TMS320C6201(Analysis, Implemention and Optimization of MPEG-4 deocderalgorithms on the RISC VLIW DSP TMS320C6201),** TU Berlin, Fachbereich 12 (Elektrotechnik). Supervisiors at HHI: B. Stabernack, M. Talmi.

M. Schubert, **Anwendungen von Smart Antennas für UMTS (Applications of Ssmart antennas for UMTS),** TU Berlin, Fachbereich 12 (Elektrotechnik). Supervisor at HHI: H. Boche.

K. Schüür, **Effizienzorientierte Optimierung eines Algorithmus zur konturangepaßten DCT für die objektbasierte Videocodierung (Efficiency-related optimization of an algorithm for shape-adaptive DCT in object-based video coding),** TU Berlin, Fachbereich 13 (Informatik). Supervisor at HHI: P. Kauff.

U. Storz, **Optische Charakterisierung von SrS:Ce-Elektrolumineszenzstrukturen (Optical characterization of SrS:CE EL-structures),** TFH-Berlin. Supervisor at HHI: B. Hüttl.

T. Tekin, **Herstellung und Charakterisierung von monolithisch integrierten MZI-Wellenlängenkonvertern (Fabrication and characterisation of monolithically integrated MZI wavelength converters),** TU Berlin, Fachbereich 12 (Elektrotechnik). Supervisor at HHI: N. Agrawal.

C. Warmuth, **Bestimmung der Amplituden- und Phasenverteilung in AWG-Wellenlängenfiltern durch Fourierspektroskopie (Determination of amplitude- and phase-distribution in**

AWG wavelength filters by Fourier spectroscopy), Technische Universität Berlin, Fachbereich 4 (Physik). Supervisor at HHI: B. Kuhlow.

J. Wei, **Wavelet Based Rotation-Invariant Texture Classification for Iris Recognition,** TU Berlin, Fachbereich 12 (Elektrotechnik). Supervisor at HHI: J. Liu.

Ch. Weißig, **Entwicklung, Aufbau und Test eines PC-Card-Moduls zur Ausgabe von gespeicherten MPEG-2 Testpattern unter Berücksichtigung des DVB Standards (Design, realisation and test of a PC-card module for storage of MPEG-2 test pattern according to the DVB standard)**, TU Berlin, Fachbereich 12 (Elektrotechnik), Institut für Meß- und Automatisierungstechnik. Supervisor at HHI: U. Höfker.

GRADUATE THESES

A. Höynck, **Anwendungen von Joint Detection in einem CITDMA Mobilfunksystem (Application of joint detection for CITDMA mobile communications system)**, TU Berlin, Fachbereich 12 (Elektrotechnik). Supervisor at HHI: H. Boche.

D. Razic, **Aufbau und Test eines optischen Phasenkonjugators in einer Polarisations-Diversität-Anordnung (Optical phase conjugator based on polarization diversity)**, TU Berlin, Fachbereich 12 (Elektrotechnik). Supervisor at HHI: H.G. Weber.

U. Rebeschieß, **Grundlegende Aspekte von CDMA-Mobilfunksystemen am Beispiel des IS-95 Standards (Some Aspects of CDMA-based Mobile Communications Systems (IS-95))**, TU Berlin, Fachbereich 12 (Elektrotechnik). Supervisor at HHI: H. Boche.

T. Ritter, **Space-Time Signalverarbeitung für Indoor Anwendungen (Space time processing for indoor applications)**, TU Berlin, Fachbereich 12 (Elektrotechnik). Supervisor at HHI: H. Boche.

U. Schwabe, **Experimentelle Untersuchung der Effizienz einer objektbasierten Videocodierung mittels starrer dreidimensionaler Modelle Experimental investigation of efficiency of object-based video coding using rigid 3D models)**, TU Berlin, FB 13 (Informatik). Supervisor at HHI: P. Kauff.

B. Utus, **Large-scale Kanalmodelle für Indoor Anwendungen (Large-scale channel models for indoor applications)**, TU Berlin, Fachbereich 12 (Elektrotechnik). Supervisor at HHI: H. Boche.

LECTURES

H.-G. Bach, Meßverfahren für Halbleiterbauelemente, TU Berlin

E.-J. Bachus, Photonische Kommunikationsnetze, TU Berlin

H. Boche, Intelligente Antennen und mehrdimensionale Signalverarbeitung in der Mobilkommunikation, TU Berlin

H. Boche, Hardy-Räume und Informationstechnik, TU Berlin

B. Kuhlow, Einführung in die optische Signalverarbeitung, TU Berlin

B. Kuhlow, Optische Signalverarbeitung und Grundlagen der Photonik, TU Berlin

J.-R. Ohm, Bildverarbeitung I, TU Berlin

J.-R. Ohm, Bildverarbeitung II, TU Berlin

J.-R. Ohm, Bildsignalverarbeitung für Multimediasysteme, TU Berlin

A. Paraskevopoulos, Halbleitertechnologie für die Integration in der Optoelektronik, TU Berlin

St. Schlüter, Chemie-Praktikum für Mediziner, FU Berlin

B. Strebel, Optische Wellenleiter, TU Berlin

H.G. Weber, Grundlagen und Anwendungen der linearen und nichtlinearen Faseroptik, TU Berlin

WORKSHOPS ORGANISED

Modellierung und Simulation integriert optischer Schaltungen und mikrooptischer Systeme, jointly organised with VDI/VDE Technologiezentrum Informationstechnik GmbH and Fachausschuss 5.3 Optische Nachrichtentechnik der ITG, Berlin, January.

European Conference on Multimedia Services, Applications and Techniques (ECMAST '98), Berlin, May.

Final Presentation of the ACTS 092 PANORAMA Project (**PA**ckage for New **Ope**Rational **A**utostereoscopic **M**ultiview Systems and Applications), Berlin, September.

Multimedia-Kommunikation auf Netzen und Terminals, Symposium in Berlin, November.

CONTRIBUTIONS TO EXHIBITIONS

LOB '98, Laser & Optik Berlin, February:
Diffractive optical elements, fiber-chip coupling module

OFC '98, San Jose, USA, February:
Photonic components and systems (jointly with u2t, Berlin)

Online '98, Düsseldorf, February:
MPEG-2 software codecs and MPEG-7 search engine

CeBIT '98, Hannover, March:
Carl Zeiss/HHI 3D-displays, high-speed receivers

Industrie-Messe Hannover '98, April:
Optoelectronic device technologies, display technologies (full color EL-display, transparent display), diffractive optical elements (jointly with Berlin Universities and Research Institutes), piezo-electronic optical scanner

ECMAST '98 (3rd Conference on Multi Media Applications, Services and Techniques), Berlin, May:
3D-video from CD-ROM, DVB-T transmission of HDTV, real-time MPEG-2 HDTV-decoder (HiBOX), Carl Zeiss/HHI 3D-display, autostereoscopic direct-view display with video-based head tracking

DVB-T Seminar, Hong Kong, July:
DVB-T transmission of HDTV, real-time MPEG-2 HDTV-decoder (HiBOX)

ECOC '98, Madrid, Spain, September:
40 Gigabit receiver, micro-optical elements

IBC '98, Amsterdam, September:
DVB-T transmission of HDTV, real-time MPEG-2 HDTV-decoder (HiBOX), stereoscopic videoconferencing with viewpoint adaptation

Caper '98, Trade Show, Buenos Aires, September/October:
HDTV, MPEG-2 decoding with HiBOX

Final Demonstrations of ACTS Project PANORAMA at HHI, Berlin, October:
Large-screen autostereoscopic display with video-based head tracking

Electronica '98, Munich, November:
HiPEG - the single chip solution for decoding MPEG-2 for HDTV (jointly with Fujitsu Microelectronics and TU Chemnitz)

INNOVATION Leipzig '98, November:
Full color EL-display, transparent display, high-speed receivers, optoelectronic device technologies, photonic components and systems

MINT-Symposium (Multimedia Communication on Integrated Networks and Terminals), final presentation, Berlin, November:
Virtual video conference system, autostereoscopic teleconference terminal with head tracking and parallax compensation, real-time MPEG-4 decoder, user interface for TV+ multimedia terminal, stereo TV from DVD and with DVB-T transmission, real-time MPEG-2 HDTV-decoder (jointly with Deutsche TV-Plattform)

COMMITTEE ACTIVITIES

Standardisation Committees

DVB Technical Module: Member

DVB Task Force "Digital Terrestrial

Television – System Aspects": Chairman

ETSI, Human Factors Group: Member

ISO/MPEG, Video Group: Chairman

VDI/VDE, Arbeitskreis Integrierte Optik: Member

Research Program Committees

COST 230, Stereoscopic Television, Management Committee: Member

COST 230, Stereoscopic Television, WG Human Factors: Chairman

COST 230, Management Committee: Member

COST 230, Psychooptics Group: Chairman

COST 239, Management Committee: Member

COST 240, Management Committee: Vice Chairman and Liason Officer COST 239/240

COST 266, Progress of Photonic Infrastructure towards the IT-Age: Member

COST 267, Semiconductor devices for signal processing WG2: Chairman

COST 268, Management Committee: Member (deputy)

MINT: Chairman of the Steering Board

Strategische Plattform Informationstechnik: Member

Conference and Workshop Program Committees

ECOC Technical Program Committee: Member

9th European Conference on Integrated Optics (ECIO '99), 1999,Turin: Program Committee Member

European Conference on Multimedia Services, Applications and Techniques (ECMAST) 1998, Berlin: Steering Committee Member and Chairman

Human Factors and Telecommunications: Permanent Steering Committee

Integrated Photonics Research Conference 1998, Victoria, Canada: Program Committee Member

11th International Conference on InP and Related Materials (IPRM '99), Davos (CH): Program Committee Area Chair

International Picture Coding Symposium (PCS '98), 1998, Berlin: Steering Committee Member

7th International Plastic Optical Fibres Conference '98 (POF '98), Berlin, National Organisation Committee: Member

2. ITG-Fachtagung Codierung für Quelle, Kanal und Übertragung, Aachen: Program Committee Member

Microwave Photonics, MWP '99, Melbourne 1999, Australia: TPC-Member

Mobile Multimedia Conference (MOMUC '98), Berlin: Program Committee Member

Münchner Kreis, Congress "The Internet of Tomorrow – New Technologies for New Applications", Chairman and Head of Program Committee

The Internet of Tomorrow – New Technologies for New Applications – Congress of "Münchner Kreis": Congress Chairman and Head of Program Committee

Editorial Boards

IEEE Signal Processing Magazine: Associate Editor

IEEE Transactions on Circuits and Systems for Video Technology: Associate Editor

Image Communication: Associate Editor and Guest Editor

Institute of Physics (GB)/Semiconductor Science and Technology: Referee

Springer Verlag Berlin, Heidelberg, Series "Photonics": Co-Editor

Other Committees

Aspen Institut Berlin: Member

COBRA, Communication Technology, Basic Research and Application at Technical University Eindhoven: Advisory Board

Competence Center for the Application of Nanostructures in Optoelectronics (NanOp): Member of Executive Board

Eduard-Rhein-Stiftung: Board of Trustees

FKTG, Urtel-Preis-Komitee: Curatorship

ITG, FA 3.1 Fernsehtechnik und elektronische Medien: Member

ITG, FG 3.1.2 Digitale Bildcodierung: Chairman

ITG, FA 5.3 Optische Nachrichtentechnik: Member

ITG, FG Optische Polymerfasern: Member (2x)

Laser- und Medizin-Technologie GmbH Berlin: Scientific Advisory Board

Münchner Kreis, Supranational Association for Communications Research: Research Committee

Nano-optoelectronics Competence Centre (NanOp), Management Committee: Member

Optoelectronics Consortium, Berlin: Member, Steering Committee

Technologiestiftung Innovationszentrum Berlin: Board of Trustees

WISTA-Management GmbH, Berlin: Advisory Committee

EXCHANGE PROGRAM

Scientists Visiting HHI

X. Bardella, University of Catalania, Spain, financed by HHI, for 7 months

K. Biermann, Max-Born-Institut, Berlin, financed by MBI, for two months

E. Cooke, DCU Dublin, Ireland, financed by MAZ Brandenburg, for 2 months

L. Jiang, Massachussetts Institute of Technology, Cambridge (MA), USA, financed by DAAD, for 3 months.

A. Krotkus, Semiconductor Physics Institute, Vilnius, Lithuania, financed by European Community, ACTS Programme, for 4 months

HHI Scientists Visiting Foreign Institutes

N. Agrawal, Lucent Technologies, Holmdel (NJ), USA, financed by HHI, for 1 year

H. Preier, University of Linz, Austria, financed by HHI, for 3 years

COOPERATIONS

Industry

AEA Technology, Harwell (UK)

Advanced Photonic Systems, Berlin

Aixtron, Aachen

Alcatel-Alsthom Recherche, Marcoussis, Paris (F)

Alcatel Telecom, Stuttgart

AMS Optotech, München

Berliner Institut für Optik, Berlin

Berliner Kraft- und Licht (Bewag) AG, Berlin

Bosch Telecom, Backnang

British Telecom, Martelsham Heath (UK)
Carl Zeiss, Jena, Oberkochen

Cybertron, Berlin

Daimler-Benz Aerospace, Ulm

Dai Nippon Printing, Tokyo (J)

Deutsche Telekom, Berlin, Bonn, Darmstadt, Wien

Deutsche Telekom-Berkom, Berlin, Darmstadt

Deutsche Thomson Brandt, Hannover, Villingen

Dornier Satellitensystme GmbH, Friedrichshafen

D-Research Digital Media Systems GmbH, Berlin

DSPecialist, Berlin

EPIGAP Optoelektronik GmbH, Berlin

France Telecom, CNET (F)

Fujitsu Mikroelektronik GmbH, Dreieich-Buchschlag

Grundig AG, Fürth

Hewlett Packard, Böblingen

Hitachi, Tokyo (J)

Holographie Design Berlin GbR, Berlin

Intracom, Athen (GR)

IOT Enwicklungsgesellschaft für Integrierte Optik-Technologie mbH, Waghäusel

Laser Components GmbH, Olching

Laser Spec GmbH, München

LKF Advanced Optics GmbH, Berlin

Loewe-Opta GmbH, Kronach

Lucent Technologies, Nürnberg, Holmdel (USA)

Mannesmann VDO AG, Babenhausen

Mikroelektronik-Anwendungszentrum GmbH im Land Brandenburg (MAZ), Werder

Mikros Image, Paris (F)

moove, Leverkusen

Nortel, Ottawa (CAN)

NTB Elektronische Geräte GmbH, Oranienburg

OptoSpeed SA, Mezzovico (CH)

Optotransmitter-Umweltschutz-Technologie, Berlin

Philips Components BV, Eindhoven (NL)

PirelliCavi e Sistemi S.p.A., Milano (I)

Planar America Inc., Beaverton (USA)

Planar International, Espoo (SF)

Quantum Devices Inc. (QDI), Yorba Linda, CA (USA)

Robert Bosch GmbH, Hildesheim, Stuttgart

2SK Media Technologies, Berlin

SEL Alcatel, Stuttgart

Sentech Instruments, Berlin

SHF Design, Berlin

Siemens Nixdorf AG, Augsburg, München

Siemens AG, Berlin, München, Regensburg

Thomson CSF Optonique, Paris (F)

U2t Innovative Optoelectronic Components GmbH, Berlin

vision pearls, Berlin

Universities and Institutes

ATR, Kyoto (J)

Bundesanstalt für Materialforschung und -prüfung (BAM), Berlin
CCETT, Rennes (F)

CNRSM, Brindisi (I)

Denmark Technical University, Kopenhagen (DK)

DFN-Verein, Berlin

DLR – Deutsches Zentrum für Luft- und Raumfahrt, Oberpfaffenhofen

ETH Zürich (CH)

ETRI, Korea

Ferdinand-Braun-Institut, Berlin

FH Lübeck

FhG Institut für Zuverlässigkeit und Mikrointegration, Berlin und Teltow

FhG Institut Siliziumtechnologie, Itzehoe

Fraunhofer Institut für Physikalische Meßtechnik (IPM), Freiburg

Freie Universität Berlin

Gesellschaft für Angewandte Optik und Spektroskopie e.V., Berlin

GMD Fokus, Berlin

Hahn-Meitner-Institut, Berlin

Helsinki University of Techniques (SF)

Humboldt-Universität zu Berlin

ICS Forthe, Crete (GR)

INRIA, Paris (F)

Institute of Technology, Carlow (IR)

Institut für Physikalische Hochtechnologie (IPHT), Jena

IRISA, Rennes (F)

Max-Born-Institut, Berlin
NHK Research Labs., Tokyo (J)

Paul-Drude-Institut, Berlin

Technical Reserach Centre of Finland, Tampere (SF)

Technical University of Loughborough (UK)

Telefonica Investigacion y Desarollo, Madrid (E)

TU Berlin

TU Braunschweig

TU Chemnitz/Zwickau

TU Darmstadt

TU Dresden

TU Eindhoven (NL)

TU Hannover

TU Ilmenau

TU München

TU Wien (A)

Universität Dortmund

Universität Erlangen-Nürnberg

Universität - GH Duisburg

Universität Karlsruhe

Universität Linz, A

Universität Marburg

Universität Stuttgart

Universität Tübingen

Universität Ulm

University of Patras (GR)

University of Thessaloniki (GR)

Walter-Schottky-Institut, München

Weierstraß-Institut für Angewandte Analysis und Stochastik (WIAS), Berlin

Weizmann Institute of Science, Rehovot (IL)

Wuhan Research Institute for Posts & Telecommunications (PR China)

START UP COMPANIES

LKF Advanced Optics GmbH, Berlin
LKF-Advanced Optics GmbH is a high-tech company, founded in 1996 by research staff members of the HHI. The mission is to convert the results of basic research to practical high end photonic components. First products are tunable mode-locked lasers in customized versions. Target for these products are leading telecommunication labs worldwide researching in ultra-high-bit time devision muliplex technique.

DSPecialists GmbH, Berlin
DSPecialists develops systems and tools for digital signal processing using digital signal processors (DSP). Its focus is to provide platforms in software and hardware for customers in various branches, such as audio, video, telecom and measurement/control. DSPecialists sells its products and provides different kinds of services, such as technical training and application development.

Virtual Photonics Incorporated (VPI)
Virtual Photonics Incorporated (formerly BNeD GmbH and Virtual Photonics Pty Ltd) is a team of thirty executives and photonics engineers in Berlin, San Francisco and Melbourne delivering new design, planning and engineering software and services to leading component and system manufacturers, system integrators and network operators. VPI attracts the brightest talent in photonics engineering to design powerful software platforms, in partnership with the world's leading research institutes. VPI invented the first generation of Photonics Design Automation systems products – BroadNed, GOLD and OPALS – and jointly developed the HPPhotonics System Designer. VPI has now consolidated and advanced this know how with the Photonics Transmission Design Suite, an integrated design tool for multi skilled corporate teamwork.

2SK Media Technologies GbR, Berlin
2SK Media Technologies develops and markets software for compression and decompression of audio and video signals according to the MPEG standards. Its main product is the MPEG SoftEngine, which currently supports MPEG-1 and MPEG-2. Future products, which will support MPEG-4 and MPEG-7, are under development.

MikroM, Berlin
MikroM develops and designs VLSI components for image and sound processing and compression. Its main product is HiPEG+, a single chip HDTV decoder according to the Main Profile@High Level of MPEG-2. This chip, which is based on the HiPEG chip previously developed at HHI, contains the video decoder and the systems demultiplex.

u2t Innovative Optoelectronic Components GmbH, Berlin
u2t Innovative Optoelectronic Components GmbH was founded in 1998 by three HHI scientists. Their intention is to support R&D-engineers with state-of-the-art optoelectronic components resulting from most recent device research. Ultrafast InGaAs photodetectors with 50 GHz bandwidth and extremely high power handling capabilities are the first products.

Usability Lab am HHI, Berlin
The company supplies Human Factors support at all stages of the product development lifecycle. It helps to design all products of information technology with a high degree of usability. Thus, the chances of the product's successful future marketing will increase. But even products already on the verge of being put into the market can be improved by adopting Human Factors procedures.

vision pearls, Berlin
The company develops software for computer vision applications. The main interest is on video based human-computer interaction using advanced object detection and tracking algorithms. The first product will support new ways of interaction with multimedia software presentations.

HHI AT A GLANCE

Government research institute (Federal Republic of Germany and State of Berlin)
Total staff at end of 1998: 249 employees

Areas of Research and Development

Photonic Networks

- Design, development and demonstration of optical communication networks and subsystems (access and customer networks, core networks)
- Investigation and development of WDM and high-speed OTDM techniques for high capacity transmission and routing
- Exploration of high speed transmission performance of photonic networks
- Development of techniques for network operation and maintenance
- Development and fabrication of photonic devices and integrated circuits (transmitters, modulators, switches, optical amplifiers, filters, multiplexers and demultiplexers, signal regenerators, transceivers, receiver frontends) based on InP, SiO_2/Si and polymers

Mobile Broadband Systems

- Development of optical microwave generation and transmission systems for cellular mobile communication systems
- Development of RF and IR mobile systems for broadband in-house communication
- Investigations on time varying transmission channels for mobile communication systems
- Design of problemspecific algorithms for signal processing and antenna arrays
- Development of methods to increase the transmission capacity in cellular mobile communication systems

Electronic Imaging Technology for Multimedia

- Development of algorithms and hardware architectures for video and audio compression
- Development of algorithms and hardware architectures for image analysis and synthesis
- Design of integrated circuits for image processing
- Development of user interfaces for multimedia applications
- Analysis and optimization of communication services
- Development of 3D display technologies
- Development of blue emitters for electroluminescent flat-panel displays
- Development of an optical pickup for DVD-systems

HEINRICH-HERTZ-INSTITUT FÜR NACHRICHTENTECHNIK BERLIN GMBH

Einsteinufer 37, D-10587 Berlin
Germany
Phone: +49 (0)30 3 10 02-0
Fax: +49 (0)30 3 10 02-213
Email: Contacts@hhi.de
http://www.hhi.de

Scientific Managing Director:
Prof. Dr. Clemens Baack
Administrative Managing Director:
Dr. Wolfgang Grunow

ISSN 1435-1587